

GERMAN PHARM-TOX SUMMIT 2021

Abstracts of the

87th Annual Meeting of the German Society for Experimental and Clinical Pharmacology and Toxicology (DGPT)

With contribution of the Arbeitsgemeinschaft für Angewandte Humanpharmakologie e. V. (AGAH)

1 March – 3 March 2021

Digital

This supplement was not sponsored by outside commercial interests. It was funded entirely by the publisher.

Structure

Oral Presentations..... 1-89

<i>Toxicology – 3R Practice/Alternative Methods.....</i>	<i>1-6</i>
<i>Toxicology – Toxins.....</i>	<i>7-12</i>
<i>Pharmacology – Cardiac pharmacology and treatment.....</i>	<i>13-18</i>
<i>Pharmacology – Cancer pharmacology and treatment.....</i>	<i>19-24</i>
<i>Pharmacology – Disease models – drug development I.....</i>	<i>25-29</i>
<i>Young Scientist Award.....</i>	<i>30-35</i>
<i>Toxicology – Carcinogenesis.....</i>	<i>36-41</i>
<i>Pharmacology – Immunopharmacology inflammation antiinfectives-Session II - Identification of immunological targets and drug development.....</i>	<i>42-47</i>
<i>Pharmacology – Disease models – drug development II.....</i>	<i>48-53</i>
<i>Toxicology – Emerging topics.....</i>	<i>54-59</i>
<i>Pharmacology – Ion channels and membrane transporters.....</i>	<i>60-65</i>
<i>Toxicology – Food Toxicology.....</i>	<i>66-71</i>
<i>Pharmacology – G-protein coupled receptors.....</i>	<i>72-77</i>
<i>Immunopharmacology inflammation antiinfectives-Session I - Functional characterization of immunopharmacological drugs.....</i>	<i>78-83</i>
<i>Pharmacology – Pharmacogenetics, Pharmacoepidemiology and Drug Safety.....</i>	<i>84-89</i>

Poster Presentations..... P01-P111

<i>Pharmacology – Cardiac pharmacology and treatment.....</i>	<i>P01-P02</i>
<i>Pharmacology – Immunopharmacology / inflammation / antiinfectives.....</i>	<i>P03-P12</i>
<i>Pharmacology – Cancer pharmacology and treatment.....</i>	<i>P13-P26</i>
<i>Pharmacology – CNS / endocrine pharmacology and treatment.....</i>	<i>P27-P29</i>
<i>Pharmacology – Pharmacoepidemiology and drug safety.....</i>	<i>P30-P31</i>
<i>Toxicology – 3R Practice/Alternative Methods.....</i>	<i>P32-P41</i>
<i>Toxicology – Regulatory toxicology.....</i>	<i>P42-P47</i>
<i>Toxicology – Inhalation toxicology/Respiratory toxicology.....</i>	<i>P48-P52</i>
<i>Toxicology – Carcinogenesis.....</i>	<i>P53-P54</i>
<i>Pharmacology – Pharmacological education.....</i>	<i>P55-P56</i>
<i>Pharmacology – G-protein coupled receptors.....</i>	<i>P57-P60</i>
<i>Pharmacology – Signal transduction and second messengers.....</i>	<i>P61-P64</i>
<i>Pharmacology – Nuclear receptors, enzymes and other targets.....</i>	<i>P65-P71</i>
<i>Pharmacology – Ion channels and membrane transporters.....</i>	<i>P72-P82</i>
<i>Pharmacology – Drug transport/delivery and metabolism.....</i>	<i>P83-P87</i>
<i>Pharmacology – Disease models, drug development.....</i>	<i>P88-P98</i>
<i>Pharmacology – Pharmacokinetics and PK/PD modeling.....</i>	<i>P99</i>
<i>Toxicology – Biogenic toxins.....</i>	<i>P100-P101</i>
<i>Toxicology – Computational Toxicology.....</i>	<i>P103-P104</i>
<i>Toxicology – Emerging topics.....</i>	<i>P105-P111</i>

Author index

Oral Presentations

Toxicology – 3R Practice/Alternative Methods

1

The E-Morph Assay: Screening for anti-estrogenic substances based on quantitative changes in cell-cell contact organization of breast cancer cells

S. Klutzny¹, M. Kornhuber¹, S. Dunst¹, G. Schönfelder¹, M. Oelgeschläger¹
¹Bundesinstitut für Risikobewertung, Deutsches Zentrum zum Schutz von Versuchstieren (Bf3R), Berlin, Germany

Question: Adverse health effects caused by the unintended exposure to endocrine disrupting chemicals (EDCs) including substances with anti-estrogenic activity in the environment, food, and consumer products are of high public concern. In view of the up to 800 substances that have been listed as suspected EDCs in recent years and the more or less unlimited number of possible co-exposure scenarios, modern cell-based high-throughput screening (HTS) approaches are increasingly playing a central role in regulatory toxicology.

Methods: The E-Morph Assay is a novel *in vitro* screening assay that addresses a human-relevant functional endpoint, i.e. the estrogen-dependent reorganization of cell-cell contacts in breast cancer cells [1, 2]. We used this assay to screen a library of 440 toxicologically relevant industrial chemicals, biocides and plant protection products that were proposed to act on nuclear hormone receptors (estrogen, androgen, glucocorticoid, thyroid). The E-Morph Assay detected 24 estrogenic substances with relative potencies that correlated very well with the ER bioactivity score published by the US EPA Endocrine Disruptor Screening Program. Moreover, the E-Morph Assay identified nine substances with yet undescribed estrogenic activity, and the two known anti-estrogens Tamoxifen and Raloxifene. These results provide a proof-of-concept study demonstrating the applicability of the E-Morph Assay in cell-based HTS approaches.

Results: In addition to toxicological testing frameworks, the E-Morph Assay is likely also applicable in the pharmaceutical sector, e.g., for (pre-)screening of novel active substances during the drug discovery process. This led us to file a European and international (PCT) patent application for the E-Morph Assay at the European Patent Office [3].

[1] Bischoff P, Kornhuber M, Dunst S, Zell J, Fauler B, Mielke T, et al. 2020. Estrogens determine adherens junction organization and e-cadherin clustering in breast cancer cells via amphiregulin. *iScience* 23:101683.

[2] Kornhuber M, Dunst S, Schönfelder G, Oelgeschläger M. 2021. The E-Morph Assay: Identification and characterization of environmental chemicals with estrogenic activity based on quantitative changes in cell-cell contact organization of breast cancer cells. *Under review*.

[3] Bischoff P, Kornhuber M, Schönfelder G, Oelgeschläger M, Dunst S, Vogl S. 2019. Screening method for estrogenic and anti-estrogenic activity. EP3517967A1, PCT/EP2019/051920. *European Patent Office*.

2

DNA strand breaks assessment using the hepatocyte-like HepaRG cell line: comparison of the automated AUREA gTOXXs and alkaline comet assay

P. Braun¹, F. K. Gehring¹, I. Pfltzner², S. Pfulher³, D. Tom³, C. Chesne⁴, D. Dressler², K. Engelhart-Jentzsch K²
¹3T GmbH & CoKG, Tuttlingen, Germany
²BioTeSys, Esslingen, Germany
³Procter & Gamble, Mason, Germany
⁴Biopredic International, St. Gregoire, France

The HepaRG cell line is an excellent model for mapping the metabolic response of hepatocytes to chemicals, including measurements of toxicity. The automated gTOXXs solution provides a sensitive and reliable *in vitro* technique to detect genotoxicity in the form of DNA strand breaks. In this study, the degree of DNA strand breaks induced by exposure of HepaRG cells to genotoxic methyl methane sulfonate (MMS) has been comparatively assessed by AUREA gTOXXs and the alkaline Comet assay.

HepaRG cells have been cultivated for 4 hours or 7 days. Cytotoxicity is determined by the MTT test measuring viability of the cells. DNA strand breaks are assessed by gTOXXs (Moreno-Villanueva, Eitze, Dressler et al 2011; *Altox*, 28, 4/11) and compared to the results obtained with the alkaline Comet assay. The gTOXXs is based on progressive DNA unwinding at "open sites" under specific conditions of alkaline pH, time and temperature and fluorescence labelling of intact double-stranded (ds) DNA. Exposure to MMS for 4h produced no cytotoxic effects on HepaRG cultivated for 7d and mere slight cytotoxic effects on HepaRG cultivated for 4h at the highest concentrations (15% and 6% reduced viability, respectively). A clear dose-dependent decline of % dsDNA is detected by the gTOXXs and the Comet assay in a highly similar manner. The detection sensitivity of gTOXXs, however, appears to surpass the one of the Comet assay. A significant reduction in % dsDNA is detected by the gTOXXs at 10 micro molar MMS, while significant increase in tail intensity is detected at 30 micro molar MMS by the Comet assay. A no-effect threshold is observed for DNA damage assessed by the Comet assay, albeit, not for the one assessed by gTOXXs. Notably, the HepaRG cultured for 4h and 7d have nearly identical dsDNA dose-response curves but higher variability

(increase in the standard deviation) of the mean %dsDNA was observed in the 4h experiment.

Conclusion: AUREA gTOXXs for automated genotoxicity assessment is a very sensitive assay for detecting DNA strand breaks similar to the alkaline Comet assay. This finding is further supported by a very recent study assessing the genotoxic potential of ten engineered nanomaterials by the two assays (unpubl. results). For MMS, the 4 h cultivation protocol for HepaRG cells appears suitable for genotoxicity assessment. It will be interesting to compare the suitability of the 4h protocol with the 7 d protocol for genotoxins needing bio-activation.

3

HepaChip-MP – An organ-like perfusable cell culture system in multiwellplate format for toxicity testing

M. Busche¹, S. Werner¹, B. Hagemeyer¹, M. Pawlak¹, H. Becker², J. Schnabel², K. Gall³, R. Hemmler³, G. Damm⁴, S. Beuck⁵, T. Klaassen⁵, J. Moer⁶, A. Ullrich⁶, T. Mayr⁷, M. Matz-Soja⁸, R. Gebhardt⁸, M. Stelzle¹

¹Natural and Medical Sciences Institute (NMI), Reutlingen, Germany

²microfluidic ChipShop, Jena, Germany

³Ionovation GmbH, Osnabrück, Germany

⁴Leibniz University Hannover, Incubator of Saxony for Clinical Translation, Leipzig, Germany

⁵A & M Labor für Analytik und Metabolismusforschung Service GmbH, Bergheim, Germany

⁶Primacyt GmbH, Schwerin, Germany

⁷Graz University of Technology, Institute of Analytical Chemistry and Food Chemistry, Graz, Austria

⁸Universität Leipzig, Rudolf-Schönheimer-Institute of Biochemistry, Leipzig, Germany

Introduction/Question: Undetected liver toxicity accounts for a major fraction of drug recalls following market entrance and is responsible for considerable health risks for patients (LeCluyse et al., 2012). Currently employed models often fail to accurately predict toxic side effects in liver due to lack of a physiologic microenvironment, rapid loss of typical liver functionality in cell culture systems and species related differences of animal models.

Methods: We established a microfluidic cell culture system in multi-well plate format (HepaChip-MP) with 24 independent culture chambers for automated, parallelized cell seeding in a liver sinusoid-like structure and toxicity testing (Busche et al., 2020). Selective, automated assembly of viable cells is accomplished by dielectrophoresis using a pipetting robot, while physiologic media perfusion during culture is realized by pumpless gravitational flow. For measuring cellular oxygen usage, sensors were integrated in the culture chamber. Chip handling can be performed easily either with a pipetting robot or manually.

Results: We adapted conventional cell biology assays to be used with the HepaChip-MP. A resazurine assay as well as an ATP assay was carried out to demonstrate cell damage of assembled cells after treatment with diclofenac and acetaminophen. To enable the analysis of the metabolism of xenobiotic substances, CYP-activity and -induction was shown via turnover of model substrates and subsequent analysis by mass spectrometry. By using the integrated oxygen sensors, we established the non-invasive and time-resolved online measurement of cellular oxygen consumption after substance treatment.

Conclusion: We were able to establish a parallelized, perfused liver model in multi-well plate format for drug and toxicity testing. Automated filling of the chip and the cell assembly facilitates use by non-expert end-users and implementation in industry and scientific work flows. The HepaChip-MP allows throughput substance testing under more physiological conditions than in currently used 2D-culture systems. Also, integrated oxygen sensors enable the non-invasive online measurement of cellular oxygen consumption. An extensive functional and cytological comparison between 2D-, 3D-culture and the HepaChip-MP as well as increased culture time and co-culture with non-parenchymal cells will be part of future research.

Acknowledgements: funding by the BMBF through grant no. 031B0481D is acknowledged.

4

In vitro testing of angiogenesis by a growth-factor free human based co-culture

B. Birk¹, N. Roth¹, S. Woelk¹, B. Flick¹, B. van Ravenzwaay¹, R. Landsiedel¹
¹BASF SE, Experimental Toxicology and Ecology, Ludwigshafen am Rhein, Germany

Angiogenesis, *de novo* formation of blood vessels, is important for (patho-) physiological processes. Chemicals can interact with this biological effect leading to desired (reduced tumor growth) or toxic effects (developmental toxicity). Several external growth factors (GF)-requiring *in vitro* angiogenesis assays have been developed in the past. We developed a human based *in vitro* angiogenesis assay without external GF to screen early anti-angiogenic effects of chemicals. Human fibroblasts (Cl-huFIB, Inscreenex) were co-cultured with human endothelial cells (HUVEC, PromoCell) in 96-well plate. Cells were treated at Day 4 and 8 with 3 angiogenesis inhibitors with known teratogenic effects (Digoxin (DI), Levamisole (LV), 2-Methoxyestradiol (ME)), two teratogenic substances without angiogenic inhibiting effects (Phenytin (PH), Methimazole (MT)) and one without anti-angiogenic and teratogenic effects (D-Mannitol (MA)). On Day 14, HUVECs were stained with rabbit- α -Factor VIII related antigen (Zytormed) to quantify the HUVEC tube formation by measurement the tubular length and network branching points (IncuCyte, Sartorius). To distinguish anti-angiogenic effects from cytotoxicity, MTT viability test was performed in parallel.

No external GF was needed to build a reproducible and tubular network. Reproducibility was proven by application of DI in several runs (>n=5). LV, DI, PH and ME showed a lower LOEC (lowest observed effect concentration defined as > 20% inhibitory effects versus vehicle control) for the tube formation than cytotoxicity assuming an anti-angiogenic effect. MT and MA neither showed any inhibitory effect for inhibition of tube formation nor cytotoxicity up to 1000 µM. The results of all test substances in our GF-free assay were in line, except PH, with the results of the method using a co-culture of HUVECs and adipose tissue plus external GF [2]. PH showed anti-angiogenic properties in our assays at >100 µM but was inactive in the assay of Toimela et al. ([2]). PH is often considered not having anti-angiogenic properties, but Eser et al. [1] could demonstrate this activity in mice.

This GF-free protocol for a human cell-based *in vitro* angiogenesis assay is easy to handle and providing reproducible results in line with literature [1, 2]. Further testing is needed but it could be a useful tool to investigate angiogenesis in the area of toxicology and pharmacology in the future.

[1] DOI: 10.1186/1471-2482-12-25

[2] DOI: 10.1016/j.reprotox.2016.11.015

5

Inhibition of human Deiodinase 1 by gold containing organic substances, anorganic salts and nanoparticles

A. G. Weber¹, C. Müller¹, B. Birk¹, S. Schneider¹, B. van Ravenzwaay¹, R. Landsiedel¹
¹BASF SE, Experimental Toxicology and Ecology, Ludwigshafen am Rhein, Germany

The disruption of the hypothalamus-pituitary-thyroid axis (HPTA) has been linked to goiter, neurodevelopmental deficits in humans and thyroid tumors in rats. Testing of substance-induced disruption of HPTA is routinely done using animal studies. Robust and predictive *in vitro* methods for the detection of substance-induced disruption of the HPTA can help to reduce animal testing.

The HPTA is a complex endocrine system, consisting of multiple enzymes and transporters responsible for hormone synthesis, distribution, action, metabolism and elimination. The Deiodinase I (DIO1), a seleno-cysteine dependent enzyme, plays an important role in the systemic production of the biologically active thyroid hormone T3 in the thyroid gland as well as the deiodination of inactive thyroid hormone metabolites preventing excess iodide excretion.

In this study the DIO1-Sandel-Kolthoff assay (DIO1-SK) was used to investigate the role of gold derivatives in deiodinase inhibition as well as to test the methods applicability towards different classes of substances. Organic and inorganic gold compounds, their analogues as well as different sizes of gold nanoparticles (AuNPs) were tested in the DIO1-SK.

The DIO1-SK uses human liver microsomes as a DIO1 enzyme source to detect substance-induced iodide release inhibition. Released iodide was quantified via the Sandell-Kolthoff reaction which uses reduction of yellow Ce4+ to colorless Ce3+ with a catalyzing function of iodide as a colorimetric readout.

Three organic gold compounds, namely aurothioglucose (ATG), sodium aurothiomalate and auranofin, inhibited iodide release activity, generating similar IC50 ranging from 0.49 to 0.75 µM. Their structural analogues lacking the gold cation did not produce iodide release inhibition. The two gold salts Gold(I) and Gold(III) chloride showed similar iodide release inhibition values as the organic gold compounds tested. Further, AuNPs with different diameters were tested regarding iodide release inhibition in the DIO1-SK assay. AuNPs with a diameter of 100 and 30 nm did not have an effect while AuNPs of 5 nm diameter inhibited iodide release with an IC50 of 9.43*1011 particles/ml.

We have shown the gold dependent effect on iodide release activity of deiodinases using multiple gold compounds and the applicability of the DIO1-SK assay towards different groups of substances including nanoparticles. The formal validation of the assay including ATG as positive control organized by ECVAM is ongoing.

6

Serotype-specific sensitivity to Botulinum neurotoxins of iPSC-derived motor neurons

M. Schenke^{1,2}, B. M. Schjeide³, G. P. Püschel³, **B. Seeger^{1,2}**

¹University of Veterinary Medicine Hannover, Institute for Food Quality and Food Safety, Hannover, Germany

²University of Veterinary Medicine Hannover, Virtual Center for Replacement and Complementary Methods to Animal Testing, Hannover, Germany

³University of Potsdam, Institute of Nutritional Science, Department of Nutritional Biochemistry, Nuthetal, Germany

Question: Botulinum neurotoxins (BoNTs) are used to treat neuromuscular dysfunctions and are applied in aesthetic medicine. Each batch of these highly potent neurotoxins, produced by *Clostridium botulinum* bacterial strains, must be tested for potency, which is still done to a significant extent with the mouse lethality assay. For BoNT batch testing, 400,000 mice are still used annually within Europe alone. BoNTs cleave proteins essential for neurotransmitter release in neurons. Approved replacement methods are only applicable to single pharmacological products using highly specific neopeptide antibodies to detect the proteolytic activity of BoNTs. To overcome this limitation and to develop a serotype-independent cell-based *in vitro* assay that is applicable to both pharmacologically used serotypes (BoNT/A1 and /B1) and prospective compounds, and

finally to replace the mouse lethality assay, the cells most representative for the toxic effects of BoNTs should be applied: human motor neurons (MNs).

Methods: Human induced pluripotent stem cells were differentiated to MNs according to three different protocols. Previously, the cells have been characterized for expression of characteristic marker genes and proteins for MNs as well as for targets of different BoNT serotypes [1]. Here, cleavage of respective substrate proteins after incubation with different concentrations of BoNT/A1 and /B1 has been quantified via Western Blot in comparison to the commonly used neuroblastoma cell line SiMa, which has been proven in the past to be sensitive to BoNT/A1, but not to BoNT/B1 [2].

Results: MNs were more sensitive to BoNT/A1 than SiMa cells. It appears that SiMa cells are not sensitive to BoNT/B1 since there was no concentration-dependent substrate cleavage. The generated MNs were sensitive to BoNT/B1.

Conclusions: Motor neurons seem to be a promising basis for the development of an *in vitro* method for the potency testing of different BoNT serotypes.

Acknowledgement: MoNLightBoNT-Assay development was funded by the German Federal Ministry of Education and Research (FKZ 031L0132A/B).

References:

- Schenke, M., et al., *Analysis of Motor Neurons Differentiated from Human Induced Pluripotent Stem Cells for the Use in Cell-Based Botulinum Neurotoxin Activity Assays*. *Toxins*, 2020. **12**(5).
- Pathe-Neuschäfer-Rube, A., et al., *Cell-Based Reporter Release Assay to Determine the Potency of Proteolytic Bacterial Neurotoxins*. *Toxins*, 2018. **10**(9).

Toxicology – Toxins

7

The enzyme subunit SubA of Shiga Toxin-Producing *E. coli* strains demonstrates comparable intracellular transport and cytotoxic activity as the holotoxin SubAB

K. Sessler¹, P. Papatheodorou¹, F. Wondany², M. Krause³, S. Noettger¹, D. Bernhardt³, J. Michaelis², H. Schmidt³, H. Barth¹

¹University Ulm Medical Center, Institute of Pharmacology and Toxicology, Ulm, Germany

²University Ulm, Institute of Biophysics, Ulm, Germany

³University of Hohenheim, Institute of Food Science and Biotechnology, Hohenheim, Germany

Shiga toxin-producing *Escherichia coli* (STEC) strains are bacterial pathogens, which are mainly found in the gastrointestinal tract of farm and wildlife animals. The bacteria can be transmitted to humans via food and causes diarrheal and extraintestinal diseases. In addition to the Shiga toxin, some STEC strains also produce a second toxin, namely the subtilase cytotoxin (SubAB) [1]. SubAB belongs to the family of AB₅ toxins, consisting of an enzymatically active A subunit (SubA) and separate B subunits (SubB), which mediate cell binding and uptake of SubAB. Inside the host cell, SubAB is transported via a retrograde pathway into the endoplasmic reticulum (ER), where it cleaves the glucose-regulated protein GRP78. SubAB-induced GRP78 cleavage activates a cellular stress response eventually resulting in cell death [1]. We previously demonstrated that SubA, without SubB, binds and intoxicates HeLa cells [2], whereas the cellular and molecular mechanisms behind this remained unclear. In the present study, we found that even in the absence of SubB, SubA is internalized into cells, reaches the endoplasmic reticulum (ER) and cleaves the chaperone GRP78. Furthermore, SubA-induced GRP78 cleavage in cells is prevented by the pre-treatment of cells with brefeldin A (BFA), which inhibits the transport of protein toxins into the ER. Obviously, SubA contains a yet undescribed ER localization signal, predicted by the software scanProsite™ as a SEEL motif at the C-terminus. Hence, a SubA mutant, lacking the SEEL motif (SubA_{ΔC344}), was generated, which exhibited no cytotoxicity alone, but only together with SubB, when tested on HeLa and HCT116 cells. Fluorescence microscopy revealed that SubA_{ΔC344} is generally taken up into cells, but further investigations regarding substrate cleavage have shown that SubA_{ΔC344}-induced GRP78 cleavage was delayed when compared to wildtype SubA. We therefore assume that the SEEL motif plays a crucial role in guiding SubA into the ER [3]. Furthermore, we confirmed our findings in the human intestinal mini-gut organoid system. Our results not only contribute to a better understanding of the mode of action of the subtilase cytotoxin, but also raise the question whether a B component-independent cytotoxic effect of the A component is also true for other bacterial AB₅ toxins.

1. Paton AW et al. (2010), *Toxins (Basel)* 2(2):215–228.

2. Funk J et al. (2015), *Infect Immun* 83(6):2338–2349.

3. Sessler K et al. (2021); *Arch. Toxicol.* (in press)

8

Inhibition of *Clostridioides difficile* toxins by ambroxol hydrochlorideS. Fischer¹, J. Baier¹, G. Fois², P. Dietl², M. Frick², H. Barth¹¹University of Ulm Medical Center, Institute of Pharmacology and Toxicology, Ulm, Germany²University of Ulm, Institute of General Physiology, Ulm, Germany

In western countries, infections with the pathogenic bacterium *Clostridioides* (*C.*) *difficile* (CDI) are coming more and more into focus, in particular in hospitalized patients after prolonged treatment with antibiotics. CDIs are responsible for up to 10 % of all nosocomial infections in Germany and are one of the most common diagnosed cause of contagious antibiotic-associated diarrhea and depending on the severity, different clinical presentations ranging from mild diarrhea to fulminant colitis are possible. After germination in the gut, *C. difficile* produces the two exotoxins TcdA and TcdB, which are the major virulence factors causing *C. difficile* associated diseases (CDAD). TcdA and TcdB are taken up into host cells via receptor-mediated endocytosis. Acidification of endosomal vesicles by vacuolar H⁺-ATPases leads to translocation of the glucosyltransferase domain across the endosomal membrane. Once in the cytosol, the enzymatic portion glycosylates and inactivates Rho-GTPases in mammalian cells leading to the destruction of the cytoskeleton, cell-rounding and typical clinical symptoms. Based on the ubiquitous occurrence of *C. difficile* and the almost uncontrollable contamination of pathogens in hospitals, novel pharmaceutical strategies to prevent and to treat toxin-associated diseases are urgently needed. Therefore, pharmacological toxin-inhibitors are required since the produced toxins are responsible for the severity and the progress of CDAD. Recently, it was shown that the approved and commercially available drug ambroxol hydrochloride (Ax-HCl) blocks acidification of lamellar bodies that derive from endosomes. Prompted by these findings, we investigated the inhibitory potency of Ax-HCl on the *C. difficile* toxins TcdA and TcdB. To investigate the inhibitory effect of Ax-HCl, different mammalian cell lines were incubated with TcdA and TcdB as well as the combination of both toxins in the presence or absence of Ax-HCl. Inhibition of the toxins was monitored by cell rounding, intracellular substrate modification and measurements of changes in transepithelial electrical resistance. Based on its ability to neutralize vesicular pH values, the widely used drug Ax-HCl also protected cultured cells from intoxication with TcdA and TcdB and might therefore be an auspicious pharmacological inhibitor to treat and to prevent CDAD.

9

Innovative and highly sensitive detection of *Clostridium perfringens* enterotoxin based on receptor interaction and monoclonal antibodiesM. Krüger¹, T. Neumann¹, S. Mahrhold², J. Weisemann², C. Feraudet-Tarisse³, C. Pöhlmann⁴, K. Schulz⁴, M. Dörner¹, D. Stern¹, U. Messelhäußer², D. Rimek⁴, F. Gessler², S. Simon³, T. Elßner⁴, A. Rummel², B. Dörner¹¹Robert Koch Institute, Centre for Biological Threats and Special Pathogens, Biological Toxins, Berlin, Germany²Hannover Medical School, Institute for Toxicology, Hannover, Germany³Atomic Energy and Alternative Energies Commission, Centre de Recherche de Saclay, Gif-sur-Yvette, France⁴Bruker Daltonik GmbH, Leipzig, Germany⁵Bayerisches Landesamt für Gesundheit und Lebensmittelsicherheit, Oberschleißheim, Germany⁶Thüringer Landesamt für Verbraucherschutz, Bad Langensalza, Germany⁷mprolab GmbH, Göttingen, Germany

Introduction: The pore-forming *Clostridium perfringens* enterotoxin (CPE) is one of the major causes of food poisoning, antibiotic-associated diarrhea and is involved in other human and veterinary gastrointestinal diseases. Fast and sensitive detection of CPE is crucial for the diagnosis of *C. perfringens* induced intoxication and differentiation from other gastrointestinal diseases.

Objectives: The objective of this work was i) to functionalize the endogenous CPE receptor claudin-4, a member of the tetraspanin superfamily, for innovative detection of the toxin, ii) to compare the performance of receptor-based and conventional antibody-based tools and detection systems for CPE and iii) to transfer conventional ELISA approaches to the automated mobile detection platform pBDi (portable BioDetector integrated).

Materials & methods: We generated nine highly affine and specific monoclonal antibodies binding five distinct epitopes of CPE by hybridoma technique. The antibodies were thoroughly characterized with respect to their binding properties by surface plasmon resonance and ELISA along with recombinantly expressed claudin-4. Antibodies were explored for their potential to functionally block the toxin's action. Sandwich ELISAs and receptor-based assays with superior sensitivity were transferred to the automated detection platform pBDi.

Results: All newly generated monoclonal antibodies displayed excellent affinities towards CPE ranging from 0.05 – 2.3 nM. Eight of the nine antibodies depicted clear blockage of toxin action in a cytotoxicity assay indicating the potential of the mAbs to bind native CPE. Integration of the mAbs into classical sandwich ELISA as well as the application of claudin-4 as capture reagent combined with mAb detection led to detection limits in the low pg/mL-range for stationary detection and in the low ng/mL-range for mobile detection using the on-site detection device. In a validation study, CPE was correctly detected in the supernatant of 30 *cpe*-positive *C. perfringens* outbreak strains out of 64 strains tested in total, providing 100% correlation to PCR results.

Conclusion: We established highly sensitive antibody- and receptor-based assays for the detection of CPE applying new monoclonal antibodies and the functionalized receptor claudin-4. For the first time, we present an automated, fast and sensitive on-site detection system detecting CPE in ng/mL-concentrations within 20 minutes, a useful advancement for clinical diagnostics.

10

Cytotoxic effects of the *Clostridioides difficile* pore-forming toxin CDTbK. Ernst¹, M. Landenberger², J. Nieland², M. Roeder², K. Nørgaard², P. Papatheodorou², H. Barth²¹Ulm University, Medical Center, Institute of Pharmacology and Toxicology, Ulm, Germany²Ulm University, Medical Center, Institute of Pharmacology and Toxicology, Ulm, Germany

The clinically highly relevant *Clostridioides* (*C.*) *difficile* produces and secretes several AB-type protein toxins that cause *C. difficile*-associated diseases (CDAD) like diarrhea and pseudomembranous colitis. In patients treated with antibiotics, the gut microbiota is disturbed which can cause *C. difficile* overgrowth and release of the large Rho/Ras-GTPase glycosylating toxin TcdA and TcdB which are considered as the major virulence factors for CDAD. A third toxin called CDT is produced in addition to TcdA and TcdB by *C. difficile* strains isolated from severe cases of colitis. CDT is a binary AB-type actin ADP-ribosylating toxin and consists of two separate protein components. The binding/translocation B-component, CDTb, is responsible for receptor-binding, as well as transport and translocation of the enzyme A-component, CDTa, into the target cell cytosol. Therefore, CDTb forms transmembrane pores through which CDTa can translocate to the cytosol where it ADP-ribosylates monomeric G-actin. This leads to depolymerization of the actin cytoskeleton and thereby rounding of adherent cells and, eventually, causes cell death. Here, we discovered that CDTb shows cytotoxic effects in the absence of CDTa. CDTb caused cell rounding and impairment of cell viability as well as of the epithelial integrity of CaCo-2 monolayers in the absence of CDTa. Cell rounding induced by CDTb alone was dependent on the presence of LSR, the specific cellular receptor of CDT, but the isolated receptor-binding domain of CDTb was not able to induce cell rounding. CDTb-induced cytotoxicity was inhibited by an enzymatically inactive CDTa mutant as well as by several tailored pore-blockers. These findings indicate that pore formation into the cytoplasmic membrane as the underlying cytotoxic mechanism of CDTb. Taken together, our results suggest two independent functions of CDTb during the intoxication process of epithelial cells by CDT: i) serving as a transporter of the A-component CDTa into the cytosol of target cells and ii) directly attacking the cell membrane by pore-formation.

11

Intoxication of mammalian cells with binary clostridial enterotoxin is inhibited by the combination of pharmacological chaperone inhibitorsM. Braune¹, K. Ernst¹, J. Sailer¹, H. Barth¹¹Ulm University, Medical Center, Institute of Pharmacology and Toxicology, Ulm, Germany

Binary toxins *Clostridioides difficile* toxin CDT, *Clostridium botulinum* C2 toxin and *Clostridium perfringens* iota toxin cause enterotoxicity. These toxins consist of a binding/translocation (B) component which facilitates binding to cells and transport of the enzymatically active (A) component into the cytosol. Here, it ADP-ribosylates G-actin leading to depolymerization of F-actin and thereby to cell rounding. The folding helper enzymes heat shock protein 90 and 70, cyclophilins and FK506-binding proteins facilitate the translocation of CDT, C2 and iota A components through pores formed by respective B components into the cytosols. Folding helper enzymes can be inhibited by pharmacological inhibitors which protect cells from intoxication.

Question: Combination of different pharmacological inhibitors of folding helper enzymes leads to enhanced protection of cells from intoxication with C2 toxin, can this be seen for CDT intoxication as well? Can the protective effect still be observed if concentrations of each inhibitor are reduced?

Methods and Results: Combination of pharmacological inhibitors of Hsp90 (radicol), Hsp70 (VER-155008), cyclophilins (cyclosporine A) and FK506 binding proteins (FK506) showed a delay of CDT-induced rounding of Vero cells compared to single inhibitors. The protective effect of the inhibitor combination on CDT intoxication was confirmed by analysis of ADP-ribosylation status of G-actin in CaCo-2 lysates from CDT-treated cells. Damage of epithelial integrity of CaCo-2 monolayers by CDT and C2 toxin, measured as reduction in transepithelial electrical resistance (TEER), was delayed by combination of inhibitors. Furthermore, inhibitor combination delayed C2 and CDT intoxication even if lower concentrations of each inhibitor were used. A protective effect of the inhibitor combination was also shown for iota toxin but was more pronounced for C2 toxin compared to CDT and iota toxin.

Conclusion: The combination of folding helper enzymes inhibitors protected cells from intoxication with CDT and C2 toxin. Inhibitor concentrations and exposure times could be reduced if inhibitors were applied in combination which might be of advantage to reduce risk of adverse effects.

Ernst, K., Sailer, J., Braune, M., & Barth, H. (2020). *Naunyn-Schmiedeberg's archives of pharmacology*. DOI: 10.1007/s00210-020-02029-3

12

European programme for the establishment of validated procedures for the detection and identification of biological toxins (EuroBioTox)

S. Worbs¹, B. Kampa¹, M. Skiba¹, K. Busschots², R. Zeleny², J. Masquelier³, A. Puustinen⁴, P. Vanninen⁴, C. Rasetti-Escargueil⁵, M. Popoff⁶, E. Lemichez⁵, A. S. Mierzała⁶, H. Volland⁶, F. Becher⁶, S. Simon⁶, B. Boran⁷, Y. Nia⁷, J. A. Hennekinne⁷, J. Weisemann⁸, A. Rummel⁹, D. Jansson⁹, M. A. Avondet¹⁰, W. Luginbühl¹¹, R. Josuran¹², C. Zaborosch¹², L. Burns¹³, K. Campbell¹³, **B. Dörner**¹

¹Robert Koch Institute, Biological Toxins, Berlin, Germany
²European Commission, Joint Research Centre, Geel, Belgium
³Sciensano, Tervuren, Belgium
⁴University of Helsinki, Finnish Institute for Verification of the Chemical Weapons Convention, UH/VERIFIN, Helsinki, Finland
⁵Institut Pasteur, Département de Microbiologie, Bactéries Anaérobies et Toxines, Paris, France
⁶CEA-SACLAY, Laboratoire d'Etudes et de Recherche en Immunoanalyse, Gif-sur-Yvette, France
⁷ANSES, Food Safety Laboratory, SBCL Unit, Maisons-Alfort, France
⁸toxogen GmbH, Hannover, Germany
⁹Swedish Defence Research Agency FOI, Umeå, Sweden
¹⁰SPIEZ LABORATORY, Spiez, Switzerland
¹¹ChemStat, Bern, Switzerland
¹²Zürich University of Applied Sciences ZHAW, Institute of Chemistry and Biotechnology, Wädenswil, Switzerland
¹³Queen's University Belfast, Institute for Global Food Security, Belfast, United Kingdom

Introduction: Biological toxins are known as causative agents of food poisoning, but some of them also have a history as warfare agents and could be used in a bioterrorism context. Previous studies showed that there is a lack of robustness in European preparedness for biotoxin incidents. There is a need for standard analytical tools and procedures, reference materials, state-of-the-art training and establishment of a European proficiency testing scheme.

Objectives: EuroBioTox is a Horizon 2020 project integrating 13 consortium partners and 50 network partners from 23 countries from the health, food, military and verification sectors. The project aims at establishing a Pan-European network of competence for the analysis of biological toxins of potential bioterrorism threat (1). The toxins in the scope of EuroBioTox comprise selected large protein toxins (ricin, abrin, botulinum neurotoxins [BoNT], staphylococcal enterotoxin B [SEB]) as well as small molecule biotoxins (saxitoxin [STX]).

Materials & methods: Using current best practice, the EuroBioTox core members develop and validate improved analytical tools, reagents and standard operating procedures based on realistic incident scenarios. Alternative and more accurate *in vitro* tests for the ethically questionable animal test for BoNT are under evaluation.

Results: Progress beyond state of the art has been achieved by production of five candidate reference materials for different biological toxins to be certified after the current comprehensive molecular characterisation. Training courses at basic and advanced levels have been conducted within the network tailored to the different methods and toxins, followed by a series of proficiency tests (currently five) to disseminate best practice methods across Europe. The creation of a European repository with proprietary toxin-specific tools was initiated to harmonise detection methods. With respect to the specific needs of first responders, new conceptual guidelines on sampling, detection and decontamination were established focusing on biological toxins.

Conclusion: EuroBioTox is implementing a comprehensive mechanism of training, method sharing, improvement of quality assurance measures and proficiency testing. It is expected that the spreading of good analytical practices will improve preparedness and response planning at national and international level.

Reference: <https://eurobiotox.eu>

Pharmacology – Cardiac pharmacology and treatment

13

Thrombin receptor PAR4 coordinates inflammatory stress platforms in diabetic atria

C. Mittendorf¹, J. Poertner¹, L. Kassler¹, T. Puzicha¹, M. Kamler², D. Dobrev¹, **A. Fender**¹

¹Medical Faculty, University Duisburg-Essen, Institute of Pharmacology, Essen, Germany
²Medical Faculty, University Duisburg-Essen, Department of Thoracic and Cardiovascular Surgery, Essen, Germany

Question: The NLRP3 inflammasome and the Unfolded Protein Response (UPR) are interconnected stress platforms driving atrial cardiomyopathy, to which patients with diabetes are particularly prone. Protease-activated receptor 4 (PAR4) is increased in right atrial appendages (RAA) of patients with diabetes and in isolated cardiac fibroblasts exposed to high glucose, thereby increasing thrombin-stimulated IL-1 β production. We now examined the candidate function of PAR4 as an upstream regulator of UPR/NLRP3-dependent stress pathways in diabetic atria.

Materials and Methods: RAA were obtained from patients \pm type 2 diabetes undergoing cardiac surgery. Atria were collected from wildtype and PAR4^{-/-} mice fed chow or a high-fat diet (HFD) for 26 weeks. Neutrophils isolated from healthy donors (Polymorphprep[®]) were primed in platelet poor plasma (PPP) \pm thrombin (1 U/mL, 3h). Atrial cardiomyocyte-like HL-1 cells were cultured in high glucose medium and stimulated for 24h \pm study drugs or neutrophil-conditioned PPP. Tissue and cell lysates and supernatants were assessed by real-time PCR, Western blot and ELISA.

Results: Expression of auto-cleaved active caspase-1, the UPR regulator GRP78, and total and phosphorylated mTOR and P70S6 kinase were higher in atria of diabetic patients and HFD-fed mice compared to controls. PAR4 deletion ameliorated these atrial stress signals in HFD-fed mice. In HL-1 cells, thrombin or a PAR4 activating peptide increased phosphorylation of mTOR, P70S6 kinase, AMP-activated kinase and Ca²⁺/calmodulin-dependent protein kinase II, without increasing the expression or secretion of GRP78 or inflammatory cytokines. The ability of HL-1 cells to produce GRP78 and IL-6 in response to stress signals was confirmed with the TLR2 agonist Pam3CSK4 and oxidised human serum albumin, a prototypical advanced oxidation protein product (AOPP) of neutrophil-derived myeloperoxidase (MPO). MPO and AOPP were elevated in atria of HFD-fed mice and in conditioned PPP from thrombin-primed neutrophils, which strongly increased expression and release of GRP78 and IL-6 in HL-1 cells.

Conclusion: Thrombin via PAR4 directly stimulates stress kinases in atrial cardiomyocytes, and indirectly promotes cardiomyocyte GRP78 and cytokine production via neutrophil-derived AOPP. PAR4 antagonists may provide a new therapeutic approach to counter interconnected stress platforms in atrial cardiomyopathy.

14

MiR-21-dependent macrophage-to-fibroblast signaling determines the cardiac response to pressure overload

D. P. Ramanujam^{1,2}, A. P. Schön^{1,2}, C. Beck^{1,2}, P. Vaccarello¹, G. Felician^{1,2}, A. Dueck^{1,2}, D. Esfandyari^{1,2}, G. Meister³, T. Meitinger^{2,4}, C. Schulz^{2,5}, S. Engelhardt^{1,6}

¹Technical University of Munich, Institute for Pharmacology and Toxicology, München, Germany
²German Centre for Cardiovascular Research, München, Germany
³University of Regensburg, Regensburg, 3Biochemistry Center Regensburg (BZR), Laboratory for RNA Biology, Regensburg, Germany
⁴Helmholtz Zentrum München, Institut für Humangenetik, München, Germany
⁵Ludwig Maximilian University of Munich, Medizinische Klinik und Poliklinik I, München, Germany
⁶DZHK (German Center for Cardiovascular Research) Partner Site, München, Germany

Rationale: Cardiac macrophages (cMP) are increasingly recognized as important regulators of myocardial homeostasis and disease, yet the role of noncoding RNA in these cells is largely unknown. Small RNA sequencing of the entire miRNomes of the major cardiac cell fractions revealed microRNA-21 (miR-21) as the single highest expressed microRNA in cMPs, both in health and disease (25 and 43% of all microRNA reads respectively). MiR-21 has been previously reported as a key microRNA driving tissue fibrosis.

Objective: To determine the function of macrophage miR-21 on myocardial homeostasis and disease-associated remodeling.

Methods and results: Mice with macrophage-specific (Cx3cr1-Cre-mediated) genetic deletion of miR-21 were protected from interstitial fibrosis and cardiac dysfunction when subjected to pressure overload of the left ventricle. Single cell sequencing of pressure-overloaded hearts from these mice revealed that miR-21 in macrophages is essential for their polarization towards a M1-like phenotype. Systematic quantification of intercellular communication mediated by ligand-receptor interactions across all cell types revealed that miR-21 primarily determined macrophage-fibroblast communication, promoting the transition from quiescent fibroblasts to myofibroblasts. Polarization of isolated macrophages *in vitro* towards a pro-inflammatory (M1) phenotype activated myofibroblast transdifferentiation of cardiac fibroblasts in a paracrine manner and was dependent on the rapid induction of miR-21 in cMPs.

Conclusions: Our data indicate a critical role of cMPs in pressure overload-induced cardiac fibrosis and dysfunction and reveal macrophage miR-21 as a key molecule for the pro-fibrotic role of cMPs.

15

Chronic effects of Hydroxychloroquine and Azithromycin on iPS cell-derived Cardiomyocytes: Cautions for COVID-19 patients treatment

W. Li¹, X. Luo¹, M. Poetsch¹, K. Nichani², M. Schneider², K. Hettwer², R. Oertel³, M. Hasse¹, R. P. Steiner¹, A. Strano¹, S. Uhlig², K. Simon², **M. Schubert**¹, K. Guan¹

¹Institute of Pharmacology and Toxicology, TUD, Dresden, Germany
²QuoData GmbH, Dresden, Germany
³Institute of Clinical Pharmacology TUD, Dresden, Germany

Severe acute respiratory syndrome coronavirus 2 (SARS-CoV-2) caused a still ongoing global pandemic. Despite known adverse effects of hydroxychloroquine (HCQ) and azithromycin (AZM) on cardiac function, HCQ and AZM have been used as a combination therapy in the treatment of SARS-CoV-2 infected COVID-19 patients. Indeed, recent clinical data indicate higher complication rates with HCQ/AZM combination treatment in comparison to monotherapy. In this study, we used human induced pluripotent stem cell-

derived cardiomyocytes (iPSC-CMs) to investigate the effects of HCQ and AZM on cardiomyocytes. In line with the clinically recognized side-effects of QT prolongation through treatment with HCQ and/or AZM, we revealed the prolongation of corrected field potential duration using multi-electrode array readouts. Furthermore, we demonstrate that treatment with HCQ and AZM in combination leads to higher cardiotoxicity, lower cell viability, structural disarrangement, as well as more pronounced contractile dysfunctions, and conduction velocity (CV) increment, compared to HCQ or AZM alone. We provide the first mechanistic insights for the increase in CV, demonstrating that HCQ and AZM strongly increased connexin 43 and slightly increased Nav1.5 protein levels in a synergistic manner. Taken together, our results underline strong cardiac adverse effects induced by the combined treatment of HCQ and AZM, which rise cautions for physicians to treat COVID-19 patients.

16

Genetic deconvolution in combination with AGO2-immunoprecipitation identifies the cellular and molecular mechanism of anti-miR-21 treatment in a failing myocardium.

C. Beck^{1,2}, D. P. Ramanujam^{1,2}, A. P. Schön^{1,2}, S. Engelhardt^{1,2}

¹Technical University of Munich, Institute for Pharmacology and Toxicology, München, Germany

²DZHK (German Center for Cardiovascular Research) Partner Site, München, Germany

MicroRNA-21 (miR-21) is one of the most prominently expressed microRNAs in the mammalian heart and strongly upregulated in failing myocardium. In vivo silencing of miR-21 using a synthetic inhibitor (anti-miR-21) attenuates cardiac dysfunction. Despite the known therapeutic effect of anti-miR-21 in the heart, the exact mechanism, i.e. the regulated targetome of miR-21, is only poorly understood. MicroRNAs are associated with Argonaute proteins enabling them to base pair with complementary target mRNAs. Based on complementarity translational repression or silencing of the target mRNAs is mediated. Using Argonaute2-ribonucleoprotein immunoprecipitation (AGO2-RIP) in the presence of anti-miR-21 followed by next generation RNA sequencing (Werfel et al. Nucl Acids Res 2017) allows us to identify high affinity and highly regulated target mRNAs of miR-21.

In our approach, we used 8 weeks-old mice subjected to a model of pressure overload-induced cardiac hypertrophy, and anti-miR-21 was injected intravenously for three consecutive days two weeks after surgery. Two days later, an AGO2-RIP was either performed from the total heart or from the four main cardiac cell types (myocytes, fibroblasts, macrophages or endothelial cells). Next generation sequencing of the AGO2-immunoprecipitated mRNA and total RNA identified the most de-enriched (RIP fold change) and most de-repressed targets (mRNA fold change) in the anti-miR-21-treated group compared to the control group for the distinct cardiac cell types. In addition, single cell sequencing was used to deconvolve bulk RNA sequencing data from the total heart to estimate cell type composition and their corresponding cell-type specific gene expression profile under treated and untreated condition.

Combining this bioinformatic and biochemical approach – genetic deconvolution and AGO2-RIP – allowed us to define the cell-type specific regulated targetome of a microRNA upon therapeutic manipulation. Our data on miR-21 identified the particular cardiac cell types, where anti-miR-21 takes its full pharmaceutical effect and elucidated the cell-cell crosstalk upon anti-miR-21 treatment within the heart.

Our genetic deconvolution and AGO2-RIP approach should be applicable to the analysis of any microRNA therapeutic intervention in the heart.

17

Remdesivir modulates the metabolism of cardiac cells.

K. Merches¹, V. Bätz¹, J. Fender¹, L. Breunig¹, Y. Reinders², A. Sickmann², K. Lorenz^{1,2}

¹University of Würzburg, Institute for Pharmacology and Toxicology, Würzburg, Germany

²Leibniz Institute for Analytical Sciences – ISAS e.V., Dortmund, Germany

Remdesivir (RDV) is the only approved drug against COVID-19 with a compassionate use authorization in the USA and a conditional marketing authorization in Japan and the EU. While the efficacy is still controversially discussed, concerns about its toxicity were risen. Cardiotoxicity and nephrotoxicity were suggested as potential adverse outcomes due to non-significant observations in patients. Therefore, the application of RDV was limited to severe cases with normal nephrological function. Since now, no epidemiologic evidence for RDV's toxicity in humans is evident and studies are pending. We aimed to extend the knowledge about potential mechanisms behind assumed toxic effects of RDV on heart and kidney.

By an *in vitro* approach we tested the cytotoxic effects of remdesivir on cardiac cells. Rat H9c2 cardiomyoblasts and mouse neonatal cardiomyocytes (NMCM) were screened for effects of RDV on viability and metabolism. Functionality was assessed by impedance measurements of NMCM and proliferation assays of H9c2 cells. In order to test if a simultaneous infection with the RNA Virus SARS-Cov-2 can alter the effects of RDV, we simulated an infection *in vitro* in NMCM. Thus, imiquimod was used to stimulate the RNA receptor Toll-like-receptor 7, which leads to cytokine expression by NMCM.

Remdesivir decreased intracellular ATP-levels in both H9c2 and NMCM at concentrations over 12 µM after 24 h of treatment. Lactate secretion was increased after 0.8 µM RDV treatment in both cell types, while lactate-dehydrogenase (LDH)-release assays did not reveal cell damage after up to 50 µM of RDV treatment for 72 hours. The impedance of NMCM monolayers was decreased by 6.25 µM of RDV after 24 hours, while the beat rate was not affected. H9c2 cells were impaired in proliferation. A simulation of a viral infection with TLR7-ligand imiquimod did not render NMCM more sensitive to RDV.

In conclusion, our results indicate that remdesivir alters the metabolism of H9c2 and NMCM at clinically relevant concentrations and might impair cell effector function. Currently, we assess similar endpoints in kidney cells. RDV is a prodrug of a nucleoside analogue, which might interfere with ATP-dependent metabolic regulators. Therefore, we are currently performing detailed analyses of mitochondrial and glycolytic activity after RDV-treatment as well as proteomic analysis to further reveal its toxicological mechanism

18

Method of Transverse Aortic Constriction in mice with reduced variability of the aortic peak pressure gradient

L. A. A. Neves¹, T. Martinez¹, A. Isbatan², S. A. K. Chowdhury³, P. Senese⁴, M. R.

Gralinski⁴, F. J. Hock⁵

¹CorDynamics, Chicago, United States

²University of Illinois at Chicago, Cardiovascular Research Core, College of Medicine, Chicago, United States

³University of Illinois at Chicago, Physiology and Biophysics, Chicago, United States

⁴CorDynamics, Chicago, United States

⁵CorDynamics, Dieburg, Germany

Introduction: Transverse aortic constriction (TAC), a common chronic pressure overload model, is a useful tool to study the effectiveness of emerging drug therapy against the progression of cardiac dysfunction. A 27G needle is usually selected to induce TAC; however, variability in the generated pressure gradient and, consequently, disease progression is frequently a problem.

Objective: This study assessed whether measuring the aorta diameter at the time of surgery and applying 65-70% constriction would decrease model variability and provide a gradual time course in the development of heart failure.

Materials and Methods: C57BL/6NcrJ mice (23.7-26.1 g) underwent TAC (n=6-7) or Sham (n=4) surgery. The transverse aorta diameter was determined at the time of surgery using a divider/caliper. For TAC animals, a ligature was tightly tied around the transverse aorta against hypodermic tubing. TAC animals were divided into 2 groups: TAC using 27G tubing (Gr1) or TAC using a tubing diameter selected to induce 65%-70% constriction (Gr2). Echocardiography was performed at 1-, 4-, 6- and 8-weeks post-surgery. Hearts and lungs were harvested at 8-weeks post-surgery and weighed.

Results: Aortic constriction was confirmed by a significant increase in the pressure gradient for Gr1 (39 to 119 mmHg; p=0.0005) and Gr2 (51 to 73 mmHg; p=0.0005) vs Sham (2.3 to 3.6 mmHg). Variance in Gr1 pressure gradient was significantly greater than in Gr2 (F=12.9; p=0.007). Morphological changes in both TAC groups were associated with concentric remodeling at Week 1 (LV mass [mg]: 138±37 in Gr1 [p=0.09] and 125±34 [p=0.11] in Gr2 vs 78±15 in Sham; RWT: 0.57±0.04 in Gr1 [p=0.002] and 0.42±0.05 in Gr2 [p=0.04] vs 0.31±0.05 in Sham) that progressed to eccentric hypertrophy by Week 8 (LV mass [mg]: 302±134 in Gr1 [p=0.04] and 252±105 in Gr2 [p=0.07]) vs 95±17 in Sham; RWT: 0.43±0.02 in Gr1 [p=0.42] and 0.43±0.07 in Gr2 [p=0.23] vs 0.36±0.05 in Sham). Systolic dysfunction was also observed at 8-weeks post-TAC as indicated by decreased LVEF (%; 20±10 in Gr1 [p=0.02] and 26±11 [p=0.03] in Gr2 vs 45±7 in Sham).

Conclusion: These results showed that when the degree of constriction is determined based on aorta diameter obtained during surgery, variability of the pressure gradient is reduced post-TAC.

Pharmacology – Cancer pharmacology and treatment

19

Synergism of the metabolic inhibitor CPI-613 and genotoxic chemotherapeutics in colorectal cancer therapy through a p53-independent mitochondrial apoptosis pathway

C. Neitzel^{1,2,3}, P. Demuth¹, N. Seiwert^{1,2,3}, B. Rasenberger², M. Christmann², K. Boengler⁴,

D. Vogel⁵, M. Huber⁵, M. Linnebacher⁶, J. Fahrer^{1,2,3}

¹Technical University of Kaiserslautern, Division of Food Chemistry and Toxicology, Department of Chemistry, Kaiserslautern, Germany

²University Medical Center, Department of Toxicology, Mainz, Germany

³Justus Liebig University Giessen, Rudolf Buchheim Institute of Pharmacology, Gießen, Germany

⁴Justus Liebig University Giessen, Institute for Physiology, Faculty of Medicine, Gießen, Germany

⁵University of Marburg, Institute for Medical Microbiology and Hospital Hygiene, Marburg, Germany

⁶University of Rostock, Division of Molecular Oncology and Immunotherapy, Department of General Surgery, Rostock, Germany

Introduction: Colorectal cancer (CRC) is the third most prevalent type of cancer worldwide, with an increasing incidence especially in newly developed countries. Despite diverse therapeutic options, long-term survival rates of advanced CRC are still low. Considering the necessity of new therapeutic approaches, the deregulated metabolism of cancer cells may provide a novel target for CRC treatment in the future.

Objectives: In the following study, the anticancer activity of pyruvate- and α-ketoglutarate dehydrogenase inhibitor CPI-613 was examined as a single treatment option and in combination with antineoplastic drugs to assess synergistic effects and underlying mechanisms.

Materials & methods: In order to evaluate the synergistic cytotoxicity of CPI-613 in combination with 5-Fluorouracil (5-FU) and Irinotecan (IT), several established and patient derived CRC cell lines as well as non-transformed human colonic epithelial cells (HCEC) were utilized. Live-cell metabolic assays, confocal microscopy, cell death and autophagy measurements by flow cytometry, Western Blot and gene expression analysis were performed to further elucidate the underlying toxicity mechanism. The therapeutic efficacy and anti-tumor activity of CPI-613 in a combination regimen with IT or as a single agent were investigated in a xenograft-mouse model, applying the CRC cell lines HCT116 and HT29.

Results: *In vitro* screening of CPI-613 as well as co-treatment with 5-FU and IT revealed cancer cell selective cytotoxic activity independent of mutational status in CRC cell lines and synergism with chemotherapeutics. Underlying mechanisms include disruption of mitochondrial respiration and membrane potential, downregulation of anti-apoptotic Bcl-xL and survivin as well as cyclins B1 and H, suppression of autophagy and blockage of DNA-damage induced p53 stabilization. Anti-tumor activity of CPI-613 and synergism with IT were confirmed in xenograft-mouse models and led to prolonged survival and enhanced therapeutic efficacy. In accordance with our *in vitro* findings, CPI-613 impeded IT-induced p53 stabilization, phosphorylation of histone H2AX and formation of the autophagy marker LC3B-II in tumor xenografts.

Conclusion: Based on its synergism with established anticancer drugs, CPI-613 revealed to be a potential addition in the therapy regimen of CRC. Our study indicates p53-independent modulation of the mitochondrial apoptosis pathway and autophagy suppression as possible mechanisms.

20

Inhibition of HER receptors reveals distinct mechanisms of compensatory upregulation of other HER family members: basis for acquired resistance to targeted cancer therapeutics and for combination therapy

D. Gutsch¹, R. Jenke¹, T. Büch¹, A. Aigner¹

¹University of Leipzig, Rudolf-Boehm-Institute for Pharmacology and Toxicology, Clinical Pharmacology, Leipzig, Germany

Introduction: Overexpression of members of the HER/erbB tyrosine kinase family like HER2/erbB2/neu is associated with various cancers. Some heterodimers, esp. HER2/HER3 heterodimers, are particularly potent inducers of oncogenic signaling. Still, from a clinical viewpoint their inhibition has yielded only moderate success so far, despite promising data from cell culture. This suggests acquired resistance upon inhibitor therapy as one putative issue, requiring further studies in cell culture also aiming at rational combination therapies.

Objectives: To elucidate molecular effects upon targeted inhibition or knockdown of individual HER receptors in ovarian and breast carcinoma cells *in vitro*, as basis for rational combination therapies *in vivo*.

Methods: Cell lines were treated with siRNAs for HER2 or HER3 gene knockdown, or with specific inhibitors. Alterations in the expression of HER family members were determined on the mRNA and protein level. Biological effects of single or combination therapies were studied in various cell culture assays (anchorage-dependent/-independent proliferation, apoptosis) as well as in an *s.c.* tumor xenograft therapy study in mice, upon treatment with siRNAs formulated in polymeric, PEI-based nanoparticles.

Results: We demonstrate in mammary and in ovarian carcinoma cells that the RNAi-mediated single knockdown of HER2 or HER3 leads to the rapid counter-upregulation of the respective other HER family member, thus providing a rational basis for combinatorial inhibition. Concomitantly, combined knockdown of HER2/HER3 exerts stronger anti-tumor effects as compared to single inhibition. In a tumor xenograft mouse model, therapeutic intervention with nanoscale complexes based on polyethylenimine (PEI) for siRNA delivery, again reveals HER3 upregulation upon HER2 single knockdown and a therapeutic benefit from combination therapy. On the mechanistic side, we demonstrate that HER2 knockdown or inhibition reduces miR-143 levels with subsequent de-repression of HER3 expression, and validate HER3 as a direct target of miR-143. HER3 knockdown or inhibition, in turn, increases HER2 expression through the upregulation of the transcriptional regulator SATB1.

Conclusions: We describe counter-upregulation processes of HER family members upon targeted inhibition, which are based on distinct molecular mechanisms. This may provide the basis for the rational combination of inhibitors in tumor therapy.

21

Role of RNA-binding proteins ZFP36L1 and ZFP36L2 and their targets in chronic myeloid leukemia: Implications on TKI resistance

M. Dworschak¹, M. Kähler¹, I. Cascorbi¹, I. Nagel^{1,2}

¹Institute of Experimental and Clinical Pharmacology, University Hospital Schleswig-Holstein Kiel, Kiel, Germany

²Institute of Human Genetics, University Hospital Schleswig-Holstein Kiel, Kiel, Germany

Question: The mRNA binding proteins ZFP36L1 and ZFP36L2 have been described to play an important role in hematopoiesis and cell quiescence, being primarily discussed as potential tumor suppressors. In an imatinib (IM)-resistant chronic myeloid leukemia (CML) cell model, elevated levels of ZFP36L1 and ZFP36L2 were detected. Using CRISPR/Cas9-genome editing to develop ZFP36L1 and ZFP36L2 knockout cell lines, we performed genome wide expression analysis in order to find potential target genes.

Further, we analyzed differences in cell proliferation and apoptosis between ZFP36L1 and ZFP36L2 knockout and wild-type cells.

Methods: ZFP36L1/ZFP36L2 single and double knockout K-562 CML cells were generated by CRISPR/Cas9-genome editing. Genome-wide expression data was analyzed with Transcriptome Analysis Console (TAC) Software. mRNA and protein levels were analyzed using RT-qPCR and immunoblotting. Further, proliferation and apoptosis were investigated by cell counting experiments, BrdU- and Caspase9-assays in treatment-naïve cells, as well as in response to IM treatment. In addition, we verified the binding of ZFP36L1 to the CDKN1A 3' untranslated region (3'UTR) performing luciferase reporter gene assays.

Results: Total cell number was reduced in all knockout cell lines compared to wild-type cells, while altered proliferation could not be detected. During the development of IM-resistance, BrdU incorporation was significantly reduced in ZFP36L1 knockout (p<0.01) and double knockout (p<0.05) cell lines. Genome-wide expression analysis of ZFP36L1 knockout cells revealed differential expression of cell cycle regulators, i.e. CCND1 (FC 4.23, p=0.0047), CCND3 (FC 3.55, p=2.02E-06) and CDKN1A (p21) (FC 4.92, p=3.81E-09), compared to wild-type cells. We further showed the direct binding of ZFP36L1 to CDKN1A 3' UTR, leading to its destabilization and degradation.

Conclusions: In summary, the ZFP36L1 and ZFP36L2 single and double knockout led to decreased proliferation of K-562-cells, both in the presence and absence of IM. Further, we were able to show the direct downregulation of CDKN1A, known as a cell cycle inhibitor, by ZFP36L1. These data suggest that the mRNA destabilizing protein ZFP36L1 cannot be generalized as tumor suppressor, but is potentially involved in the cellular response to IM treatment.

22

Comparative study on the time-dependent induction and removal of nitrogen mustard-induced DNA damage in different human cells using a combination of the rFADU assay and LC-MS/MS analysis

S. Krassnig¹, A. Mangerich¹, A. Bürkle¹

¹University of Konstanz, Biology / Molecular Toxicology, Konstanz, Germany

Nitrogen mustards (NM) are highly reactive bifunctional alkylating agents. They can form DNA interstrand crosslinks (ICLs), which cause a block of DNA strand separation, inhibiting essential processes in DNA metabolism (e.g., replication and transcription). In fast replicating cells, e.g., tumour cells, this can lead to the induction of cell death. The upregulation of ICL repair is thought to be a key factor for the resistance of tumour cells to ICL-inducing cytostatic agents, such as NMs.

To monitor the induction and repair of NM-induced ICLs, we used the automated reversed fluorometric analysis of alkaline DNA unwinding (rFADU) assay. For the additional detection of monoalkylated DNA bases, we developed an LC-MS/MS method based on a previously developed mass spectrometric platform for the quantitation of sulfur mustard-induced DNA adducts [1].

We performed a comparative analysis of adduct formation and removal, which is suggestive of DNA repair processes in a series of different human cell lines and PBMCs after treatment with HN2 and chlorambucil. Dose-dependent increases in adduct-formation were observed and suitable treatment concentrations were identified for each drug-cell line combination, which was then used for subsequent experiments to monitor the kinetics of the adduct formation. We revealed significant differences in the repair kinetics of the cell lines tested. For example, in U2OS cells and in hTERT immortalized RPE-1 cells, time-dependent repair of the monoalkylated DNA-adducts was confirmed. Regarding ICLs, repair was only observed in PBMCs and in the hTERT immortalized human podocytes, but not in HaCaT, A2780, hTERT immortalized RPE-1, and VH10 cells.

In conclusion, the combination of the rFADU technique and LC-MS/MS analyses represent powerful tools to study the molecular mechanisms of NM-induced DNA damage and repair. By applying those methods to a spectrum of human cell lines of different origin and transformation status, we obtained novel insight into the cell-type specific repair of different DNA lesions formed after treatment with NMs, which may help identify novel resistance mechanisms of tumours and to define molecular targets for therapeutic interventions.

[1] Zubeil T., et al. (2019), A mass spectrometric platform for the quantitation of sulfur mustard-induced nucleic acid adducts as mechanistically relevant biomarkers of exposure, Archives of Toxicology, 93(1), 61-79.

23

miRNA-506 replacement inhibits pancreatic cancer cells by affecting cell cycle progression, autophagy and apoptosis *in vitro* and *in vivo*

H. Borchardt¹, M. Morawski², A. Aigner¹

¹Rudolf Boehm Institute of Pharmacology and Toxicology, Clinical Pharmacology, Leipzig, Germany

²Paul Flechsig Institute of Brain Research, Leipzig, Germany

Questions: The therapeutic replacement of miRNAs pathologically downregulated in tumors, including pancreatic cancer, may represent promising treatment options. Due to the poor prognosis of pancreatic cancer, with a 5-year survival rate of only ~ 9%, novel targets or treatment options are urgently needed. In this study, we comprehensively

analyze the effect of miR-506-3p replacement on pancreatic cancer cell lines *in vitro* and in a mouse tumor model *in vivo*.

Materials & Methods: Transfection of miR-506-3p was used to target different pathways in various cell lines. Effects of transient miRNA transfection were analyzed on the molecular and cellular level, including proliferation (CCK-8), apoptosis and autophagy (caspase-3/7 activity-assay, flow cytometry), cell cycle distribution (flow cytometry) and protein deregulation (Western blot). Switching to a more relevant *in vivo* situation, tumor xenograft-bearing mice were treated with polymeric nanoparticles containing miR-506-3p or negative control miRNA (NC1). Xenografts were analyzed for tumor growth and for gene expression on the protein level / by immunohistochemistry.

Results: Transient transfection of miR-506-3p led to profoundly reduced cell viability. This was based on the induction of apoptosis and autophagy as well as decreased cell cycle progression. Concomitantly, an activation of caspase-3/7 and increase of the autophagic membrane associated LC3B-II protein were found. The miR-506-3p mediated downregulation of CDK6 and upregulation of p21 also led to cell arrest in G1- and S-phase of the cell cycle. In addition, the oncogenic transcriptional regulator MYC, regulated by CDK4/6, as well as the pro-survival factor survivin were found downregulated. By using xenograft bearing mice, a clinically more relevant *in vivo* situation was created to evaluate the efficacy of a polymeric nanoparticle formulation for miR-506 replacement. The data showed a reduction in tumor growth and increased necrotic areas of the tumor. Furthermore, immunohistochemistry revealed the reduction of the proliferation factor Ki-67, downregulation of the oncogenes MYC and survivin, and an increase in the marker of autophagosomes, LC3B.

Conclusion: The micro-RNA miR-506-3p exerts multiple anti-tumorigenic effects in pancreatic cancer cells, *in vitro* and *in vivo*. We identify the nanoparticle-based miR-506-3p replacement therapy as an effective and powerful strategy against pancreatic cancer.

24

Chemical ER stress inhibits replication of three human coronaviruses in cultured cells

M. S. Shaban¹, C. Müller², C. Mayr-Buro¹, H. Weiser¹, B. V. Albert¹, A. Weber¹, U. Linne³, N. Karf⁴, M. L. Schmitz⁵, J. Ziebuhr², M. Kracht¹
¹RBI-JLU, Gießen, Germany
²Institute of Medical Virology, Gießen, Germany
³Mass spectrometry facility of the Department of Chemistry, Marburg, Germany
⁴Institute of Biochemistry, Gießen, Germany
⁵German Center for Lung Research (DZL) and Universities of Giessen and Marburg Lung Center (UGMLC), Gießen, Germany

Objectives: Coronaviruses are RNA viruses with large genomes that infect a broad range of species, including humans. The four "common" human CoV (HCoV-229E, -NL63, -HKU1, -OC43) cause a spectrum of mild symptoms mostly limited to the upper respiratory tract. The three highly pathogenic CoV, severe acute respiratory syndrome (SARS) CoV 1 and 2 and middle east respiratory syndrome CoV (MERS-CoV) cause significant disease burden and mortality. We found that CoVs strongly activate the ER stress protein kinase PERK that is well known to confer translational suppression. This prompted a large study to reveal the role of ER stress for CoV replication and the host response. Here, we provide evidence that pharmacological reprogramming of ER stress pathways can be exploited to suppress CoV replication.

Methods: To investigate the role(s) of chemically-induced ER stress for CoV replication, we used several types of model systems, including Huh7, MRC-5 and Vero6 cell lines. The cells were infected with HCoV-229E, MERS-CoV or SARS-CoV-2 in the presence or absence of the ER stress trigger thapsigargin. Expression of viral or host proteins or mRNAs were examined using cell lysates for immunoblotting, mass spectrometry or RT-qPCR. In parallel, the supernatants were used for ELISA assays and plaque assays. Immunofluorescence assays were utilized to visualize subcellular sites of viral replication. Proteomic analyses were performed to globally uncover virus and thapsigargin-regulated components, pathways and protein networks.

Results: We found that thapsigargin efficiently inhibits replication of all three CoV in different cell types in the lower nM range with favorable selectivity indices (SI, CC50/EC50 >50). Mechanistically, the compound partially restores virus-induced translational shut-down and counteracts the CoV-mediated downregulation of IRE1 α and the ER chaperone BiP. The proteome-wide data sets further revealed multiple upregulated factors that are likely to contribute to the thapsigargin-induced antiviral state, including HERPUD1, an essential factor of ER quality control and ER-associated protein degradation complexes and p62/SQSM1, a regulator of selective autophagy.

Conclusion: The data show that thapsigargin hits a central mechanism required for CoV replication, suggesting that thapsigargin (or derivatives thereof) may be developed into broad spectrum of anti-CoV drugs.

Pharmacology – Disease models – drug development I

25

The SARS-CoV-2 main protease M^{pro} causes microvascular brain pathology by cleaving NEMO in brain endothelial cells

J. Wenzel¹, J. Lampe¹, H. Müller-Fielitz¹, K. Müller¹, R. Schuster¹, M. Zille¹, L. Zhang², M. Krohn¹, V. Neve¹, H. Altmeyden³, F. Sauve⁴, M. Pasparakis⁵, V. Prevot⁴, R. Hilgenfeld², M. Glatzel³, M. Schwaninger¹

¹University of Lübeck, Institute of Experimental and Clinical Pharmacology and Toxicology, Lübeck, Germany

²University of Lübeck, Institute of Biochemistry, Lübeck, Germany

³University Medical Center Hamburg-Eppendorf, Institute of Neuropathology, Hamburg, Germany

⁴University of Lille, Laboratory of Development and Plasticity of the Neuroendocrine Brain, Neuroscience & Cognition, Lille, France

⁵University of Cologne, Institute for Genetics, Cologne, Germany

Several lines of evidence suggest that neurological symptoms in COVID-19 patients are partially due to damage to small vessels. However, the potential mechanisms are unclear. Here, we show that brain endothelial cells express SARS-CoV-2 receptors. The main protease of SARS-CoV-2 (M^{pro}) cleaves NEMO, the essential modulator of NF- κ B signaling. By ablating NEMO, M^{pro} induces the death of human brain endothelial cells and microvascular pathology in mice that is similar to what we find in the brain of COVID-19 patients. Importantly, the inhibition of receptor-interacting protein kinase (RIPK) 3, a mediator of regulated cell death, blocks the vessel rarefaction and disruption of the blood-brain barrier due to NEMO ablation. Our data suggest RIPK as a therapeutic target to treat the neuropathology of COVID-19.

26

Human engineered heart tissue transplantation in a chronic myocardial injury model

C. von Bibra¹, A. Shibamiya¹, B. Geertz¹, E. Querdel¹, B. Hiebl², T. Eschenhagen¹, F. Weinberger¹

¹Medical Center Hamburg-Eppendorf (UKE), Institute for Experimental Pharmacology and Toxicology, Hamburg, Germany

²University of Veterinary Medicine Hannover, Laboratory Animal Science, Hannover, Germany

Introduction: Myocardial injury leads to an irreversible loss of cardiomyocytes (CM) which is replaced by fibrotic tissue. The implantation of human engineered heart tissue (EHT) has become a promising therapeutic approach to regenerate the heart after myocardial injury. Previous studies exhibited beneficial effects of human induced pluripotent stem cell (hiPSC)-derived CM transplantation in a guinea pig model in the subacute period of myocardial infarction. From a clinical standpoint it is worthwhile to explore the ability to repair myocardial function in the chronic stage of myocardial injury.

Methods: Human EHTs were generated from hiPSC-derived CMs (15x10⁶ cells). Myocardial cryoinjury was induced in guinea pigs. EHT patches were implanted epicardially four weeks after injury. Control animals received cell-free patches. Animals were sacrificed after a follow-up period of four weeks and hearts were harvested for histological analysis. Cardiac function was evaluated by serial echocardiography.

Results: Hearts revealed large transmural myocardial injuries amounting to 26% of the left ventricle. EHT recipient hearts demonstrated compact muscle islands of human origin in the scar region, as indicated by a positive staining for human Ku80 and dystrophin, remuscularizing 5% of the scar area. Grafts were vascularized by host derived endothelial vessels. Immunostaining showed that human CMs had developed immature but readily identifiable sarcomeres. Echocardiography analysis demonstrated no significant difference between animals that received EHT patches and animals in the control group (Fractional area change 36% vs. 34%).

Discussion: The present study evaluated the effect of EHT patch transplantation in a chronic myocardial injury model. EHT patches engrafted in the chronically injured heart but human grafts were smaller than after transplantation in a subacute model, indicating that the chronically scarred heart represents a more hostile environment for cell engraftment. In contrast to the subacute model, EHT patch transplantation did not improve left ventricular function, highlighting the difficulties for a regenerative approach.

27

Cardiac fibroblasts follow their individual program in 3D cultures

A. DeGrave^{1,2}, S. Al Disi^{1,3}, S. Weinbrenner¹, D. Maestro Lavin⁴, G. L. Santos^{1,2}, S. Lutz^{1,2}

¹University Medical Center Göttingen, Institute of Pharmacology and Toxicology, Göttingen, Germany

²DZHK (German Center for Cardiovascular Research) Partner Site, Göttingen, Germany

³University of Edinburgh, Edinburgh, United Kingdom

⁴University of Cantabria, Institute of Biomedicine and Biotechnology of Cantabria, Santander, Spain

Background: Understanding the behavior of cardiac fibroblasts is crucial for the development of anti-fibrotic drugs, however, use of *in vivo* and 2D models has limitations. Bridging the gap, 3D-human engineered connective tissues (ECT) allow for the analysis of various parameters without paracrine influences in a 3D context.

Methods: Human primary cardiac fibroblasts (hCF) and foreskin fibroblasts (hFF) were used for 2D-proliferation analysis by automated nuclei counting. Cell sizes were determined by electric current exclusion. ECT formed by 7.5 x 10⁵ cells and collagen were casted in a multi-well plate equipped with two flexible poles and cultured for up to 20 days. Contraction and compaction of 5 ng/mL TGF β -treated and control ECT were assessed respectively by pole deflection and cross-sectional area analysis. qPCR was performed for isolated ECT RNA.

Results: By comparing cell size with proliferation rate of 2D-cultured hCF from 3 male donors and analyzing ECT behavior over 5 days, we demonstrate that smaller cells proliferate faster, show higher contraction forces in 3D, and enhance ECT compaction. hCF from 2 female donors showed similar results, although overall activity seemed to be lower than of male cells. The contraction of all ECT plateaued after 3-4 days. Therefore, we cultured the ECT for up to 20 days to investigate a potential phenotypic steady state of the embedded cells. Only ECT with more active hCF displayed a second phase of contraction after the plateau. To test if this is a feature of active hCF, ECT were prepared with fast proliferating hFF. An opposite contraction behavior was shown with ECT relaxing and disintegrating over time after reaching maximum contraction. Treatment with pro-fibrotic TGF β from day 0 caused ECT to increase contraction by 2-fold within the first 3-4 days and had no effect on the time needed to reach the plateau, the plateau length, and the steepness of the second contraction. If applied from day 6, ECT contraction doubled within the next 6 days and showed the same dynamics as the controls. Lastly, regulation dynamics of typical genes involved in fibrosis, COL1A1, LUM, and THBS1, was analyzed in ECT. The latter two genes showed a similar time-dependent regulation as seen for ECT contraction.

Conclusion: Our data argues that 3D-cultured hCF follow an intrinsic program which is strongly dependent on their initial phenotypic state. For successful drug screening, individual as well as sex-specific differences must be considered.

28

Single cell sequencing of failing myocardium identifies lncRNA *Schlafenlnc* as a regulator of cardiac resident macrophage function

A. Dueck^{1,2}, D. Esfandyari^{1,2}, L. Althaus^{1,2}, K. Heise^{1,2}, S. Baygün³, D. P. Ramanujam^{1,2}, M. Schmidt-Suppran³, L. Maegdefessel^{2,4}, S. Engelhardt^{1,2}

¹Technical University of Munich, Institute of Pharmacology and Toxicology, München, Germany

²German Centre for Cardiovascular Research, Munich Heart Alliance, München, Germany

³Technical University of Munich, Immunopathology and Signal Transduction, München, Germany

⁴Technical University of Munich, Vascular Biology, München, Germany

Cardiac resident macrophages (MPs) are important regulators within the heart and recently shown to take part in cardiac conduction and hypertrophy. Since the underlying molecular mechanism are not yet known, we wanted to understand whether long non-coding RNAs (lncRNAs) play important roles within these immune cells.

We employed deep RNASeq (>100 million reads/sample) of purified murine cardiac MPs and single cell sequencing (scSeq) of over 30,000 cells (total myocardial cells and purified leukocyte fraction) to characterize cardiac MPs.

First, we could show that lncRNAs are of general importance for defining cell types by re-clustering analyses of our scSeq data. Using different gene sets as input, we could show that lncRNA genes improve clustering sensitivity not only as a whole group, but already by using only a few lncRNAs ($p < 0.05$). Next, using our in-depth RNASeq data, we could define the entire lncRNome of cardiac MPs from healthy and diseased murine myocardium (pressure-overload to the left ventricle). In total, we uncovered a set of 56 lncRNAs highly enriched (fold change >10) in cardiac MPs and 36 lncRNAs also deregulated during disease ($p < 0.05$). Integrating scSeq and RNASeq expression data as well as the de-regulation during disease yielded the lncRNA *Schlafenlnc* as the top candidate for further study.

Schlafenlnc is encoded within the Schlafen protein family locus, its proteins play important roles in immune cells such as differentiation, invasion and migration. We generated a *Schlafenlnc* knockout macrophage cell line using CRISPR/Cas9 and performed RNASeq of unstimulated, LPS-treated and IL4-treated *Schlafenlnc*-deficient MPs. We could show that – similarly to the function of some of the Schlafen proteins – *Schlafenlnc* impacted on genes implicated in differentiation and particularly migration. Most prominently, one gene of the matrix metalloproteinase family (degradation of extracellular matrix) was strongly down-regulated in *Schlafenlnc*-deficient cells. To validate this phenotype, we conducted different migration assays, which showed both a strongly decreased migration of *Schlafenlnc*-deficient cells in comparison to controls.

Taken together, our data establish the entire lncRNome in cardiac MPs, highlighting especially their importance for cell identity. The lncRNA *Schlafenlnc* was identified as a critical regulator of macrophage migratory functions and we could describe for the first time a function for a lncRNA in this exciting cell type.

29

Dysbiosis in experimental colitis is positively affected by the herbal preparation STW 5 (Iberogast)

M. T. Khayyal¹, S. S. Mohamed¹, N. F. Abdeltawab¹, R. M. Ammar², H. Abdel-Aziz²

¹Faculty of Pharmacy, Cairo University, Department of Pharmacology, Cairo, Egypt

²Bayer Consumer Health, Darmstadt, Germany

Aim: To study whether ulcerative colitis (UC) is associated with changes in intestinal microbiota and whether the effectiveness of STW 5 (Iberogast) in this condition is related to affecting such changes.

Methods: Ulcerative colitis (UC) was induced in rats by feeding them 5% dextran sodium sulphate (DSS) in drinking water for 7 days. Rats were treated concurrently with STW 5

and sacrificed 24 h later. Faecal samples were used to determine changes in relevant bacterial flora.

Results: Induction of UC led to dysbiosis and changes in the relative abundance of the gut microbiota exhibited by an increase in some Firmicutes genera, namely *Enterococcus*, and a decrease in others, namely *Blautia*, *Clostridium* and *Lactobacillus*. DSS further induced an increase in the abundance of *Bacteroidetes*, *Proteobacteria*, *Actinobacteria* and its genus *Bifidobacterium*. *Methanobrevibacter* levels were also increased. Microbial dysbiosis was associated with changes in parameters of colonic inflammation. STW 5 effectively guarded against these changes as well as against the changes in colonic indices, in inflammatory and apoptotic markers, and in any induced histological damage. Derangements in the microbial flora have largely contributed towards the development of DSS-induced colitis. These have been largely prevented by STW 5.

Conclusions: The findings suggest that the beneficial usefulness in UC may be attributed at least in part to ameliorating the prevalent dysbiosis.

Young Scientist Award

30

In vitro assessment of the structural elements of β -nitrostyrene responsible for its cytotoxic and genotoxic properties

J. Sündermann¹, A. Bitsch¹, S. M. Reamon-Büttner¹, H. Uphaus¹, M. Wehr¹, S. Wilde¹, C. Ziemann¹

¹Fraunhofer-Institut für Toxikologie und Experimentelle Medizin ITEM, Preclinical Pharmacology and Toxicology, Hannover, Germany

Over the last decades, the industrial chemical β -nitrostyrene (β -NS) has emerged as a potential new core-structure for anti-neoplastic drug development, since the compound exhibits strong anti-proliferative and pro-apoptotic potential, selectively in tumour cells. For risk assessment and future developments it is of utmost importance to discover and understand the underlying mechanisms and structural elements, being key for these observed effects.

Based on in silico similarity calculations, prediction of mutagenicity by QSAR-algorithms and literature data we selected nine structural derivatives of β -NS for further investigations. These were subsequently characterized regarding their (geno)toxic potential to finally determine underlying structure-activity relationships. Cytotoxicity (membrane damage; lactate dehydrogenase release assay) and genotoxicity (DNA strand breaks; alkaline comet assay) of the compounds were initially compared in L5178Y/TK⁺ mouse lymphoma cells after 1 – 4 h of incubation. Furthermore, induction of γ H2A.X (marker for DNA double-strand breaks) was immunocytochemically assessed in human WS1 fibroblasts and semi-automatically quantified using a Meta5 System (MetaSystem, Altusheim, Germany).

As chemical lead structure β -NS at 5 μ M mediated both a statistically significant cytotoxic (30 % of the Triton X-100 positive control) and clastogenic potential (tail intensity of 6.5 %), as compared to the vehicle control (0 % cytotoxicity; tail intensity of 1.5 %). These adverse biological effects were absent for structures with changes in the nitrovinyl-moiety like e.g. trans-cinnamic acid, but were enhanced by structures harboring an additional dioxole-group or nitro-group (e.g. 2-dinitrostyrene: 49 % cytotoxicity; tail intensity of 15.4 %). Interestingly, 2-methoxy-5-[(E)-2-nitroethenyl]phenol as a β -NS derivative, with hydroxy- and methoxy-groups did not induce an increase in γ H2A.X and thus DNA double-strand breaks, and thereby differs from the other compounds with a nitrovinyl-moiety.

In summary, the present study demonstrates that β -NS and its structural derivatives with a nitrovinyl-moiety possess a strong cyto- and genotoxic potential. Thus, the nitrovinyl-moiety seems to represent the activity determining structural element. Notably, even small changes in the core chemical structure of β -NS can have a major impact on mediated biological effects.

31

Validation of an animal replacement assay for in-vitro diagnostics of botulism in humans

M. Steinberg¹, L. V. Wilk¹, D. Stern¹, L. von Berg¹, S. Mahrhold², A. Rummel², U.

Messelhäußer³, M. Dörner¹, B. Dörner¹

¹Robert Koch Institute, Biological Toxins and Special Pathogens, Berlin, Germany

²Hannover Medical School, Institute for Toxicology, Hannover, Germany

³Bavarian Health and Food Safety Authority, Oberschleißheim, Germany

Introduction: Botulism is a rare and potentially fatal disease caused by botulinum neurotoxins (BoNTs), that are produced by Gram-positive, anaerobic, spore-forming bacteria of the genus *Clostridium*. BoNTs bind to specific receptors on the presynaptic membrane of the neuromuscular junction and are internalized into recycling endosomes. After translocation of the toxin's enzymatic subunit into the cytoplasm, it cleaves specific proteins of the SNARE-complex at positions unique for each BoNT-serotype. Five BoNT serotypes are known to cause botulism in humans (BoNT/A, B, E, F and HA). The serotypes can be further subdivided into more than 40 subtypes. The resulting within-serotype molecular variability heavily challenges BoNT detection. Until now, the gold standard for botulism diagnostics is still the mouse bioassay (MBA), which poses a heavy burden on the animal and is therefore ethically questionable.

Objectives: Previously, we established a prototype suspension array based on the Luminex® technology, which includes enrichment of the toxins via their receptor binding domain and subsequent detection of enzymatic activity using neopeptide-specific monoclonal antibodies. The aim of this work was to further develop this method to sensitively detect all BoNT sero- and subtypes pathogenic to humans in complex matrices (e.g. serum, food).

To this end the assay performance parameters based on two different toxin enrichment strategies – via monoclonal antibodies or via recombinant endogenous receptors – for BoNT/A and BoNT/B were determined: limit of blank (LoB), limit of detection (LoD) and quantifiable range.

Results: We could show that the new *in-vitro* assay was able to detect toxin concentrations down to 3 pg/ml BoNT/A1 and 1.2 pg/ml BoNT/B1 in buffer depending on the enrichment strategy. Quantification of BoNT/A1 was possible from 8 to 2000 pg/ml and for BoNT/B1 from LoD to 800 pg/ml. Therefore, the assay is able to detect toxin amounts equal or lower than the MBA. Ongoing work is addressing the comprehensive validation of the assay for BoNT/A and BoNT/B spiked into serum and food matrices.

Conclusion: In summary the here presented multiplex suspension array has the potential to replace the MBA for diagnostics of botulism in humans. The main advantage over other suggested replacement methods is that it is a robust, highly sensitive assay that can be performed with commonly available laboratory equipment ensuring a broad applicability in routine laboratories.

32

OCT1 of men and men: Differences in metformin and thiamine uptake – Structural causes and potential clinical consequences for hepatic metformin concentrations

M. J. Meyer¹, A. Tuerkova², S. Römer¹, C. Wenzel¹, T. Seitz², J. Gaedcke⁴, S. Oswald¹, J. Brockmöller³, B. Zdravil², M. V. Tzvetkov¹

¹University Medicine Greifswald, Institute of Pharmacology, C_DAT, Greifswald, Germany

²University of Vienna, Department of Pharmaceutical Chemistry, Wien, Austria

³University Medical Center Göttingen, Institute of Clinical Pharmacology, Göttingen, Germany

⁴University Medical Center Göttingen, Department of General, Visceral, and Pediatric Surgery, Göttingen, Germany

Metformin, the most commonly used oral antidiabetic drug, is a substrate of the hepatic uptake transporter OCT1 (gene name SLC22A1). OCT1 deficiency was shown to lead to more pronounced reductions of metformin concentrations in the mouse than in the human liver. Similarly, the effects of OCT1 deficiency on the pharmacokinetics of thiamine were reported to differ between human and mouse.

The aim of this study was to compare the uptake characteristics of metformin and thiamine between human and mouse OCT1 *in vitro* to explore underlying structural mechanisms causing differences in hepatic concentrations between humans and mice. Furthermore, we used the differences in uptake between human and mouse OCT1 as a tool to improve our understanding of the transport mechanism of OCT1.

To this end, we used HEK293 cells stably transfected to overexpress human or mouse OCT1 and targeted proteomics to scale up the results for human and mouse liver. The affinity for metformin of human OCT1 was 4.9-fold lower than that of mouse OCT1, resulting in a 6.5-fold lower intrinsic clearance. Using *in vitro* to *in vivo* extrapolation, the estimated liver-to-blood partition coefficient for metformin was only 3.34 in human compared with 14.4 in mouse and may contribute to higher hepatic concentrations in mice. Similarly, the affinity for thiamine of human OCT1 was 9.5-fold lower than that of mouse OCT1. Using HEK293 cells overexpressing human-mouse chimeric OCT1, we showed that simultaneous substitution of transmembrane helices TMH2 and TMH3 resulted in reversal of affinity for metformin. Using homology modeling, we suggested several structural explanations, of which a different interaction of leucine¹⁵⁵ in human TMH2 compared with the corresponding valine¹⁵⁶ in mouse TMH2 with residues in TMH3 had the strongest experimental support.

In conclusion, the contribution of human OCT1 to the cellular uptake of thiamine and especially to that of metformin may be much lower than the contribution of mouse OCT1. This may lead to an overestimation of the effects of OCT1 on hepatic metformin concentrations in humans when using the mouse as model organism. Nevertheless, comparative analyses of human and mouse orthologs may help to reveal mechanisms of OCT1 transport.

33

Do dimethyl fumarate and nicotinic acid elicit common, potentially HCA2-mediated adverse reactions? A combined epidemiological- experimental approach

D. Dubrall^{1,2}, R. Pflock³, J. Kosinska³, M. Schmid⁴, M. Bleich⁵, N. Himmerkus⁵, S. Offermanns⁶, M. Schwaninger³, B. Sachs^{7,8}

¹University Hospital of Bonn, Bonn, Germany

²Federal Institute for Drugs and Medical Devices, Bonn, Germany

³University of Lübeck, Lübeck, Germany

⁴Uniklinikum Bonn, Institut für Medizinische Biometrie, Epidemiologie und Informatik, Bonn, Germany

⁵Christian-Albrechts-Universität zu Kiel, Kiel, Germany

⁶Max-Planck Institute for Heart and Lung Research, Bad Nauheim, Germany

⁷Bundesinstitut für Arzneimittel und Medizinprodukte, Forschung, Bonn, Germany

⁸University Hospital (RWTH) Aachen, Clinic for Dermatology and Allergology, Aachen, Germany

Introduction: Dimethyl fumarate (DMF) and nicotinic acid (NA) can induce flushing by activation of the hydroxy-carboxylic acid receptor 2 (HCA2). So far, it is unknown if other adverse drug reactions (ADR) to DMF and NA may also be mediated by HCA2.

Objective: The first aim of our analysis was to compare the ADR profile reported for DMF and NA in order to investigate whether there are differences and similarities. As a second aim we investigated the expression of HCA2 in murine organs. The underlying assumption was that ADRs common to both substances may be mediated by HCA2 which we addressed in a combined pharmacoepidemiological and experimental approach.

Materials and methods: All spontaneous ADR reports for DMF and NA in the European ADR Database (EudraVigilance) received before 31/05/2019 were analysed with regard to the reported ADRs based on different hierarchical levels of the Medical Dictionary for Regulatory Activities (MedDRA) terminology. Odds Ratios were calculated in order to identify differences in the distribution of ADRs between DMF and NA. For the experimental approach, murine organs were screened for HCA2 expression.

Results: Similarities in the ADR profile of DMF and NA were found on different hierarchical levels of the MedDRA terminology. On a more summarizing level, "gastrointestinal signs and symptoms" (OR 0.8 [0.6-1.1]), "hepatobiliary investigations" (OR 1.3 [0.7-2.5]) and "anxiety disorders and symptoms" (OR 0.9 [0.3-2.2]) were equally distributed between DMF and NA. Likewise, "diarrhoea (excluding infective)" (OR 1.2 [0.7-1.8]) and "liver function analyses" (OR 1.3 [0.7-2.6]) were reported equally common for DMF and NA on a more detailed level of analysis. In contrast, differences were observed especially concerning ADRs referring to blood and lymphatic organs, which occurred more often in DMF treated patients. In the experimental analysis, HCA2 was expressed in the gastrointestinal tract, liver, and CNS of murine organs.

Conclusion: Similarities and discrepancies were found between the ADR profile of DMF and NA. Since gastrointestinal ADRs were frequently reported for both substances and HCA2 expression was found in the gastrointestinal tract, gastrointestinal ADRs may be mediated by HCA2. The observed discrepancies in the ADR profiles may reflect differences between the patient populations and the mechanisms that lead to these ADRs and may not involve HCA2.

34

Identification and characterization of cAMP buffering proteins by fluorescence anisotropy

C. Konrad¹, P. Annibale¹, M. Lohse^{1,2}, A. Bock¹

¹Max Delbrück Center for Molecular Medicine, Berlin, Germany

²ISAR Bioscience, Planegg, Germany

Cyclic adenosine monophosphate (cAMP) is a ubiquitous second messenger downstream of many G protein-coupled receptors (GPCRs) and modulates key signaling pathways in health and disease. To ensure GPCR signaling specificity in space and time, cAMP signaling is compartmentalized into nanodomains. We have recently shown that under basal conditions cAMP is mainly bound to cAMP binding sites and, thus, immobile. This so-called "buffered diffusion" allows phosphodiesterases to regulate cAMP signaling in nanometer size compartments [1]. Eukaryotic cells express only a limited number of cAMP binding proteins that may account for the observed buffering capacity. Typically, a cAMP buffer should have a high cAMP binding affinity and capacity to ensure efficient binding under non-stimulated conditions. Until now, only the regulatory subunits of protein kinase A (PKA), expressed at micromolar concentrations in cells, appear to fulfill these requirements.

More recently, the Popeye domain-containing (POPDC) proteins have been reported to constitute a novel class of cAMP effector proteins. However, it is largely unknown how POPDC proteins bind cAMP. Interestingly, POPDC proteins have a unique cAMP-binding domain, substantially distinct from all other cAMP binding proteins in eukaryotes. They are highly expressed in skeletal and cardiac muscle cells and even single point mutations may have severe phenotypes (AV-blocks, muscular dystrophy).

To better understand POPDCs' role in cAMP signaling, we here characterize their cAMP binding properties. We established a binding assay on the basis of fluorescence anisotropy using a novel fluorescent cAMP analog, 8-F-cAMP, to determine cAMP binding affinities in crude cell lysates without time consuming and laborious purification. We calibrated the method for the whole range of high (nanomolar) and low affinity (micromolar) binding using well characterized cAMP effectors as references. In a second step we use the assay for the determination of the cAMP affinity of full length POPDC. Interestingly, we find a low nanomolar cAMP affinity of POPDC1, which even exceeds the high affinity of PKA R1a.

Taken together, the data suggest that POPDC may be a novel cAMP buffering protein playing a pivotal role in the cAMP homeostasis of cardiac and skeletal muscle cells with important implications for several diseases.

References:

[1] Bock *et al.*, Optical mapping of cAMP signaling at the nanometer scale. *Cell*. 182, pp. 1519-1530 (2020).

The novel TRPV2-selective blocker X10056 inhibits phagocytosis and lipopolysaccharide-induced migration of primary macrophages

R. Raudszus¹, M. Schaefer¹, K. Hill¹

¹Rudolf Boehm Institute of Pharmacology and Toxicology, Leipzig, Germany

Transient receptor potential channels (TRP) form a superfamily of mainly nonselective cation channels. Affected by various chemical and physical stimuli, these TRP channels are involved in a variety of physiological and pathophysiological processes, such as nociception or thermosensation. Within the about 30 mammalian members of the superfamily, TRPV2 is a Ca²⁺-permeable ion channel, which is highly expressed in immune cells, including macrophages. However, due to a lack of potent and selective pharmacological tools, the function of TRPV2 in such cells is not very well understood. We have previously identified the dithiolane X10056 as a novel, potent and TRPV2-selective inhibitor. X10056 blocked TRPV2-mediated Ca²⁺ influx with an IC₅₀ of 6.0 μM in HEK293 cells heterologously expressing rat TRPV2 (HEK_{TRPV2}), and inhibited TRPV2 currents in electrophysiological whole-cell recordings performed on HEK_{TRPV2} cells. Since TRPV2 is believed to play a role in controlling macrophage function such as phagocytosis and migration, we isolated and cultured primary bone marrow-derived macrophages (BMDM) and peritoneal macrophages from mice. Quantitative PCR (qPCR) revealed the expression of TRPV2 in BMDM and peritoneal macrophages. 2-APB elicited a Ca²⁺ influx in BMDM and peritoneal macrophages that was inhibited by X10056, confirming the functional expression of TRPV2 in both cell types. Besides, we validated a siRNA-mediated knockdown of TRPV2 in BMDM by qPCR and fura-2-assisted single cell Ca²⁺ assays. In phagocytosis assays using pHrodo-labelled *E. coli* and *S. aureus* bioparticles, phagocytosis was significantly decreased when TRPV2 was inhibited by X10056, valdecoxib or after siRNA-mediated knockdown. Furthermore, TRPV2 inhibition and siRNA-mediated knockdown caused significant inhibitory effects on macrophage migration in a lipopolysaccharide-induced trans-well assay. In contrast, TRPV2 activation with a combination of 2-APB and probenecid resulted in an increased number of migrated cells. Taken together we establish X10056 as novel and potent TRPV2-selective inhibitor. In addition, we provide evidence that TRPV2 plays an important role in two key functions of macrophages, phagocytosis and migration.

Toxicology – Carcinogenesis

DNA oxidation damage and oxidative/nitrative stress status in obesity before and after weight loss

E. E. Bankoglu¹, H. Stopper¹

¹University of Würzburg, Institute of Pharmacology and Toxicology, Würzburg, Germany

Question: Obesity is a rising health issue of our century. Obesity has been shown to increase the DNA damage and accumulation of DNA damage can lead to mutation and can increase cancer risk in case of mis-repair or no repair. Oxidative stress plays a key role in obesity related detrimental consequences including DNA oxidation damage. Therefore, we aimed to study the association between obesity, weight loss and DNA oxidation damage in cryopreserved peripheral blood mononuclear cells and develop a further understanding on the role of two main ROS sources mitochondria and NADPH oxidase enzyme.

Methods: In order to analyse DNA damage and repair, we utilized an enhanced-throughput comet assay by preparing minigels on a Gelbond matrix. As oxidative and nitrative stress markers, advanced protein oxidation products and 3-nitrotyrosine were analysed in plasma and cryopreserved peripheral mononuclear blood cells. In addition, expression of oxidative stress related proteins HSP70 and Nrf2 together with mitochondrial enzyme citrate synthase and NADPH oxidase subunit p22 phox were analysed by using western blot.

Results: Our findings showed an elevated DNA damage in obese individuals compared to the control group. Weight loss improved the oxidative/nitrative stress by reducing protein oxidation products and 3-nitrotyrosine. However, DNA oxidation damage and oxidative stress proteins HSP70 and Nrf2 were not reduced after the weight loss. Our first findings did not yield any significant alteration in the expression of mitochondrial enzyme citrate synthase and p22 phox.

Conclusions: Overall, obesity showed association with elevated DNA strand breaks, oxidised base and oxidative/nitrative stress. Weight loss improved all over health status, reduced DNA strand breaks and improved some of the analysed oxidative/nitrative stress parameters. However, levels of cellular ROS formation and DNA oxidation damage did not fully recover after weight loss, which might be due to the burden of the weight-loss mediated fat tissue break down.

Reference: Bankoglu, E.E., et al., Influence of bariatric surgery induced weight loss on oxidative DNA damage. Mutation Research/Genetic Toxicology and Environmental Mutagenesis, 2020. 853: p. 503194.

Repair of O⁶-carboxymethylguanine adducts by MGMT in human colonic epithelial cells

N. Seiwert¹, T. Kostka^{2,3}, M. Empl², S. Geisen⁴, P. Hoffmann⁵, J. Adam², B. Seeger^{2,6}, J. Shay⁷, M. Christmann⁸, S. Sturla¹, J. Fahrer¹, P. Steinberg^{2,9}

¹Technical University of Kaiserslautern, Division of Food Chemistry and Toxicology, Kaiserslautern, Germany

²University of Veterinary Medicine, Institute for Food Toxicology, Hannover, Germany

³Gottfried Wilhelm Leibniz University Hannover, Institute of Food Science and Human Nutrition, Hannover, Germany

⁴ETH Zurich, Department of Health Sciences and Technology, Zurich, Germany

⁵University of Veterinary Medicine Hannover, Department of Physiology, Hannover, Germany

⁶University of Veterinary Medicine Hannover, Institute for Food Quality and Food Safety, Hannover, Germany

⁷University of Texas Southwestern Medical Center, Department of Cell Biology, Dallas, United States

⁸University Medical Center Mainz, Department of Toxicology, Mainz, Germany

⁹Federal Research Institute of Nutrition and Food, Max Rubner-Institut, Karlsruhe, Germany

Question: N-nitroso compounds (NOC) are DNA-alkylating agents, which occur exogenously and arise endogenously in the large intestine due to the nitrosation of amino acids. NOC cause both O⁶-methylguanine (O⁶-MeG) and O⁶-carboxymethylguanine (O⁶-CMG) adducts in DNA. Both lesions are highly mutagenic and their repair is thus crucial to prevent mutagenesis and carcinogenesis, particularly in the colorectum. O⁶-methylguanine-DNA methyltransferase (MGMT) is known to repair O⁶-MeG, but its role in repairing O⁶-CMG is under debate. Here, the function of MGMT in the repair of both types of O⁶-guanine lesions was investigated.

Methods: MGMT was inhibited in human colonic epithelial cells (HCEC) *in vitro* by the potent pharmacological inhibitor O⁶-benzylguanine (O⁶-BG), followed by the induction of O⁶-guanine adducts using azaserine or temozolomide. MGMT protein levels were determined by SDS-PAGE and Western Blot analysis. MGMT activity was determined using radioactive ³H-MNU-labelled calf thymus DNA with O⁶-MeG as substrate. Adduct levels were quantified depending on MGMT activity in HCEC using nanoLC-ESI-hrMS². DNA strand break formation in HCEC with or without MGMT inhibition was analysed with an alkaline comet assay. Finally, cytotoxicity was determined via MTS assay.

Results: Pre-treatment with O⁶-BG significantly depleted MGMT protein levels and completely abolished its activity in HCEC. Subsequent incubation with azaserine resulted in significantly higher O⁶-MeG and O⁶-CMG levels in MGMT-inhibited cells, while O⁶-CMG levels were found to be up to 18 times higher than O⁶-MeG levels. This finding provides evidence that MGMT repairs both O⁶-CMG and O⁶-MeG adducts. Interestingly, upon MGMT inhibition and azaserine exposure, higher levels of O⁶-CMG adducts did not result in increased DNA strand break formation or higher cytotoxicity. In contrast, treatment with the O⁶-methylating agent temozolomide following MGMT inhibition elevated both the number of DNA strand breaks and cellular toxicity.

Conclusions: The findings of the present study show that MGMT repairs O⁶-MeG as well as O⁶-CMG lesions. Furthermore, the data indicate that O⁶-CMG and O⁶-MeG adducts have a different potential to induce DNA strand breaks and cytotoxicity in the absence of MGMT.

Oxaliplatin-induced senescence in colorectal cancer cells is dependent on p14-mediated sustained p53 activation

M. Christmann¹, F. Krämer¹, A. Nguyen¹, M. Tomicic¹

¹University Medical Center, Department of Toxicology, Mainz, Germany

Question: Senescence, e.g. irreversible cell cycle arrest, represents an important cellular consequence of anticancer drug-based tumor therapy. Thus, upon entering a senescent state, the cells are protected against anticancer therapy. Previous reports indicate that some of these cells could either escape from senescence contributing to the formation of recurrences or they can induce the senescence-associated secretory phenotype (SASP) which may impact therapy success, either by inducing strong inflammatory responses or acting as a potent tumor promoter. Here we analyzed to which degree the anticancer drug oxaliplatin induces senescence in colorectal cancer (CRC) cells and elucidated the role of p53 in this process.

Materials & methods: Cell death, senescence, cell cycle progression and activation of the DDR was analyzed in HCT116 p53wt, HCT116 p53-/-, LoVo, SW48 and SW480 CRC cells upon exposure to oxaliplatin. The impact of p53 and p14 knockdown on oxaliplatin-induced senescence was analyzed in LoVo cells.

Results: Treatment with oxaliplatin resulted in cell cycle arrest in the G2-phase in all tested CRC cell lines (HCT116 p53wt, HCT116 p53-/-, LoVo, SW48 and SW480). Western blot analyses show that in the p53-proficient lines p53 and p21 were activated at early time points upon treatment. However, at later time points only LoVo cells showed sustained activation of the p53/p21 pathway, which was accompanied by a strong induction of senescence, as determined by senescence-associated β-Gal staining and

induction of factors characteristic of the senescence-associated secretory phenotype (SASP). The dependence of oxaliplatin-induced senescence on p53 was further proven by siRNA-mediated knockdown of p53. Opposite to LoVo cells, the p53/p21 response and senescence induction was much weaker in the p53-proficient HCT116 p53wt, SW48 and SW480 cells, which was based on deficiency for p14. Thus, among all cell lines only LoVo cells express p14 and siRNA-mediated knockdown of p14 significantly reduced sustained activation of the p53/p21 pathway and of senescence.

Conclusion: Overall, our data show that oxaliplatin-induced senescence in CRC cells is dependent on p53 proficiency, however, a significant senescence induction can only be observed upon p14-mediated stabilization of p53.

40

Investigation on mechanism of genotoxicity of selected pyrrolizidine alkaloids in HepG2 cells

H. Naji Said Aboud^{1,2}, E. E. Bankoglu¹, O. Kelber³, H. Sievers⁴, H. Stopper¹
¹Institute of Pharmacology and Toxicology, University of Würzburg, Würzburg, Germany
²School of Health and Human Sciences, Pwani University, Kilifi, Kenya
³Steigerwald Arzneimittelwerk GmbH, Bayer Consumer Health, Darmstadt, Germany
⁴PhytoLab GmbH & Co. KG, Vestenbergsgreuth, Germany

Introduction: Pyrrolizidine alkaloids (PAs) are natural compounds that are widely distributed in many plant species. Certain PAs are hepatotoxic and affect humans via food, food supplements and herbs/spices. Exposure to PAs can cause hepatic sinusoidal obstruction syndrome leading to hepatotoxicity and carcinogenicity.

Aim of the study: To investigate the chemical structure effect relationship of genotoxic PAs and to analyze their molecular mechanisms including the role of metabolic enzymes, DNA cross-linking activity and oxidative stress.

Material and methods: The genotoxicity of PAs of different chemical structure, such as europine, retrorsine and lasiocarpine, was investigated in human hepatoma HepG2 cells using the cytokinesis-block micronucleus (CBMN) assay. DNA-crosslinking activity of different ester PA-types was investigated in HepG2 cells using a modified comet assay. Oxidative stress was analyzed in HepG2 cells using DHE staining. The role of metabolic enzymes such as cytochrome P450s was investigated in HepG2 cells using the inhibitor ketoconazole.

Results: An increase of micronucleus formation was found with all PAs of different chemical structure. The lowest concentrations at which significant induction of micronuclei were detected were 3.2µM for lasiocarpine (open diester PA-type), 32µM for retrorsine (cyclic diester type) and 100µM for europine (monoester PA-type). In the modified crosslink comet assay, the diester type PAs reduced tail formation after hydrogen peroxide treatment; while an equimolar concentration of the monoester europine did not significantly reduce DNA migration. In addition, micronucleus induction by lasiocarpine was abolished after pre-treatment with ketoconazole.

Conclusion: The results show that the genotoxicity depends on the ester type of the PAs with an open diester PA-type such as lasiocarpine being the most potent while the monoester PA-type such as europine being the least potent. In the modified comet assay, the crosslinking activity was also related to the ester type of PAs.

Reference:

Naji Said Aboud Hadi, Ezgi Eyluel Bankoglu, Lea Schott, Eva Leopoldsberger, Vanessa Rame, Olaf Kelber, Hartwig Sievers, and Helga Stopper. "Genotoxicity of selected pyrrolizidine alkaloids in human hepatoma cell lines HepG2 and Huh6." *Mutation Research/Genetic Toxicology and Environmental Mutagenesis* 861 (2021): 503305. <https://doi.org/10.1016/j.mrgentox.2020.503305>.

41

Trace elements, ageing, and sex: Impact on genome stability

V. K. Wandt^{1,2}, N. Winkelbeiner^{1,2}, K. Lossow^{3,2}, J. Kopp^{1,2}, L. Simon¹, F. Ebert^{1,2}, A. Kipp^{3,2}, T. Schwerdtle^{1,2}
¹University of Potsdam, Department of Food Chemistry, Potsdam, Germany
²TraceAge – DFG Research Unit on Interactions of Essential Trace Elements in Healthy and Diseased Elderly, Berlin-Potsdam-Jena-Wuppertal, Germany
³Friedrich-Schiller-Universität Jena, Department of Molecular Nutritional Physiology, Jena, Germany

Ageing is a complex biochemical process causing a multitude of physiological and pathophysiological changes in the human body, such as ageing-associated alterations in essential trace element (TE) levels. Nevertheless, studies focusing on the interplay of nutritional TE intake, their homeostases, interactions, as well as their impact on health status in the context of ageing are scarce. Thus, the interdisciplinary research unit TraceAge investigates these research questions focusing on the essential TEs iron, copper, manganese, selenium, iodine, and zinc.

Among others, ageing-associated alterations in TE level impacts on genome stability, by interfering with DNA damage response (DDR) and DNA repair mechanisms. Its maintenance is vital to ensure a reliable cellular functionality and hence prevent diseases. To investigate the impact of alterations in the TE status on different genomic stability

related endpoints in murine liver, feeding studies in animals of different age and sex were conducted. In this context, changes in mRNA and protein expression levels of different DDR and DNA repair genes and proteins were evaluated via quantitative PCR and Western Blot analysis. Additionally, the total amount of DNA strand breaks was determined by alkaline Comet Assay and 8-oxo-7,8-dihydro-2'-deoxyguanosine levels were assessed applying an ELISA kit. Base excision repair (BER) represents the major cellular repair mechanism for oxidative DNA lesions, removing a broad and frequently occurring damage spectrum, thereby contributing greatly to the maintenance of genomic stability. BER incision activity was evaluated by a non-radioactive incision activity assay based on using DNA damage-containing oligonucleotides. Furthermore, poly(ADP-ribose)ylation status, which is an essential reversible post-translational modification of proteins with poly(ADP-ribose) as early event in DNA damage response, was quantified via stable isotope dilution liquid chromatography tandem mass spectrometry. Besides the investigation of genomic stability endpoints, TE levels in murine liver and serum were analysed via inductively coupled plasma tandem mass spectrometry.

By bringing together the mentioned endpoints, we aim to get further insights into the complex interplay between the TE status, ageing, sex, and genome stability in murine liver.

Pharmacology – Immunopharmacology inflammation antiinfectives-Session II - Identification of immunological targets and drug development

42

Dynamic mass redistribution technology decodes the dynamics of Toll-like receptor signaling

J. Holze¹, E. Kostenis², G. Weindl¹
¹University of Bonn, Pharmaceutical Institute, Pharmacology and Toxicology, Bonn, Germany
²University of Bonn, Institute for Pharmaceutical Biology, Bonn, Germany

Question: The discovery of Toll-like receptors (TLRs) established the first group of pathogen recognition receptors and represented a breakthrough in the mechanistic understanding of host pathogen interactions in innate immunity. TLR signaling leads to activation of transcription factors and inflammatory responses. However, there are still major gaps in the understanding of TLR function, especially the early dynamics of downstream TLR pathways remains less clear.

Methods: Here we present the label-free dynamic mass redistribution (DMR)-based assay as a powerful method to detect TLR activation in a native and label-free environment and to delineate the real-time dynamics of TLR pathway activation. This approach offers the possibility to bypass the use for further molecular tools that may interfere with intracellular processes. In reporter cells as well as monocytic and epidermal cells, we confirmed that DMR technology can be applied to study TLR activation.

Results: We demonstrate that DMR is sufficiently sensitive to detect TLR signaling and readily discriminates between different TLR signaling pathways. Pharmacological modulators and inhibitors of TLRs and downstream signaling molecules reduced the DMR response induced by TLR ligands, confirming that the detected signal is downstream of TLR activation.

Conclusion: We hypothesize that measuring DMR is a potential experimental approach that will change the way of analyzing TLR signaling responses. It complements traditional assays using a single endpoint and has the opportunity to open the door for future design of selective drugs that target TLRs.

43

Differential effects of B cell knockout and antibody deficiency in murine models of diet-induced non-alcoholic fatty liver disease

M. Karl¹, S. Hasselwander¹, G. Reifenberg¹, Y. O. Kim², K. S. Park², X. Wang², N. Hövelmeyer², E. Seidel¹, H. Li¹, D. Schuppan¹, N. Xia³
¹Medical center Mainz, DInstitute of Translational Immunology and Research Center for Immunotherapy department of Pharmacology, Mainz, Germany
²Medical center Mainz, Institute for Molecular Medicine, Mainz, Germany
³Medical center Mainz, Department of Pharmacology, Mainz, Germany

Background & Aims: Growing evidence suggests an important role for the adaptive immune system and in particular B cells in the development of non-alcoholic fatty liver disease (NAFLD). However, a detailed functional analysis of B cell subsets in NAFLD pathogenesis is lacking.

Approach & Results: To uncover the functional contribution of B cells, we studied high fat diet (HFD)-induced NAFLD in Bnull (*JH7*) mice compared to mice with restricted B cell function (*IgM^{-/-}*; exclusively membrane-bound IgM, no antibody secretion). In wildtype mice, 21 weeks of HFD resulted in NAFLD with massive macrovesicular steatosis, modest hepatic and adipose tissue inflammation, insulin resistance and incipient fibrosis. In contrast, mice with B cell defects exhibited attenuated development of NAFLD-related histological and immunological parameters. This was paralleled by downregulated expression of hepatic genes related to *de novo* lipogenesis, inflammation and fibrogenesis. Remarkably, *IgM^{-/-}* mice were completely protected from the development of hepatic steatosis, inflammation and fibrosis, more than Bnull mice, and almost lacked adipose tissue inflammation and dysfunction.

Conclusions: Comparative analysis of graded models of B cell deficiency suggests differential roles of B cell function in the development of high fat diet-induced obesity and NAFLD, including liver inflammation, fibrosis and adipose tissue inflammation.

44

Characterization of novel pyrimidine-based TLR8 antagonists identified by modeling-guided synthesis

M. Grabowski¹, A. Scheffler², A. Dolšak³, D. Šribar⁴, J. Holze², G. Wolber⁴, M. Sova³, G. Weindl²

¹Freie Universität Berlin, Institute of Pharmacy (Pharmacology and Toxicology), Berlin, Germany

²University of Bonn, Pharmaceutical Institute, Pharmacology and Toxicology Section, Bonn, Germany

³University of Ljubljana, Faculty of Pharmacy, Ljubljana, Slovenia

⁴Freie Universität Berlin, Institute of Pharmacy (Pharmaceutical Chemistry), Berlin, Germany

Question: Toll-like receptor 8 (TLR8) is an endosomal sensor of single-stranded RNA and initiates early inflammatory responses. Despite the importance of endosomal TLRs for human host defense against microbial pathogens, extensive activation may contribute to inflammatory and autoimmune diseases. We recently reported a novel chemotype of TLR8 antagonists that was based on a pyrimidine scaffold. In this study, we explored the chemical space around the pyrimidine-containing antagonists to get insights into the structure-activity-relationships of TLR8 antagonists.

Methods: A modeling-guided synthesis approach was performed to identify novel TLR8 modulators based on their predicted ability to bind in the binding pocket of human TLR8. HEK293T cells stably overexpressing human TLR8 were used to characterize virtual screening hits and synthesized compounds for the ability to inhibit TLR8-mediated responses.

Results: 13 out of 44 biologically tested compounds showed concentration-dependent inhibitory activity, representing a hit rate of 30%. None of the compounds appeared to have agonistic activity on TLR8. The most potent TLR8 antagonists demonstrated an IC50 value in the low μM range without affecting cell viability.

Conclusion: We experimentally confirm novel pyrimidine-derivates as TLR8 antagonists with low cytotoxicity that are relevant candidates for lead optimization and further mechanistic studies.

45

Enhanced efficacy of combinatorial RIG-I-mediated immunotherapy and radiotherapy in malignant melanoma depends on functional p53 expression

S. Lambing¹, S. Holdenrieder^{1,2}, P. Müller¹, C. Hagen¹, S. Garbe³, J. G. van den Boorn¹, E. Bartok¹, M. Renn^{1,4}, G. Hartmann¹

¹Institute of Clinical Chemistry and Clinical Pharmacology, University Hospital Bonn, Bonn, Germany

²Institute of Laboratory Medicine, German Heart Center, München, Germany

³Department of Radiation Oncology, University Hospital Bonn, Bonn, Germany

⁴Mildred Scheel School of Oncology, University Hospital Bonn, Bonn, Germany

The activation of the anti-viral innate immune receptor RIG-I offers a novel and promising approach for immunoncology, which is currently being investigated in clinical trials. RIG-I agonists elicit a strong immune response in tumor, as well as immune cells that is driven by type I interferon and can induce both direct- and immune-cell-mediated tumor cell death. This leads to the development of a tumor-specific cytotoxic T-cell response, in addition to the anti-tumor effects of the innate immune system.

In order to further increase the amount of immunogenic cell death, we investigated the activation of RIG-I in combination with radiotherapy, a well-established method for the treatment of many cancers. While irradiation is known to induce cytotoxic DNA damage that results in tumor debulking, recent studies have also shown that it can induce tumor-specific immunity, making it an ideal combination partner for RIG-I immunotherapy.

In this study, we show that concurrent administration of low-dose irradiation with RIG-I agonists (3pRNA) further enhanced the induction of RIG-I-mediated tumor cell death in human and murine melanoma cell lines as well as the uptake of dead tumor cells by antigen-presenting cells. *In vivo*, this combination treatment translated into increased T- and NK-cell activation as well as prolonged survival of mice bearing B16 melanoma. Expression analysis revealed the p53 pathway to play a major role in combinatorial RIG-I irradiation treatment. By using polyclonal p53 knockouts of B16 cells, we showed that the synergistic increase in tumor cell-cycle arrest, cell death, and exposure of calreticulin on the cell surface as well as subsequent uptake by DCs normally seen with the combination treatment was attenuated in the knockout cells. In an *in vivo* mouse model, p53-knockout tumors still responded to 3pRNA injections but the addition of irradiation produced no increase in the activation of immune cells or inhibition of tumor growth. Thus, although melanoma is generally considered radioresistant, in combination with RIG-I activation, irradiation offers a promising new approach to treat melanoma.

46

Chronic helminth infection ameliorates colitis via the soy derived metabolite

daidzein

A. Kazakov¹, D. Colon¹, P. Maier¹, A. Odainic², R. Chong¹, S. Jayagopi¹, F. Karagiannis¹, V. Schmitt³, M. Michla¹, C. Wilhelm¹

¹Institut für Klinische Chemie und Klinische Pharmakologie, Immunopathology, Bonn, Germany

²Institute of Innate Immunity, Immunogenomics, Bonn, Germany

³FM Therapeutics, Bonn, Germany

Over the last decades industrialized countries experience an increase in chronic inflammatory disorders such as asthma and allergies affecting the lung or inflammatory bowel disease (IBD) manifesting in the intestine. Simultaneously infectious diseases such as parasitic helminth infections are largely eradicated in the Western World. This observed correlation led to the formulation of the "hygiene hypothesis" by Strachan in 1989, which was improved and refined since. It proposes the concept that a general lack of infections, the absence of ambient beneficial microbes and parasitic helminths might contribute to the development of chronic inflammation disorders. Helminths in particular through co-evolution with humans for thousands of years have developed regulatory functions to suppress the immune system and induce epithelial repair to maintain chronicity. Hence understanding the interplay of parasitic infections and the epithelial cell layer may be important for unraveling basic principles of chronic inflammation and tissue regeneration and introduce new therapies for the treatment of inflammatory disorders. In order to address this experimentally we infected mice with the well-adapted whipworm *Trichuris muris*, which establishes a chronic infection in the intestine. Notably, *T. muris* infections largely attenuate disease progression and symptoms such as weight loss, diarrhea and colon shortening in a chemically induced colitis model in mice. Metabolomics analysis revealed that various compounds were increased by chronic worm infection. Among those was the dietary soy derived metabolite daidzein. Oral delivery of daidzein was able to significantly reduce weight loss and increase survival in the context of DSS colitis. Mechanistically we demonstrated a direct effect of daidzein on the differentiation of intestinal epithelial cells *in vitro*. Upon treatment translocation of YAP, the main signaling component of the hippo pathway to the nucleus is induced. Nuclear localization of YAP drives a gene expression program, inducing regeneration and repair of the epithelium. This is accompanied by downregulation of crucial stem cell and paneth cell markers *Igf1*, *offm4* and *lyz1* indicative of an alternative differentiation regime of epithelial cells. With our results we provide evidence that dietary intervention with soy metabolites might be a potent strategy for the treatment of intestinal damage experiences in the context of inflammatory bowel disease in the future.

47

The transmembrane protein tetraspanin 5 controls the effects of loss of the tumor suppressor deleted in liver cancer 1 (DLC1) on hepatocellular carcinoma (HCC) growth

L. Schreyer¹, C. Mittermeier², D. E. Martin³, S. Singer⁴, B. Liebl⁵, T. Gudermann⁶, A. Aigner⁷, S. Muehlich¹

¹Friedrich-Alexander-Universität Erlangen-Nürnberg, Department of Chemistry and Pharmacy, Erlangen, Germany

²National University of Singapore, Cancer Science Institute of Singapore, Singapore, Singapore

³Ludwig Maximilian University of Munich, Department of Chemistry and Pharmacy, München, Germany

⁴University Hospital Tübingen, Department for Pathology, Tübingen, Germany

⁵GL Bayerisches Landesamt für Gesundheit und Lebensmittelsicherheit, Oberschleißheim, Germany

⁶Ludwig Maximilian University of Munich, Walther Straub Institute of Pharmacology and Toxicology, München, Germany

⁷University of Leipzig, Rudolf Boehm Institute of Pharmacology and Toxicology, Leipzig, Germany

Megakaryoblastic Leukemia 1 (MKL1) is a coactivator of Serum Response Factor (SRF) that regulates the transcription of genes involved in cell migration, cell proliferation, cell adhesion and differentiation and plays an essential role for hepatocellular carcinoma (HCC) formation. We showed that loss of the tumor suppressor Deleted in Liver Cancer 1 (DLC1), which occurs in 50% of liver cancers, promotes expression of MKL1/SRF dependent target genes enhancing HCC growth. To identify novel gene targets induced by DLC1 loss mediating the effect on MKL1 transcriptional activation and HCC growth, we performed microarray experiments in HepG2 human hepatoma cells transduced with DLC1 shRNA using Affymetrix oligonucleotide arrays for differential expression studies. This approach revealed that Tetraspanin 5 (TSPAN5) was strongly upregulated upon DLC1 depletion in HCC cells. We provide evidence that knockdown of TSPAN5 provoked *in vitro* and *in vivo* growth arrest triggered by oncogene induced senescence (OIS). Mechanistically, depletion of TSPAN5 reduced actin polymerization and thereby MKL1-Filamin A complex formation, resulting in decreased expression of MKL1-dependent target genes and senescence induction *in vitro* and *in vivo*. Considering the increased TSPAN5 expression in human HCC and the therapeutic efficacy of a senescence-inducing strategy, TSPAN5 is a promising novel pharmacological target for HCC therapy.

Pharmacology – Disease models – drug development II

48

Treamid is a potential compound for inhibiting fibrosis and accelerating endothelial regeneration in idiopathic pulmonary fibrosis

E. Skurikhin¹, V. Nebolsin², A. Dygai^{1,3}, O. Pershina¹, N. Ermakova¹, A. Pakhomova¹, E. Pan¹, V. Krupin¹, **M. Zhukova**¹, W. D. Grimm⁴, S. Morozov³, A. Kubatiev³
¹Goldberg ED Research Institute of Pharmacology and Regenerative Medicine, Tomsk National Research Medical Centre of the Russian, Laboratory of Regenerative Pharmacology, Tomsk, Russian Federation
²Pharma Enterprises Ltd., Moscow, Russian Federation
³Institute of General Pathology and Pathophysiology, Moscow, Russian Federation
⁴University of Witten/Herdecke, Department of Dental Medicine, Witten, Germany

Question: Pirfenidone and Nintedanib drugs, which are known on the market, slow down the progression of idiopathic pulmonary fibrosis (IPF), but do not stop it and do not restore the structure of damaged lung tissue. The search of compounds with antifibrotic activity and accelerating regeneration in IPF is urgent.

Methods: The object of the study was Treamid (bisamide derivative of a dicarboxylic acid, "PHARMENTERPRISES"). Pneumofibrosis in C57BL/6 mice was modeled by bleomycin (BLM, Nippon Kayaku Co., Ltd., Tokyo, Japan). Treamid was administered intragastrically. In a histological study, we evaluated inflammatory infiltration and damage to the lungs and connective tissue deposits. Mature macrophages (F4/80+CD11b+), immature macrophages (F4/80lowCD11b+) and inflammatory cells with the phenotype CD45+Sca1+CD11b+ and CD45+CD19–Sca1+CD11b+F4/80+ were assessed by flow cytometry. ELISA evaluated the level of hydroxyproline, type I collagen, fibronectin, total collagen, and connective tissue growth factor in the lung homogenate. Using flow cytometry and cell imaging methods, we studied precursors of angiogenesis (CD45-CD309+CD117+), endothelial progenitor cells (CD45-CD31+CD34+), VEGF2 + cells, lung stem cells (CD45–CD117+CD49f+) and Clara cells (CD45-CD34-CD31-Sca1+).

Results: Treamid reduced lymph-macrophage infiltration and connective tissue area in the lungs of mice under conditions of BLM injection. Treamid inhibited alveolar destruction and increased lung capillary density in mice with pulmonary fibrosis. Treamid reduced total collagen, type I collagen, hydroxyproline, and fibronectin in the lung homogenate. We associate the regenerative effect of Treamid with a selective stimulating effect on resident endothelial progenitor cells.

Conclusion: Treamid represents a promising compound for the development of a new antifibrotic drug with the ability to accelerate the regeneration of the lung endothelium in patients with IPF.

49

Nox4-dependent upregulation of S100A4 after peripheral nerve injury modulates neuropathic pain processing

G. Wack¹, K. Metzner¹, M. S. Kuth¹, E. Wang¹, A. Bresnick², R. P. Brandes³, K. Schröder³, I. Wittig⁴, A. Schmidtko¹, **W. Kallenborn-Gerhardt**¹
¹Institute of Pharmacology and Clinical Pharmacy, Goethe University Frankfurt, Frankfurt am Main, Germany
²Albert Einstein College of Medicine, Department of Biochemistry, Bronx, United States
³Institute of Cardiovascular Physiology, Goethe University Frankfurt, Frankfurt am Main, Germany
⁴Cluster of Excellence "Macromolecular Complexes", Goethe University Frankfurt, Frankfurt am Main, Germany

Introduction: Several studies suggested that reactive oxygen species (ROS) produced by NADPH oxidase 4 (Nox4) affect the processing of neuropathic pain. However, mechanisms underlying Nox4-dependent pain signaling are incompletely understood.

Objective: Here, we aimed to identify novel Nox4 downstream interactors in the nociceptive system.

Material and methods: We generated mice lacking Nox4 specifically in sensory neurons. In addition, global S100A4-deficient mice were used. A proteome screen was performed using mass spectrometry. Tissue expression of Nox4 and S100A4 was investigated using immunostaining, qPCR and Western blot. Neuropathic pain behavior was assessed in a model of peripheral nerve injury.

Results: Mice in which Nox4 was specifically deleted in sensory neurons demonstrated reduced hypersensitivity after peripheral nerve injury. Using a proteomic approach, we detected various proteins that are regulated in a Nox4-dependent manner after injury, including the small calcium-binding protein S100A4. Expression of S100A4 was strongly up-regulated in peripheral nerves and dorsal root ganglia after injury and mice lacking S100A4 showed altered neuropathic and ROS-dependent pain behavior.

Conclusion: Our results suggest that S100A4 expression is up-regulated after peripheral nerve injury in a Nox4-dependent manner and that deletion of S100A4 leads to an increased neuropathic pain hypersensitivity.

50

Platelet-rich plasma therapy attenuates cardiac necrosis and promotes repair in rat model of isoproterenol induced cardiac toxicityS. Yadav¹, S. Srivastava¹, **G. Singh**¹¹ISF College of Pharmacy, Moga, Department of Pharmacology, Moga, India

Objectives: Platelet-rich plasma (PRP) therapy has been demonstrated to exert beneficial effects in coronary artery ligation models. Present study was designed to investigate the cardioprotective potential of intramyocardial injection of activated PRP in isoproterenol (ISO) induced cardiac injury model.

Material & Methods: All experimental groups were approved by Institutional Animal Ethics Committee of the ISF College of Pharmacy, Moga, Punjab, India. ISO was injected at a dose of 85 mg/kg subcutaneously for 2 days in wistar rats (Sharma et al., 2020). Treatment groups received intramyocardial injection (200 microlitre on both ventricles) of either thrombin activated PRP or platelet poor plasma (PPP), 2 hours after first dose of ISO administration. Hearts were isolated 24 hours after second dose of ISO injection and cardiac function assessment was performed using automatic Langendorff apparatus. Immunostaining for alpha smooth muscle actin (α -SMA) protein was done as a marker for cardiac repair and inflammatory markers (TNF- α , IL-6) were determined by ELISA kits. Cardiac necrosis and fibrosis score was determined by histological staining methods.

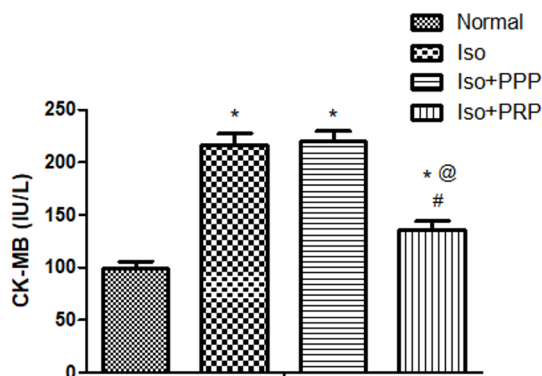
Results: Administration of ISO resulted in cardiac dysfunction as depicted by reduced maximum (dp/dt max.) and minimum (dp/dt min.) developed pressures, increased left ventricular end diastolic pressure (LVEDP) and increased relaxation constant Tau values, along with increase in lactate dehydrogenase (LDH) and creatinine kinase-MB (CK-MB) values. Moreover, ISO administered hearts exhibited a reduced immunostaining for α -SMA protein, increased inflammation, marked necrosis and fibrotic staining. PRP treatment attenuated the development of functional and histological alterations induced by ISO.

Conclusions: PRP treatment effectively retarded the ISO induced cardiac dysfunction and necrosis by suppressing inflammatory stress and preventing cardiomyocyte loss.

Legend Figure1: CK-MB levels in normal, Isoproterenol (85 mg/kg s.c), ISO + PPP (intramyocardial platelet-poor plasma injection in ISO rats), ISO + PRP (intramyocardial platelet-rich plasma in ISO rats) groups. *p<0.05 vs Normal control group, @p<0.05 vs ISO administered group, #p<0.05 vs ISO + PPP group.

Reference: Sharma S, Khan V, Dhyani N, Najmi AK, Haque SE. Icarin attenuates isoproterenol-induced cardiac toxicity in Wistar rats via modulating cGMP level and NF- κ B signaling cascade. *Human & Experimental Toxicology*, 2020; 39(2):117-26.

Fig. 1



51

Metformin reduces therapeutic effects in the new in vitro tumor therapy model**F. Meyer**¹, S. Göbel¹, C. Leovsky¹, R. Thierbach¹¹Institut für Ernährungswissenschaften; Friedrich-Schiller-Universität Jena, Humanernährung, Jena, Germany

Introduction: Despite considerable medical proceedings, cancer is still a leading cause of death. Major problems for tumor therapy are chemoresistance as well as toxic side effects. In recent years, the additional treatment with the antidiabetic drug metformin during chemotherapy showed promising results in some cases.

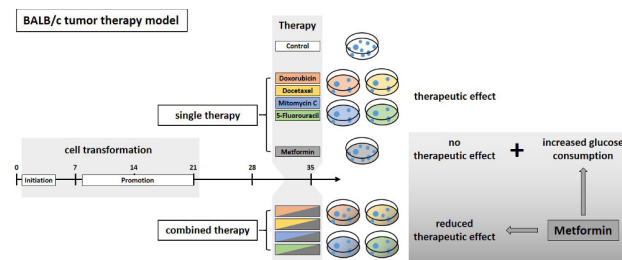
Objectives: The aim of this study was to develop an in vitro tumor therapy model in order to further investigate the potential of a combined chemotherapy with metformin.

Methods: Cytotoxic effects on BALB/c fibroblasts were proven by the resazurin assay. Based on the BALB/c cell transformation assay, the BALB/c tumor therapy model was established successfully with four different chemotherapeutics (Doxorubicin, Docetaxel, Mitomycin C and 5-Fluorouracil). Thereby, the therapeutic treatment was conducted in the late phase of malignant cell transformation (day 32-35). Moreover, glucose consumption in the medium supernatant was measured and protein expressions were determined by Western Blotting and Immunofluorescence.

Results: The anti-carcinogenic effects of the chemotherapeutic agents were confirmed in the new BALB/c tumor therapy model and significantly decreased the number of type-III-foci even in non-toxic concentrations. However, the combined treatment with metformin showed surprising results. The therapeutic effects of the chemotherapeutic agents were partly mitigated when applied simultaneously with metformin, indicating that metformin could induce chemoresistance. Mechanistically, an increased glucose consumption was observed after metformin treatment in non-transformed cells as well as in the mixed population of malignant transformed cell foci and non-transformed monolayer cells, suggesting that metformin could also increase glucose consumption in transformed cells. This observation could contribute to the chemoresistance inducing effect and is currently further investigated. So far, different glucose transporters and metabolic key proteins like AMPK and TXNIP seem to be involved in this process.

Conclusion: In conclusion, this study suggests a cautious use of metformin during chemotherapy. Moreover, the BALB/c tumor therapy model offers a potent tool for further mechanistic studies of drug-drug interactions during cancer therapy.

Fig. 1



52

Telmisartan induces a specific signature of gut microbiota, which may participate to its anti-obese potency

L. Beckmann¹, A. Künstner², I. Stölting¹, M. Freitag², U. Matschil³, S. Ibrahim², E. Langan², J. Knobloch⁴, H. Busch², **W. Raasch**¹

¹University of Lübeck, Institute of Experimental and Clinical Pharmacology and Toxicology, Lübeck, Germany

²University Lübeck, Institute of Experimental Dermatology, Lübeck, Germany

³Heinrich Pette Institute, Hamburg, Germany

⁴UKSH Lübeck, Clinic of Infectiology and Microbiology, Lübeck, Germany

Question: The AT1 receptor antagonist telmisartan (TEL) has antiobese efficacy. The mechanism is still a matter of debate. We here investigated whether a gut related mechanism is involved.

Methods: Sprague Dawley rats were fed with cafeteria diet (CD) and treated with TEL (8 mg/kg/d) while controls received vehicle. A third group (vehicle-treated) had limited food excess only receiving the amount of TEL-treated rats (pair-feed, =PF). A fourth group received chow+vehicle (CON). Animals were functionally phenotyped. Stool samples were analysed by 16S rRNA gene amplicon sequencing.

Results: After 3 months, CD fed rats developed obesity and insulin resistance. Both was prevented in TEL- and PF-rats. Alpha diversity analyses indicated that bacterial phylum became different over time. Following a BORAL analysis, CD and PF clearly differed from CON and TEL animals. Taxonomic analyses of phylum, family and genus abundances revealed differences between the groups. On phylum level, the Firmicutes/Bacteroidetes ratio was increased in CD and PF, but not in TEL rats. On family level, Lachnospiraceae, Suterellaceae and Erysipelotrichaceae increased while Prevotellaceae decreased in obese rats. In contrast, Prevotellaceae was higher in TEL compared to CD and PF rats. On genus level, Blautia, Allobaculum and Parasutterella increased while Prevotella decreased in CD compared to chow rats. This shift was almost converted in TEL but not in PF rats. Leptin positively correlated with Blautia or Parasutterella and negatively with Prevotella. Performing a co-occurrence network analyses, Kleinberg's hub scoring indicated that centralisation and stability were highest in TEL treated rats. In a machine-learning test using a random forest approach, we observed a very accurate prediction for chow-fed controls while the correct classification was less than half in CD-fed and PF controls. TEL animals were mostly classified in a correct manner.

Conclusions: TEL treatment induces a specific signature in faecal microbiota. Considering that microbiota of CD and PF rats is almost similar we further conclude that TEL influences microbiota in a food intake independent manner. Since Firmicutes was here observed to be increased in obese but not in TEL rats, we speculate that this gut-related mechanisms may participate to cardiovascular and metabolic benefits following TEL treatment.

53

Telmisartan prevents high-fat diet-induced neurovascular impairments and reduces anxiety-like behavior

G. Huber¹, M. Ogrodnik², J. Wenzel¹, I. Stölting¹, L. Huber³, O. Will², E. Peschke², U. Matschil⁴, J. B. Hövener³, M. Schwaninger¹, D. Jurk², **W. Raasch**¹

¹University of Lübeck, Institute of Experimental and Clinical Pharmacology and Toxicology, Lübeck, Germany

²Mayo Clinic, Rochester, United States

³University Hospital Schleswig Holstein, Kiel, Germany

⁴Heinrich Pette Institute, Hamburg, Germany

Beyond blood pressure regulation, there is strong evidence that the renin angiotensin system is linked to both glucose control and obesity. Commonly used angiotensin II receptor blockers, such as telmisartan, have been shown to prevent rodents from diet-induced obesity on the one hand and to improve their metabolic status on the other. Hyperglycemia as well as obesity is associated with reduced cerebral blood flow and neurovascular uncoupling which may lead to behavioral deficits. We wanted to know whether a treatment with telmisartan can prevent from these changes in obesity.

We put young mice on high-fat diet and simultaneously treated them with telmisartan. At the end of treatment, we performed laser speckle imaging and magnet resonance imaging to assess the effect on neurovascular coupling and cerebral blood flow. Different behavioral tests were used to investigate cognitive function.

Mice developed diet-induced obesity and after 16, not 8 weeks of high-fat diet, however, the response to whisker pad stimulation was about 30 % lower in obese compared to lean mice. Simultaneous telmisartan treatment increased the response again by 10 % compared to obese mice. Moreover, telmisartan treatment normalized high-fat diet-induced reduction of cerebral blood flow and prevented from a diet-induced anxiety-like behavior. In addition to that, telmisartan affects cellular senescence and string vessel formation in obesity.

We conclude, that telmisartan has protects from neurovascular unit impairments in a diet-induced obesity setting and may play a role in preventing obesity related cognitive deficits in Alzheimer's disease.

Toxicology – Emerging topics

54

Clostridial C3 toxins enter human dendritic cells, modify their functions, and are promising new carriers for drugs or vaccines

M. Fellermann¹, S. Fischer¹, C. Huchler¹, L. Fechter¹, S. Heber¹, F. Wondany², D. Mayer³, S. Stenger³, J. Michaelis², H. Barth¹

¹Ulm University, Medical Center, Institute of Pharmacology and Toxicology, Ulm, Germany

²Ulm University, Medical Center, Institute of Biophysics, Ulm, Germany

³Ulm University, Medical Center, Institute of Medical Microbiology and Hygiene, Ulm, Germany

Apart from macrophages, dendritic cells (DCs) are the most important antigen-presenting cells and play a major role in innate and adaptive immune defense. Macrophages as well as DCs both can be derived from monocytic cells. Moreover, monocytes and macrophages are known to specifically internalize clostridial C3 mono-ADP-ribosyltransferases (C3bot or C3lim) (Fahrer et al. 2010). C3bot from *Clostridium (C.) botulinum* as well as C3lim from *C. limosum* specifically modify the GTPases Rho A/B/C in the cytosol of these cells and thereby inhibit Rho-mediated signal transduction, and functions such as migration and phagocytosis. Here, we demonstrate that C3bot, C3lim as well as the fusion toxin C2IN-C3lim enter and intoxicate DCs in a time- and concentration-dependent manner. Thereby, the C3 toxins are efficiently internalized into immature as well as mature human DCs. Using stimulated emission depletion (STED) super-resolution microscopy localization of the internalized C3 protein into early endosomes was confirmed. In contrast, the mono-ADP-ribosyltransferase C2I from the binary *C. botulinum* C2 toxin was not taken up into DCs, indicating the specific uptake of C3 toxins into DCs (Fellermann et al. 2020). Moreover, in magnet-based scratch assays and via live-cell imaging, we could demonstrate that C3-treatment reduced important physiological functions of DCs like the migration, which is *in vivo* a prerequisite for antigen presentation in the lymph nodes. These findings extend the current knowledge about the pathophysiological role of the C3 exoenzymes as immune cell-modulating toxins. Additionally, this opens up novel opportunities to use the C3-toxins for local inhibition of unwanted DC functions, e.g. in auto-immune diseases or against transplant rejections. Finally, by genetic fusion of a green fluorescent protein (eGFP) to C3bot or its non-toxic mutant C3bot_{E174Q} it was demonstrated, that the uptake of the cargo model eGFP into DCs is strongly enhanced. Hence, C3bot and especially C3bot_{E174Q} can possibly be used as monocytic cell-selective drug delivery tools or vaccine carriers, what will be further investigated in the CRC1279.

Fahrer J, Kuban J, Heine K, et al (2010) Selective and specific internalization of clostridial C3 ADP-ribosyltransferases into macrophages and monocytes. Cell Microbiol 12:233–247.

Fellermann M, Huchler C, Fechter L, et al (2020) Clostridial C3 Toxins Enter and Intoxicate Human Dendritic Cells. Toxins (Basel) 12.

IgG binding to dead cells as a quantitative and tissue-based tool for liver cell intoxication

P. Erdösi^{1*}, J. Albin^{1*}, S. Dooley¹, Y. Quian², A. Teufel², M. Ebert³, A. Dropmann^{1,2}, S. Hammad^{1,4}

¹Heidelberg University, Molecular Hepatology Section, Department of Medicine II, Medical Faculty Mannheim, Mannheim, Germany

²Heidelberg University, Hepatology and Clinical Bioinformatics, Department of Medicine II, Medical Faculty Mannheim, Mannheim, Germany

³Heidelberg University, Department of Medicine II, Medical Faculty Mannheim, Mannheim, Germany

⁴South Valley University, Department of Forensic Medicine and Toxicology, Faculty of Veterinary Medicine, Qena, Egypt

* joint authorship

Introduction and objective: A frequent endpoint of liver toxicity is necrosis, apoptosis, and necroptosis-driven cellular death. Estimation of mild (solitary), early and subtypes of death requires a well-trained pathologist. To establish a sensitive, reproducible, quantifiable and pathologist-independent method for determining cellular death during acute liver intoxication.

Methodology: Adult male C57BL/6 wildtype mice were treated with one dose of carbon tetrachloride (CCl₄). To induced different grades of cellular damage, we treated the mice with doses of CCl₄ ranging from 0.25 to 0.8 g/kg, and sacrificed the mice 48h post injection. For a time course estimation, we treated the mice once with 1.6 g/kg CCl₄ and sacrificed them between 3h and 30 days post injection. Serum was collected for AST and ALT analysis. Serial liver sections were stained with HE and FITC labelled anti-mouse or -human IgG antibodies, and/or co-stained with TUNEL (apoptosis marker). Histopathological evaluation was performed from HE staining with a modified Ishak scoring system, estimating central necrosis and inflammation. The IgG signal and TUNEL positivity were quantified in confocal scans by ImageJ.

Results: Blinded Ishak scoring of HE stained slides revealed the highest scores at around 200mg/kg of CCl₄. This score (pathologist-dependent) correlated well with the IgG quantification, as well as with ALT and AST levels. Whereas Ishak scoring identifies necrotic cells only, IgG staining seems to detect apoptotic (Co-IF staining with TUNEL) and necrotic cells. In addition, early detection of cell death was possible 6h after CCl₄ injection, as indicated by the presence of IgG labelled cells, which is in agreement with the increase in ALT and AST levels. Spatial-temporal and dose quantification of anti-mouse IgG staining was in line with pathological evaluation of liver injury. First attempts on human non-diseased liver tissues indicated positive IgG signals in dying cells.

Conclusion and outlook: Our study shows that the anti-mouse-IgG antibody is binding with high affinity to necrotic and apoptotic cells and can be easily quantified. Therefore, the method can be used to detect early or mild toxicities that cannot be detected with regular staining methods. A single damaged cell is identifiable by this fluorescence based procedure, and co-IF for colocalization studies is feasible. Validation of the IgG marker in other mouse models i.e. Abcb4KO is ongoing. Further, preliminary results indicate that IgG also marks dead cells in human livers.

56

The explosive trinitrotoluene (TNT) induces carbonyl reductase in the blue mussel (*Mytilus* spp.) – a new promising biomarker for sea dumped war relicts?

J. S. Strehse¹, M. Brenner², M. Kisiela¹, E. Maser¹

¹Institute of Toxicology and Pharmacology for Natural Scientists, University Medical School Schleswig-Holstein Campus Kiel, Kiel, Germany

²Alfred Wegener Institute Helmholtz Centre for Polar and Marine Research, Biosciences - Ecological Chemistry, Bremerhaven, Germany

Question: Human carbonyl reductase (CBR1) plays an important role in the Phase I metabolism of many carbonyl group bearing xenobiotics. In addition, this enzyme metabolizes endogenous signal molecules such as steroid hormones and biogenic amines. The importance of carbonyl reductase could also be demonstrated in the model organism *Daphnia*, where it protected against oxidative and carbonyl stress, respectively. Recently, carbonyl reductase has been identified in the blue mussel *Mytilus* spp. While the mechanism of toxicity and carcinogenicity of TNT and its derivatives occurs through its capability of inducing oxidative stress in the target biota, we had the idea if TNT can induce the gene expression of carbonyl reductase in blue mussels and serves as a new biomarker for munitions in the sea.

Methods: Blue mussels (*Mytilus* spp.) were exposed to TNT in laboratory aquariums and in a field experiment at a munitions dumpsite. After treatment, mRNA was isolated from different mussel tissues for RT-PCR analysis. Gene specific primers were designed according to a bioinformatics analysis to infer the carbonyl reductase gene sequence and 18S RNA as the housekeeping gene, respectively, in *Mytilus* spp.

Results: As we did know before that TNT exhibits its toxic effects via oxidative stress, we could indeed show that TNT exposure resulted in a strong and concentration dependent induction of the carbonyl reductase gene in *Mytilus* spp. in both laboratory (Fig. 1) and in the field experiment (Fig. 2). These results are of high significance, since carbonyl reductase may now serve as the first biomarker for TNT exposure on a molecular level.

Conclusion: Millions of tonnes of munitions that have been dumped after wars pose a new threat to the seas worldwide, since the metal vessels corrode and toxic explosives (e.g. TNT) leak into the environment. Therefore, specific biomarkers are urgently sought

to detect TNT contaminations and to perform a risk assessment both for the ecosphere and the human sea food consumer. According to our finding that TNT induces the expression of the carbonyl reductase gene in *Mytilus* spp., we have identified the first biomarker for TNT exposure on a molecular level.

Fig. 1: Induction of the carbonyl reductase gene in *Mytilus* spp. gills after a 96-hour treatment with TNT. Agarose gel and densitometric analyses

Fig. 2: Induction of the carbonyl reductase gene in *Mytilus* spp. in a field experiment. (A) Agarose gels and (B) densitometric analyses

Fig. 1

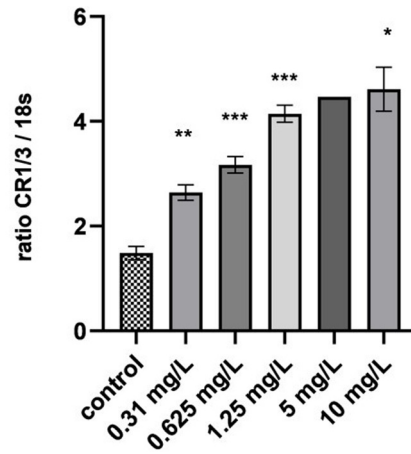
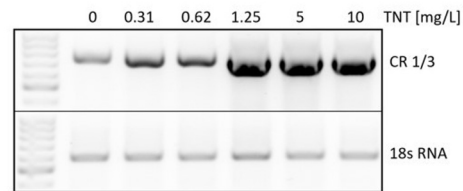
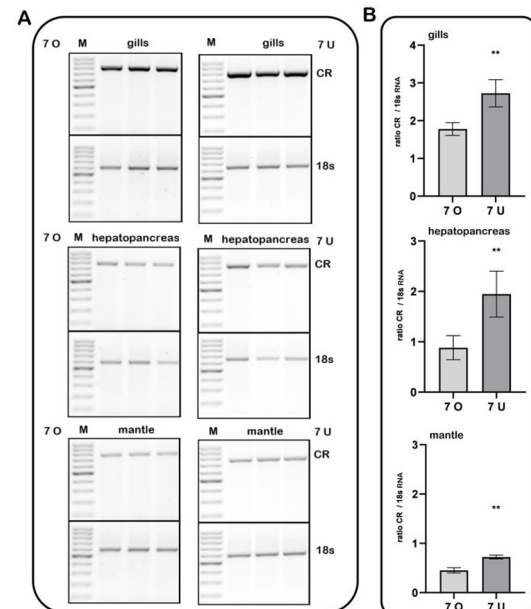


Fig. 2



57

A microfluidic thyroid-liver platform to investigate thyroid toxicities in humans and rats *in vitro*

J. Kühnlenz¹, D. Karwelat², M. Raschke², S. Bauer¹, H. Tinwell³, R. Bars³, T. Steger-Hartmann²

¹TissUse GmbH, Berlin, Germany

²Bayer AG, Pharmaceuticals Division, Investigational Toxicology, Berlin, Germany

³Bayer S.A.S., CropScience Division, Toxicology, Sophia Antipolis, France

The extrapolation of adverse effects observed in rat studies to human health continues to be a major challenge for toxicologists. Rodents, which are widely used for regulatory toxicity testing, are known to be particularly sensitive to chemical-induced perturbations of the thyroid hormone (TH) homeostasis which can be caused by direct effects or by the induction of liver enzymes. Compared to humans, their TH turnover is much higher due to shorter thyroxine (T4) half-lives. The understanding of the species-specific differences is key for the regulatory acceptance of the risk assessment. Human *in vitro* assays tackling only one particular mechanism of action cannot reflect the complex TH biology. To overcome this lack of complexity, the implementation of microfluidic microphysiological systems (MPS) offers a path forward, since they allow to recapitulate the physiological and the toxicological interaction of target organs.

Here, we present the connection of three-dimensional (3D) liver and thyroid organoids of both human and rat origin in a commercially available platform (TissUse's HUMIMIC Chip2). The thyroid models derived from respective primary tissues displayed an *in vivo*-like architecture and a release of *de novo* synthesized THs upon addition of thyroid stimulating hormone (TSH). Furthermore, the thyroid models allow to detect direct TH perturbation as demonstrated by a significant inhibition of TH secretion in response to the model compound methimazole. We also successfully established a human and rat 3D liver model generated from primary rat or human HepaRG hepatocytes. Both liver models reflected fundamental species differences, e.g. a predominant basal T4 metabolism via glucuronidation in the rat model versus T4 glucuronidation and sulfation in the human model. The application of chemical inducers like β -naphthoflavone and pregnenolone-16 α -carbonitrile increased TH metabolism in the rat model, but not in the HepaRG model. Finally, we successfully combined and co-cultivated the two organ models for more than two weeks.

Therefore, our system models the hepatic-thyroid axis within a single *in vitro* assay for two different species and thus presents a promising tool for the assessment of direct as well as indirect TH perturbations. These thyroid-liver-chips will allow to investigate similarities and differences of certain safety-related findings observed in different species and have the potential to significantly contribute to the 3R principles.

58

New aspects in deriving health based guidance values for bromate in swimming pool water

C. Röhl¹, M. Batke², G. Damm³, A. Freiberger⁴, T. Gebel⁵, U. Gundert-Remy⁶, J. Hengstler⁷, A. Mangerich⁸, F. Partosch⁹, T. Schupp¹⁰, K. M. Wollin¹¹, H. Foth¹²

¹Department of Environmental Health Protection, Neumünster, Germany

²Hochschule Emden/Leer, Emden, Germany

³Department of Hepatobiliary Surgery and Visceral Transplantation, Leipzig, Germany

⁴Bayer AG, Pharmaceuticals, Toxicology, Pathology and Clinical Pathologie, Wuppertal, Germany

⁵Federal Institute for Occupational Safety and Health, Dortmund, Germany

⁶Charité – Universitätsmedizin Berlin, Institute for Clinical Pharmacology and Toxicology, Berlin, Germany

⁷Leibniz Research Centre for Working Environment and Human Factors, Dortmund, Germany

⁸Department of Biology, Molecular Toxicology, Konstanz, Germany

⁹ITEM, Toxicology, Hannover, Germany

¹⁰University of Applied Science Muenster, Chemical Engineering, Steinfurt, Germany

¹¹Formerly Public Health Agency of Lower Saxony, Hannover, Germany

¹²University Halle, Institute of Environmental Toxicology, Halle, Germany

Question: Bromate classified as 1B carcinogen is a typical by-product occurring in drinking and swimming pool water after disinfection. The aims of this study were a) to evaluate the carcinogenic mode of action of bromate, b) to derive reliable levels of exposure by all routes under various scenarios of swimming, and c) to inform the derivation of cancer risk-related bromate concentrations in swimming pool water.

Methods: A comprehensive literature search was performed. Quality of the studies on genotoxicity and carcinogenicity were assessed by Klimisch criteria (Klimisch et al. 1997) and SciRAP tool (Beronius et al. 2018), respectively. Benchmark dose (BMD) modelling was performed using the modelling average mode in BMDS 3.1 and PROAST 66.40 (human cancer BMDL10; EFSA 2017). For the exposure, data from a wide range of sources were evaluated for their reliability. Different target groups (infants/toddlers, children and adults) and exposure scenarios (recreational, sportive swimmers, top athletes) were considered for oral, inhalation and dermal exposure. Exposure was calculated by frequency of swimming events and duration in water.

For illustration, cancer risk-related bromate concentrations in pool water were calculated for different target groups taking into account their exposure, using the hBMDL10 and a cancer risk of 10⁻⁵.

Results: There is convincing evidence from a multitude of studies that bromate induces clastogenic and aneugenic effects as well as oxidative DNA damage and DNA strand breaks formation *in vitro* and *in vivo* without discernible threshold. Hence, bromate may be considered a non-threshold carcinogen.

BMD modelling with model averaging for renal cancer studies (Kurokawa et al. 1983, 1986; DeAngelo et al. 1998) resulted in a median hBMDL10 of 0.65 mg BrO₃-/kg bw per day.

Evaluation in different age and activity groups revealed that top athletes had the highest exposure, followed by sportively active children, sportively active adults, infants and toddlers, children and adults. The predominant route of exposure was oral (73 - 98%, by swallowing water, followed by the dermal route (2 - 27%); inhalation route was insignificant (< 0.5%).

Conclusions: Accepting the same risk level for all population groups results in different guidance values due to the large variation in exposure. For example, for an additional risk of 10⁻⁵ the bromate concentrations would range between 0.011 for top athletes, 0.015 for sportive children and 2.1 mg/l for adults.

59

Inferring longitudinal cascades of mechanistic events in drug-induced liver injury from transcriptomic and histopathology data using sequential pattern and rule mining

A. Liu¹, A. Bender¹, J. Munoz-Muriedas²

¹University of Cambridge, Department of Chemistry, Cambridge, United Kingdom

²GSK, Stevenage, United Kingdom

The Adverse Outcome Pathway (AOP) framework aims to formalize knowledge on how molecular initiating events are linked to adverse outcomes, through key events on different biological levels. However, often the underlying toxicity mechanisms, in particular on intermediate cellular and tissue levels, are not completely understood and the relationship between changes on the molecular or cellular level and the adverse outcome are largely qualitative.

We aim to derive events in Drug-Induced Liver Injury (DILI) and quantify the association between these events in a data-driven manner. To do so, we use data from the TG-GATES database which contains information from single- and repeat-dose studies in rats on 156 compounds out of which many are known to be hepatotoxic. First, the dysregulation of individual genes, cellular pathways and serum marker levels is computed and sequences describing these changes over time are formulated for each compound-dose combination. We then derive events and cascades which are frequently observed in adverse conditions using sequential pattern mining and investigate association rules which provide insights on which events or a combination thereof are predictive for histopathology at a later timepoint. Among others, this identified fatty acid metabolism and NFkB signalling as events which are often followed by hepatic necrosis and inflammation, respectively.

Overall, this analysis aspires to contribute towards a computationally inferred, quantitative AOP for DILI by deriving mechanistic information on events preceding DILI, including their strength of association and longitudinal order.

Pharmacology – Ion channels and membrane transporters

60

Kcnt1 encoded sodium-activated potassium channels (**aka** Slack, Slo2.2 or KNa1.1) in ischemia/reperfusion-induced cardiac injury

A. Kuret¹, R. Ehinger¹, H. Bischof¹, A. Luczak¹, J. Adler¹, X. Zhou², R. Malli³, P. Ruth¹, R. Lukowski¹

¹Institute of Pharmacy, University of Tübingen, Department of Pharmacology, Toxicology and Clinical Pharmacy, Tübingen, Germany

²University Medical Centre Mannheim, First Department of Medicine, Mannheim, Germany

³Medical University of Graz, Gottfried Schatz Research Center, Chair of Molecular Biology and Biochemistry, Graz, Austria

Question: The sodium-activated potassium channel Slack (*sequence like a calcium-activated potassium channel, aka* Slo2.2, KNa1.1) encoded by *Kcnt1*, requires high intracellular sodium ions ([Na⁺]_i) for half-maximal channel activation. It has been hypothesized that Slack plays an important role during ischemic conditions, which result in cytotoxic increases in [Na⁺]_i. Here, we aim to identify the potential function of Slack channels in murine heart and cardiomyocytes (CMs) during ischemia and reperfusion (I/R)-induced myocardial damage.

Question: The sodium-activated potassium channel Slack (*sequence like a calcium-activated potassium channel, aka* Slo2.2, KNa1.1) encoded by *Kcnt1*, requires high intracellular sodium ions ([Na⁺]_i) for half-maximal channel activation. It has been hypothesized that Slack plays an important role during ischemic conditions, which result in cytotoxic increases in [Na⁺]_i. Here, we aim to identify the potential function of Slack channels in murine heart and cardiomyocytes (CMs) during ischemia and reperfusion (I/R)-induced myocardial damage.

Methods: Global and CM-specific Slack knockout mice (Slack KO, CM Slack KO) as well as their litter-matched controls were subjected to an *in vivo* model of acute myocardial infarction. Infarct size was measured at baseline, after mechanical conditioning and in response to pharmacological treatment with the cGMP-elevating compound cinaquat (CIN) or the mitoKATP-inhibitor 5-hydroxy-decanoate (5-HD). The expression and function of Slack in CMs was validated with real-time PCR and Western Blot approaches and by

using a genetically encoded FRET-based potassium ion indicator (GEPII) as well as patch-clamp technique.

Results: Global and CM-specific Slack KO mice showed an increased vulnerability to the I/R injury in comparison to their litter-matched controls. Accordingly, cardioprotection elicited by mechanical pre- and post-conditioning was attenuated in global and CM-specific Slack-deficient mice. While pharmacological elevation of cGMP with CIN reduced infarct size to a similar extent in CM-specific CTR and KO mice, conditional Slack mutant mice did not respond to co-treatment with 5-HD after ischemic preconditioning. Patch clamp recordings revealed reduced Slack KNa-inhibitor (*i.e.* chinidine and clofilium) sensitive outward currents in Slack-deficient CMs. Finally, GEPII-based monitoring revealed less accumulation of extracellular potassium ($[K^+]_{ex}$) in the supernatant of Slack KO CMs exposed to the membrane permeabilizing agent digitonin or the "specific" Slack activator nicosamide.

Conclusions: CM-specific Slack channels limit the I/R-induced myocardial injury in a mitoKATP-dependent manner *in vivo*. Electrophysiological and K^+ biosensor-based *in vitro* assays provide robust evidence for Slack-dependent changes in $[K^+]_{ex}$ on the plasma membrane of CMs. In sum, we suggest that Slack represents a novel modulator of key signalling pathways regulating K^+ in discrete CM compartments protecting the heart from I/R-induced damages.

61

KS0365 is a new and potent TRPV3 agonist

M. Maier¹, K. Hill¹, S. Olthoff¹, T. Magauer², L. Wein², M. Schaefer¹

¹University Leipzig, Medical Faculty, Rudolf Boehm Institute of Pharmacology and Toxicology, Leipzig, Germany

²Institute of Organic Chemistry and Center for Molecular Biosciences, Innsbruck, Austria

Ca^{2+} signaling mediated by the thermosensitive, non-selective, Ca^{2+} permeable transient receptor potential channel TRPV3 is assumed to play a critical role in regulating several aspects of skin functions, such as keratinocyte migration, skin barrier formation and wound healing. However, due to the lack of highly potent, selective and specific modulators of TRPV3, it still remains laborious to reliably study the function of TRPV3 in skin homeostasis. Most studies rely on the non-specific TRPV3 activator 2-APB, which additionally acts on a variety of other TRP channels, making it difficult to attribute 2-APB-evoked responses in native tissues to the TRPV3 channel.

Hereby we introduce a novel TRPV3 agonist KS0365, which was identified by screening a compound library and further characterized by Ca^{2+} assays, different Ca^{2+} and microscopy (TIRF, LSM) imaging approaches, electrophysiological studies, and migration assays. In fluo-4-assisted Ca^{2+} influx assays, KS0365 activated murine TRPV3 in the recombinant HEK_{TRPV3} and in the native mouse 308 keratinocyte (m308k) cell line more selectively, more potently, and with a higher efficacy compared to 2-APB. KS0365-evoked Ca^{2+} responses in m308k cells were inhibited by siRNA-mediated gene knockdown. Whole-cell patch-clamp recordings revealed that TRPV3 channels, activated by KS0365, responded with a slowly developing linear current characterized by a more dominant inward current compared to 2-APB activation. Having a closer look on the localization of recombinant TRPV3 in m308k cells by microscopy imaging, we found that TRPV3 is expressed in the leading edge. In a migration assay performed on m308k cells, KS0365 accelerated the scratch closure which was further accelerated by the co-stimulation with EGF and abrogated by ruthenium red and siRNA-mediated knockdown of TRPV3. The combination of migration assays together with Ca^{2+} imaging revealed that the increase in intracellular Ca^{2+} in response to KS0365 is higher in m308k cells located at the front of the scratch compared to cells located at the rear, as well as in the leading edge of the cell compared to the cell body.

Taken together, by applying the novel TRPV3 activator KS0365, we demonstrate that TRPV3 may play a role in wound healing, presumably by triggering Ca^{2+} influx with the most prominent signals in the leading edge of keratinocytes oriented towards the front of the scratch, thereby accelerating keratinocyte migration and scratch closure.

62

TRPA1 function in human pulmonary fibroblasts

F. Geiger¹, C. Staab-Weijnitz¹, T. Gudermann¹, A. Dietrich¹

¹Walther Straub Institute of Pharmacology and Toxicology, Member of the German Center for Lung Research (DZL), LMU-Munich Germany, München, Germany

²Comprehensive Pneumology Center, Member of the German Center for Lung Research (DZL), Helmholtz-Zentrum München, Munich, Germany, München, Germany

Transient receptor potential ankyrin 1 (TRPA1) is a non-selective Ca^{2+} permeable cation channel. While TRPA1 was mostly studied in neuronal cells, it was originally cloned from cultured human lung fibroblasts. TRPA1-mediated Ca^{2+} entry is evoked by exposure to several chemicals including allyl isothiocyanate (AITC) and inhaled components of cigarette smoke, suggesting a possible role of TRPA1 in progression of lung disease. However, a protective effect of TRPA1 activation in the development of cardiac fibrosis was proposed. Yet, the function of TRPA1 in transforming growth factor β 1 (TGF- β 1)-driven fibroblast to myofibroblast differentiation as well as the development of pulmonary fibrosis remains elusive.

TRPA1 expression and function was analyzed in cultured primary human pulmonary fibroblasts (HPF) obtained from three different donors before and after incubation with TGF- β 1. Transcriptome sequencing, qRT-PCR and immunoblotting were used to identify target genes on mRNA and protein levels. TRPA1 specific siRNAs were established to

assess the role of the channel in cell function during fibroblast myofibroblasts differentiation.

TRPA1 mRNA is highly expressed in HPF and levels were significantly reduced after adding TGF- β 1. Expression of fibrosis markers, e.g. alpha smooth muscle actin (α SMA), plasminogen activator inhibitor (PAI), fibronectin (FN1) and collagen (Col1a1), was increased after down-regulation of TRPA1-mRNA by siRNA targeting in HPF. Moreover, TGF- β 1 treatment of HPFs reduced Ca^{2+} entry evoked by the TRPA1 activator AITC, while increasing barrier function and contractile characteristics of the cells. Effects of siRNA-mediated knock-down of TRPA1 on cell contraction, migration and resistance of HPF will be quantified and compared to TGF- β 1-induced fibroblast myofibroblast differentiation.

Our results suggest an inhibitory function of TRPA1 channels in TGF- β 1-driven fibroblast to myofibroblast differentiation. Therefore, activation of TRPA1 channels might protect from the development of pulmonary fibrosis in patients.

63

Role of TRPM5 in triagonist-induced insulin secretion

P. Beyerle¹, T. Müller², T. Gudermann^{1,3,4}, N. Khajavi¹

¹Walther Straub Institute of Pharmacology and Toxicology, Faculty of Medicine LMU, München, Germany

²Institute for Diabetes and Obesity, Helmholtz Diabetes Center at Helmholtz Zentrum München, München, Germany

³German Center for Lung Research, München, Germany

⁴German Center for Cardiovascular Research, Munich Heart Alliance, München, Germany

Background: Diabetes currently affects 450 million individuals in the world. The limited effectiveness of anti-diabetic treatments is attributed to the complexity of the disease. Identification of a safe and effective medical intervention has emerged as a global priority. Recently, a unimolecular triagonist of balanced activity at three key receptors involved in metabolism and specifically the glucagon-like peptide 1 receptor (GLP-1R), glucose dependent insulinotropic receptor (GIPR) and glucagon receptor (GcgR) was reported as superior to conventional monoagonist therapy.

Question: Although the underlying mechanism by which GLP-1, GIP and glucagon act has been described, the specific downstream mechanism by which the enhanced efficacy of triagonist is delivered remains elusive. Glucagon and incretin receptors mainly induce Gs downstream signaling. Recent studies revealed that GLP-1R is capable of signaling through additional G-proteins including Gq. We have previously shown that a substantial portion of the increased insulin secretion induced by triagonist is Gq-dependent. Accumulating evidence suggested that activation of Gq signaling might lead to activation of a member of the transient receptor potential (TRP) ion channel superfamily known as TRPM5. In this study, we investigated the role of TRPM5 in triagonist-mediated responses.

Methods: Pancreatic islets were isolated from TRPM5^{-/-} and WT mice in C57BL/6J background. Gene expression was detected by real-time PCR. Insulin secretion was monitored by ELISA. Ca^{2+} transients were measured in fluo-4 loaded islets using confocal laser microscopy.

Results: Triagonist induced a significant increase in glucose-stimulated-insulin-secretion (GSIS) relative to control in pancreatic islets from WT mice. Confocal imaging of calcium transients revealed an increase in Ca^{2+} amplitude and synchronicity of Ca^{2+} oscillations in the presence of triagonist. Genetic inactivation of TRPM5 abolished triagonist-induced insulin secretion. Likewise, the TRPM5 blocker TPPO attenuated the stimulatory effect of triagonist in pancreatic islets.

Conclusion: Our data support the concept that Gq- and phospholipase C-dependent signaling pathways culminate in TRPM5 activation as a key component of triagonist-induced insulin secretion in murine pancreatic islets. These findings may explain the therapeutic benefit of triagonist treatment of diabetes mellitus and provide deeper mechanistic insight to further improve its efficacy.

64

The TRPV2 channel mediates Ca^{2+} -influx in red blood cells, dehydration and Δ 9-THC-induced decrease in osmotic fragility

A. Belkacemi¹, C. Fecher-Trost¹, R. Tinschert¹, D. Flormann², M. Malihpour¹, C. Wagner², M. R. Meyer¹, A. Beck¹, V. Flockerzi¹

¹Universität des Saarlandes, Experimentelle und Klinische Pharmakologie und Toxikologie, Homburg, Germany

²Universität des Saarlandes, Experimentalphysik, Saarbrücken, Germany

Transient receptor potential (TRP) cation channels, conserved in mammals, flies, fish, sea squirts, worms and fungi essentially contribute to cellular Ca^{2+} signalling. In this study we identified the transient receptor potential vanilloid (TRPV) 2 channel protein in mouse and human red blood cells (RBCs) using specific antibodies and mass spectrometry. Osmotic fragility was significantly increased in *Trpv2* KO RBCs accompanied by a compensatory decrease of the amount of proteins involved in hydration and by a possible impairment of the antioxidant protective system. TRPV2 currents and TRPV2-dependent Ca^{2+} entry were activated by the specific TRPV2 channel agonists cannabidiol or Δ 9-tetrahydrocannabinol in the presence of antagonists of cannabinoid receptor type 1 and 2 and were significantly reduced in *Trpv2* KO RBCs. Both cannabinoids changed the morphology and osmotic tolerance of the RBCs. Our data demonstrate that the TRPV2 channel is the specific

molecular target for cannabinoids in mouse and human RBCs mediating part of their protective effects.

65

HCS-microscopy monitoring of endogenous type-II PKA in sensory neurons identifies scorpion toxin MeuNaTxalpha-1 to sensitize nociceptors via Nav1.2

M. van Cann¹, A. Kuzmenkov², J. Isensee¹, A. Andreev-Andrievskiy³, S. Peigneur¹, G. Khusainov^{2,5}, A. Berkut², J. Tytgat⁴, A. Vassilevski^{2,5}, **T. Hucho**¹
¹Universität zu Köln, Translationale Schmerzforschung, Köln, Germany
²Shemyakin-Ovchinnikov Institute of Bioorganic Chemistry of the Russian Academy of Sciences, Moscow, Russian Federation
³Lomonosov Moscow State University, Moscow, Russian Federation
⁴KU Leuven, Toxicology and Pharmacology, Leuven, Belgium
⁵Moscow Institute of Physics and Technology (State University), Dolgoprudny, Germany

Introduction: In neuroscience, venoms are often analyzed for their modulation of electric activity. But neuronal plasticity greatly depends on intracellular signaling activity. We established how to analyze cultured primary sensory neurons on a single neuron level for modulation also of intracellular signaling activity such as endogenous type II PKA or ERK1/2 in using an automatized High Content Screening (HCS) microscopy approach.

Objectives: We set out to test venoms for their modulating activity of endogenous type II PKA signaling in primary sensory neurons, to purify the active toxin in rounds of monitoring and biochemical fractionation, and to characterize the mode of action.

Materials & methods: Venoms of various species such as scorpions, spiders, and anemones were tested on primary sensory neuron cultures of rat and mice. After varying time intervals, cells were fixed, permeabilized, and immunofluorescently labeled with antibodies against phosphorylation sites of type II PKA and ERK1/2. Single cell based intensities were acquired using a HCS-microscopy approach.

Results: We identified MeuNaTxalpha-1, a sodium channel-selective scorpion alpha-toxin from *Mesobuthus eupeus*, which affected both PKA-II and ERK1/2. Recombinant MeuNaTxalpha-1 showed identical activity to the native toxin on mammalian voltage-gated sodium channels expressed in *Xenopus laevis* oocytes and induced thermal hyperalgesia in adult mice. The effect of MeuNaTxalpha-1 on sensory neurons was dose-dependent and tetrodotoxin-sensitive. Application of inhibitors and toxin mutants with altered sodium channel selectivity demonstrated that signaling activation in sensory neurons depends on Nav 1.2 isoform. Accordingly, the toxin was more potent in neurons from newborn rats, where Nav 1.2 is expressed at a higher level.

Conclusion: Our results demonstrate that HCS microscopy-based monitoring of intracellular signaling is a novel and powerful tool to identify and characterize venoms and their toxins affecting sensory neurons.

Toxicology – Food Toxicology

66

The natural phenylpropene methyleugenol induces p53-mediated apoptosis in liver cells via the mitochondrial pathway

M. J. Carlsson¹, A. S. Vollmer², D. Heylmann², H. Damm¹, B. Rasenberger³, M. Christmann², J. A. Fuhlbrueck¹, S. Stegmüller¹, A. Cartus¹, J. Fahrer¹
¹TU Kaiserslautern, Food Chemistry and Toxicology, Kaiserslautern, Germany
²Justus Liebig University Giessen, Rudolf Buchheim Institute of Pharmacology, Gießen, Germany
³Universitätsmedizin Mainz, Toxicology, Mainz, Germany

Introduction: Methyleugenol (ME) is a naturally occurring secondary plant constituent and belongs to the group of phenylpropenes. It is part of the essential oils of different herbs and spices and is used in flavouring compounds and cosmetics. ME and its metabolite 1'-Hydroxymethyleugenol (OHME) have shown to be carcinogenic in rodent studies. In the liver ME is converted into OHME by different CYP450-enzymes and further converted into an unstable sulfo-species which decays into an DNA-reactive carbocation that forms two DNA-adducts. The induced cell death mechanisms have not been characterised yet.

Methods: HepG2 cells and primary murine hepatocytes (pMH) were used in the present study. DNA-adduct formation was examined via mass spectrometry. Gene expression was analysed with qPCR and Western Blot was used for detection of protein expression. Caspase cleavage and activity was examined by Western Blot and Caspase 3/7 activity assay. Cell viability was tested with resazurin assay and cell death was characterised with annexinV-FITC/PI-staining by flow cytometry. Mdm2 was inhibited by Nutlin3a and caspases by zVAD-FMK. Due to the metabolic profile of the employed cells OHME, instead of ME was used throughout the study.

Results: OHME forms two different DNA-adducts in a time and dose dependent manner, with N2-(trans-methylisoeugenol-3'-yl)-2'-deoxyguanosin as predominantly formed adduct. Gene expression analysis shows the time dependent induction of pro-apoptotic Bcl2-family members, like Noxa and Puma as well as other relevant p53 target genes like p21 and Mdm2. Western Blot showed an accumulation of p53. Cell viability is reduced in dose and time dependent manner and the occurring cell death shows characteristic apoptotic features in annexinV-FITC/PI-staining. Strong induction of caspase 9 and 3 cleavage and a lack of caspase 8 cleavage supports the assumption of mitochondrial apoptosis as the

induced cell death pathway. Caspase inhibition via zVAD-FMK results in an inhibition of OHME induced effects. Activation of the p53-axis via Mdm2 inhibition leads to a strong induction of p21 and a higher apoptosis rate.

Conclusion: The study suggests that the main OHME induced cell death pathway is mitochondrial apoptosis mediated by p53. The displayed caspase cleavage pattern argues for mitochondrial apoptosis. Induction of p53-axis via Mdm2 inhibition as well as caspase inhibition confirm these results.

67

2-Methylfuran - metabolic activation and adduct formation

V. Kirsch¹, E. Richling¹
¹Technical University of Kaiserslautern, Food Chemistry and Toxicology, Kaiserslautern, Germany

Objectives: 2-Methylfuran (MF) occurs mainly in coffee as a head induced contaminant [1]. *In vivo* studies showed a distribution primarily to the liver where toxicological effects as necrosis were overserved [2]. The underlying mechanism is assumed to be a metabolic activation of MF to acetylacrolein (AcA), which reacts for example with amino acids [3]. The aim of our study was to characterise the enzymatic conversion of MF to AcA using liver microsomes from rats (RLM) and humans (HLM) investigating species-specific differences. Additionally, incubations with single cytochrome P450 enzymes (supersomes) were performed to identify responsible enzyme(s). Due to the reactivity of AcA, after formation it was scavenged with Nε-acetyl-L-lysine (AcLys).

Material & methods: The adduct of AcLys and AcA, AcLys-AcA, was synthesised and characterized. Likewise, the product of the furan analogue *cis*-1,2-buten-1,4-dial (BDA), AcLys-BDA, was synthesised to serve as internal standard. MF (10-750 µM) was incubated with RLM or HLM (1.5 mg/mL) as well as supersomes (CYP P450 1A2, 2A6, 3A4, 2C9, 2D6 or 2E1; 120 nM) for one to 120 min. Afterwards, the enzymes were precipitated and AcLys-AcA as well as AcLys-BDA (internal standard) determined in the supernatant by HPLC-ESI-MS/MS in MRM mode.

Results: MF was converted by RLM, HLM and CYP 2E1 to AcA in a time and dose dependent manner. The activation of MF was more pronounced in HLM than RLM. Within the selected supersomes, CYP 2E1 revealed to be the key enzyme for the metabolic activation of MF - analogous to the enzymatic conversion of furan to BDA [4].

Conclusion: The oxidative ring opening of MF as phase I of the xenobiotic metabolism results in the α,β-unsaturated carbonyl, namely AcA, an intermediate highly reactive towards nucleophilic cell components such as proteins and DNA [5]. Hence, the formation of such adducts is crucial to investigate for the usage as biomarkers and the risk assessment of the ubiquitously occurring substance MF in food.

- [1] A. Becalski *et al.*, *Journal of Food Composition and Analysis* **2016**, *47*, 113-119.
 [2] S. Gill *et al.*, *Toxicologic Pathology* **2014**, *42*, 352-360.
 [3] V. Ravindranath *et al.*, *Science* **1984**, *224*, 884-886.
 [4] L. A. Gates *et al.*, *Drug Metabolism and Disposition* **2012**, *40*, 596-601.
 [5] L. A. Peterson *et al.*, *Chemical Research in Toxicology* **2006**, *19*, 1138-1141.

68

Food safety research and risk assessment of submicro- and nanoplastics

H. Sieg¹, M. Paul¹, V. Stock¹, L. Böhmert¹, A. Braeuning¹
¹German Federal Institute for Risk Assessment, Food Safety, Berlin, Germany

The topic of microplastics has been increasingly researched due to the growing public interest in plastic waste and its possible transfer into the human food chain with unknown impact on human health. Microplastics is defined as polymer particles of different materials in a size range between 1 µm (0.001 mm) and 5 mm. Although, methodological challenges still exist for these particles, there have been scientific investigations, to get a clearer view on its intestinal toxicity. Particles bigger than 1.5 µm are unlikely to be bioavailable and effects are only detected in overload situations, decades above realistic exposure scenarios. The situation for particles smaller than 1 µm, however, is much more challenging.

The BfR conducts research projects to compare microplastic particles of food-relevant materials (polyvinylchloride, melamin resin, metacrylate, polylactide, polystyrene) with particles with sizes below 1 µm, down to 25 nm. Cellular particle uptake and transport over the intestinal barrier as well as toxicological mechanisms are investigated using human *in vitro* cell models. Aim is the quantification of cellular uptake and the investigation of possible mechanisms which could have an impact on human health, to achieve a better understanding of the risks which could be caused by submicro- and nanoplastic particles. A special focus lies on the material differences between the broad spectrum of different plastic materials.

According to experiences from nanotoxicology, an increased uptake and biodistribution can be possible for smaller particles in the submicro- and nano-range. While no intentionally produced nanoplastics are known, it is plausible that these particles can emerge from bigger plastic particles by weathering and decomposition, although quantitative investigations are very limited due to insufficient analytical methods for these small polymer particles. The fate of such particles remains still unclear, making it necessary to investigate particles below 1 µm in size in toxicological approaches. This talk

will give an overview about micro- and nanoplastics research, the state of knowledge and the approaches for risk assessment.

69

Pyrrrolizidine alkaloids induce different transcription patterns in rat liver, lung, and kidney

J. Buchmüller¹, J. Ebmeyer¹, H. Sprenger¹, J. D. Rasinger², J. Hengstler³, D. Schaudien⁴, O. Creutzenberg⁴, A. Braeuning¹, **S. Hessel-Pras¹**

¹German Federal Institute for Risk Assessment, Food Safety, Berlin, Germany

²Institute of Marine Research (IMR), Bergen, Norway

³IfADo, Dortmund, Germany

⁴Fraunhofer-Institut für Toxikologie und Experimentelle Medizin ITEM, Hannover, Germany

Objectives: Pyrrolizidine alkaloids (PAs) are secondary plant metabolites synthesized against herbivores. PAs occur in more than 6,000 plants worldwide. Humans and livestock can be intoxicated by the uptake of PA-contaminated food and feed. PA poisoning can lead primarily to severe liver damage, but the lung can also be affected as a secondary target organ. In the last years, molecular PA-induced mode of action was often elucidated using hepatic *in vitro* models. However, there is still a knowledge gap regarding the effects of PAs in human-relevant doses in a whole organism. Therefore, we conducted a subacute 28 days study in rats using different PAs in human-relevant doses and examined effects on liver, lung, and kidney gene expression patterns.

Materials & methods: Male rats were treated orally with six different PAs echimidine, heliotrine, senecionine, lasiocarpine, senkirkine and platyphylline in the doses 0.1, 0.33, 1.0 and 3.3 mg PA per kg body weight per day over 28 days. Organ RNA was isolated for whole genome microarray analysis. Possible damages of the organs were examined histopathologically. Hepatotoxicity was also assessed by analyzing aspartate (AST) and alanine aminotransferase (ALT) activity in blood plasma.

Results: All animals showed no signs of intoxication neither in the blood plasma levels of ALT and AST nor on histopathological examination. Whole-genome microarray analyses revealed effects only in the high-dose treatment groups. After software-based pathway analysis of differential regulated genes, PAs induced hepatic gene expression changes associated with cell cycle regulation processes and DNA damage response in animals treated with heliotrine, senecionine and senkirkine. In lungs, pathways involved primarily in immune response of the cells were predicted to be regulated in the animals exposed to echimidine, heliotrine and senecionine. For kidney, microarray analysis was exemplarily conducted for the highest dose of senecionine or senkirkine. However, no PA-induced changes in gene expression were identified.

Conclusion: In this *in vivo* study, molecular effects of PAs involved in the induction of hepato- and pneumotoxicity were investigated for the first time. Genotoxicity- and inflammation-associated pathways were identified in liver and lung, respectively. In the kidney, no changes in gene expression were identified. This leads to new insights into the PA-induced toxicity in liver and lung and shows different modes of action in both organs.

70

Structure-dependent genotoxicity and cytotoxicity of eleven pyrrolizidine alkaloids in HepG2 cells with CYP3A4 overexpression

M. Haas¹, K. Wirachowski¹, J. H. Küpper², D. Schrenk¹, J. Fahrer¹

¹Technical University of Kaiserslautern, Food Chemistry and Toxicology, Kaiserslautern, Germany

²Brandenburg University of Technology Cottbus-Senftenberg, Molecular Cell Biology, Brandenburg, Germany

Introduction: Pyrrolizidine alkaloids (PAs) are secondary metabolites that occur as contaminants in various plant-based foods and dietary supplements. Following metabolic activation by CYP450 enzymes, PA cause hepatotoxicity and induce DNA damage that can lead to the development of liver tumours. Several lines of evidence suggest that PAs are not equally toxic and differ in their genotoxic and cytotoxic potential, which is important for their risk assessment in food and phyto-pharmaceuticals.

Objectives: The aim of the study was to detail the relative genotoxic and cytotoxic potential of eleven pyrrolizidine alkaloids in human liver cells depending on their structure and degree of esterification.

Material & Methods: CYP3A4 overexpressing HepG2 cells were used for metabolic activation of PAs. The cells were incubated with eleven different PAs for 24 h or 72 h. The cytotoxic effects of PAs were determined by the resazurin viability assay and EC50 values were calculated to assess the relative cytotoxicity. The genotoxic potential was investigated using western-blot analysis of the DNA damage markers γ H2AX and p53. Data were subject to BMD modelling via PROAST software to derive BMD values for assessing the relative genotoxicity.

Results: In general, monoesters such as lycopsamine display the lowest and cyclic diesters including lasiocarpine the strongest cytotoxic effects. The determined EC50 values of the tested PAs are in a broad range from 4 μ M up to 500 μ M and above, with lowest determined EC50 values for di-esters and the highest for mono-esters. Additionally the results show a structure-dependent cytotoxicity. Furthermore, a concentration-dependent formation of γ H2AX and p53 was observed, which was also structure-dependent and most pronounced for di-esters and cyclic esters. The lowest BMDL values ranging from 0.2 – 0.8 μ M were obtained for retrorsine, lasiocarpine and echimidine.

Conclusion: The results show a concentration- and structure-dependent toxicity based on the degree of esterification. In addition, p53 was revealed as a similarly sensitive marker of genotoxicity as γ H2AX. Our data support the view to classify PAs according to their relative potency, which is relevant for their risk assessment.

71

Decrease of DNA integrity by topoisomerases poisoning effects of secondary plant metabolites

L. Müller¹, L. Schütte¹, M. Esselen¹

¹Westfälische Wilhelms-Universität Münster, Institute of Food Chemistry, Münster, Germany

DNA topoisomerases are essential nuclear enzymes, which are highly associated with DNA integrity. If the catalytic process of these enzymes is disturbed by endogenous or exogenous noxious agents, genotoxic, mutagenic, or even lethal consequences for the cell are most likely. For this reason, topoisomerase poisons and inhibitors are used as cytostatic agents in cancer therapy. [1,2] In addition to the mentioned clinical use, several topoisomerase poisons such as quercetin, genistein and (-)-epigallocatechin gallate have already been characterised in common foods. [3,4] In spite of low concentrations in the mg/kg scale, it must be considered that these substances are consumed daily and, consequently, an accumulative effect may occur. The presented study is therefore focusing on the effects of nevadensin, a major polyphenol of basil, on human topoisomerase I activity and subsequent cell response. Firstly, the influence on topoisomerase I activity was examined with the relaxation assay, a cell-free pre-test. In this *in vitro* test system, a partial inhibition of topoisomerase I activity was determined. To clarify the underlying mode of action of the topoisomerase inhibitory properties of nevadensin the "isolating *in vivo* complexes of enzyme to DNA" assay (ICE assay) was performed in HT29 cells. Interestingly, nevadensin was identified as a selective topoisomerase I poison. Based on this finding the impact of nevadensin on DNA integrity was focused. Therefore, the Comet assay as well as cell cycle analysis were performed. Besides an increase of DNA strand breaks a strong arrest in the G₂/M cell cycle phase and caspase activation after nevadensin treatment was found. In sum, the results assume that cell cycle disruption and apoptotic events play key roles in the cellular response to topoisomerase I poisoning caused by nevadensin in HT29 cells.

[1] Pommier Y, Pourquier P, Fan Y, Strumberg D.; Mechanism of action of eukaryotic DNA topoisomerase I and drugs targeted to the enzyme. (1998). *Biochim Biophys Acta* 1400,83-105.

[2] Wang J. C.; DNA topoisomerases. (1996). *Annu Rev Biochem* 65,635-692.

[3] Pommier Y.; DNA topoisomerase I and II in cancer chemotherapy: Update and perspectives. (1993). *Cancer Chemother Pharmacol* 32,103-108.

[4] Esselen M., Barth S. W.; Food-borne topoisomerase inhibitors: Risk or benefit. (2014) *Advances in Molecular Toxicology* (Bd 8).

Pharmacology – G-protein coupled receptors

72

The role of (xeno)estrogens and GPER1/GPR30 receptor for centrosome amplification and chromosomal instability *in vitro*

M. Bühler¹, G. Schönfelder^{1,2}, M. R. Schneider¹, **A. Stolz-Ertych³**

¹Bundesinstitut für Risikobewertung, Zentralstelle zur Erfassung und Bewertung von Ersatz- und Ergänzungsmethoden zum Tierversuch, Berlin, Germany

²Charité – Universitätsmedizin Berlin, Berlin, Germany

³German Federal Institute for Risk Assessment, Experimental Toxicology and ZEBET, Berlin, Germany

Introduction: Recent studies reported GPER to promote the development and progression of colon cancer upon exposure of (xeno)estrogens by affecting cellular proliferation, migration and invasion. However, the underlying molecular mechanisms of this (xeno)estrogen/GPER-induced risk potential are widely unclear.

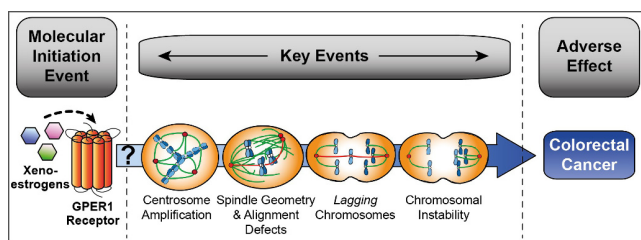
Objectives: Given a largely unexplored connection between (xeno)estrogens, GPER and colon tumorigenesis on the one hand, and the widely accepted colon cancer-prone lesions, i.e. whole chromosome instability (w-CIN) and supernumerary centrosomes on the other hand, we aim to uncover a potential link between (xeno)estrogens, GPER, centrosome amplification and w-CIN *in vitro*.

Materials & Methods: Normal colon and colorectal cancer-derived cell lines were treated with 17 β -estradiol, bisphenol A or diethylstilbestrol in the presence or absence of (active) GPER1 using gene-specific RNAi or selective GPER antagonists. Subsequently, numerical and structural abnormalities of the cellular centrosome were visualized by using state-of-the-art high resolution fluorescence microscopy and live cell imaging. Genome instability was evaluated by w-CIN-analyses using chromosome counting from metaphase spreads following karyotype analyses.

Results: Our results show that the (xeno)estrogen/GPER-axis triggers the abnormal formation of centrioles, which represent the functional subcomponents of each centrosome. These defects in centrosome integrity are associated with centrosome amplification and the generation of abnormal mitotic spindles, finally causing chromosome segregation defects during mitosis, which manifest in whole chromosomal instability.

Conclusions: Our results significantly contribute to the understanding of the mode-of-action of (xeno)estrogens with regard to colon tumorigenesis, that involves GPER-mediated centrosome amplification and genome instability.

Fig. 1



73

Gα₃ proteins are essential for brown and white adipocyte function on control diet

V. Leiss¹, J. Kerner¹, T. Gnad², A. Pfeifer², B. Nürnberg¹

¹Institute of Experimental and Clinical Pharmacology and Pharmacogenomics, Department of Pharmacology, Experimental Therapy and Toxicology, Tübingen, Germany
²Institut für Pharmakologie und Toxikologie, Bonn, Germany

Question: G proteins transduce signals from ligand-activated G protein-coupled receptors to intracellular target proteins. Among the three highly homologous inhibitory G proteins (Gα₁-Gα₃) the Gα₂ protein isoform is predominantly and ubiquitously expressed, whereas Gα₃ represents a minor isoform. The role of adipocyte Gα₂ was shown recently (Leiss *et al.*, *Mol. Metab.* 2020), whereas Gα₃-dependent pathways in brown and white adipocytes have to be deciphered.

Materials & methods: Using the tamoxifen-inducible Cre-loxP system, adipocyte-specific *Gnai3*-deficient mice (*Gnai3*^{Cre/loxP}) were generated and challenged with a control diet (CD) or a 45% high fat diet (HFD). In these mice, we analyzed the impact of Gα₃ deficiency on body weight gain, body composition and glucose homeostasis in comparison to littermate controls.

Results: Despite significantly reduced Gα₃ protein levels in both brown (BAT) and white adipose tissue (WAT) compartments, no obvious phenotype was observed in *Gnai3*^{Cre/loxP} mice on HFD in comparison to littermate controls. Body weight gain, glucose tolerance, fat cell size and adipocyte-driven lipolysis were similar in *Gnai3*^{Cre/loxP} and control animals. In contrast, although body weight gain on CD was comparable in *Gnai3*^{Cre/loxP} and control mice, our data indicate decreased BAT and WAT masses and a slightly improved glucose tolerance of *Gnai3*^{Cre/loxP} animals.

Conclusion: Whereas lack of Gα₃ had no effect on HFD, our data suggest an isoform-specific role of adipocyte Gα₃ for normal brown and white adipocyte function on CD. We speculate that Gα₂ and Gα₃ have isoform-specific functions in adipocytes: adipocyte Gα₂ is relevant for increased weight gain under excessive food intake by reducing oxygen consumption and inhibiting cAMP synthesis and consequently lipolysis, whereas adipocyte Gα₃ is mainly responsible for controlling fat storage under normal dietary conditions.

Leiss V, Schönsiegel A, Gnad T, Kerner J, Kaur J, Sartorius T, Machann J, Schick F, Birbaumer L, Häring HU, Pfeifer A, Nürnberg B. Lack of Gα₂ proteins in adipocytes attenuates diet-induced obesity. *Mol Metab.* 2020 Oct;40:101029. doi: 10.1016/j.molmet.2020.101029.

74

Illuminating the signaling enigma of Carvedilol

T. Benkel¹, M. Zimmermann², S. Monteleone³, V. Lim³, N. Pavlaki⁴, D. Malan⁵, E.

Matthees⁶, M. Szpakowska⁷, E. Miess⁸, J. Zeiner¹, F. Häberlein¹, K. Simon¹, J. Gomeza¹, A. Inoue⁹, S. Schulz⁹, A. Chevine⁹, C. Hoffmann⁹, P. Sasse⁹, V. Nikolaev⁴, P. Kolb⁵, M. Waldhoer², E. Kostenis¹

¹University of Bonn, Institute of Pharmaceutical Biology, Bonn, Germany

²InterAx Biotech GmbH, Villingen, Switzerland

³Philipps-University Marburg, Pharmaceutical Chemistry, Marburg, Germany

⁴University Medical Center Hamburg-Eppendorf, Institute of Experimental Cardiovascular Research, Hamburg, Germany

⁵University of Bonn, Institute of Physiology I, Bonn, Germany

⁶University Hospital Jena, Institute for Molecular Cell Biology, Jena, Germany

⁷Luxembourg Institute of Health, Department of Infection and Immunity, Esch-sur-Alzette, Luxembourg

⁸University Hospital Jena, Institute of Pharmacology and Toxicology, Jena, Germany

⁹Tohoku University, Graduate School of Pharmaceutical Science, Sendai, Germany

Question: Carvedilol is classified as a third generation β-blocker associated with survival benefits for patients suffering from heart failure in early clinical trials¹. These benefits are, in part, ascribed to its unique signaling mechanism at the β₂ adrenergic receptor (β₂AR) subtype, frequently designated as “arrestin-biased signaling”². A central tenet of the above signaling paradigm is that both G proteins and arrestins are viewed as independent transducers, each transmitting receptor signals in their own right. In contrast to this purported mode of action, recent literature³ and our own unpublished observations

indicate that Carvedilol does indeed signal, but relies on a G protein-driven, arrestin-scaffolded mechanism to do so.

Methods: In an attempt to resolve the above controversy, we analyzed the molecular underpinnings of Carvedilol’s mode of action using different cellular systems (immortalized and primary) along with a variety of cell biological and signaling assays. We examined canonical G protein interaction and signaling using mini G proteins from various Gα families, EPAC-based FRET sensors and TR-FRET-based cAMP accumulation assays, phosphorylation of receptor proximal sets of serine/threonine residues within the carboxy-terminal tail, recruitment of arrestin-2 and -3 in the absence and presence of G protein-coupled receptor kinases, phosphorylation of ERK1/2-MAPkinases, internalization, but also global cell activation, cAMP production and beating frequency in rodent neonatal and adult cardiomyocytes.

Results and Conclusions: Our results provide both a compelling molecular explanation for the enigmatic Carvedilol pharmacology in particular, and a deeper understanding of the mechanisms of β-blocker action in general. Because β-blockers are widely used to prevent, treat or improve cardiac function in cardiovascular diseases such as cardiac failure, we expect our findings to be of prime importance for choosing the appropriate β-blocker medication and for devising future therapeutic strategies that intend to modulate the function of this relevant adrenergic receptor subfamily.

References

1 Poole-Wilson PA *et al.*, *Lancet.* 2003 Jul 5;362(9377):7-13. doi: 10.1016/S0140-6736(03)13800-7.
2 Wisler JW *et al.*, *Proc Natl Acad Sci U S A.* 2007 Oct 16;104(42):16657-62. doi: 10.1073/pnas.0707936104. Epub 2007 Oct 9.

3 Grundmann M *et al.*, *Nat Commun.* 2018 Jan 23;9(1):341. doi: 10.1038/s41467-017-02661-3.

75

Investigating the impact of the sphingosine-1-phosphate-receptor-1 on hemostasis

C. Tolksdorf^{1,2}, R. Wolf^{1,2}, B. Brinschwitz^{1,2}, T. Janker¹, G. Jedlitschky¹, E. Moritz^{1,2}, B. H. Rauch^{1,2}

¹University Medicine Greifswald, Department of General Pharmacology, Greifswald, Germany

²DZHK (German Centre for Cardiovascular Research), Partner site Greifswald, Greifswald, Germany

Objective: Sphingosine-1-phosphate (S1P) is a versatile lipid mediator concerting inflammatory cellular responses. Platelets produce and upon activation release large amounts of S1P, which can bind to five G-coupled receptors (S1PR₁₋₅). Besides its key role in inflammation, S1P functions in both activation of platelets and affecting coagulation processes are under debate. However, the impact of the respective S1P receptors remains to be elucidated. Thus, we investigated the effects of specific agonists and antagonists for each of the S1PRs 1-5 on platelet aggregation and thrombin generation with a particular focus on S1PR₁.

Methods: Platelet aggregation was determined in platelet-rich-plasma (PRP) from healthy volunteers by light transmission aggregometry (LTA). Thrombin generation was quantified by calibrated automated thrombography (CAT). Cytosolic Calcium (Ca²⁺) was determined in washed platelets by fura-2-fluorescence.

Results: Incubation of PRP with both agonists or antagonists for each of the S1PRs 1-5, respectively, did not affect platelet aggregation directly. When platelets were stimulated with ADP (2.5 μM), the extent of activation weakens over a time period of 2 h by up to 40%. Preincubation of PRP with the S1PR₁ agonist CYM5442 (10 μM) prior to stimulation with ADP did maintain and even elevate the time-dependent extent of ADP-induced platelet aggregation for up to 1.5 h. This effect was reversed in part by the specific S1PR₁ antagonist Ex26. None of the compounds for the other S1PRs 2-5 showed comparable platelet responses modifying effects. The time-dependent thrombin generation measured by CAT was accelerated by incubation of PRP with ADP (5 μM) or collagen (5 μg/ml). Coincubation with agonists for S1PRs 1, 3 and 4 reduced the time to peak of thrombin formation for collagen and S1PR₄ activation shortened the lag time for ADP-enhanced thrombin formation. However, overall thrombin generation was not affected. In addition, platelet Ca²⁺-signals were slightly decreased by preincubation of platelets with the S1PR₁ agonist CYM5442 and resulted in a markedly faster Ca²⁺-influx evoked by ADP.

Conclusion: Activation of S1PR₁ maintains platelet responses to agonists such as ADP, fastens thrombin generation and accelerates Ca²⁺ influx. Consequently, S1P may play an important role in the fine tuning of the processes of hemostasis. This may become particularly relevant under conditions of elevated S1P levels such as during inflammation.

76

cAMP nanodomains at G protein-coupled receptors

S. Anton¹, I. Maiellaro², C. Konrad¹, J. Möller¹, A. Bock¹, M. Lohse^{1,3}

¹Max Delbrück Center for Molecular Medicine, Berlin, Germany

²University of Würzburg, Institute of Pharmacology and Toxicology, Würzburg, Germany

³ISAR Bioscience, Planegg, Germany

G protein-coupled receptors (GPCRs) are therapeutically relevant membrane proteins that relay extracellular stimuli (e.g. from neurotransmitters and hormones) into specific cellular

functions by modulation of second messengers such as cAMP. Cells express many different GPCRs and can spatialize GPCR signals to exert precise control over complex cell functions. However, it is entirely unknown how spatial information is encoded in GPCR signals and how cells orchestrate such spatial information from different GPCRs by using only very few diffusible second messengers. Here we show that picomolar glucagon-like peptide 1 (GLP-1) exclusively generates a GLP-1 receptor-associated cAMP pool that does not equilibrate with other cellular cAMP compartments. Moreover, this cAMP compartment is protected from cAMP influx originating from β -adrenergic receptors. Using novel GLP-1 receptor-targeted cAMP sensors, i.e. *GPCR-nanorulers*, we show that cAMP levels gradually decrease at nanometer distances from the receptor. This cAMP nanodomain exclusively activates nanodomain-anchored protein kinase A, thereby constituting a self-sufficient GPCR signalosome. In summary, we provide direct evidence for GPCR-associated cAMP nanodomains and propose that cells use those cAMP nanodomains to exert spatial control over GPCR signals.

77

Revised PTH1R biosensors with improved assay window enable monitoring of activation and modulation

K. Nemeč¹, A. Isbilir¹, H. Schihada^{2,3}, E. O. Grushevskiy¹, I. Maiellaro^{4,3}, M. Lohse^{3,1}

¹Max Delbrück Center for Molecular Medicine, Berlin, Germany

²Karolinska Institutet, Section of Receptor Biology & Signaling, Stockholm, Sweden

³University of Würzburg, Institute of Pharmacology, Würzburg, Germany

⁴University of Nottingham, School of Life Sciences, Queen's Medical Centre, Nottingham, United Kingdom

G-protein-coupled receptors (GPCRs) are the largest membrane protein family. They regulate a plethora of cellular functions and represent the target of around 40 % of marketed drugs. To develop new and more specific drugs is crucial to understand their mode of activation and modulation.

The binding of a ligand induces a change in the conformation of its cognate receptors. Tagging the receptor at conformation-sensitive sites with fluorescent proteins represents a valuable method for monitoring the activation of GPCRs in living cells. Different receptor biosensors have been optimized based on fluorescence or bioluminescence resonance energy transfer- (FRET or BRET)^{1,2}, and more recently single fluorophore (SF)³-sensor design.

Here we focus on the parathyroid hormone 1 receptor (PTH1R), a class B GPCR, an important regulator of mineral ion homeostasis and bone metabolism⁴.

Using prototypical PTH1R FRET-based biosensor we generated two new biosensors. In detail - we exchanged cyan and yellow fluorescent tags with 1) more photostable and bright variants - mTurquoise2 and mCitrine, 2) with the single fluorophore cpGFP obtaining PTH1RcpGFP. To characterize them, we used advanced microscopy methods and a plate reader to look at their signal amplitude, kinetics, and capability for use in high throughput screenings (HTS).

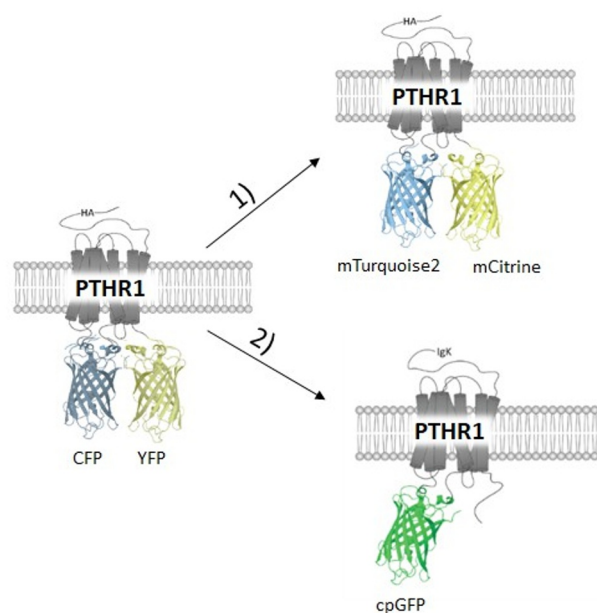
We demonstrate that both new biosensors have improved, two times bigger dynamic range and allow us to monitor activation processes in single and HTS format, while the kinetic properties and potency stay unchanged. Both sensor variants are unique among known class B GPCR biosensors - PTH1R FRET biosensor is first in class B, which activation is able to monitor in HTS format, while PTH1RcpGFP is first for which was showed that SF design works also for class B GPCRs.

Thus, revised biosensors will be of fundamental importance in the further investigation of activation and modulation of PTH1R, and may facilitate drug design.

References

1. Vilardaga, J. P. et al. (2003) *Nature biotechnology*, 21(7), 807-812.
2. Schihada, H., et. al. (2018) *Communications biology*, 1(1), 1-8.
3. Patriarchi, T., et. al. (2018) *Science*, 360(6396).
4. Cheloha, R. W., et. al. (2015). *Nature Reviews Endocrinology*, 11(12), 712.

Fig. 1



Pharmacology – Immunopharmacology inflammation anti-infectives-Session I - Functional characterization of immunopharmacological drugs

78

C81 prevents the inflammatory activation of endothelial cells and impairs leukocyte-endothelial cell interactions by interfering with the TNF1-NFκB activation cascade

G. M. Krishnathas¹, B. Strödeke², L. Mittmann³, T. Zech¹, C. Reichel³, S. Rösser⁴, T. Schmid⁴, S. Knapp⁵, S. Müller⁵, F. Bracher², R. Fürst¹, I. Bischoff-Kont¹

¹Goethe University Frankfurt, Institute of Pharmaceutical Biology, Frankfurt am Main, Germany

²Ludwig Maximilian University of Munich, Department of Pharmacy – Center for Drug Research, München, Germany

³Ludwig Maximilian University of Munich, Department of Otorhinolaryngology and Walter Brendel Centre of Experimental Medicine, München, Germany

⁴Goethe University Frankfurt, Institute of Biochemistry I, Faculty of Medicine, Frankfurt am Main, Germany

⁵Goethe University Frankfurt, Institute for Pharmaceutical Chemistry and Buchmann Institute for Molecular Life Sciences, Frankfurt am Main, Germany

Chronic inflammatory diseases such as psoriasis or rheumatoid arthritis are characterized by an ongoing leukocyte infiltration into the inflamed tissue, which finally leads to severe tissue damage. The vascular endothelium plays a major role in this pathophysiological condition as it represents a barrier for immune cells and tightly controls leukocyte extravasation. In this study, we characterized the actions of a natural compound-derived carbazole derivative (C81) in a preclinical setting and found that C81 reduces leukocyte-endothelial cell interactions by interfering with endothelial activation processes.

In a first step, an *in vivo* assay was performed employing intravital microscopy to monitor leukocyte trafficking after C81 treatment and TNF activation in postcapillary venules of a murine cremaster muscle. Moreover, *in vitro* cell adhesion (under static conditions and under flow) and transmigration assays using human umbilical vein endothelial cells (HUVECs) and monocytes were implemented. The impact of C81 on cell adhesion molecules and the NFκB signaling cascade was analyzed *in vitro* in HUVECs. Effects of C81 on protein translation were determined by incorporation of a puromycin analogue-based approach and polysome profiling.

We found that C81 significantly reduced TNF-activated leukocyte trafficking in postcapillary venules *in vivo*. Similarly, C81 reduced leukocyte-endothelial cell interactions significantly *in vitro*, indicated by a reduced leukocyte adhesion onto TNF-activated HUVECs under static conditions and under flow. Moreover, C81 reduced the transmigration of the THP-1 monocytic cell line through a HUVEC monolayer. Analyzing endothelial cell adhesion molecules, we found that C81 significantly reduced the levels of ICAM-1, VCAM-1 and E-selectin. Focusing on the NFκB signaling cascade, we showed that C81 reduced the activation on multiple levels of the cascade through promoted IκBα recovery by attenuation of IκBα ubiquitination and through reduced total levels of TNFR1 caused by protein translation inhibition. We conclude that C81 represents an interesting lead compound that warrants further preclinical analysis as inhibitor of inflammation-associated leukocyte-endothelial cell interactions.

Xenocoumacin-2 inhibits pro-inflammatory and pro-angiogenic processes

P. Erkok^{1,2}, M. Schmitt¹, R. Ingelfinger^{1,2}, I. Bischoff-Kont¹, L. Kopp^{2,3}, H. B. Bode^{2,4}, S. Schiffmann^{2,3}, R. Fürst^{1,2}

¹Goethe University Frankfurt, Institute of Pharmaceutical Biology, Faculty of Biochemistry, Chemistry and Pharmacy, Frankfurt am Main, Germany

²LOEWE, Center for Translational Biodiversity Genomics (LOEWE-TBG), Frankfurt am Main, Germany

³Fraunhofer, Institute for Translational Medicine and Pharmacology (ITMP), Frankfurt am Main, Germany

⁴Goethe University Frankfurt, Molecular Biotechnology, Department of Biosciences, Frankfurt am Main, Germany

In many severe disorders, such as rheumatoid arthritis, Crohn's disease or cancer, inflammation and angiogenesis are involved as interdependent pathogenetic processes. Both processes are closely associated with the activation of vascular endothelial cells (ECs) leading to increased leukocyte-EC interactions and the occurrence of angiogenic key events. In this study, for the first time, we explored the pharmacological potential of xenocoumacin (Xcn) 1 and 2 – two natural products isolated from the insect-pathogenic bacterium *Xenorhabdus nematophila* – to inhibit inflammation- and angiogenesis-related processes.

In vitro, the pro-inflammatory activation of ECs was blocked particularly by Xcn2: Concentrations ≥ 100 nM diminished the adhesion of ECs onto leukocytes in response to both tumor necrosis factor (TNF) and interleukin 1 β under static and flow conditions, without impairing EC viability. Xcn2 treatment reduced protein levels of cell adhesion molecules and inhibited key stages of the NF- κ B activation pathway, such as phosphorylation of the I κ B α kinase- β and of the inhibitor of κ B- α as well as nuclear translocation of the NF κ B subunit p65. Besides EC, also leukocytes were directly influenced: In macrophages, the lipopolysaccharide-induced release of pro-inflammatory mediators and the expression of their synthesizing enzymes was assessed: Xcn1/2 did not influence the lipopolysaccharide-induced levels of prostaglandin E2 and cyclooxygenase-2, but reduced the levels of nitric oxide (NO) and the inducible NO synthase. Regarding angiogenesis-related processes, Xcn2 efficiently decreased the proliferation, undirected and chemotactic migration, sprouting and network/tube formation of ECs. Most importantly, we found that Xcn2 decreases the *de novo* protein synthesis in ECs by approximately 50 %. As a result, the levels of (short-lived) proteins such as TNF receptor 1 and the vascular endothelial growth factor receptor 2, which represent key mediators of anti-inflammatory and anti-angiogenic responses, were strongly reduced.

In conclusion, our research highlights the pharmacological activity of Xcn2 in the context of inflammatory and angiogenic processes. Overall, Xcn2 is worth further preclinical characterization.

Chloroquine enhances pro-inflammatory responses to IL-1 β in non-immune cells

C. Lübow¹, G. Weindl¹

¹University of Bonn, Pharmaceutical Institute, Pharmacology and Toxicology, Bonn, Germany

Question: Chloroquine is known for its immunomodulatory effects as well as for its ability to inhibit cellular processes like autophagy and endocytosis. Previously, we showed that chloroquine and other lysosomotropic drugs increase the pro-inflammatory response to interleukin (IL)-1 β in dendritic cells and macrophages which was strongly dependent on inhibition of autophagic flux and internalisation of the IL-1 receptor. However, it still remains unclear, if this effect is restricted to innate immune cells. In the present study, we used HEK293 cells as a model system to study the regulation of sterile inflammatory processes by lysosomotropic drugs.

Methods: HEK293 cells as well as secreted embryonic alkaline phosphatase (SEAP) reporter HEK293 cells transfected with the IL-1 receptor (HEK blue IL-1 β cells) were exposed to IL-1 β in the presence or absence of chloroquine or the endocytosis inhibitor dynasore. Protein levels of cytokines were detected by ELISA. SEAP secretion was determined by QUANTI-blue assay. Gene expression was studied by quantitative real-time RT-PCR.

Results: Chloroquine slightly increased IL-1 β -induced CXCL8 secretion in HEK293 cells whereas it had no effect in HEK blue IL-1 β cells. Moreover, chloroquine failed to induce SEAP secretion in HEK blue IL-1 β cells. However, gene expression of CXCL8 and CXCL2, another IL-1 β -inducible chemokine, were upregulated up to 1000-2000-fold in the presence of chloroquine compared to IL-1 β stimulation alone. The endocytosis inhibitor dynasore also increased CXCL8 gene levels under sterile inflammatory conditions suggesting an involvement of endocytosis inhibition.

Conclusion: Our data indicate that the pro-inflammatory mechanisms of lysosomotropic drugs under sterile inflammatory conditions are cell-type independent. Future analysis may elucidate the detailed underlying molecular mechanisms using HEK293 cells as they are easily genetically modified.

The vasoconstrictor adenosine tetraphosphate activates NLRP3 inflammasome

J. Bockstiegel¹, G. Weindl¹, M. Tölle², M. Schuchhardt²

¹University of Bonn, Pharmaceutical Institute, Pharmacology and Toxicology Section, Bonn, Germany

²Charité – Universitätsmedizin Berlin, Department of Nephrology and Medical Intensive Care, Berlin, Germany

Question: Adenosine triphosphate (ATP) is a well-known activator of the NLRP3 inflammasome leading to secretion of interleukin (IL)-1 β in primed myeloid immune cells like macrophages by binding to the purinergic P2X7 receptor. The endogenous mononucleotide adenosine tetraphosphate (Ap4) is a potent endothelium-derived vasoconstrictor by activation of P2X1. However, immunoregulatory effects of Ap4 have not yet been reported. Due to structural similarities to ATP, we hypothesized that Ap4 is also able to induce pro-inflammatory immune response. Thus, the present study aims to identify the role of Ap4 on NLRP3 inflammasome activation and to further investigate the underlying mechanisms of Ap4 recognition.

Methods: THP-1 and U937 cells were differentiated with phorbol 12-myristate 13-acetate (PMA) into macrophage-like cells. Flow cytometry analysis was used to characterize macrophage-specific cell surface markers. To study NLRP3 activity, macrophages were primed with Pam3CSK4 for 3 h followed by stimulation with ATP or Ap4. IL-1 β production was quantified by ELISA.

Results: Ap4 increased IL-1 β secretion in THP-1-derived macrophages in a concentration-dependent manner, although the magnitude of IL-1 β release was lower compared to ATP. However, Ap4 stimulation led to a 24-fold higher IL-1 β release in U937-derived macrophages compared to THP-1-derived macrophages, whereas ATP stimulation was less potent and induced a 5-fold increase. The NLRP3 inflammasome inhibitor MCC950/CRID3 suppressed nucleotide-induced IL-1 β release.

Conclusion: Our findings indicate that Ap4-induced IL-1 β release in macrophages depends on NLRP3 activation. The differential effects of Ap4 and ATP on IL-1 β release in THP-1- and U937-derived macrophages suggests the involvement of different receptors or pathways.

Vioprolide A reduces pro-inflammatory processes in human endothelial cells - inhibition of protein translation as central mechanism?

L. Burgers¹, B. Luong¹, M. Fabritius², Y. Li³, C. Reiche⁴, S. Michalak³, R. Müller¹, R. Fürst¹

¹Goethe University Frankfurt, Institute of Pharmaceutical Biology, Frankfurt am Main, Germany

²Clinical Centre at the University of Munich, Department of Otorhinolaryngology, München, Germany

³Ludwig Maximilian University of Munich, Department of Ophthalmology, München, Germany

⁴Saarland University, Helmholtz Institute for Pharmaceutical Research Saarland, Department of Microbial Natural Products and Department of Pharmaceutical Biotechnology, Saarbrücken, Germany

Inflammation is a multicellular biological process, which protects the body against pathogens and altered cells. Although inflammation is of great physiological importance, it can also be part of severe pathological conditions, e.g. rheumatoid arthritis. Since vioprolide A (vioA), a cyclic peptide derived from the myxobacterium *Cystobacter violaceus*, was identified in a screening to influence endothelial cells (ECs), we aimed to investigate its effect and mode of action on inflammatory processes in primary human umbilical vein ECs (HUVECs).

Leucocyte-EC interactions were analysed by cell adhesion assay *in vitro*. The influence of vioA on cell adhesion molecules (CAMs), which are indispensable for leucocyte adhesion to ECs, and on the underlying NF- κ B signalling pathway were investigated by flow cytometry, western blot and qPCR. NF- κ B p65 nuclear translocation was detected by immunofluorescence. Recently published data indicate that vioA interferes with protein biosynthesis in Jurkat cells. Thus, *de novo* protein synthesis in HUVECs was analysed by a protein synthesis assay. Anti-inflammatory actions of vioA were further monitored *in vivo* by intravital microscopy of postcapillary venules of the cremaster muscle and microglia/macrophage infiltration after laser-induced choroidal neovascularization in mice.

VioA diminished TNF-induced leucocyte adhesion to and expression of CAMs in HUVECs *in vitro* without impairing cell viability up to 10 nM. *In vivo* experiments underlined the anti-inflammatory potential of vioA. According to a decreased overall protein translation, vioA reduced the protein level of the TNF receptor 1, which activates pro-inflammatory NF- κ B signaling upon ligand binding. As a result, activation of the downstream kinases TAK1 and IKK α / β was prevented, whereas TNF-evoked I κ B α degradation, which allows nuclear translocation of NF- κ B, was not impaired. On the contrary, vioA alone already reduced the I κ B α protein level. Still, TNF-induced NF- κ B p65 nuclear translocation was decreased without affecting p65 protein level.

Taken together, viOA inhibits pro-inflammatory processes in ECs. Although this might be partially based on the reduced overall protein translation, the experimental data implicate a more complex mode of action, which puts viOA in a unique position compared to other translational inhibitors. Thus, viOA represents an interesting compound for the inhibition of inflammatory processes that warrants further in-depth investigations.

83

Trained immunity in nucleic acid sensing

M. Adamson¹, K. Bayrak¹, E. Hartmann¹, S. Schmitz¹, S. Herberhold², K. Andryka¹, S. Marx¹, M. Renn¹, E. Bartok¹, G. Hartmann¹

¹University Hospital Bonn, Institute for Clinical Chemistry and Clinical Pharmacology, Bonn, Germany

²Waldkrankenhaus Bonn, Department of Otolaryngology, Bonn, Germany

Background: Recent research has shown that not only the adaptive but also the innate immune system can adapt to pathogenic challenges. Termed *trained immunity*, studies to date have focused on the enhanced release of pro-inflammatory cytokines after repeated treatment of myeloid cells with C-type Lectin receptors (CLR) followed by Toll-like receptors (TLR) agonists. However, the role of trained immunity in the antiviral, type-I interferon (IFN) response has not yet been systemically investigated. Our study aimed to characterize potential training effects resulting from stimulation of the antiviral cytosolic RNA receptor retinoic acid-inducible gene I (RIG-I).

Methods: On day 0, synthetic 5'-triphosphorylated RNA (3pRNA), a specific RIG-I ligand, was transfected into primary human monocytes, epithelial cells and fibroblasts. Cells were then rechallenged with 3pRNA at day 6 and compared to cells not stimulated at day 0. RIG-I signaling was characterized using ELISA, FACS, RT-PCR and 3'mRNA Sequencing.

Results: At the mRNA level, RIG-I stimulation at day 0 enhanced expression of interferon stimulated genes (ISG) in all cell types upon rechallenge at day 6. At the protein level, repetitive stimulation also enhanced proinflammatory cytokine release. Repetitive RIG-I stimulation induced broad transcriptomic changes, resulting in an increase in differentially expressed genes and higher fold change than single stimulation on day 6. Moreover, RIG-I stimulation on day 0 induced transcriptomic changes which were still detectable on day 6, including ISG expression.

Conclusion: Our results indicate that *trained immunity* may be a broader phenomenon within the innate immune system. In nucleic acid sensing, training the innate immune system could have a vital role in protecting the integrity of the host during viral infection. Moreover, RIG-I-mediated training could be applied to novel vaccination and other prophylactic strategies against pathogenic viruses.

Pharmacology – Pharmacogenetics, Pharmacoepidemiology and Drug Safety

84

Personalized risk profiles in emergency adverse drug reactions

K. Just¹, J. Stingl¹

¹University Hospital of RWTH Aachen, Institute of Clinical Pharmacology, Aachen, Germany

Question: Most adverse drug reactions (ADR) are dose-related[1], while individual differences in drug exposure exist based on pharmacogenomics (PGx) profiles. Preemptive PGx testing is expected to prevent ADRs, however trials are ongoing to prove this hypothesis[2].

Methods: The prospective multi-center observational study on ADRs in emergency departments (ADRED) aims to personalize drug safety by assessing individual profiles for an increased ADR risk. ADR cases were collected in four large EDs in Germany (N=2215) and PGx samples obtained and analyzed from a subsample (n=776).

Results: Patients enrolled were mostly older and multi-medicated with a median age of 76 years (IQR 58; 80) and 7 drugs taken (IQR 3; 10) in the total and 70 years of age (IQR 56; 79) and 8 drugs taken (IQR 5; 11) in the subsample [3,5]. Antithrombotics were commonly suspected for causing an ADR leading to ED admission in the total population (OR 2.94, 95%CI 2.49-3.47)[3]. The risk for bleeding ADRs was more than doubled in older adults with OR 2.46 (95%CI 1.77-3.41) for gastrointestinal and OR 2.89 (95%CI 1.37-6.11) for hemorrhage from respiratory passages[4]. In the genotyped subsample, clopidogrel-associated bleeding events were associated with age (OR 1.05, 95%CI 1.02-1.08) and higher CYP2C19 activity (OR 4.97, 95%CI 1.73-14.27). A tendency for an association of phenprocoumon-risk profiles (low VKORC1/CYP2C9 activity) with phenprocoumon-suspecting ADRs was observed (p=0.052)[5].

Conclusion: Older adults are often affected by emergency bleeding ADRs associated with the intake of antithrombotic drugs. While PGx profiles might add to the individual ADR risk, more work on the interpretation of PGx profiles in the context of age and multi-medication is urgently needed.

Funding: This project has received funding from the European Union's Horizon 2020 research and innovation program under grant agreement No. 668353. And this work was supported by the framework of the AMTS focus of the German Federal Ministry of Health (BMG), grant number ZMVI5-2514ATA004.

References: [1] Edwards IR, Aronson JK. Lancet 2000;356:1255-9. [2] van der Wouden CH, Bohringer S, Cecchin E, et al. Pharmacogenet Genom 2020;30:131. [3] Just KS, Dormann H, Böhme M, et al. Eur J Clin Pharmacol 2020;76:439-48. [4] Just KS, Dormann H, Schurig M, et al. Br J Clin Pharmacol 2020;86:2144-54. [5] Just KS, Dormann H, Schurig M, et al. J Clin Med 2020;9:1801.

85

MTOR polymorphisms and *de novo* diabetes mellitus in liver transplantation patients treated with everolimus

A. Hagemann^{1,2}, P. Husen³, K. Straub⁴, K. Willuweit⁴, H. Wedemeyer⁴, H. S. Bachmann^{5,6,2}, K. Herzer⁴

¹Universität Witten/Herdecke, Pharmacology and Toxicology, Witten, Germany

²University of Witten/Herdecke, Zentrum für Biomedizinische Ausbildung und Forschung, Witten, Germany

³University Hospital Essen, Department of General, Visceral, and Pediatric Surgery, Essen, Germany

⁴University Hospital Essen, Department of Gastroenterology and Hepatology, Essen, Germany

⁵University of Witten/Herdecke, Pharmacology and Toxicology, Witten, Germany

⁶Universitätsklinikum Essen, Pharmacogenetics, Essen, Germany

Question: The impact of immunosuppressive drugs in patients following liver transplantation (LT) is very individual. Despite the multiple beneficial effects of the mammalian target of rapamycin (mTOR) inhibitor Everolimus (EVR) in LT recipients, some patients do not benefit from EVR administration. We investigated whether the presence of common single-nucleotide polymorphisms (SNPs) in the mTOR gene are predictive for adverse events following the introduction of EVR after LT.

Methods: The feasibility and efficacy of EVR in 127 liver transplant recipients who were converted to EVR-based immunosuppression was documented retrospectively. Blood samples of these patients were analyzed for the occurrence of four SNPs in the mTOR promoter region (mTOR3099/rs2295079 C>G, mTOR3162/rs2295080 A>C) and the mTOR 3' untranslated region (mTOR8167/rs12139042 C>T, mTOR8600/rs2536 A>G); the specific allele variants were also associated with the incidence of adverse events (AEs).

Results: Of all patients, 21 (16.5%) did not tolerate the medication and had to discontinue. Of those patients who continued, 37% developed signs of reduced tolerance within the first 6 months, resolving after 12 months. When the cohort was divided according to genotype and allele frequency, patients with the mTOR3162/rs2295080 CC variant had a significantly higher risk (odds ratio = 5.89; 95% confidence interval = 1.48 - 23.40; P = 0.012) of developing new-onset diabetes mellitus following EVR treatment than AA or AC genotype carriers.

Conclusion: Our results suggest that the SNP mTOR3162/rs2295080 CC genotype is associated with the development of new-onset diabetes mellitus following EVR treatment.

86

Drug repositioning by using OpenVigil 2.1-MedDRA with U.S. FDA pharmacovigilance data identifies female sex hormones, anti-diabetics, neuropharmacological sigma-receptor modulators, tyrosine kinase inhibitors and various other agents as possible candidate drugs against *coronaviridae* infections

R. Böhm¹, C. Bulin¹, V. Wätzig¹, I. Cascorbi¹, H. J. Klein², T. Herdegen¹

¹University Hospital Schleswig Holstein, Institute of Experimental and Clinical Pharmacology, Kiel, Germany

²Christian-Albrechts-Universität zu Kiel, Institut für Informatik, Kiel, Germany

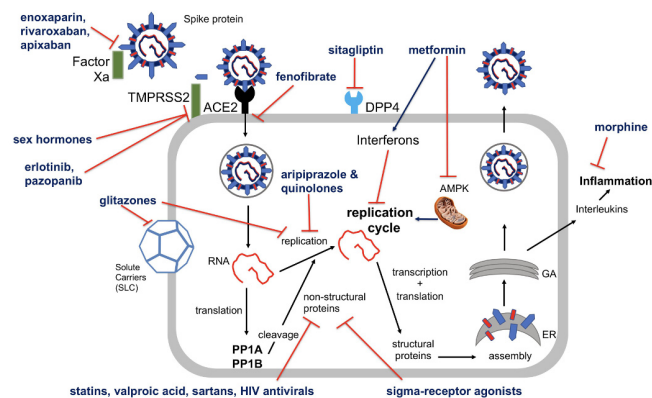
Question: Pharmacovigilance is the ongoing and systematic monitoring of the safety of medicinal products, relying on spontaneous reporting of incidents. Those reports are primarily used for identifying new adverse drug reactions (ADR) by screening for disproportionate reporting, i.e. there are unexpectedly more reports of certain combinations of adverse events and drugs than estimated as occurring by chance. However, scanning for associations of drugs and adverse events that occur less frequently than expected can provide hypotheses for drug repositioning, i.e. a known drug could be therapeutically beneficial for a new indication like the coronavirus disease (COVID-19). Since coronavirus related adverse event reports are lacking in pharmacovigilance data prior to 2020, we searched for drugs suitable against similar infections (e.g., caused by similar RNA viruses, respiratory manifestation).

Methods: We performed a retrospective, observational, pharmacovigilance study: Drugs associated with viral respiratory tract infections and/or diseases caused by RNA-viruses, which are phylogenetically similar to SARS-CoV-2, were extracted from the U.S. pharmacovigilance data 2004Q1 to 2020Q2 using OpenVigil 2.1-MedDRA17, filtered for statistically significant inverse associations, checked for clinical infeasibility (e.g., having strong cytotoxic effects) or for implausibility (e.g., only topically usable), and grouped according to their WHO Anatomical Therapeutic Chemical (ATC) classification code. For each signal, a literature search in Google Scholar and PUBMED was performed, to consolidate known effects and putative mechanisms of this drug against COVID-19.

Results: The clustering of the resulting 112 candidate drugs using ATC codes revealed female sex hormones/anti-androgens, anti-diabetics, neuropharmacological sigma-receptor modulators, peptidase inhibitors, antiviral drugs, nicotinic acetylcholine receptor agonists and tyrosine kinase inhibitors as putatively antiviral. (Hydroxy-)Chloroquine appears as a statistically significant risk factor to contract viral diseases.

Conclusions: Inverse signals in pharmacovigilance data provide new hypotheses for drug repositioning. This could be done for all indications. Concerning the treatment of viral respiratory infections like *coronaviridae* infections, there is affirmative data for some candidate drugs; the remaining proposed drugs, for which no antiviral mechanism is known yet, shall stimulate further exploration.

Fig. 1



87

Why we should replace the term "antibiotics" by "antibacterial drugs"

R. Seifert¹, B. Schirmer¹

¹Medizinische Hochschule Hannover, Pharmakologie, Hannover, Germany

The term "antibiotics" was coined as umbrella term for antibacterial drugs in the 1940s. The term antibiotic actually implies that the drug is effective against all forms of life which is (fortunately) not the case. During the past decades, medicine has witnessed a dramatic increase in resistance against many "antibiotics" including so-called "broad-spectrum antibiotics". In addition, there are recent developments in which classic "antibiotics" are used for indications other than bacteria-caused diseases. Conversely, several "non-antibiotics" are being repurposed for treatment of diseases caused by bacteria resistant to classic "antibiotics". This situation calls for a thorough revision of terminology in the area of antipathogenic drugs. This revision is part of a broader initiative to implement a mechanism- and chemistry-driven nomenclature of drug classes rather than the traditional indication-driven nomenclature. Most importantly, we propose to replace the term "antibiotic" by "antibacterial drug", "antibiogram" by "antibacteriogram" and "antibiosis" by "antibacteriosis". These terms are consistent with the words "bacteriostatic" and "bactericidal". The terms "biostatic" and "biocidal" have a completely different meaning. The term "agent", traditionally used in the field, should be replaced by "drug". Along the same line, there is a lot of terminological inconsistency with respect to "tuberculostatics". The term antimycobacterial drugs with the subclasses of mycobacteriostatic and mycobactericidal drugs is more precise. Some terms such as narrow-spectrum- and broad-spectrum-antibiotics should be abandoned altogether because the spectrum of antibacterial activity of drugs varies substantially, both geographically and temporarily. The arbitrary use of imprecise terms also renders literature searches increasingly difficult. While abandoning traditional terms may be inconvenient and take time, the use of correct terms will increase accuracy of antibacterial treatment in the future and facilitate the understanding of drug repositioning. The proposed nomenclature has already been implemented in a recent pharmacology textbook and into the list of drugs used for the federal medical exam in Germany (<https://www.impp.de/pruefungen/allgemein/gegenstandskataloge.html>). It is hoped that the proposed new nomenclature will improve precision of medical education, pharmacotherapy and antibacterial stewardship.

88

Increased patient and physician satisfaction in guide-based prescription talks (AMPEL: Aspects of Medication and Patient participation – an Easy guideline)

V. Kirsch¹, J. Matthes¹

¹University of Cologne, Centre of Pharmacology, Cologne, Germany

Objectives: Patients want to receive more information on a drug therapy and to actively participate in medical decisions. Information and active participation correlate with increased adherence. To support physicians in effective and efficient prescription talks, we developed the conversation guide AMPEL that combines patient-relevant drug information with steps of shared decision-making (AMPEL: Arzneierordnungsgespräche unter Berücksichtigung Medikamentöser Aspekte und der Partizipativen Entscheidungsfindung - ein Leitfaden / Aspects of Medication and Patient participation – an Easy guideline). In a pilot study we tested effects on patient and physician satisfaction with prescription talks in primary care.

Material & methods: Six residents in community-based primary care practices participated in a controlled pilot study in sequential pre-post design. Initially, they

conducted 41 prescription talks as usual, i.e. without knowing the guide (control phase). Then, they conducted 23 talks considering the guide (intervention phase). Immediately after the talks, patients filled in a questionnaire on satisfaction with the information on medication and physician-patient interaction, and physicians about their satisfaction with the talk and the application of the guide.

Results: Patients felt better informed after guide-based prescription talks (e.g., SIMS-D inventory in median 10 vs. 17, $p < 0.05$), more actively involved (KPF-A inventory for patient activation 2.9 ± 0.8 vs. 3.6 ± 0.8 , $p < 0.05$), and more satisfied with the physician-patient interaction. Physicians rated the guide helpful and feasible. During the intervention phase, their satisfaction with the conversation was significantly increased. Of note, the evaluation of the duration of the talk was not affected.

Conclusion: The promising results argue for further studies to verify whether the increase in perceived patient information and activation can be confirmed and validated and whether it may influence treatment adherence. Furthermore, the significant effects of our guide on satisfaction with the prescription talk encourage testing its use in everyday medical practice.

89

Arrhythmia-risk stratification of antipsychotics and antidepressants through analysis of the summaries of product characteristics of the brand-name products approved in Germany

M. Elsayed¹, E. Abdel-Kahaar^{2,3}, M. Gahr¹, B. J. Connemann¹, M. Denkinger¹, C. Schönfeldt-Lecuona¹

¹Department of Psychiatry and Psychotherapy III, University of Ulm, Ulm, Germany

²Institute of Pharmacology of Natural Products and Clinical Pharmacology, University of Ulm, Ulm, Germany

³Department of Pharmacology, Qena Faculty of Medicine, South Valley University, Qena, Egypt

Background: Most psychotropic drugs such as antidepressants (AD) and antipsychotics (AP) may induce different forms of cardiac arrhythmias. However, this risk varies considerably among the different agents and hence, it is of utmost clinical importance to create an arrhythmia-risk stratification of these agents. In this study we utilized the summaries of product characteristics (SmPCs) of the brand-name AD and AP approved in Germany to create a ranking list of these agents concerning their risk to induce different types of cardiac arrhythmias.

Methods: We identified all the brand-name AD and AP approved in Germany and collected their SmPCs. In a second step, we extracted the frequency category of each form of arrhythmia (QT-prolongation, Torsade de Pointes tachycardia, and ventricular arrhythmia) listed in the "Undesirable effects" section of the SmPCs and performed a risk assessment.

Results: We obtained the SmPCs of 24 AD and 26 AP identified as brand-name drugs. Regarding AP: Invega® (paliperidone) and Serolect® (sertindole) carried the highest risk of QT-Prolongation (frequency $\geq 1/100$ and $< 1/10$) and Serolect® (Sertindole) carried the highest risk for Torsade de Pointes tachycardia ($\geq 1/1000$ to $< 1/100$) while Solian® (amisulpride), Xomolix® (droperidol), Zyprexa® (olanzapine) were associated with the highest risk of ventricular tachycardia ($\geq 1/10,000$ and $< 1/1000$). The reported cardiac arrhythmias of AD were less than of AP with Zoloft® (sertraline) carried the highest risk to induce QT-Prolongation ($\geq 1/10,000$ and $< 1/1000$) and both Zoloft®, and Trevilor® (venlafaxine) carried the highest risk of Torsade de Pointes tachycardia ($\geq 1/10,000$ and $< 1/1000$) while the risk of ventricular tachycardia was highest with Trevilor® ($\geq 1/10,000$ and $< 1/1000$).

Conclusion: Arrhythmia-risk stratification of AP and AD is of extreme clinical importance. The utilization of SmPCs to assess the cardiac risk based on the frequency categories of the various forms of cardiac arrhythmias might help to identify the high-risk drugs and avoid them in predisposed patients. Based on our analysis of SmPCs, Serolect® (sertindole) carries the highest risk of cardiac arrhythmias among AP while Zoloft® (sertraline), Trevilor® (venlafaxine) carry the highest risk among AD. The interpretation of the reported risk assessment should, however, be done carefully considering the limitations of SmPCs.

Poster Presentations

Pharmacology – Cardiac pharmacology and treatment

P01

Specific COX-dependent signaling of bradykinin in small dermal blood vessels of mice

M. Krybus¹, E. Gholamreza-Fahimi¹, F. Khosravi¹, M. Bisha¹, G. Kojda¹

¹Institute of Pharmacology and Clinical Pharmacology, Heinrich Heine University Düsseldorf, Düsseldorf, Germany

Introduction: The inflammatory mediator bradykinin (BK) is a key mediator in non-allergic angioedema such as hereditary angioedema or angioedema induced by ACE inhibitors. In larger blood vessels BK signals via the Gq-coupled BK receptor type 2 (B2) and activates phospholipase A2 as well as endothelial NO synthase (eNOS). However, using eNOS knockout mice we found that eNOS does not contribute to BK-induced extravasation in

small dermal blood vessels. Hence, arachidonic acid metabolites like prostaglandins (PG) formed by cyclooxygenases (COX) might play a decisive role in BK induced edema.

Methods: We used the Miles assay to quantify dermal extravasation of Evans blue, a dye with a strong affinity to the plasma peptide albumin, in mice's dorsal skin. For this purpose, anaesthetized C57BL/6 mice received the dye intravenously (i.v.). After shaving the dorsal skin, phosphate-buffered saline (PBS), 2 nmoles of BK, the proteolytically stable BK-analogue labradimil (LD) and histamine (His) were injected intradermally (i.d.). The resulting extravasates were excised after sacrificing those mice. Finally, the dye was extracted and quantified spectrometrically.

Results: In C57BL/6, BK induced a dose-dependent increase of extravasation expressed as fold increase (\pm SEM) in comparison to PBS reaching at 2 nmoles 4.26 ± 0.07 ($n=6$, $P<0.0001$). In striking contrast, intraperitoneal (i.p.) pre-treatment of C57BL/6 with the unspecific COX inhibitor diclofenac reduced the extravasation to 2.26 ± 0.28 ($n=6$, $P<0.0001$). Likewise, ibuprofen reduced the extravasation to 2.72 ± 0.15 ($n=5$, $P<0.0001$) and similar effects were seen for both drugs using LD. A lesser reduction was observed using the COX-2 specific drug etoricoxib both before i.d. BK ($n=6$, to 3.04 ± 0.12 , $P=0.0311$) and before i.d. LD (to 2.81 ± 0.18 , $P=0.0010$). To determine the impact of PG on extravasation we used the corresponding PG receptor (PGR) antagonists. While DP antagonist laropiprant, EP2 antagonist PF-04418948 and EP4 antagonist grapiprant had no effect, IP antagonist RO1138452 significantly decreased dermal extravasation induced by both i.d. BK ($n=6$, to 2.94 ± 0.13 , $P<0.0001$) and i.d. LD (to 2.89 ± 0.29 , $P=0.0002$). No effect was observed on His-induced extravasations by any COX inhibitor or PGR antagonist.

Conclusion: Our results suggest that the generation of prostacyclin predominantly formed by COX-1 likely contribute to B2-mediated edema formation in small dermal blood vessels of mice.

P02

Molecular regulation of right ventricular failure in rats

S. Werner¹, L. Jurida¹, O. Dittich-Breiholz², F. Knapp³, S. Rohrbach³, M. Kracht¹
¹Justus Liebig University Giessen, Rudolf Buchheim Institute of Pharmacology, Gießen, Germany
²Medizinische Hochschule, RFU Transcriptomics, Hannover, Germany
³Justus Liebig University Giessen, Institute of Physiology, Gießen, Germany

Question: Heart failure is among the leading causes of death globally. Ventricular failure progresses through a hypertrophic compensatory phase followed by failure of the ventricle function through rapid decompensation. While several treatment options for left ventricular failure are established, they often prove ineffective in right ventricular disease. In order to unravel right heart specific mechanisms of disease and to develop specific treatment options, it is important to establish appropriate animal models that (i) reflect the slowly progressive mode of compensation / decompensation and (ii) allow comparative analyses of left versus right heart failure in the same experimental set up.

Methods: To model the slowly occurring progression of right or left heart failure, in weanling rats non-restrictive clips around either the pulmonary artery (PAB) or the aorta (AOB) were surgically applied and the animals were monitored functionally and by imaging. Upon animal growth, increasing vessel constriction results in compensatory hypertrophy after 6 weeks and heart failure at week 21 (PAB) or 24 (AOB). Individual ventricle samples from both phases of AOB or PAB and from sham animals were collected and analysed by mRNA-seq as well as ChIP-seq for the chromatin markers H3K27ac and H3K4me1 to unravel transcriptomic changes and correlate them to the active enhancer landscape for both disease conditions. Bioinformatics analyses were used for a detailed comparison to identify deregulated pathways and interaction networks.

Results & Conclusion: We found little changes of the transcriptomes during compensatory phases of both PAB or AOB. However, upon decompensation numerous ventricle-specific deregulated gene sets were identified, including genes previously implicated in pathological heart remodelling. We observed a clear difference in expression patterns between right and left ventricle. The characteristic gene expression patterns of right ventricular failure were mirrored in the right ventricle of AOB rats, suggesting that the right ventricle reacts also to left ventricular failure with a specific gene expression programme. Protein interaction analyses based on the transcriptomic data reveal ventricle-specific protein networks which are assembled of co-regulated factors. Together, these data obtained in a rat model which closely resembles the course of human disease identify profound molecular differences between right and left heart failure.

Pharmacology – Immunopharmacology / inflammation / anti-infectives

P03

Evaluation of immunomodulatory activity of SKB_Gutbiotic in laboratory animals
 Immunomodulatory activity of SKB_Gutbiotic was studied using various models such as delayed type hypersensitivity, neutrophil adhesion test, carbon clearance test, immune organ index and measuring Immunoglobulin levels.

M. Mohan¹, P. Saudagar¹, G. Guthale¹, **K. Chaudhari¹**
¹MGV's Pharmacy College, Mumbai-Agra Road, Panchavati, Nashik-03, Maharashtra, INDIA, Department of Pharmacology, Nashik, India

Methods: The present study was undertaken to evaluate the immunomodulatory potential of SKB_Gutbiotic, a three combined species of probiotics i.e. *B. subtilis*, *B. vallismortis* and *B. licheniformis* on laboratory animals i.e. rats and mice by using various models such

as delayed type hypersensitivity, neutrophil adhesion test, carbon clearance test and immune organ index. The effect of SKB_Gutbiotic on haematological parameters and humoral immunity was evaluated by determining the complete blood count & Immunoglobulin levels. Acute toxicity study was also carried out as per OECD 425 guideline.

Results: Significant increase in the blood serum immunoglobulin levels i.e. IgA, IgM and IgG of rats are the important achievements in our work. It was observed that SKB_Gutbiotic (50 billion CfU/kg, p.o) showed the same significant increase in immunoglobulin levels as of Levamisole (33mg/kg, p.o). Thus this data it may help us deduce the possible synergistic effect of SKB_Gutbiotic with levamisole for enhancing the Immunostimulant activity, which in turn would be helpful for treatment of various immune diseases.

Conclusion: SKB_Gutbiotic shows stimulatory effect on both cellular as well as humoral immunity and didn't show any signs of toxicity in animals treated up to dose of 2000mg/kg.

Fig. 1

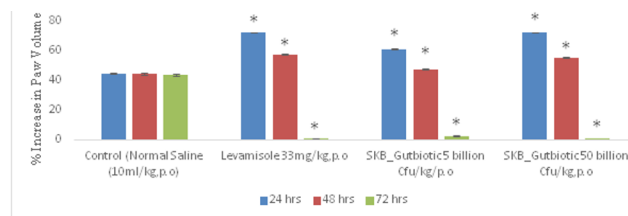
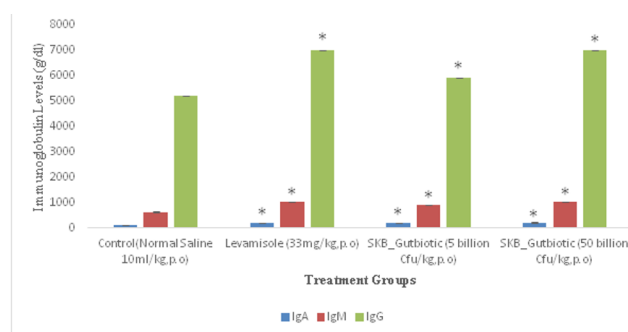


Fig. 2



P04

Interaction of reactive oxygen species and the JAK/STAT pathway in the sensory perception of itch

J. Wilzopolski¹, P. M. Canbolat¹, W. Bäumer¹
¹Freie Universität Berlin, Institute of Pharmacology and Toxicology, Department of Veterinary Medicine, Berlin, Germany

Question: Reactive oxygen species (ROS) are involved in physiological and pathophysiological processes in mammals. They are constantly produced as second messengers in keratinocytes as a reaction to exogenous and endogenous stimuli. A role of oxidative stress is discussed in the context of atopic dermatitis (AD) and itch, as intradermal injection of the naturally occurring ROS H₂O₂ into the neck of mice leads to a robust scratching response. The role of the Janus kinase/Signal Transducers and Activators of Transcription (JAK/STAT) pathway in AD and itch has recently gained particular attention and two JAK-inhibitors are approved for their therapy in human and veterinary medicine, respectively. Various studies show that ROS modulate the activity of JAK/STAT. The exact mechanisms in itch perception and AD mediated through ROS in association with JAK/STAT are not clear yet. Various studies indicate an increase or a decrease in JAK activity depending on the cell type, stimuli and study conditions. According to literature a possible intersection seems to be the modulation of JAK2 through H₂O₂. Therefore, the aim of this study is to investigate the role of JAK/STAT in the signalling of ROS induced sensory perception.

Methods: Primary small diameter mouse dorsal root ganglion (DRG) neurons are exposed to H₂O₂ and subtype selective JAK inhibitors of different profile and their activation is measured via real-time fluorescence Ca²⁺ imaging.

Results: Murine DRG neurons are activated by H₂O₂ (7.2 %). This signal is not altered by the preferentially selective JAK3-inhibitor tofacitinib (7.8 %). In combination with the relatively selective JAK1-inhibitor oclacitinib approximately twice as many neurons reacted to H₂O₂ (14.2 %). The signal is reduced in combination of H₂O₂ with the relatively selective JAK2-inhibitor BMS911543 (3.0 %) or the JAK1/2-inhibitor AZD1480 (3.6 %).

Conclusion: The above-mentioned results indicate an involvement of JAK1 and JAK2 in H₂O₂ activation of sensory neurons.

P05

Unexpected effects in a mouse model of calcipotriol induced skin inflammation

H. Oltmanns¹, V. Filor¹, P. Hagedorn¹, K. Becker², W. Baumgärtner², M. Kietzmann¹, J. Meißner¹

¹University of Veterinary Medicine Hannover, Department of Pharmacology, Toxicology and Pharmacy, Hannover, Germany

²University of Veterinary Medicine Hannover, Department of Pathology, Hannover, Germany

Question: The calcipotriol model which is described by NAIDOO et al. (Journal of Investigative Dermatology 138, 2606-2616, 2018) as a mouse model of atopic dermatitis was used to study effects of H1/H4 histamine receptor antagonists in the inflammatory process. Murine keratinocytes were used as well to gain information about the effect of calcipotriol treatment on cytokine release.

Methods: Female Balb/C mice and histamine H4 receptor knockout mice were used. They were topically treated (20 µl/ear) with calcipotriol (MC 903) over 14 days. Different amounts of calcipotriol (0.5 nmol and 1 nmol) were administered onto the ear skin. The ear thickness and histology, the cervicale lymph node weight and cell number, and the concentration of thymic stromal lymphopoietin (TSLP, measured by enzyme-linked immunosorbent assay) in the skin were determined. The effect of systemically administered H1 receptor antagonist mepyramine as well as H4 receptor antagonist JNJ 39758979 was studied in mice treated with 0.5 nmol calcipotriol, as well. The glucocorticoid dexamethasone was used as positive control. Furthermore, murine keratinocytes were treated with calcipotriol *in vitro* and were analyzed for TSLP concentration.

Results: Redness, scaling and swelling were observed after calcipotriol treatment in ear skin with invasion of inflammatory cells like lymphocytes, macrophages and neutrophils. The TSLP concentration in the skin was significantly enhanced. Also, an increase of the cervical lymph node weight and cell number were detected. In comparison to the wildtype mice, the inflammatory response was more pronounced in H4 knockout mice. In contrast to dexamethasone, the treatment with JNJ 39758979 and mepyramine showed only slight effects. Furthermore, an increase of TSLP concentration was observed *in vitro* after dexamethasone and calcipotriol treatment.

Conclusion: The calcipotriol model exhibits some characteristics of atopic dermatitis, like swelling, redness and scaling. Significant effects of histamine receptor antagonists were not found. The role of dexamethasone in the inflammation pathway in this model is not yet understood in detail. Therefore, we aspire more *in vitro* studies to define the effect of dexamethasone in this inflammation model.

P06

Monoclonal antibody therapy in spontaneous chronic urticaria – A case-based approach

E. G. Ban¹, **P. Lechsner**¹, C. Ureche¹, M. A. Balan¹, S. Patzelt¹

¹UMFST Targu Mures, Targu Mures, Romania

Introduction: Chronic spontaneous urticaria (CSU) is a condition characterized by the presence of periods with urticaria lasting for more than 6 weeks, associated or not with the presence of angioedema. It is a common type of urticaria, causing notable deterioration in the patient's quality of life. Recently, besides the classic therapeutic approach, monoclonal antibody therapy was approved.

Objective: By presenting our case-based approach we want to point out that even strongly positive lab results must be considered in correlation to patients' physical sign and symptom status and other results.

Material and methods: The prescription of monoclonal antibody therapy requires a complex previous medical examination and a correct balance setup between risk and benefit. We evaluated a patient for a probable recommendation for Omalizumab. Evaluation consisted of physical examination, allergy testing, laboratory and paraclinical evaluation and pharmacotherapy with antihistamines under monitoring.

Results: An 83-year-old male patient visited our allergology setting complaining of urticaria in the last 3 years, with periods lasting for more than 4 weeks. Physically, we observed scars of previous severe pruritus episodes and allergy examination lacked relevancy. We established therapy with a first-generation antihistamine and referred the patient to further laboratory evaluation. This returned paradox results with very high total IgE values (2836, UI/mL; normal < 158 UI/mL) without other immune-allergy parameters sustaining it. CSU presented resistant to antihistaminic therapy – as the patient stated for previous therapies with different antihistamines. Seemingly the patient fit a recommendation for MAB therapy after completion of the guideline approach. But the special situation: No correlation between IgE values and other lab results, which should raise questions. The lab results returned clues of underlying anemia and an increased monocyte level. Despite the patient insisting to initiate a MAB therapy we decided to continue paraclinical evaluation into the direction of anemia and elevated monocyte level and their etiology. A complete evaluation with ultrasound and endoscopy of the GIT, finally revealed a tumorous formation on the descending colon.

Conclusion: The MAB therapy should be prescribed after a careful evaluation of the patient and in full knowledge of the monoclonal antibodies.

P07

Could MAB therapy improve polypragmasia rates in chronic asthmatic patient?

B. Erika¹, **P. Simon Andreas**¹, B. Attila¹, U. Corina¹

¹UMFST, Pharmacology, Tirgu Mures, Romania

Background: Chronic allergic asthma is a frequent disease affecting patients for a lifetime and having a strong effect on the quality of life of the patient. The disease itself in an ongoing one, requiring a chronic therapy in the late adulthood and elderly patients. This will lead inevitably to a multiple drug association.

Material and methods: We effectuated a clinical pharmacology analysis of the therapy administered to a 78-year-old male patient. During the evaluation we have taken into consideration personal parameters of the patient, medical history and medications which were used concomitantly. We also performed a risk-benefit study of a probable use of monoclonal antibody therapy.

Results: We have decided to effectuate a clinical pharmacological analysis of a patient's pharmacotherapy by choosing randomly from a group of adult patients, older than 60 years-of-age, suffering from allergic asthma for more than 5 years, without MAB therapy. Our patient is 78-year-old, suffering from allergic asthma since he was 16-years-old. He's current medication include a number of 16 medicines, taken regularly, every day, for a period longer than 2 weeks. From these 16 medications 4 are used for the treatment of allergic chronic asthma. When performing the analysis, we found minor and serious drug-drug interactions and also drug use and drug combinations which are not recommended in respiratory pathology and/or worsening respiratory pathology. The associated diseases requiring medical treatment in our patient – and representatively for the population studied – are: cardiovascular pathology, psychiatric pathology, ophthalmologic and rheumatologic pathology. Meaning that the used medications include 2-3 medications for the cardiovascular condition – requiring special attention, since angiotensin-converting enzyme inhibitors and/or beta-blockers have relative contraindications in these patients. Also the glaucoma therapy and the non-steroidal anti-inflammatory medicines can cause side effects and failure of the treatment.

Discussion: The evaluation of patients with chronic allergic asthma into the direction of a therapy with monoclonal antibodies should be considered. The monthly treatment with a MAB could improve signs and symptoms and also quality of life of the patient especially by reducing the use of corticosteroids – which are also in the line of drug-drug interactions.

P08

***In vitro* cytotoxicity and an apoptotic assay of *Eucalyptus globulus* essential oil in colon and liver cancer cell lines**

H. Khazraei¹

¹Shiraz University of Medical Sciences, Pharmacology, Shiraz, Iran

Purpose: The vegetable toxicity effect has been investigated in recent years. The *Eucalyptus globulus* of the Myrtaceae family is used in the treatment of various infectious disorders traditionally. The aim of this study was to assay the potential anticancer effect of *Eucalyptus globulus* essential oil *in vitro* and compare the cytotoxicity effects between cancerous and non-cancerous human cell lines.

Methods: The cytotoxicity of the *eucalyptus globulus* essential oil was evaluated on the colon cancer cell line SW48, liver cancer cell line HepG2, HEK293t, skin fibroblast, and fat human cells using MTT assay. 5-FU was used as a control treatment of cancer in this study.

Results: Different concentrations of *eucalyptus globulus* essential oil reduced the viability of human cancer cell lines, SW48 (0.05% - 5%), and HepG2 (0.5% and more). *Eucalyptus* essential oil has some side effects and might not be safe at high doses (0.5% and 5 %).

The comparison between the cytotoxic effect of 5-FU and eucalyptus on fibroblast cells and cancerous SW48 cell line indicated that eucalyptus, by itself, had a significant effect on the cell viability of normal cells such as fibroblast cells, and its cytotoxic effect mildly decreased.

The findings of the present study showed that eucalyptus essential oil suppresses the proliferation of the human colon cancer cells via induction of apoptosis.

Conclusion: *Eucalyptus* essential oil might be a good candidate for colon cancer treatment. Further investigations could be helpful to confirm our obtained results.

P09

Evaluation of the effects of antidepressants against acetic acid-induced colitis in rats

H. Khazraei¹

¹Shiraz University of Medical Sciences, Pharmacology, Shiraz, Iran

Question: High prevalence of psychological comorbidities in patients with ulcerative colitis supports the premise that adding an anti-depressant drug to medical treatment. Clomipramine, Risperidone, and Escitalopram could be some good candidates for investigation of the anti-colitis activity.

Methods: In this study colitis was induced by intracolonic instillation of 2 ml of 3% v/v acetic acid solution in rats. Anti-colitis effects of Clomipramine, Risperidone, and Escitalopram were evaluated in rats. Clomipramine (25 mg/kg/day), Escitalopram (10 mg/kg/day) and Risperidone (2mg/kg/day) were orally administered daily after the colitis induction. Prednisolone (5 mg/kg/day) as the reference drug and normal saline as the control were also orally administered daily after colitis induction. All the treatments continued daily for seven days. The effect was assessed based on inflammatory cytokines (TNF α , IL-6) and biochemical myeloperoxidase changes and also histopathological evaluations.

Results: IL-6 level was decreased ($p < 0.05$) after administration of clomipramine and it was effective to reduce colitis severity through a reduction in the macroscopic and microscopic colonic parameters. Although, prednisolone decreased myeloperoxidase (MPO) and TNF-alpha levels, However, it was statistically non-significant ($p > 0.05$).

Conclusion: Clomipramine as an antidepressant drug has anti-inflammatory properties, which could be introduced as a good candidate for people who suffered from IBD disorders.

P10

NLRP3-independent inflammasome activation by proteasome inhibitors

F. Ullrich^{1,2}, K. Andryka¹, S. Schmitz¹, S. B. Soler¹, T. Zillinger^{1,3}, G. Hartmann¹, E. Bartok¹

¹University of Bonn, Institute of Clinical Chemistry and Clinical Pharmacology, Bonn, Germany

²University Hospital Essen, Department of Hematology and Stem Cell Transplantation, Essen, Germany

³University of Marburg, Institute of Immunology, Marburg, Germany

Introduction: Proteasome inhibitors (PIs) such as Bortezomib (BTZ) have revolutionized multiple myeloma (MM) treatment. PIs selectively target MM cells by inhibiting Nuclear factor κ light chain enhancer of activated B cells (NF- κ B) and inducing apoptosis. However, their efficacy is limited by the emergence of drug resistance and treatment-limiting side effects including peripheral neuropathy and lymphopenia. Resistance to PIs as well as their side effects may partly be immune-mediated. Thus, we set out to investigate the impact of PI treatment on innate immune responses.

Materials and Methods: PIs were applied to a variety of inflammasome-competent human immortalized and primary cells, including the cell line THP-1 (monocytic), primary human peripheral blood mononuclear cells (PBMC), M-CSF or ascites-derived macrophages, keratinocytes, and epithelial cells. [EB1] Inflammasome activation was characterized via Interleukin-1 β (IL-1 β) release in cellular supernatants (ELISA, all cell types) and ASC-speck formation using an ASC-GFP reporter (THP-1). To characterize the contribution of Nod-like receptor pyrin domain-containing protein 3 (NLRP3) and caspase-1 (CASP-1) to inflammasome formation, NLRP3 and CASP-1-deficient THP1 cells were generated using CRISPR/Cas9-mediated genome engineering, and NLRP3 was pharmacologically inhibited using MCC-950 (Invitrogen).

Results: We report PI-mediated activation of the inflammasome in all cells tested. Treatment with BTZ induced secretion of IL-1 β by THP1 cells and PBMC with an EC50 that was similar to the IC50 in BTZ-sensitive, but not BTZ-resistant KMS-11 MM cells. We observed hallmarks of canonical inflammasome activation such as the formation of ASC specks and abrogation of IL-1 β secretion in caspase-1-deficient cells. A variety of inflammatory stimuli induce inflammasome formation via activation of NLRP3, the only inflammasome receptor currently targetable by a small molecule and investigated in clinical trials. Surprisingly, neither genetic ablation of NLRP3 nor MCC-950 treatment could abrogate IL-1 β signaling following BTZ exposure.

Conclusion: Few small-molecule, NLRP3-independent inflammasome activators have been identified. Consequently, the observation that PIs activate the inflammasome via an NLRP3-independent mechanism is of considerable interest. Further investigation will include the identification of the receptor mediating BTZ-driven inflammasome assembly in order to identify mechanisms of action that may be amenable to therapeutic intervention.

P11

Identification and functional analysis of potent TLR7- and TLR8-specific RNA-oligonucleotide agonists for immunotherapy

A. Wieland¹, T. Zillinger¹, E. Bartok¹, M. Suresh², S. Menne², B. Sawatsky³, V. von Messling³, W. Barchet¹, C. Coch¹, G. Hartmann¹

¹University Hospital Bonn, Institute of Clinical Chemistry and Clinical Pharmacology, Bonn, Germany

²Georgetown University Medical Center, Department of Microbiology and Immunology, Georgetown, United States

³Paul-Ehrlich-Institute, Division of Veterinary Medicine, Langen, Germany

Sensing of nucleic acids by innate immune receptors such as TLR7 and TLR8 can elicit a potent immune response. Both TLR7 and TLR8 are located in the endolysosome but of different immune cells. While TLR7 preferentially detects short dsRNA, TLR8 is activated by ssRNA and its cleavage products. TLR7 is primarily expressed in pDCs and B cells, but TLR8 is highly expressed and functional in human primary monocytes. TLR7 activation in pDCs induces the secretion of high amounts of type I interferons. TLR8 activation in primary monocytes results in the secretion of Th1, thus inducing IL-12p70 and pro-inflammatory cytokines but not type I IFN.

Based on previous structural insights, we designed an array of TLR7- and TLR8-specific RNA oligonucleotides. The minimal structural motif sufficient for full TLR7 activation is a single G:U wobble base pair within a non-U-containing sequence context. Based on these rules for TLR7 agonist activity, we were able to develop TLR8-selective RNA-oligonucleotide agonists. By comparing our RNA-oligonucleotide agonists to different small-molecule agonists of TLR7 and TLR8 *in vitro*, we demonstrated that our ligands were less toxic and more potent than the small molecules. Interestingly, the cellular response to our TLR8 ligands showed not only a substantial quantitative difference but also exhibited a superior qualitative response pattern, when compared to the respective small-molecule TLR7/8 ligands. Because rodents do not have a functional TLR8 receptor they cannot be used as *in vivo* models in preclinical development of TLR8 agonists, therefore ferrets (influenza) and woodchucks (hepatitis B) were identified as suitable animal models. Our results suggest that RNA-based TLR8 ligands are highly attractive compounds for clinical development as anti-infectives, vaccine adjuvants as well as for cancer immunotherapy due to their favorable functional characteristics, but our initial *in vivo* results show that delivery of these RNA agonists still requires further optimization.

P12

Functional analysis of human genes regulated by HCoV-229E using genome-editing by CRISPR-Cas9

B. V. Albert¹, M. S. Shaban¹, S. Werner¹, J. Meier-Soelch¹, C. Mayr-Buro¹, H. Weiser¹, T. Hain², L. Schmitz³, M. Kracht¹

¹Rudolf Buchheim Institute of Pharmacology, Justus Liebig University Giessen, Gießen, Germany

²Institute of Medical Microbiology, Gießen, Germany

³Institute of Biochemistry, Gießen, Germany

Questions: Human coronavirus 229E is the member of genus *Alphacoronavirus* associated with mild upper respiratory tract infections. The virus replicates in the host cell cytoplasm and triggers immunomodulatory and ER-associated stress responses by poorly characterized mechanisms. HCoV-229E infection in Huh7 cells upregulated 1,073 genes at the genome-wide level (Poppe et al., doi: 10.1371/journal.ppat.1006286) which include transcription factors (ANKRD1, EIF2AK3, ATF4, BHLHE40/41, ZNF165, and KLF6) and metabolic factors (CHAC1, FICD, EDEM1, FUT1, CTH, and ERO1LB), whose role for the virus-host response is unknown. By performing loss-of-function approaches will reveal the significance of the most strongly regulated host cell factors, the underlying mechanisms involved and how they may form a CoV-regulated signaling network that controls (positively or negatively) HCoV-229E replication or the expression of host cell genes.

Methods: To obtain more insight into the functional relevance of coronavirus (CoV) induced genes in viral replication; we used CRISPR-CAS9 mediated loss-of-function approaches to suppress these host cell factors in Huh7 cells. We also used an unbiased approach to identify the genes needed for HCoV-229E replication based on the genome-scale CRISPR-CAS9 knockout (GECKO) lentiviral sgRNA library consisting of more than 100,000 sgRNAs targeting the human genome with 6 sgRNAs per gene.

Results and Conclusion: Genomic editing and knockout/knockdowns were confirmed by Sanger sequencing of PCR-amplified genomic regions and by immunoblotting of cell extracts of stable cell lines. The roles of these host cell factors were systematically assessed for virus replication by measuring viral titers, viral transcripts and viral protein expression by qRT-PCR and western blotting. However, we have observed no major phenotype with the knockout cell lines on HCoV-229E replication. We have successfully generated stable transduced Huh7 cell line with GECKO library and the screening strategy would then be analyzing the enrichment of integrated sgRNAs by deep sequencing in the cells, which survive upon HCoV-229E infection. Our deep sequencing data identified numerous genes that are required for replication and/or cell-survival. Further validation of these hits will provide more insights into the functional relevance of these genes, which might be responsible in different stages of replication including viral entry, viral-host response and budding.

Pharmacology – Cancer pharmacology and treatment

P13

Targeting the SCAP factors c-IAP1, c-IAP2 and Bcl-2 eliminates senescent cells and enhances TMZ-induced cell killing of glioblastoma cells

C. Schwarzenbach¹, L. Tatsch¹, B. Kaina¹, M. Tomacic¹, M. Christmann¹
¹University Medical Center Mainz, Toxicology, Mainz, Germany

Introduction: Senescence represents an important outcome of alkylation drug-based tumor therapy. In previous work, we showed that following temozolomide (TMZ) exposure most glioma cells evade apoptosis, entering a senescent state and thereby they are protected against anticancer therapy. The senescent cells could either escape from senescence, contributing to the formation of recurrences, or they can induce the senescence-associated secretory phenotype (SASP), which may impact therapy success. Therefore, a direct targeting of senescent cells might be favorable to improve the effect of TMZ-based anticancer therapy. Agents that specifically kill senescent cells are called "senolytics". Their discovery was based on the observation that senescent cells are resistant to apoptosis due to upregulation of specific senescent-cell anti-apoptotic pathways (SCAPs).

Question: Which SCAPs are involved in the prevention of TMZ-induced cell death in senescent glioblastoma cells?

Methods: Cell death, senescence, cell cycle progression and expression of anti-apoptotic factors were analyzed by flow cytometry, β -Gal assay, qPCR and immunodetection in LN229, U87 and A172 glioblastoma cells upon exposure to TMZ. Furthermore, the impact of inhibition of these potential SCAPs on cell death was evaluated by flow cytometry.

Results: TMZ-induced senescence is a frequent event in glioblastoma cells, which is associated with an accumulation of cells in the G2-phase and a significant formation of polyploid cells. During senescence a strong upregulation of c-IAP1, c-IAP2, Bcl-2 and Bcl-XL was observed. Treatment of senescent cells with non-toxic concentration of the inhibitors embelin (targets XIAP), AT406 (targets c-IAP1 > XIAP), BV6 (targets c-IAP1, c-IAP2 and marginal XIAP) and Venetoclax (targets Bcl-2) clearly showed that inhibition of c-IAP2 and Bcl-2 strongly triggers death of TMZ-induced senescent cells. COMBENEFIT analysis further showed that combination of BV6 and Venetoclax further enhances this response.

Conclusions: During TMZ-induced senescence upregulation of the antiapoptotic factors c-IAP1, c-IAP2 and Bcl-2 are key events in the protection from cell death, and inhibition of these factors effectively kills senescent glioblastoma cells.

P14

The impact of cell adhesion signaling in tyrosine kinase inhibitor resistance in chronic myeloid leukemia cells

M. Litterst¹, I. Nagel², I. Cascorbi¹, M. Kähler¹
¹Institute of Experimental and Clinical Pharmacology, University Hospital Schleswig-Holstein Kiel, Kiel, Germany
²Institute of Human Genetics, University Hospital Schleswig-Holstein Kiel, Kiel, Germany

Question: Tyrosine kinase inhibitors (TKI), such as imatinib, improved significantly the therapy of chronic myeloid leukemia (CML). They inhibit the tyrosine kinase BCR-ABL1, which is constitutively active in CML. However, therapy resistance remains a problem. Gene expression profiling of imatinib resistant cells showed alterations of cell adhesion signaling, in particular of the matrix protein fibronectin (FN1). Therefore, we analyzed, if changes in FN1-expression could play a role in imatinib-resistance.

Methods: The role of FN1 in imatinib-resistance was analyzed using an in vitro-K-562 imatinib resistance model using treatment-native cells and two biological replicate cell lines, resistant to 0.5mM imatinib. The mRNA and protein expression of FN1 was determined by RT-qPCR and immunoblotting, respectively. Further, cell adhesion capability was measured using the Vybrant cell adhesion assay. The impact of FN1 on the cell adhesion signaling was further investigated by siRNA-transfection of K-562 sensitive cells and by transfection of an FN1-coding plasmid into the two biological replicates of cells, resistant to chronic 0.5 mM imatinib exposure. Subsequently, cell adhesion capability and the response to imatinib were analyzed on the level of total cell count, cell viability and proliferation.

Results: FN1 expression on mRNA and protein level was decreased in all tested imatinib-resistant cells compared to K-562 sensitive cells. FN1-downregulation in K-562 sensitive cells led to reduction of cell adhesion ($p=0.02$), but to an increase in total cell count ($p=0.04$) and proliferation ($p=0.005$) when exposed for 48h to 2mM imatinib. Restoration of FN1-expression in both imatinib-resistant cell lines resulted in a higher capability of cell adherence ($p=0.03$, $p=0.04$) and increased cytotoxicity ($p=0.04$, $p=0.03$). Total cell count ($p=0.03$, $p=0.03$) and viability ($p=0.01$, $p=0.004$) were decreased in all tested FN1-restored imatinib resistant cell lines under imatinib exposure.

Conclusion: Our data suggest that FN1 could be involved in imatinib-resistance, as reduction of FN1-expression was associated with reduced imatinib-susceptibility and cell adherence. Interestingly, imatinib resistance could be restored by transfection of FN1 resulting in increased imatinib-susceptibility and cell adherence. This allows us to

hypothesize that alterations in the cell adhesion signaling play a role in tyrosine kinase inhibitor resistant chronic myeloid leukemia cells.

P15

Identification of senolytic agents for sequential treatment of glioblastoma with temozolomide

L. Beltzig¹, B. Stratenwerth¹, M. Christmann¹, B. Kaina¹
¹Institute for Toxicology, University Medical Center Mainz, Mainz, Germany

Introduction: Glioblastoma multiforme (GBM) is the most common malignant brain tumor in adults. Despite a stringent treatment schedule, the median survival rate is only 15 months after diagnosis due to recurrences. Temozolomide (TMZ) induces not only apoptosis, but also survival pathways, one of which is senescence. If GBM cells escape the senescent state, they may give rise to recurrent tumors. Therefore, treatments that target senescent cells, "senolytics", may lead to a better outcome.

Objectives: Here we tested two natural substances and ionizing radiation (IR) for their senolytic capacity. Also, several proteins involved in the induction of senescence were assessed regarding their role in maintaining the senescent state.

Materials & Methods: The GMB cell line LN229 was used for analysis of cell death and senescence following TMZ with and without senolytic treatment. Apoptosis and senescence were measured via flow cytometry, using annexin V-PI or C12FDG staining, respectively. Natural substances tested were fisetin and curcumin. The specific signaling pathway inhibitors were ABT-737, AZD1390, VE-821, UCN-01, Chk2-II, NF- κ B-I κ B, UC2288, 3-MA, BV6, pifithrin- α , pifithrin- μ and chloroquine.

Results: Eight to ten days following TMZ treatment up to 80% of senescent cells and 20-30% of apoptotic cells were measured in the population. Fisetin, ABT-737, chloroquine and 3-MA significantly reduced senescence while cell death was increased significantly. The ATM and ATR inhibitors and pifithrin- α were also able to reduce senescence, but only slightly increased cell death by apoptosis. No such effects were seen after treatment of senescent cells with IR, curcumin, the inhibitors of Chk1, Chk2, NF- κ B or p21 and pifithrin- μ .

Conclusion: Fisetin, chloroquine, ABT-737 and 3-MA were identified as senolytics by a decrease in senescence and increase in cell death. ATM, ATR and p53 play critical roles in the induction of senescence. They also seem to be important in maintaining senescence, since inhibition led to a decrease of the senescent population. However, since no significant increase in the cell death rate was observed, the corresponding inhibitors do not have senolytic properties. Inhibition of Chk1, Chk2, p21, NF- κ B and p53 had no effect on senescent cells. Therefore, they neither seem to play a critical role in maintaining senescence nor can they be used as senolytics. Since IR did not reduce the senescence level, it cannot be considered to be senolytic.

P16

Targeting mechanisms of the DNA damage response (DDR) to overcome acquired resistance to conventional anticancer therapeutics (CATs)

J. Mann¹, G. Fritz¹
¹Heinrich Heine University Düsseldorf, Institute of Toxicology, Medical Faculty, Düsseldorf, Germany

Question: Acquired drug resistance of malignant cells limits the therapeutic efficacy of conventional anticancer therapeutics (CATs). A common target of approved CATs is the genomic DNA of tumor cells. Due to induction of DNA damage, the DNA damage response (DDR) gets activated and coordinates cell cycle arrest, DNA repair and apoptosis. Alterations in these signaling pathways can contribute to CAT-resistance, which makes DDR components attractive targets for developing new therapeutic approaches. To overcome acquired drug resistance, we aim to evaluate the usefulness of selected DDR modifiers to evoke cell death in CAT-resistant cell variants if used as mono- or co-treatment.

Methods: Previously isolated cisplatin-resistant bladder cancer cells were analyzed regarding their sensitivity to various CATs and pharmacological DDR modifiers by measuring the cell viability via AlamarBlue™ Assay. This screening approach was applied to identify DDR-modulatory compounds that (i) effectively resensitize/kill the cisplatin-resistant cell variant and (ii) provide hints for putative molecular mechanism contributing to acquired cisplatin-resistance. Based on the obtained results, we investigated the effect of selected DDR modifiers on proliferation (EdU incorporation assay), cell cycle distribution (flow cytometry-based analysis) and DNA damage formation and repair by western blot analyses of selected DDR components.

Results: The cisplatin-resistant variant of the bladder cancer cell line J82 (J82^{CisPt}) showed to be more sensitive to monotherapy with substances that cause replication stress (i.e. 5-Fluorouracil, Chk1-inhibitor LY2603618¹) than their parental cells. Surprisingly, J82^{CisPt} cells were less responsive to the RAD51-inhibitor B02 as compared to wild-type. The viability data with B02 were confirmed by flow cytometry-based analyses and EdU incorporation. Combined treatment regimen with low and moderate doses of Chk1-inhibitor PF477736 and B02 revealed synergistic killing efficacy in J82^{CisPt}.

Conclusion: We suggest Chk1 to be a promising target to overcome acquired cisplatin resistance of bladder carcinoma cells. In addition, as concluded from the cross-resistance of J82^{Cis^R} cells to B02, we speculate that the molecular mechanisms of acquired cisplatin resistance of these cells involve RAD51-regulated functions.

¹Höhn et al. Distinct mechanisms contribute to acquired cisplatin resistance of urothelial carcinoma cells. *Oncotarget* vol. 7,27 (2016): 41320-41335

P17

Synergistic effect of the RAD51-inhibitor B02 on doxorubicin-induced cytotoxicity in mismatch repair (MMR) deficient cancer cells Leonie Schürmann and Gerhard Fritz
Institute of Toxicology, Medical Faculty, Heinrich Heine University Düsseldorf, Germany

L. Schürmann¹, G. Fritz¹

¹Heinrich Heine University Düsseldorf, Toxicology, Düsseldorf, Germany

Question: Targeting of mechanisms of DNA repair and DNA damage response (DDR) is considered as a powerful approach to improve anticancer therapy. The anthracycline derivative doxorubicin (Doxo), which induces DNA double-strand breaks (DSBs) via inhibition of DNA topoisomerase II, is applied for adjuvant chemotherapy of Triple Negative Breast Cancer (TNBC). Dysfunctional mismatch repair (MMR) has been reported for a subset of colon and mammary carcinomas and can contribute to Doxo resistance. Here, we aim to investigate the outcome of a pharmacological inhibition of DSB repair on the Doxo response of MMR deficient tumor cells.

Methods: To this end, we analyzed the influence of inhibitors of DNA repair, notably of DSB repair by homologous recombination (HR) and Non-homologous end-joining (NHEJ), on Doxo-induced changes in cell viability, apoptotic cell death, cell cycle progression, mitochondrial homeostasis, formation of DSBs and activation of DDR mechanisms in MMR-deficient cancer cells. Since an established *in vitro* model of MMR-defective TNBC is not yet available, we employed MLH1-deficient HCT-116 colon carcinoma cells in our study.

Results: After mono- and co-treatment with Doxo and various DNA repair inhibitors (i.e. inhibitors of HDAC, PARP, MRE-11, RAD52, RAD51), we identified the RAD51-inhibitor B02 as the most powerful DNA repair inhibitor to synergistically increase the Doxo-induced loss of cell viability in HCT-116 cells. Based on the data obtained we suggest that the synergistic toxicity of Doxo and B02 is due to a reduced repair of DSBs by HR, leading to a higher number of DSBs, altered DDR and, most important, a substantial increase in caspase-driven apoptosis. Moreover, B02 largely disturbed mitochondrial homeostasis if used in combination with Doxo. Of note, B02 also promoted the cytotoxic effects of oxaliplatin and 5-FU in HCT-116 cells. Furthermore, it increased Doxo-induced cytotoxicity in MDA-MB-231 mammary carcinoma cells.

Conclusions: Pharmacological inhibition of RAD51 by B02 is suggested as a promising approach to synergistically increase the anticancer efficacy of Doxo in MMR-defective carcinoma cells. B02 may also be effective in combined treatment regimen with other types of conventional anticancer drugs and in different tumor entities. Forthcoming pre-clinical *in vivo* studies are required to elucidate the anticancer efficacy of B02 and its therapeutic window in a clinically relevant experimental setting.

P18

Effects of DNA damage response-inducing natural compounds on human bladder carcinoma cell lines

M. Sekeres¹, G. Fritz¹

¹Institute of Toxicology, Medical Faculty, Heinrich Heine University of Düsseldorf, Düsseldorf, Germany

Background and Aim: Natural compounds (NC) have been an important source of clinically useful anticancer drugs and continue to serve as a pool for new lead structures targeting cancer-related molecules. A previous study has identified 5-epi-nakijiquinone Q (NQ), 5-epi-illimaquinone (IQ) and secalonic acid F (SA) as the most promising NC that induce the DNA damage response (DDR) on their own or in combination with the conventional anticancer therapeutics (cAT) cisplatin and doxorubicin in pancreatic carcinoma cell lines. Therefore, the aim of this study was to further characterize these NC regarding their cytotoxic and DDR-modulating potency in the parental bladder carcinoma cell line J82 and the respective cisplatin-resistant variant J82 Cis^R.

Methods: The *in vitro* cytotoxic effects of the NC, used alone or in combination with the cAT cisplatin and doxorubicin, on human bladder carcinoma cell lines were evaluated by determination of cell viability using a fluorescence-based method (Alamar Blue Assay[®]). The valuation of the combination treatments was done by calculating the combination index (CI) using the CompuSyn software. Furthermore, the DDR-modulating potency of the NC was investigated via Western Blot analysis of selected DDR-related factors.

Results: The dose-response curves obtained with the bladder carcinoma cell lines are in line with the biological activity of the NC as described for pancreatic carcinoma cells. While both bladder carcinoma cell lines responded equally to NQ, the parental J82 cell line seems to be more sensitive to IQ than the cisplatin-resistant variant. In contrast, SA is more cytotoxic to J82 Cis^R cells. All combination treatments displayed additive toxicity in both bladder carcinoma cell lines at 72 h. The NC tested activate the DDR in mono- or combination-treatment with cAT. Thereby, the cisplatin-stimulated DDR was highly promoted by NQ in J82 cells.

Conclusion and Outlook: The data confirm the hypothesis that all NC tested also interfere with the DDR of bladder cancer cells. However, the NC did not increase the sensitivity of bladder cancer cells to cisplatin, suggesting that the NC may promote both DDR-related pro-death and pro-survival pathways at the same time. An objective of the ongoing work is to investigate whether a combination treatment of NQ and cisplatin affects apoptosis. To this end, flow cytometry-based analyses of cell cycle distribution are currently performed.

P19

The inducible dual-specificity phosphatases 2 influences gene expression in a cell model for diffuse large B-cell lymphoma

V. Tenhaken¹, J. Bruckmüller², B. Anangi³, B. Johansen³, H. Kildalsen³, J. Mejlvang³, I.

Nagel⁴, I. Cascorbi¹, O. M. Seternes³, H. Bruckmüller^{1,3}

¹Institut of Experimental and Clinical Pharmacology, University Hospital Schleswig-Holstein Kiel, Kiel, Germany

²Solana Research GmbH, Windeby, Germany

³Department of Pharmacy, Faculty of Health Sciences, UiT The Arctic University of Norway, Tromsø, Norway

⁴Institute of Human Genetics, University Hospital Schleswig-Holstein Kiel, Kiel, Germany

Background: Diffuse large B-cell lymphoma (DLBCL) as most common neoplasia in the mature lymphatic system is characterized by a high clinical and genetic heterogeneity. While 60% of patients can be cured by the standard chemotherapy (R-CHOP) the remaining develop progressive disease or relapses. To improve clinical outcome an increased understanding of underlying molecular processes and altered signaling pathways is needed. The identification of dysregulated molecular processes potentially responsible for inefficient treatment regimes paves the way for more personalized therapeutic strategies with improved patient efficacy. Although the frequently dysregulated Ras/ERK/MAP kinase signalling pathway is associated with disease progression and drug resistance in DLBCL, the exact underlying mechanisms are only poorly understood. Recent studies in DLBCL patients suggest a crucial role of the inducible dual-specificity phosphatase 2 (DUSP2) a key negative regulators of MAPK-signalling.

The aim of the present study was to investigate the effect of DUSP2 on the cellular transcriptome using a DLBCL cell line model. Analysis of gene expression levels was performed for WT and KO cell lines with two aims: 1. identification of genes induced by cell stimulation (unstimulated vs. stimulated cells) and 2. identification of genes related to DUSP2 activity (WT vs. KO).

Methods: CRISPR/Cas9 genomic editing was used to generate DUSP2 knockout cell clones in a B-cell lymphoma cell line (WSU-DLCL2). Whole transcriptome analysis was performed on unstimulated and stimulated wild-type (WT) and knock-out (KO) cells.

Results: Pathway analysis revealed that a 2h stimulation of WT and KO cells led to expression changes of genes associated with NF-kappa B-, MAPK- or B cell receptor-signalling. In contrast, the genes affected by DUSP2 activity could not be clearly assigned to specific overrepresented pathways. However, some of these deregulated genes are associated with MAPK-signalling. The early growth response protein 1 (EGR1), a downstream target of the MAPK pathway showed e.g. a significant induction (4,6-fold, adjusted p-value < 0,01) in WT cells after stimulation while no significant expression change was detectable in KO cells.

Conclusion: In conclusion, the initial analysis of our transcriptome data suggests that DUSP2 can influence the MAPK signaling pathway which results in an altered MAPK-related transcriptional programs.

P20

Isolation and characterization of radioresistant cell variants

N. Sivakumar¹, G. Fritz¹

¹Institute of Toxicology, Düsseldorf, Germany

Questions: The anti-tumor effects of radiotherapy (RT) are limited by acquired radio-resistance (RR) of tumor cells. In order to identify and characterize mechanisms of RR, murine tumor cells (4T1 breast cancer cells and B16-F1 skin melanoma cells) were subjected to a clinically oriented fractionated irradiation scheme. The aim of this work was to isolate and characterize the ionizing radiation (IR) response of the two different tumor cell lines.

Methods: Parental murine cell lines 4T1 and B16-F1 were exposed to fractionated irradiation scheme. The radiosensitivity of the selected cell variants was determined by use of colony formation assay and by determining cell viability using Alamar Blue assay. To investigate the cell cycle progression of the parental and radio-selected cells in response to irradiation, flow cytometry-based analyses were performed.

Results: The colony formation ability and cell viability of 4T1 and B16-F1 parental did not distinguish from that of the IR-selected 4T1^{IR} and B16-F1^{IR}. Flow cytometry-based analyses also failed to show substantial differences in the basal cell cycle distribution of 4T1 wild-type as compared to 4T1^{IR}. However, differences in cell cycle distribution were observed 24–72 h after IR treatment. Here, IR exposure of parental 4T1 cells caused more pronounced disturbances in cell cycle distribution as compared to the corresponding IR-selected 4T1^{IR} variants. Regarding B16-F1 melanoma cells, we observed differences in the cell cycle distribution under basal situation in the wild-type as compared to B16-F1^{IR}.

Conclusion: Analysis of colony formation and cell viability did not reveal the expected acquired radio-resistant phenotype of IR-selected 4T1^{IR} and B16-F1^{IR}. However, the flow cytometry-based analyses brought out differences in the cell cycle distribution between the parental and IR-selected cell lines under basal situation and/or following IR treatment. This finding indicates that fractionated irradiation causes sustained changes in cell cycle-related checkpoint mechanisms which eventually promote growth under situation of repeated IR exposure. In currently ongoing analyses we comparatively investigate the formation and repair of IR-induced DNA double-strand breaks (gH2AX/53BP1 foci analyses), monitor the activation of DNA damage response-related factors (Western blot analyses) and, furthermore, analyze mRNA expression of selected target genes via qRT-PCR in parental vs IR-selected cells of both cell types.

P21

The role of CDK-NF- κ B crosstalk in the IL-1 signaling pathway

J. Knauff¹, M. Kracht¹

¹Rudolf Buchheim Institute of Pharmacology, Justus Liebig University Giessen, Giessen, Germany

Question: The transcription factor nuclear factor kappa-B (NF- κ B) activates multiple genes with overlapping roles in inflammation, cell proliferation and cancer in response to pathogens or inflammatory stimuli such as interleukin-1 (IL-1). IL-1 is a fundamental driver of inflammation, but also contributes to reprogramming of the tumor microenvironment. The synthesis of secreted inflammatory factors is not only regulated by receptor-based cytokine pathways but also through the cell cycle. Important regulators of the cell cycle are cyclin-dependent kinases (CDKs). Selective inhibitors of CDK4/6 have been approved as anti-proliferative drugs for treating advanced breast cancer. CDK6 is also involved in the transcription of IL-1 target genes and was furthermore identified as a kinase that phosphorylates p65, the major transcriptionally active NF- κ B subunit. Apparently, several other CDKs have nuclear, transcription-associated functions considered to operate through the phosphorylation of the C-terminal domain (CTD) of RNA polymerase II. Unpublished phospho-proteomics experiments from our group revealed that IL-1 (transiently) induces the phosphorylation of additional CDKs or new putative CDK substrates (CDKs 1, 10, 11, 12, 13, NUCKS). We aim to unravel the mechanistic roles of classical and "novel" cyclin-dependent kinases in IL-1 driven gene expression and protein secretion of NF- κ B target genes.

Methods: HCT116 cells and HeLa cells were treated with the pan-CDK inhibitor flavopiridol or the selective CDK12/13 inhibitor THZ531. Western Blot analysis, RT-qPCRs and ELISAs were performed to analyze the function of the different kinases. Furthermore, an auxin-inducible degron system for a rapid and transient depletion of selected CDKs was established.

Results: The pan-CDK inhibitor flavopiridol profoundly suppresses the expression and secretion of NF- κ B target genes such as *IL8* or *CXCL2*. The inhibition of CDK12/13 with the selective inhibitor THZ531, in turn, augments the expression of IL-1 target genes. This may result from a stalled re-synthesis of I κ B.

Conclusions: These results strengthen the evidence for a tight crosstalk between CDKs and the NF- κ B signaling system. As different CDK inhibitors have differential effects on gene expression, it will be important to identify the underlying molecular basis of these effects at the transcriptional and translational levels and to assess the roles of individual CDKs on the cytokine driven tumor secretome.

P22

Effect of silver nanoformulations functionalized with rutin on human colorectal adenocarcinoma cells

I. Pinzaru^{1,2}, D. Coricovac^{1,2}, A. Dolghi^{1,2}, C. Dehelean^{1,2}

¹"Victor Babes" University of Medicine and Pharmacy Timisoara, Faculty of Pharmacy, Toxicology and Drug Industry, Timisoara, Romania

²Research Center for Pharmaco-toxicological Evaluations, Faculty of Pharmacy, "Victor Babes" University of Medicine and Pharmacy Timisoara, Timisoara, Romania

Questions: Rutin (Rut) is a phytochemical known for a wide range of biological and pharmacological activities, such as: antioxidant, anti-inflammatory, antihypertensive, anticarcinogenic, cytoprotective, anti-thrombotic, antidiabetic, neuro- and cardio-protective etc., but its low water solubility limits the *in vivo* bioavailability [1,2]. The present study proposes a new approach to enhance the biological activity of rutin via functionalization with silver nanoparticles (AgNPs) in a liposomal (L) formulation.

Methods: The functionalized compounds were obtained by a bottom-up chemical approach, being subsequently included in a liposomal formulation. The physicochemical characterization was realized through UV-Vis absorption, Fourier-transform infrared, Raman and photon correlation spectroscopy. The biological assessment involved the use of a tumor cell line, namely human colorectal adenocarcinoma (HT-29).

Results: Following the physicochemical characterization were obtained the subsequent results: the size of the nanoparticles was established in the range 94-122 nm (Rut_L 94 nm, AgNPs_L 108 nm, Rut_AgNPs_L 122 nm), good stability (negative zeta potential around -28 mV) and a percentage of encapsulation efficiency over 70 %. Biological studies on human colorectal adenocarcinoma cells highlight the cytotoxic effect of the new nanoformulation based on rutin functionalized silver nanoparticles in a liposomal form, obtaining an IC50 value below 10 and observing a series of morphological changes indicating concentration-dependent cell death.

Conclusions: These results indicate that the rutin formulations can be a promising drug carrier which preserves and intensifies the effect of active biomolecules. Further *in vitro* and *in vivo* studies will be performed to elucidate the cytotoxic mechanism of action.

References

- [1] Caparica R, Júlio A, Araújo MEM, et al. Anticancer Activity of Rutin and Its Combination with Ionic Liquids on Renal Cells. *Biomolecules*. 2020 Feb 4;10(2):233.
- [2] Pinzaru I, Tanase A, Enatescu V, et al. Proniosomal Gel for Topical Delivery of Rutin: Preparation, Physicochemical Characterization and In Vitro Toxicological Profile Using 3D Reconstructed Human Epidermis Tissue and 2D Cells. *Antioxidants* 2021, 10, 85. This work was also supported by Romanian National Authority for Scientific Research and Innovation, CNCS – UEFISCDI, grant number PN-III-P1-1.1-TE-2019-2134.

P23

Inhibition of the guanine nucleotidase exchange factor Epac1 inhibits cell growth of prostate carcinoma and renal cell carcinoma cells

L. Tänzler¹, F. Lezoualc'h², A. Mustea³, M. Schmidt⁴, M. Stope³

¹University Medicine Greifswald, Department of Urology, Greifswald, Germany

²Inserm UMR-1048, Université Toulouse III, Institut des Maladies Métaboliques et Cardiovasculaires, Toulouse, France

³University Hospital Bonn, Department of Gynecology and Gynecological Oncology, Bonn, Germany

⁴University of Groningen, Department of Molecular Pharmacology, Groningen, Netherlands

Introduction & Objectives: Monomeric GTPases are essential regulators of cell growth and motility and therefore have a central role in tumor progression. Activation occurs through interaction with a specific guanosine nucleotide exchange factor that substitutes GDP for GTP. A primary regulator of GTPase-dependent signaling cascades is the exchange factor directly activated by cAMP 1 (Epac1), which thus represents a promising target for novel anticancer therapies.

Materials & Methods: LNCaP and PC-3 (prostate carcinoma, PC) and 786-O and Caki-1 (renal cell carcinoma, RCC) cell lines were used as cancer cell culture models. The expression of Epac1, Rap1, Rap2, RhoA, Rac, Ran, and Rit1 was detected by quantitative RT-PCR and Western blotting. The activity of the GTPases Rap1, RhoA, and Rac1 was determined using commercial kits. For modulation of Epac1 activity, the Epac-specific cAMP analog 8-pCPT-2Me-cAMP and the Epac1-specific inhibitor CE3F4 were used. Proliferation was monitored by a cell analyzer.

Results: Epac1 was expressed at very low levels in the PC and RCC cells used and was only detected at the mRNA level. Epac1-dependent GTPases Rap1, Rap2, RhoA, Rac, and Ran were expressed in all 4 cell lines, Rit1, however, was detectable only in the two RCC lines. Rap1 activity could be modulated by Epac1 activation and inhibition in PC and RCC cells, whereas RhoA activity was modifiable only in RCC. Alterations in Rac1 activity were not detectable. Incubation experiments with the Epac1-specific inhibitor CE3F4 showed time- and concentration-dependent growth inhibitory effects for both PC and RCC cells.

Conclusion: Resistance represents a major challenge in all chemotherapy regimens. Therefore, it is even more important to identify new targets for novel antiproliferative agents. Inhibition of Epac1 leads to suppression of cell growth in PC and RCC cells. Thus, specific Epac1 inhibitors such as CE3F4 may represent promising therapeutics for oncological treatment.

P24

Cell morphology of a certain type of pigmented melanoma in the presence of ultraviolet radiation

A. Roman¹, A. Motoc¹

¹Victor Babeş University of Medicine and Pharmacy, Timisoara, Romania

Objectives: The WHO reviewed the classification of melanomas in 2018. According to these classifications, melanomas fall into two broad categories: melanomas caused by sun exposure (with low cumulative sun damage - with superficial spread - or high - lentigo maligna and desmoplastic melanomas) and nonsolar exposure melanomas (acral melanomas, congenital or blue nevi melanomas, Spitz melanomas, mucosal and uveal melanomas) [1]. In the present study, the evaluation of the morphological changes of a certain type of pigmented melanoma cells was performed, both in the presence and in the absence of ultraviolet radiation.

Materials & methods: The samples were obtained from an excision biopsy from a skin sample of a patient diagnosed with pigmented melanoma and were processed according to the protocols (storage in PBS with antibiotic mixture, removal of stained samples, placement in alcoholic solution, etc. during fourteen days) and cytological smears were performed for morphology and immunohistochemistry. Morphological changes were analyzed on an Olympus BX46 light microscope and histopathological analysis on a Leica Light Microscope DM750

Results: The primary culture of melanoma showed a pronounced polymorphism of epithelial shape being also present some obvious fusiform shape. Following irradiation, the cells are affected and lose their shape, highlighting the apoptotic phenomena.

Conclusions: Cell morphology is an essential parameter in assessing the development and progression of melanoma. All the information obtained is valuable and needs to be correlated with a 3D model in order to observe the mechanisms involved and to establish the relevant markers in approaching the type of disease.

References:

[1] Elder DE, Barnhill RL, Bastian BC, et al. Melanocytic tumour classification and the pathway concept of melanoma pathogenesis. In: Elder DE, Massi D, Scolyer RA, Willemze R, eds. WHO Classification of Skin Tumours. 4th ed. Lyon, France: IARC, 2018, 66–71.

P25

Lemongrass essential oil induces cytotoxic effects in HT-29 and Caco-2 colon carcinoma cell lines

A. Dolghi^{1,2}, I. Pinzaru^{1,2}, D. Coricovac^{1,3}, C. Dehelean^{1,2}

¹Research Center for Pharmacotoxicological Evaluations, Faculty of Pharmacy, "Victor Babeş" University of Medicine and Pharmacy Timisoara, Timisoara, Romania

²Victor Babeş University of Medicine and Pharmacy, Toxicology and Drug Industry, Timisoara, Romania

³Victor Babeş University of Medicine and Pharmacy, Department of Toxicology and Drug Industry, Timisoara, Romania

Background: According to current statistics (GLOBOCAN 2018), colorectal cancer occupies the fourth position as the most frequently diagnosed type of cancer globally. Despite the significant progress recorded in early detection methods and therapy alternatives, the incidence of this type of cancer is still on an ascending trend. Lemongrass (*Cymbopogon citratus*), known for its lemon odor and flavour in culinary industry, exhibits various pharmacological properties such as: antimicrobial, anti-inflammatory, antimutagenic, antidiabetic and anticancer effects.

Aim: Based on its known efficacy in gastrointestinal disorders and on its anticancer potential, the present study focused on verifying the cytotoxic potential of lemongrass essential oil in two colon carcinoma cell lines - HT-29 and Caco-2.

Methods: The cells were stimulated for 48 h with different concentrations of lemongrass essential oil (5-75 µg/mL) solubilized in dimethyl sulfoxide (DMSO) and the cytotoxic potential was evaluated in terms of cell viability (MTT assay), changes in cells' morphology and migratory capacity (scratch assay).

Results: Our results indicated a dose-dependent cytotoxic effect of the essential oil in both cell lines (HT-29 and Caco-2) by decreasing cell viability percentage and inducing changes in cells' shape (round cells) and adherence (floating cells in the culture medium). The lowest concentrations tested inhibited cells migration. It was also observed a higher susceptibility of HT-29 cells as compared to Caco-2 cells after lemongrass essential oil stimulation.

Further studies will be conducted to elucidate the cytotoxic underlying mechanism and to verify the impact of lemon grass essential oil in combination with standard therapy.

P26

The role of endolysosomal ion channels in cancer

C. Abrahamian¹, P. Netcharoensirisuk^{1,2}, P. Rüh³, A. Scotto Rosato¹, R. Tang¹, W. De-Eknamkul², F. Bracher³, C. Grimm¹

¹Ludwig Maximilian University of Munich, Walther Straub Institute of Pharmacology and Toxicology, Faculty of Medicine, München, Germany

²Chulalongkorn University Bangkok, Department of Biochemistry and Microbiology/Pharmacognosy, Faculty of Pharmaceutical Sciences, Bangkok, Thailand

³Ludwig Maximilian University of Munich, Department of Pharmacy – Center for Drug Research, München, Germany

Question: The endo-lysosomal system is an interconnected tubulovesicular network. Several ion channels including members of the mucolipin subfamily (TRPML) and two-pore channels (TPCs) are found in the membranes of endolysosomes. Interest has grown in recent years to investigate these endolysosomal ion channels in cancer due to the roles these channels play in a variety of processes closely linked to cancer metabolism such as cell growth, migration, growth factor signalling, and antigen presentation. In this study, we describe novel antagonists for TRPML1 and TPC2 and by use of these we have investigated the role of these channels in breast cancer and melanoma in more detail, respectively.

Methods: Screening and identification of potent and selective antagonists for TRPML1 and TPC2 were carried out. Expression of different endolysosomal ion channels was assessed in different cancer models via qPCR. CRISPR/Cas9 gene editing was used to create knockout (KO) models of TRPML1 in breast cancer lines and TPC2 in melanoma lines, which were validated via PCR, sanger sequencing, and the endolysosomal patch clamp technique. Cancer hallmarks were studied using transwell chambers for invasion, CellTiter Blue proliferation assay, migration scratch assay, melanin generation and tyrosinase activity assays. Underlying molecular mechanisms and effects on autophagy were explored using biochemical assays such as western blotting and immunocytochemistry.

Results: First, we provide the first in-class highly potent, isoform-selective TRPML1 inhibitors. By using these inhibitors, we demonstrate TRPML1-mediated inhibition of autophagy and TFEB translocation and inhibition of estrogen receptor negative breast cancer cell migration and invasion. Second, we have carried out a screening of 44 flavonoid compounds from South East Asian plant extracts and tested their effects on melanin production in melanoma lines. Two hit candidates were obtained that potently inhibited TPC2. Using these inhibitors and genetic ablation in melanoma, we show an inverse correlation between melanin production and melanoma progression due to the dual activity of TPC2 in endolysosomes and melanosomes. Our data suggest that loss of TPC2 results in reduced protein levels of a major regulator of melanoma progression but an increased activity of the melanin-generating enzyme, tyrosinase.

Conclusion: Endolysosomal cation channels, in particular TRPML1 and TPC2 have been extensively studied in recent years and a plethora of functions in the endolysosomal system have been discovered to be associated with lysosomal trafficking and autophagy regulation, activation of TFEB translocation, ROS sensing, regulation of lysosomal motility and positioning, and cancer. While activation of TRPML1 may be beneficial in neurodegenerative and lysosomal storage disease therapy, inhibition appears useful for cancer treatment. We show that migration and invasion of estrogen receptor negative breast cancer cells are both reduced upon treatment with EDME and genetic KO of TRPML1, corroborating its suitability to effectively interfere with major hallmarks of cancer progression. TPCs are expressed in endosomes, lysosomes, and lysosome related organelles such as melanosomes; they are of increasing interest as well as novel drug targets to treat neurodegenerative, metabolic, or infectious diseases. Here, we demonstrate that disruption of TPC2 function in different organelles, endolysosomes and melanosomes, is providing a promising new approach for melanoma treatment.

Pharmacology – CNS / endocrine pharmacology and treatment

P27

Medical cannabis is very well-tolerated in elderly pain patients and reduces comedicated opioid dosage – retrospective data from a German GP's practice

K. Gastmeier¹, F. Rottmann², V. Wätzig², A. Gastmeier³, T. Herdegen², R. Böhm²

¹GP practice, Potsdam, Germany

²University Hospital Schleswig Holstein, Institute of Experimental and Clinical Pharmacology, Kiel, Germany

³GP practice, Kleinmachnow, Germany

Question: Medial cannabinoids (MC such as THC/Dronabinol, extracts or flowers) are relevant therapeutics in particular for neuro-psychiatric dysfunctions and disorders. Its extended use is limited by insufficient data of prescription patterns, patient adherence or tolerability, particularly in elderly.

This analysis addressed the indication and dosages of MC and opioids differentiated by age and gender.

Methods: In this retrospective, observational intra-cohort analysis, we analysed prescription data of all patients in a GP's practice, who were prescribed MC.

Results: This study comprised of 178 patients with 1179 MC prescriptions, 55% dronabinol oil (557 prescriptions), 32% full-spectrum extract (328 prescriptions) or 6,6% spray (66 prescriptions). In 5% (50 prescriptions), two or more types of medical cannabis were prescribed.

Median THC dosages ranged from in median 8 mg/d for extract to 10.1 mg/d for spray with no statistical difference. The median dosages did not statistically vary for different ICD coded indications.

There was a small trend of increasing THC dosages over time ($p < 0.01$, Mann-Kendall trend test).

As patients were unevenly distributed concerning gender and age group (subgroups: <65, 65-79 and >79 years), subgroup analyses were not possible (Fig. 1).

MC was well tolerated and 143 patients (80%) continued the treatment during the observation period. 10 patients (5.6%) stopped due to ineffectiveness, 7 patients (3.9%) discontinued because of missing coverage by the health insurance. Only 5 patients (2.8%) stopped MC use due to adverse events (diarrhoea, cardiac problems, spasms of GIT, muscle cramps). Median time till dropout was 155 days (range 31 – 704).

119 patients (66%) used opioids concomitantly. Independent of THC dosage, prescription of opioid analgesics was significantly reduced by 22 morphine equivalents, i.e. 50% of opioid dosage ($p < 0.001$, one-sample t-test, Fig. 2), in line with previous findings (J Pain. 2016 Jun;17(6):739-44).

Conclusions: In elderly patients and under medical control, low-dose MC are a safe, well tolerated and may help to reduce opioid dosages. Thus, MC are a relevant option for neuro-psychiatric dysfunctions such as chronic pain in patients of high age.

Fig. 1

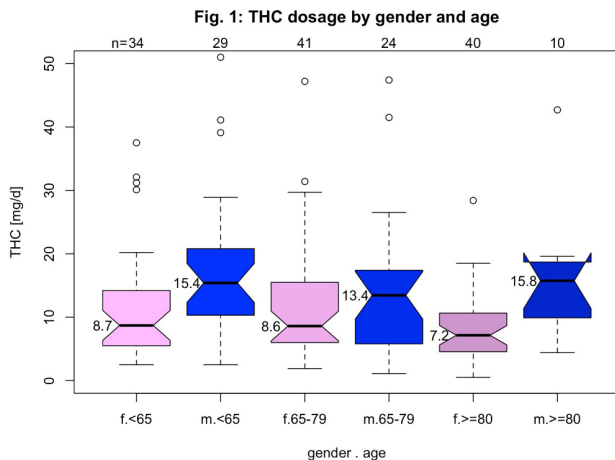
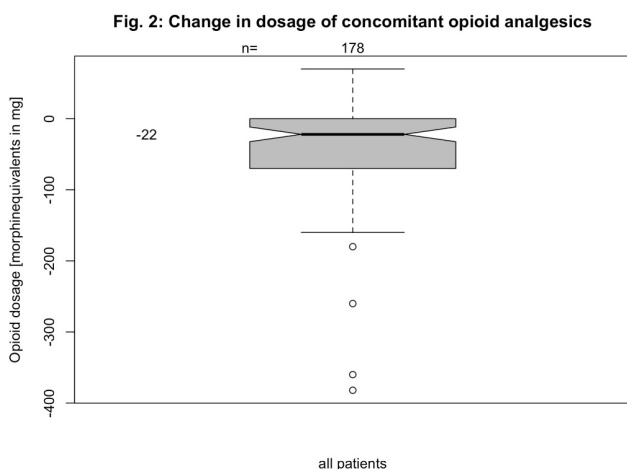


Fig. 2



P28

Neuroscientific research applications of a fully validated method for the monitoring of escitalopram and atomoxetine in human plasma

R. Regenthal¹, J. B. Rowe¹, K. D. Ersche¹, N. Skandali¹, J. Sacher¹, A. Aigner¹, J. Teichert¹
¹Institute of Pharmacology and Toxicology, Leipzig University, Clinical Pharmacology, Leipzig, Germany

Background: The exposure of healthy human volunteers or patients to neuro-psychopharmacological drugs coupled with functional magnetic resonance imaging is a common design in neuroscience. When aiming at a highly specific pharmacological modulation of neurotransmitter levels of neuronal networks involved in cognition, learning, memory, impulsivity, behavior, and functional execution, the most selective and potent specific serotonin-reuptake inhibitor (SSRI), escitalopram, and the specific noradrenergic reuptake-inhibitor (SNRI), atomoxetine, are nowadays often preferred over other approved drugs.

Methods: We developed a simple, sensitive, robust, and fully validated HPLC method for the description of complete plasma kinetics of escitalopram or atomoxetine as a useful tool for drug monitoring and the study of pharmacokinetics in neuroscientific study designs. Using photo diode array detection with UV absorption at 205 nm, the variation of internal standard within one chromatographic method enabled separate drug monitoring for concentration-controlled explorative studies in healthy humans and patients with Parkinson's disease.

Results: The method described here was found to be linear in the range of 0.002 - 1.4 mg/L for atomoxetine and 0.0012 - 0.197 mg/L for escitalopram. The lower limits of detection (LLOD) were found to be 1.2 ng/ml and 2.0 ng/ml for escitalopram and atomoxetine, respectively, and thus nearly equivalent to published LC-MS/MS methods. Results of the successful application of our method in neuroscience studies are presented, analyzing effects of escitalopram or atomoxetine in healthy humans as well as in patients with Parkinson's disease.

Conclusion: A simple, sensitive, robust HPLC method capable for monitoring escitalopram and atomoxetine in plasma is presented and validated, as a useful tool for

drug monitoring and for studying drug plasma kinetics in neuroscientific study designs. Our results point to the high inter-individual variability of plasma concentration in healthy human and patients, emphasizing a concentration-effect relationship as more predictive over a dose-effect relationship with regard to neurofunctional consequences, as detected by alterations in functional neuroimaging. Individual atomoxetine or escitalopram concentrations thus may qualify as one factor correlating with functional outcome, thus allowing to better differentiate between different degrees of neural responsivity.

P29

Pharmacological & phytochemical investigations of Kratom (*Mitragyna speciosa* Korth.) in the nematode *Caenorhabditis elegans*

C. Veltri¹, S. Hughes², **O. Grundmann**^{3,1}

¹Midwestern University Glendale, Department of Pharmaceutical Sciences, College of Pharmacy, Glendale, United States

²HAN University of Applied Sciences, Institute of Applied Biosciences and Chemistry, Nijmegen, Netherlands

³University of Florida, Department of Medicinal Chemistry, College of Pharmacy, Gainesville, United States

Objectives: *Mitragyna speciosa* Korth., commonly referred to as Kratom, is a Southeast-Asian plant whose leaf consumption results in dose-dependent stimulant and analgesic or sedative effects. Given the increasing reports of toxicity associated with Kratom consumption, especially in Western countries, it is essential to further investigate the safety of Kratom preparations using a viable *in vivo* model and well-defined Kratom leaf powders. The leaf material has gained much attention for its varied pharmacological effects, most prominently due to the activity of the alkaloids mitragynine and 7-hydroxymitragynine at opioid receptors. However, uncertainty remains over the toxicity and mechanism of action of Kratom.

Methods: In this study, we purchased three different commercially available Kratom products to prepare water and hydroalcoholic extracts for both chemical composition analysis and pharmacological evaluation. Extracts were analyzed by liquid chromatography high resolution mass spectrometry. To assess the biological effects in a whole-organism 3R compliant system, we used the nematode *Caenorhabditis elegans*. The developmental and reproductive effects of the Kratom extracts were observed.

Results: The variety of Kratom and extraction solvent (H₂O, MeOH, EtOH) were found to play large roles in the extraction efficiency of the Kratom alkaloids. All samples contained significant, but variable, levels of mitragynine, 7-hydroxymitragynine, and rhynchophylline. None of the Kratom products had detectable quantities indicating adulteration with common prescription or illicit opioids or benzodiazepines. In the worm model, we found that fertility, but not development, was impacted by all varieties of Kratom, with the severity of the reduction in brood size relating to elevated levels of alkaloids.

Conclusions: Our study shows that *C. elegans* can be used to dissect the mechanism of action and potential toxicities of Kratom, and due to the presence of an opioid-like system in the nematodes, we will show the effect of these alkaloids on opioid pathways.

Pharmacology – Pharmacoepidemiology and drug safety

P30

Pooled analysis of safety and tolerability of the fixed dose combination (FDC) of 400 mg ibuprofen plus 100 mg caffeine, compared to placebo: Data from 3 clinical trials.

M. Plomer¹, **A. Lampert**², **T. Weiser**²

¹Sanofi Aventis Deutschland GmbH, Medical Affairs, Frankfurt am Main, Germany

²Sanofi Aventis Deutschland GmbH, Medical Affairs, Frankfurt am Main, Germany

Introduction: In the first clinical efficacy study on the FDC ibuprofen/caffeine 400/100 mg, analgesic superiority versus ibuprofen 400 mg, caffeine 100 mg and placebo was demonstrated together with safety and tolerability (1). Since then, more clinical data on that FDC became available. Here we present a pooled analysis of safety and tolerability data in comparison to placebo.

Methods: Pubmed and clinicaltrials.gov were searched for clinical studies testing the above mentioned FDC versus placebo. These data were supplemented with unpublished data of trials (1) and (2). Pooled data of adverse event (AE) frequencies in verum and placebo groups were compared, and risks ratios were calculated.

Results: Three studies were identified (1, 2, 3). Two studies (1, 2) allowed for comparisons after a single dose of the FDC and placebo, study 3 provided data for 6 days administration of 3 doses daily (i. e. 18 doses). 28 (of 374) patients treated with a single dose of FDC, and 11 (of 122) patients under placebo reported AEs, which all were of mild to moderate intensity. The relative risk (RR) was 0.83 for the FDC compared to placebo (p=0.58). After 6 days treatment, 20 of 256, and 7 of 126 patients under FDC and placebo, respectively, reported AEs (which all were of mild to moderate intensity), giving a RR of 1.40 (p=0.42). 93% of FDC-treated patients rated tolerability as "good", "very good", or "excellent" (97.6% with placebo, p=0.32).

Conclusion: In clinical trials, the FDC ibuprofen 400 mg plus caffeine 100 mg was safe and showed high tolerability. AE incidences after single or repeated dosing, as well as patient assessment of tolerability, were not statistically different from placebo.

References:

- 1: Weiser T et al. (2018) Eur J Pain. 22:28ff
 - 2: Predel HG et al. (2019) J Pain Res. 12:2771ff
 - 3: Anonymous (2019) <https://clinicaltrials.gov/ct2/show/NCT02863575>
- Funding: This study was funded by Sanofi-Aventis Deutschland GmbH.

P31**COVID-19 vaccination program in Romania: an overview on implementation and monitoring of adverse reactions**

C. Morgovan¹, A. M. Juncan¹, L. L. Rus¹, A. A. Chis¹, **A. Arseniu**^{1,2}, C. M. Dobraea¹, A. Frum¹, L. Vonica¹, A. Butuca¹, F. Gligor¹, S. Ghibu³

¹"Lucian Blaga" University of Sibiu, Preclinical Department, Sibiu, Romania

²"Iuliu Hatieganu" University of Medicine and Pharmacy, Cluj-Napoca, Romania

³UMF "Iuliu Hatieganu" Cluj-Napoca, Pharmacology, Physiology and Pathophysiology, Cluj-Napoca, Romania

Questions: After first appearing in Wuhan (China) in December 2019, the novel Coronavirus (2019-nCoV) has led to the most challenging public health problems because of its complications^{1,2}. During a period of one year, this virus has caused more than 87 million cases and 1.9 million deaths³. In this context, drug manufacturers and researchers have focused on finding an appropriate treatment, especially vaccines; their efficiency, stability and safety being the most important issues.

Methods: The work techniques used were logical analysis and comparison^{4,5}. We realized a longitudinal retrospective study. To carry out this study, data were collected from the Romanian Ministry of Health daily reports released between December 27, 2020 and January 10, 2021.

Results: Like all EU countries, Romania started the Coronavirus vaccination program at the end of December 2020. A rapid temporary authorization has been released for Comirnaty (tozinameran or Pfizer–BioNTech COVID-19 vaccine) on December 2, 2020 (UK) and December 21, 2020 (EU). At the date of this study, only a single vaccine (Comirnaty) was available on the Romanian market. The first doses of Comirnaty were delivered to Romania on December 25, 2020, and the first doses were administered 2 days later, at 07.00 GMT. The vaccination program was designed to be administered in 3 steps: 1) to health and social workers from the public and private system; 2) to high-risk population and workers in key essential areas; 3) to the general population. During a 15-day period, in Romania 0.56% of the citizens (108,294 people) were vaccinated, from which 0.36% (388 people) presented adverse reactions (ADRs). According to the scientific literature⁶, these ADRs are: 40% (n=140) local pain reactions (pain, swelling) and 60% (n=210) general disorders (headache, arthralgia, myalgia, fatigue, chills, pyrexia, hives, asthenia, or anxiety etc)⁷.

Conclusions: The global health issues and the low rate of non-severe ADRs justify the acceleration in the vaccination program.

References:

1. Huppert et al, Semin Respir Crit Care Med. 2019 Feb;40(1):31-39. doi: 10.1055/s-0039-1683996
2. Tsai et al. Int J Mol Med., 2021 Jan;47(1): 3-22. doi: 10.3892/ijmm.2020.4794.
3. <https://covid19.who.int/>
4. Cuc et al., Farmacia, 2015, 63(4): 607-612
5. Morgovan et al., Farmacia, 2019, 67(3): 537-544, doi.org/10.31925/farmacia.2019.3.24
6. Chung et al., Adv Drug Deliv Rev., 2020170:1–25. doi: 10.1016/j.addr.2020.12.011.
7. <https://vaccinare-covid.gov.ro/>

Toxicology – 3R Practice/Alternative Methods**P32****Investigations of acute effects of polystyrene and polyvinyl chloride micro- and nanoplastics in an advanced *in vitro* triple culture model of the healthy and inflamed intestine**

M. Busch¹, G. Bredeck¹, A. Kämpfer¹, R. Schins¹

¹IUF – Leibniz Research Institute for Environmental Medicine, Düsseldorf, Germany

The continuous degradation of plastic waste in the environment leads to the generation of micro- and nanoplastic fragments and particles. Due to the ubiquitous presence of plastic particles in natural habitats as well as in food, beverages and tap water, oral exposure of the human population with plastic particles occurs worldwide. We investigated acute toxicological effects of polystyrene (PS) and polyvinyl chloride (PVC) micro- and nanoplastics in an advanced *in vitro* triple culture model (Caco-2/HT29-MTX-E12/THP-1) mimicking the healthy and inflamed human intestine to study the effect of inflammatory processes on plastic particle toxicity. We monitored barrier integrity, cytotoxicity, cell layer integrity, DNA damage, the release of pro-inflammatory cytokines (IL-1 β , IL-6, IL-8 and TNF- α) and mucus distribution after 24 h of particle exposure. In addition, we investigated cytotoxicity, DNA damage and IL-1 β release in monocultures of the three cell lines. Amine-modified polystyrene nanoplastics (PS-NH₂) served as a positive control for particle-induced toxicity. No acute effects in the investigated endpoints were observed in the model of the healthy intestine after PS or PVC exposure. However, during active inflammatory processes, exposure to PVC particles was found to augment the release of IL-1 β and to cause a loss of epithelial cells. Our results suggest that prevalent intestinal inflammation might be an important factor to consider when assessing the hazard of ingested micro- and nanoplastic particles.

P33**Upregulation of the expression of M-cells, enteroendocrine cells and goblet cells in porcine intestinal organoids**

J. Lehmann¹, B. Seeger^{1,2}

¹University of Veterinary Medicine Hannover, Institute for Food Quality and Food Safety, Research Group Food Toxicology and Alternative/Complementary Methods to Animal Experiments, Hannover, Germany

²University of Veterinary Medicine Hannover, Center for Replacement and Complementary Methods to Animal Testing, Hannover, Germany

Question: The pig is a valuable model for human gastrointestinal disease research as there are similarities between these two species. Nevertheless, there are species-specific differences in pathophysiological processes, such as the infection with *Yersinia enterocolitica*, which leads to gastroenteritis in humans, whereas pigs remain asymptomatic. Intestinal organoids became an important tool to study underlying mechanisms. During long-term culture, organoids are enriched for the expression of proliferating intestinal stem cells. To provide models to investigate molecular mechanisms during bacterial infection or toxin effects, the aim of the presented study is to adapt the expression of specialized intestinal epithelial cells in porcine intestinal organoids.

Methods: Small intestinal organoids were generated after isolation of intestinal stem cells from porcine jejunum and cultured in long-term culture medium containing the niche factors Wnt3a, R-spondin and noggin. To achieve a physiological cell population, bFGF and IGF-1 were added [1]. To induce overexpression of specific epithelial cells various small molecules were added to the cell culture medium: RANKL for M-Cells [2], DAPT for goblet cells and DAPT, IWP2 and PD0325901 for enteroendocrine cells [3]. The organoids are analyzed for the expression of characteristic markers for specialized epithelial cells via RT-qPCR and immunofluorescence staining.

Results: The organoids survive treatment with the different factors for several days, changing their morphology. Their characterization is ongoing.

Conclusions: While the initial results appear promising, cell characterization will provide further insight into whether differentiation of specific epithelial cells was successful. It remains to be seen whether these cells are functional and thus could be used to study pathomechanisms in the porcine intestinal epithelium.

References

1. Fujii, M., et al., *Human Intestinal Organoids Maintain Self-Renewal Capacity and Cellular Diversity in Niche-Inspired Culture Condition*. Cell Stem Cell, 2018. 23(6): p. 787-793 e6.
2. Rouch, J.D., et al., *Development of Functional Microfold (M) Cells from Intestinal Stem Cells in Primary Human Enteroids*. PLoS One, 2016. 11(1): p. e0148216.
3. Basak, O., et al., *Induced Quiescence of Lgr5+ Stem Cells in Intestinal Organoids Enables Differentiation of Hormone-Producing Enteroendocrine Cells*. Cell Stem Cell, 2017. 20(2): p. 177-190.e4.

P34**Establishment of an *in vitro* Transgenic Rodent assay for the detection of potential mutagens**

A. Göpfert¹, D. M. Schuster¹, C. Rülker¹, N. Honarvar¹, C. Gomes¹, B. van Ravenzwaay¹, R. Landsiedel¹

¹BASF SE, Experimental Toxicology and Ecology, Ludwigshafen am Rhein, Germany

Mutagenicity is a critical endpoint in the hazard assessment of industrial chemicals, biocides and pesticides. The induction of gene mutation by test substances can be assessed *in vivo* by the transgenic rodent (TGR) assay which has been adopted by the OECD (test guideline no. 488). This assay uses the bacterial lacZ gene as a reporter gene to easily and reliably detect mutations. Multiple copies of this gene are integrated in the mouse chromosome.

There is currently no corresponding OECD method *in vitro*. We adapted an *in vitro* mutagenicity assay described by Cox *et al.* (2019) based on the protocol used for the *in vivo* TGR assay (OECD 488). In this *in vitro* version, "*in vitro* TGR assay", primary hepatocytes (PHs) isolated from transgenic mice (MutaMouse) instead of the living animal are treated with the test substance. Due to the similarity of the *in vivo* and the corresponding *in vitro* assay, this approach is aimed to predict the *in vivo* outcome better than other *in vitro* genotoxicity assays.

MutaMouse PHs were treated for six hours with N-ethyl-N-nitrosourea, Benzo[a]pyrene, Ethyl methanesulfonate, Mitomycin C and Azathioprine. To assess the mutagenic potential, isolated DNA from treated cultures were packaged in λ phages. Mutations of the lacZ gene were quantified by infection of *E. coli* C lacZ-galE- cultures and co-treatment with Phenyl- β -D-galactopyranoside (P-Gal). LacZ mutant frequency (MF) was evaluated by referring the number of phages containing lacZ mutations (selective conditions (with P-Gal)) to the total number of phages (non-selective conditions (w/o P-Gal)).

All tested mutagens showed an increase in lacZ MF ranging from 4- to 13-fold compared to vehicle control; the increase of the MF was concentration-dependent.

In conclusion, the *in vitro* TGR assay was able to detect the mutagenic potential of direct-acting and pro-mutagens with a performance qualitatively similar to the *in vivo* TGR assay. Further assessments using more test substances including moderate and weak mutagens are still required to corroborate the above data.

Cox et al. (2019). *Environ. Mol. Mutagen.*, 60(4), 348. <https://doi.org/10.1002/em.22277>

OECD (2020). *Test Guideline No. 488*, DOI: <https://doi.org/10.1787/9789264203907-en>

P35

Gap junction intercellular communication: A functional biomarker of testicular toxicity

I. Virmani¹, E. Sychrová¹, I. Sovadinová¹
¹RECETOX, Faculty of Science, Brno, Czech Republic

Abstract Text: Effects of the individual environmental contaminants and their responses are well reported in the literature; yet, overlooking the consequences of their mixture exposure. The male reproductive system as a target for these contaminants is understudied. However, there is an evidence of an interference of organochlorine cocktails with male reproductive health from previously conducted *in vivo* and *in vitro* studies. Environmentally relevant organochlorine mixtures have been associated with a worldwide decline in male fertility. The biomarkers closely associated with an adverse outcome in male reproductive health at the molecular and cellular level are considered essential elements in environmental quality and drug assessments. Testicular gap junction intercellular communication (GJIC) plays a central and critical role in cellular and tissue homeostasis in the male reproductive system and a vital role in spermatogenesis and steroidogenesis. Additionally, the inhibition of GJIC is regarded as one of the key hallmarks for the identification of non-genotoxic carcinogens. Thus, untimely dysregulation of localization and functions of GJIC in testes at sensitive periods of life may result in male reproductive dysfunctions such as decreased fertility or testicular cancers. However, testicular GJIC as a biomarker of testicular toxicity is often overlooked due to the lack of a suitable HTS (High-throughput Screening) /HCS (High Content Screening) method.

Objective: This talk will address testicular GJIC as a functional biomarker of testicular toxicity for environmental quality assessment.

Material and Methods: We evaluated the effects of a human-relevant organochlorine mixture with known reproductive toxicity *in vivo* and *in vitro* on GJIC in murine prepubertal testicular (Leydig Tm3 and Sertoli Tm4) cells using a semi-high throughput cell imaging assay for a simultaneous assessment of GJIC, cell viability and cell density/growth in adherent cultures.

Results: The human relevant organochlorine mixture inhibited testicular GJIC at the non-cytotoxic concentrations in both Leydig (Tm3) and Sertoli cells (Tm4), respectively.

Conclusion: Besides a key hallmark for identifying non-genotoxic carcinogens, GJIC seems to be also an important biomarker of testicular toxicity.

P36

Quantifying concentrations of selected compounds in Balb/c 3T3 cells and culture medium

D. Dimitrijević¹, E. Fabian¹, B. Nicol², B. Birk¹, B. van Ravenzwaay¹, R. Landsiedel¹
¹BASF SE, Experimental Toxicology and Ecology, Ludwigshafen am Rhein, Germany
²Unilever U.K., Sharnbrook, United Kingdom

The implementation of *in vitro* assays including research in chemical exposure (*In vitro* dosimetry) allows to more precisely link *in vitro* effect data to *in vivo* doses. Nominal concentrations (C_{Nom}) are prevalently used to describe concentration effect relationships in *in vitro* toxicology. However, C_{Nom} is an inaccurate dose metric as e.g. adsorption to medium constituents, evaporation or degradation of test substances may have an impact on its concentration in the *in vitro* test system. The determination of free concentrations *in vitro* would better describe toxic events at molecular targets. Here, Balb/c 3T3 cells were treated with nine compounds to determine medium (C_{Med}) and intracellular concentrations (C_{Cell}). A steady-state mass balance model was implemented to predict total C_{Med} , C_{Cell} and free C_{Med} ($C_{FreeMed}$) which were compared to experimental results.

Balb/c 3T3 cells were incubated at 6, 24 and 48 h with the test compounds (Acetaminophen, Caffeine, Fenarimol, Flutamide, Genistein, Methyltestosterone, Tamoxifen, Trenbolone, Warfarin) at subtoxic C_{Nom} , showing $\geq 80\%$ viability as previously determined in an MTT-assay. The total concentrations in medium and cells were determined via HPLC-MS/MS. Fraction unbound in medium (f_u) was measured via rapid equilibrium dialysis and used for the correction of total C_{Med} .

The C_{Med} of 8/9 compounds retained stable over time, barely deviated from the initial test concentrations and agreed with predicted total C_{Med} . Further, the correction by f_u shows lower amount of free substance with $C_{FreeMed}$ down to 5 % of the total C_{Med} for 7/9 compounds. However, $C_{FreeMed}$ of 5/9 compounds matched with the predicted $C_{FreeMed}$. Two trends are observed for C_{Cell} : Whereas a steady state situation was observed for 6/9

compounds, C_{Cell} of Flutamide, Tamoxifen and Genistein increased over time. Predictions for 3/9 compounds agreed to the experimental derived C_{Cell} .

Further strategies are currently investigated to determine and predict (free) C_{Cell} . As a future perspective, total or free concentrations from *in vitro* dosimetry may be applied as point of departure (POD) for optimized *in vitro* to *in vivo* extrapolations.

P37

Impact of fetal growth restriction on the developing brain using an *in vitro* neurosphere model

B. A. Kühne^{1,2}, P. Vázquez^{1,2}, M. Fuentes-Amell¹, C. Loreiro², F. Crispí², E. Gratacós², J. Gómez-Catalán¹, E. Fritsche³, M. Illa², M. Barenys^{1,2}
¹University of Barcelona, Pharmacology, Toxicology and Therapeutic Chemistry, Barcelona, Spain
²Hospital Clínic and Hospital Sant Joan de Déu, BCNatal Fetal Medicine Research Center, Barcelona, Spain
³IUF – Leibniz Research Institute for Environmental Medicine, Düsseldorf, Germany

Introduction: Intrauterine growth restriction (IUGR) is defined as a significant reduction in the fetal growth rate. Placental insufficiency, the main cause of IUGR, reduces placental blood flow leading to fetal development under chronic hypoxia which is associated with neurodevelopmental damage, cognitive dysfunctions and cardiovascular adverse outcomes (Eixarch et al. 2012). The characterization of neurostructural changes in fetus with IUGR is essential to design therapeutic strategies directed to limit its deleterious effects.

Methods: The induction of IUGR was performed in one of the uterine horns of pregnant rabbits at gestational day 25 (GD25). Neurospheres were obtained from the whole brain of IUGR and normal grown rabbit pups immediately after caesarean delivery at GD30. For the establishment of the neurosphere culture the ability to mimic basic processes of brain development was evaluated, including proliferation, migration, differentiation, synaptogenesis and cellular viability (Baumann et al. 2014; Kühne et al. 2019). To find a neuroprotective therapy preventing/reversing adverse effects of IUGR six different compounds at increasing concentrations (Docosahexaenoic acid (DHA), choline, lactoferrin, melatonin, zinc, and 3,3',5-Triiodo-L-thyronine (T3)) were tested. Basic processes of neurogenesis were assessed to determine the maximum tolerated concentration (MTC) and the effective concentration (EC).

Results: We have established for the very first time an *in vitro* model based on primary rabbit neuronal progenitor cells (NPCs) cultured as three-dimensional cell aggregates called neurospheres, which are able to proliferate, migrate and differentiate into neurons, oligodendrocytes and astrocytes (Barenys et al. 2020). We successfully developed new endpoints like neurite outgrowth, branching and synaptogenesis. By comparing the functionality of control and IUGR neurospheres we identified that rabbit NPCs from IUGR individuals have a significantly reduced ability to form oligodendrocytes. DHA (MTC=10µM; EC=1µM), melatonin (MTC=3µM; EC=1µM) and T3 (MTC=30nM; EC=0,1nM) have been selected as the most promising therapies due to their promoting effects on oligodendrogenesis.

Conclusion: The established *in vitro* model allows us to evaluate different processes of neurogenesis in a fast, economic and ethic way and contributes to a better understanding of IUGR induced neurodevelopmental damage and to the selection of new neuroprotective therapies.

P38

Influences on fat content, fat density and lipid droplets in *C. elegans* liquid culture

T. M. Tran¹, G. Steinberg¹, A. Wagner¹, R. Menzel², M. Oelgeschläger¹, G. Schönfelder^{1,3}, S. Vogl¹
¹Federal Institute for Risk Assessment, Berlin, Germany
²Humboldt University, Berlin, Germany
³Charité – Universitätsmedizin Berlin, Berlin, Germany

C. elegans has gained popularity as a model system in toxicology. In recent years, the fat content of the worms has moved into focus, as many fundamental pathways regulating energy homeostasis are conserved between *C. elegans* and humans. Thus, the analysis of lipid homeostasis and fat accumulation in *C. elegans* could provide insights into metabolic diseases and the activity of potential obesogens. Moreover, these effects are suspected to be transmitted to subsequent generations. Thus, lipid metabolism might be a promising read-out to address this important issue in *C. elegans*.

In a first step, we studied the influence of different food regimes on worm development, fat content and changes on the level of lipid droplets (LD), the worm's major form of fat storage, to characterize "low body fat" or "high body fat" phenotypes in our experimental setup.

Therefore, we exposed *C. elegans* to different OP50 concentrations in liquid culture for three days from L1 to adulthood and measured worm sizes. Triacylglyceride (TAG) contents were determined in adult worms employing a fluorometric/colorimetric method. In addition, changes of LD density, distribution and size, were investigated by confocal microscopy combined with 3-D image analysis. Furthermore, fatty acid (FA) patterns and amounts of "fat" and "lean" worms determined with GC/MS-MS. After three days, worms fed with higher food amounts did not only show an increase in body size, they also exhibited higher TAG levels per worm as well as per worm volume. This increase in fat density is in line with 3D-imaging data indicating the increase of LD size and LD volume

per μm^3 in the anterior part of the intestine. Moreover, FA analysis showed significant differences in the FA pattern of adult worms and their eggs, when comparing the two phenotypes ("fat" and "lean").

Taking this as a starting point, we want to investigate if these phenotypes are influenced or can be caused by environmental chemicals including potential (anti-)obesogens. First experiments with orlistat show that this anti-obesogenic drug also lowers the fat density in *C. elegans* and changes FA patterns in adults and eggs. In further experiments, we will test additional substances and investigate whether the observed effects can be transmitted to subsequent generations.

P39

Programmable iPSCs-derived 3D liver organoids as a novel in vitro model for toxicology studies by metabolomic phenotyping

S. Ramirez Hincapie¹, D. Mishra², B. Birk¹, M. Herold³, V. Haake³, V. Giri¹, S. Sperber¹, N. Summers², H. Kamp¹, R. Weiss², B. van Ravenzwaay¹

¹BASF SE, Experimental Toxicology and Ecology, Ludwigshafen am Rhein, Germany

²Massachusetts Institute of Technology, Synthetic Biology Center, Cambridge, United States

³BASF Metabolome Solutions GmbH, Berlin, Germany

Liver toxicity is an important and the most common toxicological endpoint for chemicals and drugs. BASF has developed a metabolomics in vitro (MIV) method that enables to predict modes of action of liver toxicants in HepG2 cells [1]. Although HepG2 liver cells are useful, as a cancer cell line, these cells have a reduced functionality and limited xenobiotic metabolism. Therefore, there is an urgent need to find a relevant, reliable and reproducible in vitro system that can better recapitulate human sensitivity to hepatotoxicants. Through synthetic biology, scientist from MIT (see author list), have developed a human stem-cell derived cell system, from which human liver organoids that include all liver cell types can be developed with a three-dimensional liver-specific morphology as found in vivo [2]. The aim of the project was to characterize this new in vitro model from a toxicological perspective.

As a proof of concept, the suitability of iPSCs-Liver Organoids as an in vitro system for toxicological studies was tested using 28-days old liver organoids treated for 48h with bezafibrate (50 μM , 500 μM and 1000 μM), pooled in groups of 1, 3 and 6 organoids. After exposure, some organoids were assessed for cell viability while others were chemically fixed/quenched, flash frozen in liquid nitrogen and shipped on dry ice to BASF Metabolome Solutions (Berlin, Germany) for metabolomic analysis using mass spectrometry.

First results showed a clear metabolic shift in bezafibrate treated groups using 3 and 6-pooled organoids. The lipid metabolism was particularly altered, consistent with the in vivo MoA of bezafibrate which acts as a lipid-lowering agent. Noteworthy, the treated organoids showed a weight increase, suggesting an adaptation to bezafibrate exposure not unlike the in vivo liver weight increase in bezafibrate treated rats.

Thus, iPSCs-Liver Organoids could indeed be a more reliable matrix for the identification of liver toxicity in vitro. Additional substances will be analysed in the future to further characterize this new test system.

[1] Ramirez et al., Arch Tox, 2018, doi: 10.1007/s00204-017-2079-6

[2] Guye et al., Nature Comm, 2016, doi: 10.1038/ncomms10243

P40

Refinement of h-CLAT by multiplexing analyses of inflammatory cytokines

J. Carstensen¹, C. Kneuer¹, **M. Peiser**¹

¹Bundesinstitut für Risikobewertung, Toxikologie der Wirkstoffe und ihrer Metaboliten, Abteilung Sicherheit von Pestiziden, Berlin, Germany

Background: In addition to the Direct Peptide Reactivity Assay (DPRA, OECD TG442C) and the ARE-Nrf2 Luciferase Test Method (OECD TG442D), the Human Cell Line Activation Test (hCLAT, OECD TG442E) is one of the new OECD testing systems for regulatory testing of chemicals for the endpoint skin sensitization. In addition to the former first choice test in vivo, the local Lymph Node Assay, all three in vitro assays are included in the amendments of the guidelines for cosmetic ingredients and biocidal active substances. However, several approaches are underway to enhance the predictivity of different combinatory testing strategies of in vitro, (Q)SAR and in chemico methods within the concept of Integrated Approaches to Testing and Assessment, IATA). Here, we propose a different approach by focusing to increase the predictivity of one single assay, the h-CLAT. In our proposal for technical refinement, we asked, if protein levels for inflammatory cytokines by multiplexing platform and new markers CD40 and CD83 by FACS could be established within the current h-CLAT protocol.

Methods: The hCLAT was performed according to OECD TG442E. Performance standards of the h-CLAT, DNCB, PPD, MBT and Limonene with known extreme to weak potential in three subtoxic concentrations each, irritant SDS and vehicle controls were used. After 48 h, release of cytokines in the cell supernatants was detected by Magpix-analyses. Costimulatory CD40 and maturation marker CD83 were analysed by FACS. Positive or negative results were calculated as RFI (Relative Fluorescence Intensity).

Results: In multiplexing analyses, the release of IL-8 was significantly enhanced after exposure to DNCB, MBT, and PPD comparing to vehicle controls. Also significantly increased release was found for IL-1 β after stimulation with DNCB and MBT, for MIP-1 α after stimulation with DNCB and PPD and for TNF- α after stimulation with DNCB and MBT. Irritant SDS induced IL-8 and TNF- α , but not IL-1 β and MIP-1 α . For the new cell surface markers, DNCB increased CD40 expression after highest non-cytotoxic concentrations of DNCB (up to RFI of 394, $p < 0.001$) and expression of CD83 (up to RFI of 265, $p < 0.01$). Vehicle controls or irritant SDS did not increase CD40 and CD83. **Conclusion:** Inflammatory cytokines IL-1 β and MIP-1 α and further biomarkers CD40 and CD83 within the OECD test system h-CLAT may be appropriate candidates to refine the in vitro test and could therefore contribute to animal free biocide and pesticide testing.

P41

3D Models and Multi-Organ-Chips: Scaffold-free 3D tissue models – from static to microphysiological applications

O. Frey¹, E. Thoma¹, B. Yesildag¹, A. Wolf¹, J. Lichtenberg¹

¹InSphero AG, Schlieren, Switzerland

Studying and understanding the etiologies of diseases, with the goal of developing novel therapeutic approaches translated into safe and efficient drugs, presents manifold challenges. In-vitro cell-based assays represent one of the key group of techniques and with the evolution of complex 3D tissue models receive more and more attention and a greater share in the drug discovery process. Routine implementation of novel in-vitro systems requires control over the sometimes-complex tissue- and disease-relevant parameters and at the same time simple and robust methods for handling, experimentation, and readout. This becomes particularly true when studying organ-organ interactions involving tissue models from different types in fluidic communication.

Our new generation of readily available and screening-compatible 3D microtissues models are able to emulate the healthy and various diseased states of different organ models including human liver and pancreatic islets as well as a large set of tumors. Accessing the biology of the models in a reliable and reproducible way to a large extent depends on the platforms, in which the microtissues are cultured and handled in. We therefore specially engineered and matched our 96 and 384-well plates to the microtissue morphology considering easy, but highest quality optical inspection, reliable and efficient medium exchange and compound dosing preserving maximal functionality and allowing seamless integration into automation systems. Together with the uniform, functionally robust, and long-lived characteristics of the microtissues a complete screening platform for a wide set of efficacy and safety testing can be offered.

The next steps toward more complex in-vitro models includes the combinations of such advanced microtissues in a microphysiological system to study their interactions. We extended our technology platform by a microfluidic plate based on SBS standards, which enables culturing of the same microtissues also under physiological flow conditions, and with the flexibility to interconnect and culture different types of microtissues multi-tissue configurations. Up to 10 same or different microtissues can be interconnected and cultured in 8 identical or different conditions in parallel per plate.

Providing continuity of the microtissue models enables maximal translatability between the different pre-clinical applications and control over the increasing model complexity along the drug discovery process.

Toxicology – Regulatory toxicology

P42

Adaptation of the *in vitro* micronucleus assay (OECD 487) for the assessment of the mutagenic potential of nanoparticles

N. Honarvar¹, C. Ulrich¹, N. Partosa¹, C. Comes¹, S. Berit-Seiffert¹, R. Landsiedel¹

¹BASF SE, Ludwigshafen am Rhein, Germany

Current OECD guidelines for *in vitro* genotoxicity testing may not be directly applicable for the assessment of the mutagenic potential of nanoparticles. This is explicitly stated in the OECD guidelines for the *in vitro* micronucleus assay (OECD 487) and the thymidine kinase assay (OECD 490). Both guidelines require adaptation of the respective protocol for nanoparticle testing.

In a joint effort organized by the EU Joint Research Centre (JRC) a protocol was developed for the testing of nanoparticles using the *in vitro* micronucleus assay. The adapted protocol was applied using the (adherent) cell line V79 and primary human lymphocytes (suspension cultures using human buffy coat as well as whole blood cells). The mutagenic potential of five nanoparticles (BaSO₄, CeO₂, Au5nm, Au30nm and SiO₂) was analysed using this protocol. Concurrently, Tungstencarbide Cobalt (WCa-Co) nanoparticles were used as a potential particulate positive control and Ethylmethane sulphionate (for V79 cells), Mitomycin C (for human lymphocytes) and Colcemid (for both cell types) as chemical positive controls. The cellular dose of nanoparticles was quantified by the Laser Ablation Inductively Coupled Plasma Mass Spectrometry (LA-ICP-MS) method after the treatment period.

None of the five tested nanoparticles induced a treatment-related increase in the micronucleus frequency. The putative particulate positive control WCa-Co increased the micronucleus frequencies only in the human lymphocyte cultures, but not in V79 cells. The results with lymphocytes obtained from buffy coats were more reliable than those using whole blood. LA-ICP-MS data showed concentration related increases of particle mass associated with the target cells.

In conclusion the data show that nanomaterials can be tested for their genotoxic potential *in vitro*: primary human buffy coat cells are more suitable for testing nanoparticles in the *in vitro* micronucleus assay as V79 cells; the particle burden of the cells can be quantified by LA-ICP-MS and WCa-Co can be used as a particulate positive control for these nanomaterial genotoxicity tests.

P43

Investigation of toxicokinetic mixture effects of co-formulants and active substances in plant protection products using Caco-2 cells

M. Karaca¹, B. Fischer¹, C. T. Willenbockel¹, M. D. Marzo Solano¹, P. Marx-Stoelting¹, D. Bloch¹

¹German Federal Institute for Risk Assessment, Pesticides Safety, Berlin, Germany

Background: Plant protection and biocidal products consist of one or more active substance(s) and a varying number of co-formulants. Currently, the active substance is assumed to contribute primarily to the toxicity of the product. Hence, the admission process for products relies on the testing of acute toxicity only, while in contrast the evaluation of active substances includes a more comprehensive set of toxicity studies. However, in some cases mixture effects of active substances and co-formulants might result in increased toxicity. Therefore, we propose the development of a testing strategy including *in vitro* and non-animal tests to identify and prioritize products with health-relevant mixture effects for regulatory purposes. In a first step, we investigated the effect of emulsifiers on the toxicity of the product, since these co-formulants can influence toxicokinetics due to their surface-active properties. In a second step, toxicokinetic effects were qualitatively and quantitatively assessed.

Methods: Two plant protection products (PPPs) were analysed for their cytotoxicity as compared to their respective active substances (abamectin and fluroxypyr-meptyl) and the combination of the active substances and the respective emulsifiers using Caco-2 cells. Additionally, the effect on the permeation of the active substances by several co-formulants was investigated by transport studies in Caco-2 cells and quantified using LC-MS/MS. To investigate potential mixture effects on kinetics, fluorescence anisotropy measurements and an ATPase assay were conducted.

Results: First results show that the co-formulants significantly increase cytotoxicity of investigated PPPs in different cytotoxicity assays. Analytical investigation show altered transported amount of both active substances upon combination with emulsifiers. ATPase assay results provide inhibition of P-gp transport caused by various emulsifiers investigated (EMULSOGENä EL400, RHODACALä 60/BE, SOPROPHORä BSU and SOPROPHORä 3D33). Furthermore, fluorescence anisotropy measurements demonstrate increased membrane fluidity after incubation with both PPPs, TWEENä 80, EMULSOGENä EL400 and RHODACALä 60/BE.

Conclusion: Our findings support the hypothesis that the increased cytotoxicity of the investigated PPPs may be due to the increased bioavailability of active substances enhanced by different emulsifiers. Consequently, the consideration of toxicokinetic mixture effects in a tiered test strategy is required.

P44

A proof-of-concept applicability assessment of the ocular irritation assay (OECD test guideline 496) to agrochemical formulations

M. Remmele¹, N. Schmitt¹, S. Kollé¹, R. Landsiedel¹

¹BASF SE, Experimental Toxicology and Ecology, Ludwigshafen am Rhein, Germany

Until 2021 there is no non-animal test predicting UN GHS category 1 agrochemical formulations with sufficient sensitivity (e.g., Schrage, et al. 2010, Kollé et al., 2015, Kollé, et al. 2017). In consequence, the conduct of the *in vivo* rabbit eye irritation test (OECD test guideline 405) remains necessary for agrochemical formulations where experimental data is needed to differentiate between UN GHS category 1 and UN GHS category 2 ocular irritants.

An OECD test guideline describing the Ocular Irritation assay for the identification of chemicals inducing serious eye damage (UN GHS category 1) and chemical not requiring classification for eye irritation or serious eye damage (no UN GHS category) was adopted in 2019. The assay is commercially available as test kit, is vegan and can be used of-the-shelf. The Ocular Irritation test is applicable to solid and liquid chemicals whose 10% solution/dispersion have a pH in the range between 4 and 9. The test's applicability to agrochemical formulations has, however, not yet been described.

In the present study we have assessed seven suspension concentrate formulations with available *in vivo* studies (2x UN GHS category 1, 3x UN GHS category 2, 2x no UN GHS category).

In the assay, after 24 hours of incubation, the denaturation of the proprietary protein components are determined photometrically and translated into Irritation Scores. Using the prediction model provided in OECD test guideline 496, the test chemical is then either predicted as no UN GHS category or UN GHS category 1. A classification cannot be derived directly for those test chemical resulting in the mid range ("no prediction can be made").

All of the seven agrochemical formulations tested neat resulted the same range ("no prediction can be made"). While this was expected for the 3 UN GHS category 2 formulations, the 2 UN GHS category 1 formulations were underpredicted, while the 2 no

UN GHS category formulations were overpredicted. In addition to the neat testing of the same agrochemical formulation set, the two UN GHS category 1 formulations as well as one of the UN GHS category 2 agrochemical formulations were tested diluted (surfactant protocol). All three formulations produced results closely above or below the threshold for UN GHS category 1 prediction.

In summary, the Ocular Irritation neat protocol based on the small data set available seems not to be directly applicable to agrochemical formulations.

P45

New aspects in deriving health based guidance values for bromate in swimming pool water

U. Gundert-Remy¹, C. Röhl², M. Batke², G. Damm², A. Freiburger², T. Gebel², J.

Hengstler², A. Mangerich², F. Partosch², T. Schupp², K. M. Wollin², H. Foth²

¹Institute of Clinical Pharmacology and Toxicology, Charité, Berlin, Germany

²Department of Environmental Health Protection, Neumünster, Germany

Question: Bromate classified as 1B carcinogen is a typical by-product occurring in drinking and swimming pool water after disinfection. The aims of this study were a) to re-evaluate the carcinogenic mode of action of bromate, b) to derive reliable levels of exposure by all routes under various scenarios of swimming, and c) to inform the derivation of cancer risk-related bromate concentrations in swimming pool water.

Methods: A comprehensive literature search was performed. Quality of the studies on genotoxicity and carcinogenicity were assessed by Klimisch criteria (Klimisch et al. 1997) and SciRAP tool (Beronius et al. 2018), respectively. Benchmark dose (BMD) modelling was performed using the modelling average mode in BMDS 3.1 and PROAST 66.40 (human cancer BMDL10; EFSA 2017). For the exposure, data from a wide range of sources were evaluated for their reliability. Different target groups (infants/toddlers, children and adults) and exposure scenarios (recreational, sportive swimmers, top athletes) were considered for oral, inhalation and dermal exposure. Exposure was calculated by frequency of swimming events and duration in water.

For illustration, cancer risk-related bromate concentrations in pool water were calculated for different target groups taking into account their exposure, using the hBMDL10 and a cancer risk of 10⁻⁵.

Results: There is convincing evidence from a multitude of studies that bromate induces clastogenic and aneugenic effects as well as oxidative DNA damage and DNA strand breaks formation *in vitro* and *in vivo* without discernible threshold. Hence, bromate may be considered a non-threshold carcinogen.

BMD modelling with model averaging for renal cancer studies (Kurokawa et al. 1983, 1986; DeAngelo et al. 1998) resulted in a median hBMDL10 of 0.65 mg BrO₃-kg bw per day.

Evaluation in different age and activity groups revealed that top athletes had the highest exposure, followed by sportively active children, sportively active adults, infants and toddlers, children and adults. The predominant route of exposure was oral (73 - 98%, by swallowing water, followed by the dermal route (2 - 27%); inhalation route was insignificant (< 0.5%).

Conclusions: Accepting the same risk level for all population groups results in different guidance values due to the large variation in exposure. For example, for an additional risk of 10⁻⁵ the bromate concentrations would range between 0.011 for top athletes, 0.015 for sportive children and 2.1 mg/l for adults.

P46

Influence of pregnancy and non-fasting conditions on the plasma metabolome in a rat prenatal toxicity control study

S. Ramirez Hincapie¹, V. Giri¹, J. Keller¹, H. Kamp¹, V. Haake², E. Richling³, B. van Ravenzwaay¹

¹BASF SE, Experimental Toxicology and Ecology, Ludwigshafen am Rhein, Germany

²BASF Metabolome Solutions GmbH, Berlin, Germany

³University of Kaiserslautern, Food Chemistry and Toxicology, Department of Chemistry, Kaiserslautern, Germany

Embryotoxicity can result as a secondary consequence of maternal homeostasis alterations. For this reason, prenatal toxicity studies (PTS) aim to provide information concerning the effects of substance exposure on both, the pregnant animal and the developing fetus. Due to the pregnancy and the sensitivity of the fetus, assessment of maternal toxicity is limited to clinical parameters and body weight development. Therefore, the current maternal toxicity parameters lack specificity and are likely to underestimate the extent of toxicity. A previous report has highlighted the use of plasma metabolomics, by gas- and liquid-chromatography-tandem mass spectrometry techniques, for an improved and mechanism-based identification of maternal toxicity. To establish base line metabolite profiles of healthy pregnancies we compared the metabolic profiles of non-pregnant fasted rats (standard controls in previous toxicometabolomics studies) with those of 1) non-pregnant, non-fasted 2) pregnant, fasted 3) pregnant, non-fasted animals.

Metabolites changes in response to pregnancy, food consumption (non-fasting) as well as the interaction of both conditions were identified. In dams, both conditions, non-fasting

and pregnancy, had a marked influence on the plasma metabolome and built individual patterns of changed metabolites. Non-fasting was characterized by increased plasma concentrations of amino acids, diet related compounds and lower levels of ketone bodies. The metabolic profile of pregnant rats was characterized by lower amino acids and glucose levels and higher concentrations of plasma fatty acids, triglycerides and hormones, capturing the normal biochemical changes undergone during pregnancy.

This work provides a first comprehensive overview of metabolome changes due to pregnancy. In addition, several of the well-known metabolome changes when comparing fasted and non-fasted animals were now also confirmed for pregnancy. Further, sever interactions of metabolite profiles related to pregnant and non-fasting were observed.

P47

Toxicological evaluation of the hydroethanolic corm extract of *Gladiolus psittacinus* Hook (Iridaceae)

O. Salako¹, I. Onifade¹, K. Salako², O. Akinloye^{1,3}

¹Faculty of Basic Medical Sciences, University of Lagos, Nigeria, Medical Laboratory Science, Idi-Araba, Mushin, Nigeria

²University of Lagos, Pharmaceuticals and Pharmaceutical Technology, Lagos, Nigeria

³University of Lagos, Pharmacology, Therapeutics and Toxicology, Lagos, Nigeria

Objective: *Gladiolus psittacinus* Hook. (Iridaceae) is a medicinal plant commonly used in native medicine for the treatment of diarrhoea, dysentery and gonococcal infection in man. This study aimed to evaluate the toxic potential of the hydroethanolic corm extract of this plant.

Methods: Acute toxicity of *G. psittacinus* corm extract (GP) was carried out using albino mice. Median lethal dose (LD50) of extract for oral route was determined using probit analysis. Root inhibition potential of GP (1, 5, 10 and 20 mg/ml) was evaluated using *Allium cepa* assay. The standard drug used was cyclophosphamide (CY; 15 mg/ml) and distilled water as the negative control. GP (50, 100 and 200 mg/kg) was also administered orally to albino mice for 28 days to determine the sub-acute toxicity of the extract. Mice in the standard group received CY (3 mg/kg *p.o.*) while negative control group received distilled water (10 ml/kg *p.o.*). Also micronuclei assay was used to assess the mean polychromatic erythrocytes in the femoral bone marrow of the mice while comet assay was used to evaluate DNA damage using the blood of the mice. The liver and kidney of the mice were also collected for histopathology assessment.

Results: The oral LD50 of the extract was determined to be 2238.72 mg/kg. GP especially at the highest concentration used, that is 20 mg/ml, caused considerable inhibition and wilting of *Allium cepa* roots which was comparable to that caused by CY (15 mg/ml). GP caused increase in the total mean polychromatic erythrocytes in a dose-dependent manner with peak value of 54.67 at 200 mg/kg. CY (3 mg/kg) significantly ($p < 0.05$) increased the total mean polychromatic erythrocytes with value of 60.67. The comet assay revealed an increase in olive tail moments as dose of the extract increased with peak effect seen at 200 mg/kg (2.036 μ m). This was comparable with that of CY (2.055 μ m). However, the differences were not statistically significant. Histopathological assessment revealed some abnormalities in the cytoarchitecture of the representative liver and kidney samples from the treated mice.

Conclusion: This study revealed that the hydroethanolic corm extract of *G. psittacinus* showed considerable cytotoxic and mutagenic potential. Hence, it is recommended that the use of *G. psittacinus* corms in humans should be with caution.

Toxicology – Inhalation toxicology/Respiratory toxicology

P48

An in vitro systems toxicology assessment of novel electronic vapor device by using air-liquid interface buccal, bronchial, small airway, and alveolar culture models

A. Iskandar¹, F. Zanetti¹, A. Giral¹, A. Kondylis¹, A. Sewer¹, L. Ortega-Torres¹, S. Majeed¹, S. Acali¹, D. Marescotti¹, E. Guedj¹, C. Merg¹, K. Trivedi¹, S. Frentzel¹, N. Ivanov¹, F. Martin¹, M. Peitsch¹, J. Hoeng¹

¹Philip Morris International, Neuchâtel, Switzerland

Aerosols of electronic vapor (e-vapor) products have a different composition than cigarette smoke (CS). Most studies rely on testing the effects of the liquid formulations applied directly to cell cultures. But, this setup does not mimic real-life aerosol exposure to e-vapor product (EVP) users. Using advanced cellular models (air-liquid interface human organotypic buccal, bronchial, small airway, and alveolar cultures), we examined the biological effects of acute exposure to the whole aerosol generated by the EVP P4M3 with "Classic Tobacco" flavor (Philip Morris International). The concentrations of nicotine and carbonyls deposited in the exposure chamber were measured as exposure markers. The effects of EVP exposure were compared with those of CS exposure at similar concentrations of deposited nicotine. Using a systems toxicology approach, we complemented histological and cytotoxicity endpoints with analysis of molecular changes (profiles of mRNA and secretory proteins). The results showed that CS exposure caused culture damage and reduced ciliary beating frequency (in ciliated epithelial cultures), while the EVP aerosol exposure induced minimal changes despite resulting in higher concentrations of deposited nicotine than CS exposure. Carbonyl concentrations increased with an increasing dose of CS; however, of their concentrations following EVP aerosol exposure were below the detection limits. The magnitude of alterations in gene expression and secreted mediator were greater following CS exposure than EVP aerosol exposure at all tested doses. We consistently detected increased concentrations of secreted matrix metalloproteinase 1 (MMP-1) following CS exposure in all culture types.

MMP-1 concentrations following EVP aerosol exposure were comparable with those following air exposure. Using a network perturbation amplitude methodology, greater biological impacts were detected at the earlier than at the later post-exposure time points for all exposure conditions tested. In all culture models, the biological impacts following EVP aerosol exposure were generally less than those following CS exposure at comparable concentrations of deposited nicotine. In conclusion, the studies showed that the effects of exposure to aerosol from P4M3 were lower than those of CS exposure in epithelial cultures of the aerodigestive tract. These studies demonstrated the suitability of air-liquid interface aerodigestive culture models for toxicity testing of inhalation products.

P49

Nanoparticle aerosol exposition of a A549 culture on a 3D system

D. Schneider¹, F. Glahn¹, B. Schumann¹, H. Foth¹

¹Medical Faculty of Martin Luther University, Environmental Toxicology, Halle, Germany

In many products of the daily-use, e.g. tooth paste, nanoparticles (NP) are part of the ingredients list. NP could be emitted at different stages of the product's life-cycle from production until recycling. The main entrance port for NP into the body is the respiratory system. For detecting the effects of NP in the lung, the need for human cell culture systems in inhalational toxicology increases. We are establishing a novel cell culture exposure system on inserts (MatriGrid = MG) shaped like alveoles with a lung tumor cell line (A549), respectively a Co-culture of primary peripheral lung cells (PLC) and an endothelial cell line (EA.hy926) as a model for the blood lung barrier.

Viability of A549 was determined by Resazurin-assay and Lactatdehydrogenase-assay, ROS-Assay was performed by incubating with H2DCFDA-dye. The confluency of the culture was detected by TEER-measurement (transepithelial/transendothelial electric resistance). The size-distribution of the particles in the aerosol was determined by SMPS and OPS.

First of all we exposed A549 to BaSO₄- and TiO₂-NP aerosols. In Resazurin-assay exposure of A549 to 0.9 g/l (conc. of stock suspension resulting in averagely 3 x 10⁴ particles/cm³ for BaSO₄ in the aerosol) BaSO₄-aerosol shows a slight but not significantly decreasing effect. The exposure of A549 to 0.9 g/l (conc. of stock suspension resulting in averagely 1 x 10⁵ particles/cm³ for TiO₂ in the aerosol) TiO₂-aerosol shows no significant effect, too. The LDH-assay shows no significant toxic effect at the same concentrations. TEER values of the A549-culture in MGs increases at the beginning of the experiment. TEER-measurement was used for control of the confluency, because confluency cannot be visualized with a standard light microscope. For the ROS-assay A549 were incubated with BaSO₄- and TiO₂-aerosols (0.9 g/l) for 1 h. The NP-aerosols show a 2.5-fold (BaSO₄) and a 10-fold (TiO₂) induction of ROS. The particle size of both aerosols was measured during every exposure. Based on the number size distribution the median diameters in the BaSO₄- and TiO₂-aerosols were 56 and 74 nm, respectively.

The applied NP aerosols of BaSO₄ and TiO₂ cause no relevant toxic effects in A549 cultures for 24 or 72 h. These results show that tumor cells are not affected by NP aerosols. In the future we will also investigate the transferability of these findings to Co-culture (PLC and EA.hy926) and mini-organocultures (MOC) of the lung.

P50

MicroRNA-21 as a potential therapeutic target in idiopathic pulmonary fibrosis

P. Vaccarello¹, D. P. Ramanujam¹, H. Schiller², C. Staab-Weijnitz², S. Engelhardt¹

¹Technical University of Munich, Institute of Pharmacology and Toxicology, München, Germany

²Helmholtz Zentrum München, Comprehensive Pneumology Center, München, Germany

Idiopathic pulmonary fibrosis (IPF) is a life-threatening interstitial lung disease characterized by progressive inflammation and fibrotic remodeling. MicroRNAs are increasingly recognized as important molecular mediators that contribute to development and progression of disease. The concept of preventing fibrosis through synthetic antimicroRNA molecules that selectively bind to a microRNA has been validated in various disease models in vivo, but only to a very limited extent in the lung. Here, we sought to determine the entire miRNome of mouse lung cells and thereby identify new therapeutic targets to treat pulmonary fibrosis.

8-12 weeks old wild type mice were subjected to intratracheal instillation of bleomycin (or PBS as control) using a microsprayer. One week later, bronchoalveolar lavage fluid (BALF) and lungs from untreated or PBS/bleomycin-treated mice were harvested and small RNA sequencing was performed. Our miRNome data revealed that, in the fibrotic lung tissue, miR-21 is the significantly upregulated ($p\text{-adj} < 0.05$ and $\log_2\text{FC} > 2$) microRNA with the highest expression.

To further identify the cell type in which miR-21 exerted its pathological role, different pulmonary cell types were isolated through magnetic- and fluorescence- activated cell sorting (MACS and FACS). Small RNA sequencing identified miR-21 among the top 10 expressed micro-RNAs in the total lung as well as several cell fractions, i.e., macrophages, neutrophils, T cells and epithelial cells. In endothelial cells and fibroblasts it ranked among the top 20 expressed microRNAs.

In summary, we quantified for the first time the full range of microRNAs in the main murine lung cell types at basal state and under fibrotic conditions. In particular, our data predict miR-21-expressing immune cells as key players in lung fibrotic processes and as potential therapeutic targets.

P51

Particle in vivo to in vitro extrapolation (IVIVE): Using in vivo lung burden for in vitro dose settingL. Ma-Hock¹, J. G. Keller^{1,2}, E. Ruggiero¹, W. Wohlleben¹, R. Landsiedel^{1,2}¹BASF SE, Experimental Toxicology and Ecology, Ludwigshafen am Rhein, Germany
²FU Berlin, Pharmacology and Toxicology, Berlin, Germany

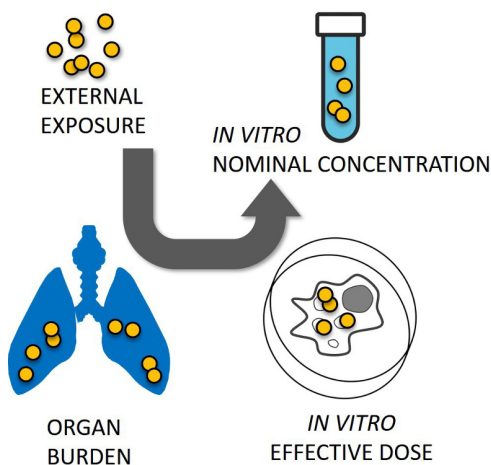
Background: The in vitro predictivity of in vivo particle toxicity is often unsatisfactory. An appropriate particle dose setting is indispensable to ensure the qualitative and quantitative relevance of in vitro findings. Accordingly, in vitro concentrations should reflect the in vivo target organ burden (internal dose) elicited by a pre-defined particle concentration (external dose) after a given exposure duration. We suggest extrapolating from the target organ burden at the particle's lowest observed adverse effect concentration (LOAEC) since this approximates the in vivo "effect threshold".

Results: To facilitate meaningful IVIVE of particle dose, we present an organ burden database covering 16 metal oxide and barium sulfate nanoparticles, colloidal amorphous silicon dioxide, and one micron-scale zinc oxide. Inhalation is an important exposure route for many particles, and the lung the primary target organ. Therefore, the database focuses on lung burden measured in short-term rat inhalation toxicity studies, complemented by liver burden data, as available. A case study exemplifies how the lungburden data can be used for IVIVE for dose and is then generalized to describe a six-step approach for Using Nanomaterial In Vivo Lung Burden for In Vitro Dose Setting: (1) Determine in vivo exposure to be reflected in vitro; (2) identify in vivo lung burden at (or close to) LOAEC; (3) extrapolate in vivo lung burden to in vitro effective dose; (4) extrapolate in vitro effective dose to in vitro nominal concentration; (5) set in vitro dose range around LOAEC-equivalent dose to allow establishing a dose-response relationship; and (6) consider uncertainties and identify specificities of in vitro test system potentially affecting in vitro findings. A variant of OBIV describes how to extrapolate the in vitro dose if lung burden data are unavailable for the given particle.

Conclusions: Application of this IVIVE results in in vitro concentration ranges that are generally much lower than those used and reported to have an effect in previously published in vitro studies. Differences between in vivo and in vitro models regarding their type of effect/read-out and potency should be considered when assessing results of in vitro studies. This and relevant in vitro concentrations will enhance the predictivity of in vitro studies.

UG Sauer et al. (2013) <https://doi.org/10.1016/j.tiv.2012.10.007>JG Keller et al. (2020) <https://doi.org/10.1080/17435390.2020.1836281>.

Fig. 1



P52

Covid 19 infection: Is it only a respiratory disease?G. Bode¹, R. Bass², K. Pueschel^{2,3}, A. Tzankov^{4,5}¹University Medical Center Göttingen, Institute for Pharmacology and Toxicology, Göttingen, Germany²Universität Berlin Charité, Pharmacology and Toxicology, Berlin, Germany³University Hamburg UKE, Legal Medicine, Hamburg, Germany⁴Universitätsspital Basel, Institut für Genetik und Pathologie, Basel, Switzerland⁵Universitätsspital Basel, Genetik + Pathologie, Basel, Switzerland

Introduction: Aerosols have been identified as the main responsible carriers of SARS-CoV-2 viruses. From noses or mouths, SARS-CoV-2 penetrate ciliated cells of the respiratory tract down to the lungs, where they, via pneumocytes and endothelial cells,

initiate a self-perpetuating process of alveolar and vascular damage. Clinical experience indicate a pulmonary thromboinflammation, often requiring machine supported assisted respiration.

Objectives: Autopsy findings and literature information stress that COVID-19 is an angiocentric syndrome with massive thrombotic diathesis, leading to a risk for multiorgan failure. The better awareness of such mechanisms will improve clinical success.

Materials and Methods: The authors reviewed autopsy findings at the Institutes for Pathology of the Universities of Hamburg and Basel and compared the morphological findings with data from clinical observations.

Results: Invasion pathways: The virus seem to enter cells via the angiotensin-converting enzyme 2 (ACE2), found in many cells, e.g. in alveoli. Particularly the surfactant-producing pneumocytes type 2 are rich in ACE2. The virus initializes an acute diffuse alveolar damage leading to vascular dysfunctions due to thromboinflammation and severe disruption of oxygen exchange.

Main organ targets: The respiratory tract is the main target of COVID-19, but other organs like heart, kidneys, gut or brain can be affected too, mainly through the mechanism of generalized thromboinflammation.

Thrombosis, thromboembolism and vascular damage: These serious complications characterize the lethal COVID-19 infections, observed in lungs, pelvis or lower extremities, often aggravating preexisting vascular dysfunctions like elevated blood pressure, atherosclerosis, diabetes mellitus, obesity, amyloidosis. This review should raise the awareness of clinicians that COVID-19 is a complex disease, not at all restricted to the lung, but capable of inducing organ damage mainly via the mechanism of thromboinflammation. Accordingly, the avoidance of blood clotting by [ct1] very early prophylactic anticoagulation therapy will reduce hospitalizations, intensive care and deaths.

Conclusion: Severe COVID-19 affects mainly the respiratory system; severe oxygen exchange impairment is often due to thromboinflammation, also leading to multiple organ failures. Therapeutic anticoagulation improves the outcomes.

Toxicology – Carcinogenesis

P53

Impact on bladder cancer of 4 SNPs, related to the genes PSCA, FGFR3 - TACC3 and CBX - APOBEC3AT. Kadhum¹, S. Selinski¹, M. Blaszkewicz¹, J. Reinders¹, E. Roth², F. Folkert², D. Ovsianikov³, O. Moormann³, H. Gerullis⁴, T. Otto⁴, S. Höhne¹, J. Hengstler¹, K. Golka¹¹Leibniz Research Centre for Working Environment and Human Factors, Dortmund, Germany²Evangelic Hospital, Paul Gerhardt Foundation, Department of Urology, Lutherstadt Wittenberg, Germany³St.-Josefs-Hospital, Department of Urology, Dortmund, Germany⁴Lukasklinik, Department of Urology, Neuss, Germany

Questions: Bladder cancer (BC), which is a smoking and occupation related disease, was a subject of several genome-wide association studies (GWAS). However, studies on bladder cancer risk and on the course of the disease differentiating between muscle invasive bladder cancer (MIBC) and non-muscle invasive bladder cancer (NMIBC) are rare. Thus this issue was investigated for 4 SNPs detected in GWAS, related to the genes TACC3 (transforming acidic coiled-coil containing protein 3) – FGFR3 (fibroblast growth factor receptor 3; located on 4p16.3), PSCA (prostate stem cell antigen; located on 8q24.3), and CBX6 (chromobox homolog 6) – APOBEC3A (apolipoprotein B mRNA editing enzyme, catalytic polypeptide-like 3A; located on 22q13.1).

Methods: This study is based on 712 bladder cancer patients and 875 controls from 3 different case control studies in Germany; Evangelisches Krankenhaus Paul Gerhardt Foundation Lutherstadt Wittenberg (203 cases, 210 controls), St.-Josefs-Hospital Dortmund (156 cases, 237 controls), and Lukaskrankenhaus Neuss (353 cases, 428 controls). The 4 SNPs of interest (PSCA rs2294008 and rs2978974, FGFR3-TACC3 rs798766, and CBX6-APOBEC3A rs1014971) were detected with standard methods.

Results: The frequencies of the investigated SNPs in the whole case group (controls in brackets) were as follows: PSCA rs2294008 AA 26%, AB 50%, BB 24 % (control group: AA 27%, AB 50%, BB 23%), PSCA rs2978974 AA 12%, AB 47% BB 41% (control group: AA 11%, AB 46%, BB 24%), FGFR3-TACC3 AA 61 %, AB 35%, BB 4 % (control group: AA 64 %, AB 33 %, BB 3 %), CBX6-APOBEC3A: AA 45%, AB 45%, BB 10% (control group: AA 44%, AB 44%, BB 13%). In the non-muscle invasive group (NMIBC, n = 581) the frequencies were as follows: PSCA rs2294008 AA 25%, AB 49%, BB 26%; PSCA rs2978974 AA 13%, AB 46%, BB 41%; FGFR3-TACC3 AA 61%, AB 35%, BB 4%; CBX6-APOBEC3A AA 45%, AB 45%, BB 10%. In the muscle invasive group (MIBC, n = 131) the frequencies were as follows: PSCA rs2294008 AA 22%, AB 56%, BB 18%; PSCA rs2978974 AA 9%, AB 51%, BB 40%; FGFR3-TACC3 AA 63%, AB 35%, BB 2%; CBX6-APOBEC3A AA 44%, AB 47%, BB 9%. The differences between the subgroups of muscle invasive (MIBC) and non-muscle invasive (NMIBC) bladder cancer were not significant.

Conclusion: The 4 investigated SNPs do not noticeably contribute differently to the bladder cancer risk for the clinically important subgroups of muscle-invasive (MIBC) and non-muscle invasive (NMIBC) bladder cancer.

P54

BP-induced DNA adduct formation in mixtures with non-carcinogenic PAH in HepaRG cells

A. John¹, L. Goedtke², A. Lampen², A. Braeuning², S. Hessel-Pras², A. Seidel¹
¹Biochemical Institute for Environmental Carcinogens, Prof. Dr. Gernot Grimmer Foundation, Grosshansdorf, Germany
²Federal Institute for Risk Assessment, Berlin, Germany

Polycyclic aromatic hydrocarbons (PAH) like the human carcinogen benzo[a]pyrene (BP) and the non-carcinogens fluoranthene (FA) and pyrene (PYR) occur as food contaminants. To examine the BP DNA-damaging potential according to mixture effects, human liver HepaRG cells were treated with BP alone and in binary or ternary mixtures with the lower molecular weight PAH FA and PYR. FA and PYR were selected due to their high relative occurrence in PAH mixtures. In contrast to BP, FA and PYR are only weak AhR agonists but interact with CAR. DNA damage was investigated using the formation of anti-BPDE-DNA adducts, as revealed indirectly by measuring the hydrolysis product BP-tetrol with HPLC fluorescence detection.

Incubation times of 8, 12, 18, 24, 48 and 72 h were chosen for the treatment of HepaRG cells with 5, 10 or 20 µM BP. An incubation time of 12 h was performed with mixture compositions of BP, FA and PYR like they occur in grilled meat. PAH incubated cells were washed and DNA was isolated (Goedtke et al., 2021). The DNA sample was hydrolyzed in an aqueous solution of 0.1 N HCl at 70°C for 16 hours. After neutralization of the solution with 1 N NaOH, released BP-tetrol was determined by HPLC with fluorescence detection and BPDE-DNA adduct levels were calculated (Alexandrov et al. 1992; 2006).

A BP concentration-dependent increase in DNA adducts was detected. BP-induced DNA damage was only weakly affected by the mixtures. At the lowest concentrations of BP (1 µM), no mixture effects were observed. Treatments with 5 and 10 µM BP alone and in binary or ternary mixtures generated a similar DNA adduct profile for both concentrations, whereas the mixture of 5 µM BP + 12.5 µM PYR generated significantly less DNA adducts compared to the other incubations.

Anti-BPDE-DNA adducts represent an important endpoint for the genotoxic MOA of BP. Their indirect determination as BP-tetrol served as a useful tool for the examination of mixture-based effects on PAH carcinogenicity in human exposure. The results indicate that the genotoxic activity of BP remains unaffected by non-carcinogenic PAH like FA or PYR in PAH mixtures occurring upon food processing.

References: Alexandrov et al. Cancer Res. 52, 6248 (1992); Alexandrov et al. Cancer Res. 66, 11938 (2006); Goedtke et al. Food Chem. Toxicol. in press (2021)

Pharmacology – Pharmacological education

P55

Seventh "Pharmacologic – Historical Forum": Scope, development and perspectives

H. Greim^{1,2}, A. Philipp^{3,4}
¹Technical University of Munich, Toxikologie und Umwelthygiene, Freising-Weihenstephan, Germany
²University, Toxicology, Freising-Weihenstephan, Germany
³University, Pharmacology and Toxicology, Innsbruck, Austria
⁴University, Pharmacology and Toxicology, Innsbruck, Austria

The "Pharmakologie - Historisches Forum" was established eight years ago. Aim of the Forum is to honour personalities of Pharmacology, Clinical Pharmacology and Toxicology of the various Universities of Germany who, with their research, have greatly contributed to the development of their scientific disciplines. Further scope of the Forum is to inform young pharmacologists and toxicologists about the achievements of our famous predecessors.

The first Forum was initiated by Roland Seifert. It was organized by Brigitte Lohff and Athineos Philippou and was held during the 80th Annual Meeting of the DGPT in Hannover. Theme was the life and scientific work of Marthe Vogt and Edith Bülbring. The following Forums have been organized by Athineos Philippou. The second one (Kiel, 2015) was dedicated to Heinz Lüllmann. The third Forum (Berlin 2016) was dedicated to the Pharmacologists of Berlin who worked there after the Second World War (Hans Herken, Friedrich Jung, Helmut Coper, Helmut Kewitz) including the years that Wolfgang Heubner has spent in Berlin. The fourth Forum (Heidelberg 2016) was honouring Wolfgang Heubner and Franz Gross, both Professors and Heads of the Pharmakologische Institut. The fifth Forum¹ (Göttingen, 2018) was dedicated to Ludwig Lendle who, besides his scientific work, also founded a second Chair for Pharmacology and Neuropharmacology. The sixth Forum (Stuttgart, 2019) was dedicated to Clinical Pharmacology. Ulrich Klotz and Helmut Greim spoke about the history of the Dr. Margarete Fischer-Bosch Institute for Clinical Pharmacology and Emil Starckenstein, Prague. The seventh Forum, held in Leipzig last year was dedicated to Fritz Hauschild and Reinhard Ludewig and the Papyrus Ebers presented by the Leipzig historian Reinhold Scholl.

During the upcoming eighth Forum in Bonn, Gunter Hartmann will honour Hans J. Dengler, Heinz Bönisch Manfred Göthert, and Helmut Greim Rudolf Buchheim.

P56

We need to talk. An approach to teaching students how to conduct a prescription conversation

V. Kirsch¹, J. Matthes¹
¹University of Cologne, Centre of Pharmacology, Cologne, Germany

Objectives: Conveying relevant information in a prescription talk is essential to ensure a safe and effective drug therapy. We analysed simulated prescription talks conducted by 5th year medical students and whether the quality of these talks changed after discussing the scenario with peer students. Furthermore, we analysed whether there were differences between prescription-talk contents named four days later by students who attended the above-mentioned simulation and those who did not.

Materials & methods: During a one-week course preparing 5th year medical students for their final year (Kirsch et al., GMS J Med Educ 2019; 36(2):Doc17), one out of a group of four was to prescribe an antibiotic in a simulated doctor-patient conversation. Fellow students observed this and then discussed the situation with the student under moderation by a pharmacist. Immediately afterwards, the same student conducted the prescription talk again. Conversations were videotaped and evaluated by means of content analysis on the basis of a self-developed checklist (Hauser et al., GMS J Med Educ 2017; 34(2):Doc18) in a pre-post comparison. Four days after the simulated conversation, all students attending the course were asked to describe a prescription talk in a written test based upon a case vignette. The test results of students who participated in the above scenario (either as the "doctor" or as an observer) were compared with the results of fellow students who attended the course but not the scenario.

Results: Data from 38 simulated doctor-patient conversations were obtained. Initial analyses show that in the spontaneous first try, students mainly did not inform about drug risks, while they did in almost all cases in the second try, often along with measures to be taken. Four days after, all students who attended the scenario named adverse effects as part of a prescription talk, and 64% also named measures to be taken. 27 of 61 the students who had not participated in the simulation scenario mentioned adverse effects, and only 5 of them measures to be taken.

Conclusion: Students seem to be sensitised to patient-relevant information on drug therapy through the immediate repetition of a simulated prescription talk. Four days later, we saw differences in this regard between students who participated in the simulated prescription talks and those who did not. The sustainability of this simple intervention should be tested by re-evaluating the students during their final year.

Pharmacology – G-protein coupled receptors

P57

A split luciferase complementation assay for the quantification of β-arrestin2 recruitment to dopamine D₂-like receptors

L. Forster¹, L. Grätz¹, D. Mönnich¹, G. Bernhardt¹, S. Pockes¹
¹University of Regensburg, Pharmaceutical/Medicinal Chemistry II, Regensburg, Germany

Investigations on functional selectivity of GPCR ligands have become increasingly important to identify compounds with a potentially more beneficial side effect profile. In order to discriminate between individual signaling pathways, the determination of β-arrestin2 recruitment, besides G-protein activation, is of great value. We established a sensitive split luciferase-based assay with the ability to quantify β-arrestin2 recruitment to D_{2long} and D₃ receptors and measure time-resolved β-arrestin2 recruitment to the D_{2long} receptor after agonist stimulation. We were able to characterize several standard ligands at the D_{2long}R and D₃R subtypes, whereas for the D_{4,4}R, no β-arrestin2 recruitment was detected, confirming previous reports. Extensive radioligand binding studies and comparisons with the respective wild-type receptors confirm that the attachment of the Emerald luciferase fragment to the receptors does not affect the integrity of the receptor proteins. Studies on the involvement of GRK2/3 and PKC on the β-arrestin recruitment to the D_{2long}R, D₃R, as well as at the D₁R using different kinase inhibitors showed that the assay could also contribute to the elucidation of signaling mechanisms.

P58

Biased antagonism of the human Mas-related G protein-coupled receptor D

D. M. F. Hanna¹, S. Müller¹, M. Arbogast¹, I. von Kügelgen¹
¹University of Bonn, Department of Pharmacology, Bonn, Germany

Question: The GPCR MRGPRD (MrgD) is expressed in sensory neurons of dorsal root ganglia and has been implicated to play role in nociception. Recently, MrgD was proposed to control cardiovascular function owing to its active contribution in the non-classical renin-angiotensin system. Amino acids as "β-alanine and 3-aminoisobutyric acid", and peptides as "alamandine and angiotensin 1-7" have been reported to be agonists. Some compounds such as chlorpromazine and related structures have been shown to act as low affinity antagonists. In the present study, we studied inhibitory actions of chlorpromazine and structurally related compounds at the human MrgD receptor. That was achieved by investigating both G-protein-dependent and β-arrestin-dependent pathways.

Methods: G-protein-dependent functional assays including the nuclear factor of activated T cells (NFAT)-reporter gene assay and the [3 H]cAMP radioaffinity assay were used to study the interaction in Chinese hamster ovary (CHO) Flp-In cells stably expressing the human MrgD receptor. Receptor coupling to the β -arrestin pathway was studied using the PathHunter β -arrestin recruitment GPCR assay (Pro-link tagged human MrgD and enzyme-acceptor-tagged β -arrestin-2 co-expressed in CHO cells).

Results: In the NFAT-reporter gene assay, pre-incubation of cells stably expressing human MrgD receptors with chlorpromazine [10 μ M], thioridazine [10 μ M] and rimcazole [20 μ M] caused a significant rightward shift of the concentration-response curve of β -alanine with apparent pKB values of 5.1, 5.2 and 5.2, respectively. β -Alanine inhibited the forskolin-induced cAMP accumulation as observed in the [3 H]cAMP radioaffinity assay. Thioridazine (10 μ M) and rimcazole (20 μ M) shifted the concentration-response curve of β -alanine to the right with apparent pKB values of 4.8 and 5.2, respectively. β -Alanine caused a concentration-dependent activation of the β -arrestin pathway. Surprisingly, chlorpromazine, thioridazine and rimcazole failed to inhibit responses to β -alanine in recruitment of β -arrestin-2.

Conclusion: The data suggest a biased antagonism of G-protein dependent responses to β -alanine mediated by the human MrgD receptor by chlorpromazine, thioridazine and rimcazole.

P59

Stable isotope resolved metabolomics to assess the effect of PI3K β inhibition on metabolic pathway activities in a PTEN-Null breast cancer cell line

M. Lackner¹, U. Hofmann¹, M. Haag¹, S. Beer-Hammer², B. Nürnberg², M. Schwab¹
¹Dr. Margarete Fischer-Bosch - Institut für Klinische Pharmakologie, Analytik, Stuttgart, Germany
²Institut für Experimentelle und Klinische Pharmakologie & Toxikologie, Abteilung für Pharmakologie & Experimentelle Therapie, Tübingen, Germany

Introduction: Understanding the regulation of aberrant cancer cell metabolism requires – beyond steady-state metabolite profiling - knowledge of the intracellular fluxes throughout the different metabolic pathways thus providing novel insights for personalized therapy. Stable isotope resolved metabolomics (SIRM) uses stable isotope tracer substrates and determination of labelling patterns in metabolites to derive relative pathway activities. Here we applied SIRM for qualitative assessment of drug-induced changes in pathway activities in a PTEN-Null breast cancer cell line upon selective inhibition of the PI3K β isoform.

Methods: The breast cancer cell line MDA-MB-468 was cultivated in [13 C, 15 N] glutamine enriched medium and treated with AZD8186 for up to 24 hours. Effects of the inhibitor were assessed by immunoblotting of PI3K/AKT pathway biomarkers and cell growth assays. Cell extracts were further analyzed applying mass spectrometry based quantitative metabolomics and SIRM.

Results: Western blot analysis demonstrated modulation of PI3K signaling at the protein level and impaired cell growth upon inhibition with AZD8186. Quantitative metabolomics revealed a significant decrease in glycolytic metabolite concentrations and Krebs cycle intermediates, whereas the majority of amino acids displayed elevated intracellular amounts. These drug-induced changes were confirmed by the SIRM approach, which displayed differences in the incorporation of stable isotopes i.a. for the Krebs cycle intermediates α -ketoglutarate and succinate and for aspartate. The most prominent alteration upon PI3K β inhibition, however, occurred within purine ribonucleotide *de novo* biosynthesis as indicated by a diminished incorporation of both nitrogen and carbon labels in adenosine nucleotides upon treatment.

Conclusion: The results obtained by conventional quantitative metabolomics showed an influence of PI3K β inhibition on the steady state levels of various metabolites in key metabolic pathways. However, specific changes in pathway activities remained uncovered by this approach. Consequently, our results demonstrate the importance of using the SIRM approach, where changes in pathway activities related to the production of energy intermediates upon PI3K β inhibition could be shown. To confirm these preliminary findings and extend the insight into affected pathways, further investigations employing the SIRM platform in combination with other tracer substrates are warranted.

P60

Characterization of SNPs in putative enhancer regions and in the promoter of the human adenosine A_{2B} receptor gene

S. Hinz¹, D. Jung¹, D. Hauert¹, H. S. Bachmann¹
¹Institute of Pharmacology and Toxicology, Faculty of Health, Witten, Germany

Question: The adenosine A_{2B} receptor (A_{2B}AR) is a novel target for the (immuno)therapy of cancer because its inhibition results in antiproliferative and antimetastatic effects. The A_{2B}AR is activated under pathological conditions such as hypoxia and inflammation where extracellular adenosine levels increase up to micromolar concentrations. Moreover, an upregulation of the A_{2B}AR expression is observed by hypoxia inducible factor 1- α (HIF-1 α) and by the transcription factors (TFs) *v-myb* and *b-myb*. Currently, the genetic variability of the A_{2B}AR gene is not entirely investigated. A few single nucleotide polymorphisms (SNPs) are described in the literature and are linked to chronic heart failure, cardioembolic stroke and diabetes. In the present study, we characterized 14 unpublished SNPs which are located in potential enhancer regions and in the putative promoter of the human A_{2B}AR gene.

Methods: The binding of TFs to the 14 SNPs (harboring either the wild-type or the variant allele) were investigated by bioinformatic analysis and by electrophoretic mobility shift assays (EMSAs). The nuclear protein fraction was extracted from HEK293T and HeLa cells. Sequences of unlabeled and 5'-DY-682 fluorescence-labeled oligonucleotides of the double-stranded DNA probes were used. The 14 SNPs were screened using HEK293T and HeLa cell nuclei extracts and SNPs with differences in the transcription factor binding pattern at the wild-type allele compared to the variant allele were further evaluated.

Results: The wild-type A-allele of rs7224967 showed the clearest difference in the TF binding pattern compared to the variant T-allele. Bioinformatic analysis revealed that the A-allele of rs7224967, unlike the T-allele, is part of a predicted binding site of CREB (cAMP response element binding protein) transcription factor. A subsequent TF matrix screening showed that TF binding to the A-allele increases when elongating the oligonucleotide probe sequence at the 5' end.

Conclusions: Characterization of genetic variants of the A_{2B}AR gene is essential to interpret and understand the different mechanisms in diseases. Our studies revealed that the SNP rs7224967, located in a potential enhancer region of the human A_{2B}AR gene, is an interesting candidate with differences in TF binding to the wild-type A-allele compared to the variant T-allele. Further studies are necessary to identify the TFs and their functional role in A_{2B}AR expression.

Pharmacology – Signal transduction and second messengers

P61

Reduction of intracellular pro-arrhythmic triggers via cGMP-stimulated PDE2

J. Klehr¹, E. Cachorro¹, M. Günscht¹, F. Nowakowski¹, H. Berning¹, K. Lorenz², A. El-Armouche¹, S. Kämmerer¹
¹TU Dresden, Institute of Pharmacology and Toxicology, Dresden, Germany
²Julius-Maximilians-Universität Würzburg, Institute of Pharmacology and Toxicology, Würzburg, Germany

Introduction: With a high mortality rate and substantial reduction of life quality, heart failure is one of the leading cardiac diseases. Heart failure is accompanied by arrhythmia often resulting in sudden heart death. New therapeutic strategies supporting cardiac actions of cGMP-generating natriuretic peptides showed protection against sudden cardiac death and arrhythmia development. Phosphodiesterase 2 (PDE2) is upregulated in HF and stimulated by cGMP. Here we studied, if PDE2 mediates antiarrhythmic effects of natriuretic peptides reducing pro-arrhythmic triggers in cardiac myocytes via a negative cGMP/cAMP-crosstalk.

Materials and methods: Using isolated cardiomyocytes from cardiac-specific PDE2-knockout mice (KO), patch-clamp-technique was applied to measure the late sodium current (I_{NaL}) as well as delayed afterdepolarizations (DAD), and confocal microscopy to determine calcium spark frequency (CaSpF). ECG was measured to detect arrhythmias in ex-vivo perfused Langendorff hearts.

Results: Upon incubation with isoprenaline (ISO, 10-100 nM, 10 min) isolated cardiomyocytes showed a significant increase in CaSpF and I_{NaL} amplitude in both wildtype mice (WT) and KO. The simultaneous stimulation of PDE2 with cGMP-generating C-type natriuretic peptide (CNP, 1 μ M) clearly reduced both arrhythmogenic triggers in WT. The CNP effect was attenuated once PDE2 was inhibited specifically with BAY-607550 (100 nM). Moreover, in KO cells simultaneous incubation with ISO and CNP did not affect either CaSpF or I_{NaL}. Similar results were observed for the occurrence of DADs after pacing the cardiomyocytes at 4 Hz.

In WT ex-vivo perfused hearts, CNP significantly reduced the number of arrhythmias such as ventricular extrasystoles and bigemini after reperfusion injury. Hearts of PDE2 KO mice displayed significant higher number of arrhythmias compared to WT.

Conclusions: The activation of the PDE2-mediated cGMP/cAMP crosstalk leads to both, a significant reduction of cardiac arrhythmogenic triggers and arrhythmias ex-vivo. Thus, cGMP-mediated PDE2 stimulation might be a promising novel strategy for future antiarrhythmic treatments.

P62

cGMP and cAMP crosstalk in brown adipocytes

D. Rowland¹, D. De Coninck¹, A. Pfeifer¹
¹Institute of Pharmacology and Toxicology Bonn, AG Pfeifer, Bonn, Germany

Obesity is characterized by an abnormal expansion in white adipose tissue (WAT) mass resulting in comorbidities such as metabolic syndrome, type 2 diabetes mellitus, cardiovascular disease, and certain types of cancer. Brown adipose tissue (BAT) is distinguished by its ability to dissipate energy in the form of heat through a process called non-shivering thermogenesis (NST), making it a promising target to combat obesity. Previous research has shown that cyclic nucleotides, such as cyclic adenosine monophosphate (cAMP) and cyclic guanosine monophosphate (cGMP) play a major role in BAT function. They enhance brown adipocyte (BA) differentiation, lipolysis, thermogenesis, mitochondrial biogenesis, energy expenditure and cause browning of WAT. While the effects of cGMP-mediated stimulation of protein kinase G (PKG) have been previously investigated, the crosstalk with the cAMP signalling pathway remains poorly understood in adipocytes. Here, we focused on modulation of cAMP levels by dual-specific phosphodiesterases (PDE) 2 and 3. To address the role of cGMP-mediated

modulation of PDEs 2 and 3, we isolated brown adipocytes from new-born transgenic mice expressing the cytosolic cAMP Förster Resonance Energy Transfer (FRET) biosensor Epac1-camps¹⁰, allowing us to monitor cAMP levels in real-time via changes in intramolecular FRET efficiencies. Our results demonstrate that PDE3, but not PDE2, is heavily involved in cytosolic cAMP degradation, even without previous adrenergic stimulation. Furthermore, stimulation of the soluble guanylylase (sGC) by BAY-412272 or natriuretic peptide receptor B (NPRB) by C-type natriuretic peptide (CNP) create rapid increases in cytosolic cAMP via cGMP mediated inhibition of PDE3 in murine brown preadipocytes. However, stimulation of natriuretic peptide receptor A (NPRA) by atrial natriuretic peptide (ANP) induced no changes in cAMP levels. Interestingly, the effects of cGMP mediated cAMP modulation were comparable to the effects of beta-adrenergic receptor agonist isoproterenol or PDE3 inhibitor clobutamide. Lastly, we show that the cGMP mediated increases in cAMP are also present after previous adrenergic stimulation, demonstrating a synergistic effect.

[1] Nikolaev, Viacheslav O.; Bünnemann, Moritz; Hein, Lutz; Hannawacker, Annette; Lohse, Martin J. (2004): Novel single chain cAMP sensors for receptor-induced signal propagation. In: The Journal of biological chemistry 279 (36), S. 37215–37218.

P63

Changes underlying restricted cardiomyocyte function in the diabetic remote myocardium

E. Funk¹, A. Kronenbitter¹, K. Beck^{1,2}, M. Krüger², J. P. Schmitt¹

¹Universitätsklinikum Düsseldorf, Institut für Pharmakologie und Klinische Pharmakologie, Düsseldorf, Germany

²Universitätsklinikum Düsseldorf, Institut für Herz- und Kreislaufphysiologie, Düsseldorf, Germany

Question: Among patients with myocardial ischemia/reperfusion (I/R), type-2 diabetes mellitus (T2DM) is highly prevalent and increases mortality. Here we aimed at identifying mechanisms restricting contractile performance of diabetic cardiomyocytes (CM) under basal conditions and in the non-infarcted remote myocardium (RM) 24 h after I/R.

Methods: 10-12 weeks old male leptin receptor-deficient db/db mice were used as a model of T2DM. Heterozygous littermates served as non-diabetic controls. Mice were harvested either naïve or 24 h after 1 h ischemia (closed-chest model of I/R). Ca²⁺ cycling (Fura-2 method) and contractile function (video-based tracking of sarcomere lengths) were measured in electrically paced CM isolated from the RM or the corresponding tissue region of sham-operated mice. Expression and phosphorylation of key proteins for CM Ca²⁺ handling and contraction were analysed by western blot. Ca²⁺ dependence of force generation was measured in skinned strips of isolated papillary muscles (Myoscope System, Myotronic).

Results: At the age of 10-12 weeks, db/db mice were obese and hyperglycemic without signs of heart failure. Compared to non-diabetic mice, Ca²⁺ cycling was suppressed in diabetic CM under basal conditions and in the RM after I/R. Mechanistically, excessive SERCA2a inhibition resulting from reduced phosphorylation of its main regulator phospholamban (PLN) led to slower cytosolic Ca²⁺ clearance. Decreased PLN phosphorylation at S16 by about 30% (p<0.05) was already present under basal conditions and further reduced by about 60% after I/R (p<0.05). In diabetic mice, PLN phosphorylation but not Ca²⁺ cycling could be normalized by β-adrenergic stimulation. Consequently, reduced PLN phosphorylation only partly contributed to the slower Ca²⁺ cycling in diabetic mice. Despite slow Ca²⁺ cycling of diabetic CM, kinetics of sarcomere contraction and relaxation were indistinguishable from non-diabetic CM under basal conditions whereas the contractile amplitude was impaired after I/R. Preserved sarcomere function could be attributed to increased myofilament Ca²⁺ sensitivity. In this context, reduced troponin I phosphorylation was identified as a contributing factor.

Conclusion: Additionally to I/R, T2DM suppresses cardiomyocyte Ca²⁺ cycling in the RM, thereby contributing to cardiac dysfunction. Increased myofilament Ca²⁺ sensitivity acts as a compensatory mechanism to maintain sarcomere function at baseline but this adaption fails after I/R.

P64

Proximity labeling of p65 NF-κB interactomes

J. Julf¹, L. Leib¹, U. Linne², A. Weber¹, M. Kracht¹

¹Rudolf Buchheim Institute of Pharmacology, Justus Liebig University Giessen, Gießen, Germany

²Competence Centre for mass spectrometry, Faculty of Chemistry, Philipps-University Marburg, Marburg, Germany

Question: The transcription factor NF-κB p65 plays a key role in innate and adaptive immunity. It functions as a master regulator of the inflammatory response by inducing the expression of pro-inflammatory genes including secreted cytokines (IL6), chemokines (IL8, CXCL2), and multiple regulatory intracellular proteins (NFKBIA). NF-κB is activated by the so-called canonical, noncanonical and atypical signalling pathways. In the canonical pathway, activation of the Interleukin-1 receptor complex triggers degradation of the cytosolic p65 inhibitor IκBα followed by nuclear translocation of p65 where it is directed by unknown pathways to the enhancers and promoters of pro-inflammatory genes. Despite its pleiotropic functions in adaptive and innate immunity or stress reactions, the entire repertoire of p65 interacting factors that contribute to its general or stimulus-specific functions within the nucleus or other cell compartments is still elusive.

Methods: To identify the p65 interactomes in intact cells, we fused p65 to the biotin ligase miniTurbo (mTb), which biotinylates proteins within close proximity to the bait protein.

miniTurbo is an engineered *E.coli* biotin ligase, which enables fast biotin tagging of interactors within 10 min. We used doxycycline-inducible p65-mTb constructs to obtain a snap shot of the dynamic p65 interactome. In this analysis, we also addressed the question, which interactions depend on p65 dimerization or DNA binding by means of p65 point mutants abolishing either function. Subsequently, the biotinylated proteins were affinity purified by streptavidin matrices, identified by mass spectrometry and extensively analysed by bioinformatics.

Results & Conclusion: Filtering and statistical testing of the proximity labeling data sets confirmed the known components of the canonical p65 pathway and revealed several hundred additional high confidence interactors. Most of these proteins map to a range of gene regulatory pathways in line with p65's transcriptional functions. Interestingly, only 20% of p65 interactors require direct DNA binding, but 70% of the p65 interactome requires dimerization. Besides the known interactors found in this analysis, there are multiple novel factors that have not been reported in the literature. This rich data set can now be validated functionally in the IL-1 system by ChIP-seq or LOF screens and also allows the intersection with other genome-/proteome-wide data sets.

Pharmacology – Nuclear receptors, enzymes and other targets

P65

Identification of novel pregnane X receptor antagonists in the Tübingen kinase inhibitor collection (TüKIC) compound library

E. K. Mustonen¹, T. Pansar^{2,3}, A. Rashidian⁴, S. Laufer², M. Schwab^{1,5,6}, O. Burk¹

¹Dr. Margarete Fischer-Bosch - Institut für Klinische Pharmakologie, Stuttgart, Germany

²University of Tübingen, Pharmaceutical and Medicinal Chemistry, Tübingen, Germany

³University of Eastern Finland, Pharmacy, Kuopio, Finland

⁴University Hospital Tübingen, Internal Medicine VIII, Tübingen, Germany

⁵University of Tübingen, Clinical Pharmacology, Tübingen, Germany

⁶University of Tübingen, Pharmacy and Biochemistry, Tübingen, Germany

Introduction: Pregnane X receptor (PXR) is a major regulator of genes involved in xenobiotic detoxification. In cancer cells, PXR activation has been shown to promote tumor growth and cancer drug resistance. Therefore, PXR antagonism is proposed as a potential approach to overcome cancer drug resistance. This approach is hindered by the limited number of available PXR antagonists.

Objectives: Our aim was to identify and characterize novel PXR antagonists from the Tübingen Kinase Inhibitor Collection (TüKIC) compound library. As kinase inhibitors represent an important group of molecularly targeted cancer drugs, dual kinase and PXR inhibitors may be of special interest for the prevention of cancer drug resistance.

Material and Methods: The TüKIC compound library was screened in silico to identify potential PXR ligands. Reporter gene assays were utilized to investigate the PXR activation potential and nuclear receptor selectivity. Binding of compounds to the PXR ligand-binding domain (LBD) was investigated with limited proteolytic digestion in vitro and cellular LBD assembly assays. Mammalian two hybrid assays were used to investigate the interaction of PXR with transcriptional coregulators. Effects on endogenous gene expression in LS174T colorectal adenocarcinoma cells were analyzed by quantitative real-time PCR. Kinome profiling was conducted to assess actual kinase inhibition.

Results: In our contribution we will discuss our key results and their implications.

Conclusion: We identified and characterized selected kinase inhibitors for their modulation capabilities of PXR.

P66

Mitotoxicity and induction of CYP1A1 by two phenolic antioxidants present in consumer related product

M. T. Ho¹, A. Luch¹, S. Zellmer¹

¹German Federal Institute for Risk Assessment, Department of Chemical and Product Safety, Berlin, Germany

Phenolic antioxidants (pAO) are well known secondary plant products and are also man-made chemicals to protect consumer related products and food from degradation by oxidation. The pAOs may consist of one or several phenolic ring structures with different side chains. A well known single ring structure is 2,6-di-*tert*-butyl-p-cresol (BHT), also known as food additive E321. The two-ring structure 2,2-bis(4-hydroxyphenyl)propane (BPA) has been studied for several years and it was classified recently as endocrine disruptor. Another two-ring structure, the AO 2246 (2,2'-Methylen-bis(4-methyl-6-*tert*-butylphenol)) has been evaluated by the European Food Safety Agency (EFSA) and occurs in food contact materials. A chemically similar two-ring structure, AO 1081 (2,2'-sulfinatediylbis(6-*tert*-butyl-4-methylphenol)) has been not been evaluated by EFSA and has been detected in consumer related products without food contact. Here, we present data on different toxicological endpoints of AO 2246 and AO 081 in HepG2 cells.

HepG2 cells were incubated with non-toxic doses of AO 2246 and AO 1081 and the effects on mitochondrial membrane potential, the ATP concentration, the activation of the AhR signalling pathway and the expression of CYP1A1 was studied.

In HepG2 cells, the EC50 of pAO 2246 and AO 1081 were 101 ± 15 µM and 331 ± 117 µM, respectively. Treatment of HepG2 cells by the pAOs resulted in a decrease of the

relative mitochondrial membrane potential ($\Delta\Psi$). The ATP concentration decreased significantly at 200 μM AO 1081 and 150 μM AO 2246. An induction of AhR mRNA occurred in the presence of both pAO. In summary, AO 2246 and AO 1081 differed in their toxicity, affected the $\Delta\Psi$ and increased the expression of CYP1A1.

The financial support of the BfR is gratefully acknowledged.

P67

Cysteine-rich LIM-only protein 4 (CRP4) regulates vascular smooth muscle cell (VSMC) plasticity and the pathogenesis of atherosclerosis

N. Längst¹, J. Adler¹, A. Peter², K. Boldt³, R. Lukowski¹

¹Institute of Pharmacy, University of Tübingen, Experimental Pharmacology, Department of Pharmacology, Toxicology and Clinical Pharmacy, Tübingen, Germany

²Institute for Clinical Chemistry and Pathobiochemistry, University Hospital Tuebingen, Department for Diagnostic Laboratory Medicine, Tübingen, Germany

³Institute for Ophthalmic Research, University of Tuebingen, Molecular Biology of Retinal Degenerations, Tübingen, Germany

Question: LIM domain-containing members of the cysteine-rich protein (CRP) family play an important role as bridging factors between proteins. Via their double zinc-finger-like LIM domain(s) they associate with the actin cytoskeleton and have thus been implicated in cell proliferation and differentiation. Along these lines, CRP4 was shown to regulate the VSMC-specific gene expression downstream of the 3',5'-cyclic guanosine monophosphate (cGMP) pathway. Because the expression of VSMC-specific genes and proteins is massively perturbed during the phenotypic modulation of VSMCs, we hypothesized that CRP4 may contribute to VSMC plasticity and thereby to vasculo-proliferative diseases such as atherosclerosis and restenosis.

Methods: CRP4 WT and KO aorta were dissected to obtain primary and highly passaged VSMCs, which were subsequently studied for their migratory and proliferative properties. Furthermore, putative pro- or anti-atherogenic roles of CRP4 were investigated *in vivo* in plaque-prone CRP4 and ApoE double-mutant mice fed a Western diet. To analyze the composition of the plaques in detail, *en face* Oil-red O as well as immunohistochemical staining methods for multiple markers of atherosclerosis were applied on aortic cryosections.

Results: In VSMCs, CRP4 is localized in the cytoplasm, especially in the perinuclear region, whereas only a minor fraction of CRP4 could be identified in the nucleus itself. The initial shape change of freshly isolated VSMCs as well as the protein expression profile in synthetic VSMCs was altered in the absence of CRP4. Moreover, proliferative and migratory behaviors differed between contractile and synthetic VSMCs in a CRP4-dependent manner. Combined these data imply a lower susceptibility to develop atherosclerotic plaques as confirmed by a ApoE/CRP4 double-mutant mouse model. Interestingly, CRP4-deficient atherogenic mice exhibited lower plaque numbers and areas and displayed a reduced VSMC content in the fibrous caps. Our ongoing analyses will validate the impact of CRP4 on oxidative stress and the further cellular composition of the atherosclerotic lesions.

Conclusion: The combined analyses of a CRP4-proficient *versus* -deficient mouse model revealed a pro-atherogenic role for CRP4. Accordingly, CRP4 contributes to the proliferative and migratory capacity of VSMCs *in vitro*. Thus, pharmacological targeting of CRP4 may be beneficial in vasculo-proliferative diseases, commonly found in hypertension and hyperlipidemia.

P68

The simultaneous determination of intracellular nucleoside triphosphates and cyclic dinucleotides with LC/MS/MS

O. Reinhard¹, R. Bertold¹, B. Rayk²

¹TU Dresden, Institute of Clinical Pharmacology, Dresden, Germany

²TU Dresden, Institute for Immunology, Dresden, Germany

Introduction: The determination of nucleoside triphosphates and cyclic dinucleotides in cells is of interest for various issues: The cyclic dinucleotides adenosine monophosphate-guanosine monophosphate (cGAMP) and diGMP could be a tumor marker in human fibroblasts. The quantification of deoxynucleoside triphosphates (dNTPs) and the corresponding ribonucleotide triphosphates (NTPs) can be used to measure enzyme activity in knockout cells

Objectives: The aim of the study was the determination of different nucleotides in different matrices with only one method and a complete chromatographic separation of the isomers ATP and dGTP and of the isomers CTP, UTP and dTTP, which have very similar masses.

Methods and Materials: ATP and dGTP are isomers, CTP, UTP and dTTP have very similar masses. Therefore a complete chromatographic separation was an aim of the study. An HPLC-Method with a reversed phase column and a mobile phase gradient were applied to separate all analytes in less than 10 min. Two transitions per substance were used in multiple reaction monitor (MRM) mode of the tandem mass spectrometer. The supernatants of cell pellets of 106 cells were examined to quantify the dNTPs.

Results: An 8-point external calibration curve in buffer at the range from 7.8 – 1000 ng/mL for 10 nucleoside triphosphates and cyclic dinucleotides was prepared and measured with samples of the assay. Quantification was performed by peak area method.

A weighted (1/x) regression first order was performed to determine the concentration of the analytes. The calibration curves were accurate and precise over the range from 7.8 – 1000 ng/mL and the correlation coefficient (r) exceeded 0.996 in all cases. The concentrations 7.8 and 1000 ng/mL are the lower and the upper limit of quantification (LLOQ and ULOQ). Coefficients of variation and accuracy were calculated for each standard and are supposed to vary by less than 15%. All tested real samples contained nucleotide. To estimate the matrix effect, the samples were additionally analyzed by the standard addition method.

Conclusions: A simple and sensitive LC / MS / MS method was developed to separate different, partially isomeric nucleotides. The method provides a convenient tool for measuring intracellular dNTP / NTP levels that can be used to measure the molecular phenotype of mouse cells. In addition, cyclic dinucleotide concentrations in human cells were determined to be potential tumor markers.

P69

Non-essential functions of the canonical cap-binding complex in the IL-1 pathway

J. Meier-Soelch¹, J. Knauff¹, D. Newel¹, H. Weiser¹, S. Werner¹, M. Heiner², M. Kracht¹

¹Justus Liebig University Giessen, Rudolf Buchheim Institute of Pharmacology, Gießen, Germany

²Justus Liebig University Giessen, Department of Internal Medicine II and Cardio-

Pulmonary Institute, Gießen, Germany

Question: In all eukaryotes, co-transcriptional fusion of the m7G cap structure to the 5'-end of mRNAs serves as the initiator signal for all subsequent splicing and RNA processing steps. The cap binds to the highly conserved nuclear cap-binding complex (CBC), which is considered as the generic regulator of downstream RNA biogenesis. The canonical CBC is a heterodimer formed by the nuclear cap-binding protein 2 (NCBP2), which directly associates with the RNA cap, and NCBP1, which stabilizes NCBP2 and serves as an adaptor for other RNA processing factors. We discovered that NCBP1 is transiently phosphorylated in response to the pro-inflammatory cytokine IL-1 raising the major question if NCBP1 or the CBC can also execute specific functions in diverse (patho)physiological conditions such as inflammatory cell reactions.

Methods: To analyze the function of NCBP1 in the IL-1 pathway, an auxin-inducible degron system was established in HCT116 colon carcinoma epithelial cells, which enables rapid and reversible depletion of NCBP1. The last exon of the NCBP1 gene was fused to a minimal auxin-inducible degron (mAID) domain by CRISPR/Cas9. The mAID tag enables inducible proteasomal degradation of the NCBP1-mAID fusion protein by the phytohormone auxin in cells co-expressing the plant-specific E3 ligase TIR1. Using this system, we explored the effects of NCBP1 depletion at multiple levels, including chromatin-association (by ChIP-seq), regulation and subcellular localization of unprocessed and mature transcripts (by RNA-seq), and cytokine secretion (by PEA technology).

Results: Homozygous monoclonal cell lines expressing the NCBP1-mAID fusion protein show a complete but reversible NCBP1 degradation and a co-depletion of NCBP2 within 24 h of auxin exposure. Functionally, depletion of NCBP1/2 results in reduced cellular viability paralleled by a global change of the cellular transcriptome. In contrast, the IL-1-induced mRNA expression as well as cytokine secretion are only partially reduced.

Conclusions: Using a sophisticated conditional depletion system, we reveal the CBC as a central factor for cell survival and integrity of the transcriptome. However, so far our data suggest that in the IL-1 pathway loss of the CBC is compensated by an additional mechanism which helps to maintain the expression of inflammatory factors. This putative CBC-independent pathway may represent a new and specific pharmacological target to control inflammatory processes.

P70

Non-redundant functions of p-body proteins DCP1a and DCP1b

D. Heylmann¹, O. Othman¹, K. Beuerlein¹, U. Tenekeci¹, M. Heiner², M. Kracht¹

¹Rudolf Buchheim Institute of Pharmacology, Justus Liebig University Giessen, Gießen, Germany

²Universities of Giessen and Marburg Lung Center (UGMLC), Gießen, Germany

Introduction: There is limited knowledge concerning physiological functions of processing-body (p-body) components DCP1a and DCP1b. Both proteins are regulatory subunits of the decapping complex which assembles within p-bodies but also in the cytoplasm and contributes to the DCP2-dependent decay of mRNA. Because external stimuli such as IL-1 affect p-body formation it is interesting to reveal the biological role of DCP1a and DCP1b in cytokine pathways. Previously, our group demonstrated IL-1 triggered phosphorylation, ubiquitination and activation of DCP1a and investigated the *in vivo* role of DCP1a in mouse knockout models. Constitutive ablation of DCP1a in mice revealed an essential role for embryonic development suggesting non-redundant functions of DCP1a. To find out if this is also the case for the related DCP1b, we have started to investigate this rarely studied protein.

Objectives: Here we present new results suggesting that DCP1b, unlike DCP1a, is required for tumor cell proliferation and prevention of cell death.

Material and Methods: HeLa cells were transfected with DCP1a and DCP1b siRNA using HiPerFect transfection reagent. Cells transfected with Luciferase siRNA were used as controls. Transfection efficacy was determined by Western Blot and quantitative real-time PCR (RT-qPCR). Cell numbers were counted between 24 and 96 h after transfection

using light microscopy. For subG1-assays, cells were incubated after ethanol fixation with Propidium iodide and cell death was quantified by flow cytometry. Gene expression of various target genes was analyzed by RT-qPCR.

Results: Knockdown of DCP1b downregulates proliferation of HeLa cells as shown by reduced cell numbers after siRNA transfection. Furthermore, DCP1b downregulation significantly induces DNA fragmentation determined by an increase of the subG1 fraction, which is an indication of cell death. In contrast, DCP1a knockdown did not induce DNA fragmentation or cell death of HeLa cells. Moreover, gene expression analysis using RT-qPCR indicated a higher expression of the cell cycle regulator p21 upon DCP1b knockdown.

Conclusion: DCP1b seems to have an essential role for the proliferation and viability of HeLa cells suggesting further non-redundant functions. Future work will focus more closely on the mechanisms of the DCP1b pathway in cytokine-activated immune and cancer cells with the aim to explore if DCP1a or DCP1b regulated decapping pathways are amenable for pharmacological intervention.

P71

Alkylating antineoplastic agents induce DNA modifications which potentiate cGAS activation.

K. Andryka¹, T. Zillinger², C. Mertens¹, S. Schmitz¹, P. Müller¹, E. D. Giammarino¹, W. Barchet^{1,3}, G. Hartmann¹, E. Bartok¹

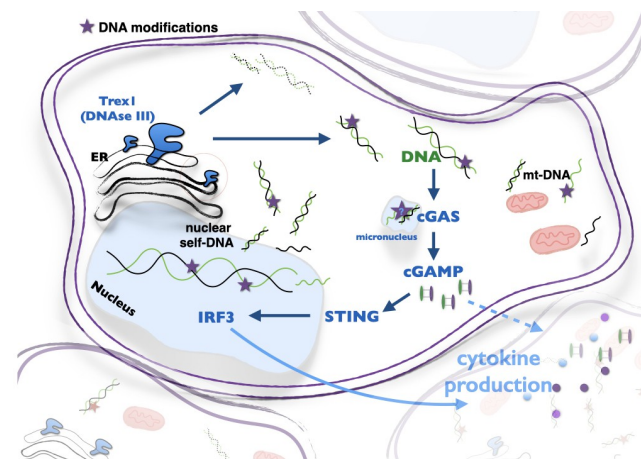
¹Institute of Clinical Chemistry and Clinical Pharmacology, University Hospital Bonn, Bonn, Germany

²Philipps-University Marburg, Medical Faculty, Marburg, Germany

³German Center for Infection Research (DZIF), partner site Bonn-Cologne, Cologne, Germany

The detection of microbial nucleic acids by the innate immune system is essential for protection of the host against pathogens. However, the release of self-DNA can also activate the cGAMP synthase (cGAS) / Stimulator of interferon genes (STING) pathway, contributing both to autoimmunity but also to the elimination of malignantly transformed cells. In this project, we show that a direct treatment of tumor cells by DNA-damaging cytostatic drugs can induce a type I interferon response in a cGAS/STING dependent manner. Moreover, our data demonstrate that these agents cause DNA modifications which increase resistance to degradation by three-prime repair exonuclease 1 (TREX1) in the cytoplasm thus licensing cGAS activation. This effect can be observed at concentrations at and below the peak plasma level of these drugs during tumor chemotherapy, and it can be elicited both in myeloid cells and in tumor cells competent in cGAS/STING signaling. Further studies will be necessary to investigate the contribution of cGAS/STING signaling during chemotherapy to tumor immunogenicity and the tumor microenvironment.

Fig. 1



Pharmacology – Ion channels and membrane transporters

P72

Species-specific and developmental influences on the expression of xenobiotic transporters

A. Weyrich¹, M. Frericks¹, T. Hofmann¹, M. Eichenlaub², S. Schneider¹, B. van Ravenzwaay¹

¹BASF SE, Experimental Toxicology and Ecology, Ludwigshafen am Rhein, Germany

²BASF SE, Bioscience Research, Ludwigshafen am Rhein, Germany

Introduction: Teratogenic effects, which can occur in animal testing, play a crucial role in the registration of drugs and plant protection agents. The explanation of such effects is difficult due to the high complexity of the system and many unknown parameters. Species differences in developmental toxicity can be due to varying expression of xenobiotic

transporters. Transporters play an important role in ADME especially for substances which require active transport into cells. The two super families of transporters well known for their role in the distribution of xenobiotics and endogenous substances are the ATP-binding cassette transporter (ABC) and the solute carrier (SLC) families. In view of embryo-foetal developmental toxicity the liver and the kidneys of the embryo, the foetus and the dam, as well as the placenta, are important organs for xenobiotic transport. The data about the expression of xenobiotic transporters is very limited and virtually absent in rabbit.

Objectives: The aim of this study was to assess gene expression of xenobiotic transporters in liver, kidney and placenta of rat and rabbit at different pre- and postnatal developmental stages.

Materials & methods: Rats and rabbits were sacrificed at different pre- and postnatal time points. Liver, kidney and placenta of embryos, foetus or offspring were harvested, snap frozen, and stored at -80°C for further analysis. mRNA was extracted and expression rates of BSEP, MRD1, MRP1-6, BCRP, OAT1-3 and several OATPs were determined by 2-Step RT-qPCR.

Results: Data analysis showed large differences in transporter expression in development and between species. Several transporters displayed a significantly lower expression in foetus that increases with progressing development while some transporters showed similar expression across development.

Conclusion: A better understanding of expression rates of xenobiotic transporters in placenta, liver and kidney during the embryonic and foetal development across species is important for the understanding of teratogenic effects. The generated gene expression data can be used to better evaluate developmental toxicity findings in non-clinical species and their relevance for humans.

P73

Deletion of two-pore channel 1 affects EGFR signalling pathways in multiple ways

S. Großmann¹, T. Müller¹, R. T. Mallmann¹, C. Rommel¹, L. Hein¹, N. Klugbauer¹
¹Albert-Ludwigs-Universität Freiburg, Institut für Experimentelle und Klinische Pharmakologie und Toxikologie, Freiburg im Breisgau, Germany

Introduction: Two-pore channels (TPCs) comprise a small family of ion channels with only two representatives in rodents and humans, TPC1 and TPC2. TPCs are key components for regulating intracellular Ca^{2+} current from endosomal and lysosomal compartments to the cytosol. This spatiotemporally restricted Ca^{2+} -increase forms the basis for fusion and fission events between endolysosomal membranes and thereby for intracellular trafficking processes.

Objectives: We investigated the function of TPC1 and TPC2 for uptake, recycling and degradation of epidermal growth factor receptor (EGFR) using MEF cells with either single or double TPC knockouts. Deletion of TPCs increases expression of EGFR in all TPC knockout cells and alters trafficking and signalling of EGFR. To investigate whether deletion of TPCs affects gene expression in a global manner, we performed an RNA sequencing analysis of wildtype and TPC1 knockout cells.

Material and Methods: A global RNA sequencing of three independent samples of WT and TPC1-KO MEF cells was performed. Computational analysis and evaluation of the data was made using tools integrated in the Galaxy platform and ClueGO software.

Results: Deletion of TPC1 causes a massive change in gene expression in comparison to wildtype MEF cells, with 674 genes more than twofold upregulated and 1141 genes more than twofold downregulated in KO cells. Gene ontology enrichment analysis revealed numerous affected pathways such as calcium signalling, MAPK signalling pathway and pathways involved in cancer progression. We studied changes in gene expression of proteins in the EGFR signalling pathways and identified numerous quantitative changes in gene expression levels. Both up- and downregulation was observed. *Egfr*-expression itself was 3.2-fold upregulated in TPC1-KO cells, whereas expression of some downstream proteins like *Jak1/Jak2* were almost cut in half (0.54 and 0.58 respectively) compared to wildtype cells.

Conclusion: RNA-seq data indicated that loss of TPC1 has a strong impact on the transcription of numerous different genes and diverse pathways. We conclude that deletion of TPC delays endolysosomal EGFR trafficking and thereby prolongs EGFR signalling and activation of associated signalling pathways, causing a positive feedback loop leading to elevated *Egfr* transcription. This dysregulation in receptor trafficking and signalling has an impact on transcriptional levels of diverse proteins – not only in the EGFR pathway.

P74

Why endogenous TRPV6 currents are not detectable-what can we learn from bats?

U. Wissenbach¹, W. Karin¹, N. Erhardt¹, H. Löhr¹, C. Wesely¹, C. Fecher-Trost¹

¹Universität des Saarlandes, Institut für Experimentelle und Klinische Pharmakologie und Toxikologie, Homburg, Germany

The human TRPV6 protein is a calcium selective ion channel which is expressed in the placental trophoblast layer, pancreatic acini and a few glands. Although TRPV6 activity is easily detectable using imaging or patch clamp based approaches, endogenous TRPV6

activity was not convincingly detected in the mentioned tissues. We showed that the translation of the TRPV6 protein is initiated at an ACG triplet which is translated into methionine. The ACG triplet is located 120bp upstream of the first in frame AUG present in the *TRPV6* mRNA. The family of bats and fruit bats comprises at the corresponding position of the ACG codon of the human sequence a classical initiation codon (AUG). We studied structural nucleotide differences between human and bats by developing chimera and mutants of human/bat TRPV6 channels. Our data indicate that the initiation of the translation of the human TRPV6 is relatively inefficient which results in a poor synthesis of the TRPV6 protein. The sequence of the human *TRPV6* mRNA which is located in between the ACG codon and the first AUG codon provokes the initiation of the translation at the ACG codon. We suggest that the mechanism involves most likely the deceleration of ribosome scanning by stem-loop formation and the use of the common initiator tRNA which is placed onto the inappropriate ACG codon resulting in low protein synthesis. In contrast the corresponding sequence of bats causes the initiation of translation at the first AUG codon of the bat *TRPV6* mRNA. The low efficiency of the translation of the human *TRPV6* mRNA may be a mechanism to avoid toxic calcium overload as consequence of the activity of the TRPV6 protein. Bats may use a more efficient translation mechanism as an adaptation to low calcium amounts present in the natural nutrition. Our data present an explanation why endogenous activity of the human TRPV6 protein is not detectable.

Wolske et al., 2020. Why endogenous TRPV6 currents are not detectable-what can we learn from bats? *Cell Calcium*. 92:102302.

Fecher-Trost, Weissgerber and Wissenbach, 2014. TRPV6 channels. *Handb Exp Pharmacol*. 222:359-84.

Fecher-Trost et al., 2013. The in vivo TRPV6 protein starts at a non-AUG triplet, decoded as methionine, upstream of canonical initiation at AUG. *J Biol Chem*. 288(23):16629-44.

P75

Postsynaptic bk channels promote schaffer collateral LTP and hippocampal memory formation in The Morris Water Maze

T. Pham¹, H. Bischof¹, S. Simonsig¹, D. Kalina¹, R. Ehinger¹, P. Ruth¹, R. Lukowski¹, L. Matt¹

¹Institute of Pharmacy, University of Tübingen, Department of Pharmacology, Toxicology and Clinical Pharmacy, Tübingen, Germany

Question: Mutations in large-conductance Ca²⁺- and voltage-activated potassium channels (BK) are associated with cognitive impairment that occurs in schizophrenia, autism and Alzheimer's disease and is characterized by impaired plasticity of glutamatergic synapses. BK's role in synaptic plasticity, the bi-directional modification of synaptic strength underlying learning and memory, however, remains unknown. Because global BK knockout mice (BK^{-/-}) suffer from cerebellar ataxia rendering them unable to perform behavioral tasks, we used hippocampal CA1 pyramidal neuron-specific conditional BK knockout (CA1BK^{fl/fl}) and littermate control mice to study BK's role in hippocampal synaptic plasticity and formation of hippocampus-dependent memory.

Methods: Conditional knockout mice were created by Cre/loxP-directed excision of floxed BK alleles. Electrophysiological long-term potentiation (LTP) and AMPA receptor phosphorylation after chemical LTP induction (cLTP) was measured in acute hippocampal slices. Motor abilities and hippocampus-dependent cognitive performance was studied using open-field, beam-walk and Morris Water Maze (MWM) paradigms. Intracellular potassium dynamics in dissociated hippocampal neuron cultures during cLTP induction was monitored in real-time by genetically encoded FRET-based potassium ion indicators (GEPII).

Results: Western blot and immunofluorescence confirmed selective and effective BK deletion from hippocampal CA1 pyramidal neurons in CA1BK^{fl/fl}. As expected, CA1BK^{fl/fl} displayed normal motor functions in open-field and beam-walk confirming their suitability for behavior-based assays. Indeed, CA1BK^{fl/fl} exhibited significantly increased latency to platform in the MWM acquisition phase and spent significantly less time in the target quadrant during probe trial, both indicating impaired hippocampus-dependent learning *in vivo*. This was further corroborated *in vitro* by significantly reduced CA3 to CA1 Schaffer collateral LTP in CA1BK^{fl/fl} and significant reduction of LTP-associated AMPA receptor phosphorylation at Ser845 after cLTP induction. GEPII recordings in dissociated hippocampal neurons revealed a massive BK-dependent reduction of intracellular potassium during cLTP induction.

Conclusion: We conclude that BK channel-mediated potassium outflow occurring during LTP induction in hippocampal neurons crucially supports synaptic plasticity *in vitro* and *in vivo*, suggesting BK modulation as therapeutic option for treating cognitive impairment.

P76

Transient receptor potential vanilloid 6 (TRPV6) protein controls the extracellular matrix architecture of the placental labyrinth

M. Winter¹, P. Weissgerber¹, K. Klein¹, F. Lux¹, V. Flockerzi¹, C. Fecher-Trost¹

¹Saarland University, Experimental and Clinical Pharmacology and Toxicology / Center for Molecular Signaling, Homburg, Germany

The high calcium selective Transient Receptor Potential Vanilloid (TRPV6) channel is expressed in maternal and fetal tissues in the placenta and uterus during pregnancy necessary for sufficient calcium supply, embryo growth, and bone development. Wild-type mice and two *Trpv6*-deficient mouse models (*Trpv6*^{-/-} and *Trpv6*^{mut/mut}) were studied to characterize the role of TRPV6 proteins. Compared to *wild-type* embryos the embryos of

"KO"-strains were less provided with calcium. The growth of *Trpv6*-deficient embryos was retarded and their bones were less mineralized. Especially the labyrinth zone of the placenta which builds the fetomaternal barrier was altered in morphology in *Trpv6*-deficient placentae. Therefore, the mature cell type of the labyrinth zone, the trophoblast cells were isolated and cultured for both genotypes. Calcium uptake by *Trpv6*^{-/-} trophoblasts and cell-cell contacts during cell culture were reduced. *Trpv6*^{-/-} and *wt* trophoblasts show a distinct calcium-dependent phenotype in cell culture. Deep proteomic profiling of *wt* and *Trpv6*^{-/-} trophoblasts by mass spectrometry leads to the identification of 2778 proteins. Among those, different proteases, including high-temperature requirement A serine peptidase 1 (HTRA1) and different granzymes (granzyme C, E, F, and G) are exclusively or more abundantly expressed in *Trpv6*^{-/-} trophoblasts, whereas the extracellular matrix adapterprotein fibronectin and the fibronectin-domain-containing protein 3A (FND3A) were markedly reduced. *Trpv6*^{-/-} placenta lysates possess a higher intrinsic proteolytic activity increasing fibronectin degradation. Our results show that the morphology of the placental labyrinth depends on TRPV6; a functional deletion in trophoblasts correlates with the increased expression of proteases controlling the architecture of the extracellular matrix in the placental labyrinth during pregnancy.

P77

Deletion of two-pore channels uncovers the importance of JNK-pathway for EGFR-receptor expression

R. T. Mallmann¹, N. Klugbauer¹, S. Großmann¹, T. Müller¹

¹Albert-Ludwigs-Universität Freiburg, Experimentelle und Klinische Pharmakologie und Toxikologie, Freiburg im Breisgau, Germany

Introduction: Two-Pore Channels (TPCs) – TPC1 and TPC2 – are located in membranes of intracellular acidic organelles of the endo-lysosomal system. TPC1 and TPC2 have been shown to be involved in the efflux of Ca²⁺ from intracellular organelles and thereby contribute to fusion and fission events of endosomes and lysosomes. Recent studies indicate that signalling of the epidermal growth factor receptor (EGFR) does not only occur during surface localization, but also after internalization and presence of activated EGFRs in endosomal compartments. Therefore, EGFR can be used as a model to uncover the specific functions of TPCs for receptor uptake, trafficking and expression. Our studies revealed an increased transcription of EGFR and an altered expression level of EGFR-pathway related genes in TPC1 and TPC2 deficient cells.

Objectives: We took advantage of MEF cells with single, but also with a TPC1/2 double gene deletion to investigate its consequences on EGFR signalling. A prolonged presence of activated EGFRs in endolysosomal signalling platforms, caused by genetic inactivation of TPCs, may not only affect EGFR-signalling pathways, but also *de novo*-synthesis of EGFR itself. The JNK-pathway is a main signalling pathway within the EGFR-signalling network, that has been shown to initiate and maintain increased EGFR-expression levels. Therefore, we investigated the basal expression as well as the phosphorylation of c-Jun in wildtype and TPC-deficient cells.

Material & methods: CRISPR/Cas9 gene editing, FACS, Western Blot

Results: We compared phospho-c-Jun levels under basal and EGF-stimulated conditions of wildtype and TPC-deficient MEF cells. TPC1-, TPC2- and TPC1/2 double knockout cells demonstrated a significantly increased phosphorylation of c-Jun under basal conditions. EGF-stimulation induced higher phospho-c-Jun levels in all MEF cell-lines, whereby phospho-c-Jun levels of EGF-stimulated wildtype cells achieved values comparable to that of TPC-deficient cells under basal conditions. EGF-stimulation of TPC-deficient cells even reached still higher phospho-c-Jun levels.

Conclusion: Increased JNK-signalling, indicated by elevated phospho-c-Jun-levels, contributes to the high EGFR expression observed in TPC deficient cells and maintains a positive feedback loop that may explain the strongly increased amounts of surface accessible EGFRs found in TPC-deficient cells.

P78

Of dogs and men: Cloning of dog OCT1 and OCT2 and comparative characterization with human and other known orthologs

S. Falk¹, M. J. Meyer¹, S. Römer², J. Geyer², S. Simm³, M. V. Tzvetkov¹

¹University Medicine Greifswald, Institute of Pharmacology, C_DAT, Greifswald, Germany

²Justus Liebig University Giessen, Institute of Pharmacology and Toxicology, Giessen, Germany

³University Medicine Greifswald, Institute of Bioinformatics, Greifswald, Germany

OCT1 and OCT2 are polyspecific membrane transporters. In humans, OCT1 is predominantly expressed in hepatocytes, whereas OCT2 is expressed in renal proximal tubules. Both transporters contribute to the hepatic and renal clearance of a variety of drugs.

Similar to rodents, also dogs are commonly used preclinical models in drug development. In contrast to rodents, very little is known about OCT1 and OCT2 in dog. The aim of this study was to clone dog OCT1 (dOCT1) and OCT2 (dOCT2) and to characterize them comparatively to human and mouse OCT1 (hOCT1, mOCT1) and human OCT2 (hOCT2).

dOCT1 and dOCT2 were cloned and sequenced from dog liver and kidney. The obtained gene structure was verified with available RNA-Seq datasets. The cloned dOCT1 and dOCT2 were stably transfected into HEK293 cells and the uptake kinetics of metformin, trospium, and fenoterol were measured and compared with those of the human and mouse orthologs.

Our analyses revealed an intron-exon structure of dOCT1 different from the published annotation. Sequencing dOCT1 of liver cDNA from Beagle dog demonstrated a previously not identified exon 3. This was confirmed by sequencing of six additional dog breeds. *In silico* analyses suggest a gap in the available dog genome sequence leading to erroneous annotation of exon 3. Metformin transport kinetics of dOCT1 (V_{max} of 10974 pmol/min/mg protein, K_M of 156 μ M) were similar to mOCT1 and not to hOCT1. Also fenoterol transport kinetics of dOCT1 (V_{max} of 1259 pmol/min/mg protein, K_M of 16 μ M) were more similar to mOCT1 than to hOCT1. In contrast, trospium transport kinetics of dOCT1 (V_{max} of 749 pmol/min/mg protein, K_M of 5.7 μ M) were similar to hOCT1 but not to mOCT1. For OCT2, metformin transport kinetics of dOCT2 (V_{max} of 21578 pmol/min/mg protein, K_M of 222 μ M) were lower but close to hOCT2. Trospium transport kinetics of dOCT2 (V_{max} of 224 pmol/min/mg protein, K_M of 2.2 μ M) were higher than those of hOCT2, whereas for fenoterol, no transport of dOCT2 was detectable.

In conclusion, we report a new gene structure for dOCT1, which will facilitate future analyses of this OCT1 ortholog. The results of this study will also help to better understand OCTs in dog, which is essential for the preclinical use of the dog as a model. In addition, species comparisons, including the here cloned and characterized dog orthologs, may reveal important insights into structure-function relationships and therewith the transport mechanism of OCT1 and OCT2 in general.

P79

Electrocardiological effects of ranolazine and lidocaine on normal and diabetic rat atrium

H. Khazraei¹

¹Shiraz University of Medical Sciences, Pharmacology, Shiraz, Iran

Purpose: Cellular changes occurring in diabetic cardiomyopathy include disturbances of calcium and sodium homeostasis. Voltage-gated sodium channels are responsible for the initiation of cardiac action potentials, and the excitability would create relevance. The effect of ranolazine as a sodium channel blocker on atrium electromechanical parameters is investigated and compared with lidocaine in streptozocin-treated diabetic rats.

Methods: After an 8-week induction of diabetes type I, the effect of cumulative concentrations of ranolazine and lidocaine on the electrophysiology of isolated atrium was studied. Ranolazine's effects were evaluated on cardiac sodium current in normal- and high-glucose medium, with the whole-cell patch-clamp technique.

Results: Ranolazine at therapeutic concentrations had no significant statistical effect on the refractory period in the normal and diabetic isolated hearts. Ranolazine (10 μ M) caused a hyperpolarizing shift of $V_{1/2}$ for steady-state inactivation in normal media, while it significantly elicited a depolarizing shift in high-glucose media ($p < 0.05$).

Conclusion: It is concluded that in the isolated rat atrium preparation, ranolazine and lidocaine have no benefit on diabetic cardiomyopathy. Although refractoriness and contractility were not much different in normal and diabetic atria, there was a definite effect of ranolazine and lidocaine on sodium current in varying concentrations. This may have significance in future therapeutics.

P80

Functions of the voltage-gated calcium channel auxiliary subunit Cav β 3 in the pancreas

H. Salah¹, B. Wardas¹, D. Martus¹, V. Flockertz¹, A. Belkacemi¹

¹Saarland University, Experimentelle und Klinische Pharmakologie und Toxikologie, Homburg, Germany

Voltage-gated calcium channels (Cav), are multi-subunit protein complexes containing the pore-forming Cav α 1 subunit and the auxiliary subunits Cav β and Cav α 2 δ . Cav β subunits are cytoplasmic proteins and are required for trafficking the pore-forming Cav α 1 subunit to the plasma membrane and to modulate its current kinetics. We have generated a global Cav β 3 knockout (KO)-1 mice. In these mice, Cav β 3 decreased glucose clearance during glucose tolerance tests when compared with Cav β 3 KO. We have now generated a second mouse strain using a completely different targeting strategy, Cav β 3 KO-2. Also, in these mice, glucose clearance during oral or intraperitoneal glucose tolerance tests is more efficient. After challenging these Cav β 3 KO-2 mice with high amounts of glucose by intraperitoneal injection, insulin concentrations in the blood were significantly enhanced compared to wild-type (WT) controls, whereas the sensitivity to insulin was not affected in the insulin tolerance test. Similarly, after stimulating *in vitro* the pancreatic islets isolated from these mice with high concentrations of glucose, insulin secretion was significantly increased compared with the WT control islets. To be sure that the changes in glucose clearance and insulin secretion are not caused by morphological changes within the pancreatic islets, we determined islets' densities, islets' areas, and islets' cellular composition that shows no variance. In parallel, we developed protocols to elicit calcium oscillations induced by extracellular glucose stimulation in primary islets isolated from wild-type and Cav β 3 KO-2 mice. In calcium imaging experiments the presence of the Cav β 3 subunit declined the frequency of intracellular calcium oscillations. In both Cav β 3 knockout mouse lines, Cav β 3 gene was deleted in the whole mouse. To exclude the possibility that the absence of Cav β 3 in cells other than pancreatic β -cells plays a role in the observed phenotype, we generated now a pancreatic β -cell specific Cav β 3 KO mouse line and we are investigating the functions of Cav β 3 specifically in the pancreatic β -cells.

P81

Phosphorylation by protein kinase CK2 inhibits TRPM3 ion channels in pancreatic beta cells

A. Becker¹, R. Scheuer², C. Götz², S. E. Philipp¹

¹Saarland University, Experimental and Clinical Pharmacology and Toxicology / Center for Molecular Signaling, Homburg, Germany

²Saarland University, Medical Biochemistry and Molecular Biology / Center for Molecular Signaling (PZMS) Saarland University, Homburg, Germany

TRPM3 proteins build ionotropic steroid receptor channels in pancreatic β -cells and increase the intracellular Ca^{2+} concentration and the insulin release after stimulation with pregnenolone sulfate and CIM0216 [1, 2]. We recently showed, that TRPM3-deficient mice display impaired blood sugar regulation after intraperitoneal and oral administration of glucose [3]. Accordingly, TRPM3-deficient pancreatic β -cells of the line INS-1 cells lacked the pregnenolone sulfate-induced Ca^{2+} signals just like the pregnenolone sulfate-induced insulin release. Both, the glucose-induced Ca^{2+} signals and insulin release were strongly reduced [3].

INS-1 cells display increased glucose-induced Ca^{2+} signals and insulin release in the presence of the protein kinase CK2 inhibitor silmitasertib [4], which has been proposed as a putative target for the therapy of diabetes [5]. Since TRPM3 proteins contain a number of predicted CK2 phosphorylation sites, we hypothesized whether CK2 phosphorylation may control the activity of TRPM3 channels.

Here, we show that TRPM3 α 2 is phosphorylated *in vitro* by CK2. Recombinant TRPM3 α 2 channels overexpressed in HEK293 cells displayed enhanced Ca^{2+} entry in the presence of silmitasertib and their activity was strongly reduced after overexpression of CK2. Accordingly, the pregnenolone sulfate / CIM0216-induced Ca^{2+} entry in INS-1 cells was strongly increased in the presence of silmitasertib and reduced after introduction of recombinant CK2. We tested all 32 putative CK2 phosphorylation sites within TRPM3 by *in vitro* phosphorylation of 15-mer peptides containing the CK2 recognition sequence S/T XX D/E or A XX D/E as control and found one single peptide to be selectively phosphorylated by CK2. Accordingly, a TRPM3 α 2 mutant containing the corresponding Serin to Alanin mutation displayed enhanced Ca^{2+} entry.

Our data show that CK2 phosphorylation of a single serine residue within TRPM3 significantly reduces the TRPM3 channel activity and might therefore contribute to TRPM3-mediated control of insulin release.

1. Wagner, T.F., et al. (2008) Nat Cell Biol, 10(12): 1421. 2. Held, K., et al. (2015) Proc Natl Acad Sci U S A, 112(11): E1363. 3. Becker, A., et al., (2020) 54(6): 1115. 4. Scheuer, R., et al. (2020) Int J Mol Sci., 21(13): 4668. 5. Ampofo, E., et al. (2019) Int J Mol Sci., 20(18) : 4398.

P82

Top-down and bottom-up approaches revealed new categories of peptides from the venom of Moroccan scorpion *Androctonus mauretanicus*

K. DAOUDI^{1,2}, J. Chamot Rooke³, R. CADI⁴, N. Oukkache⁵

¹Pasteur Institute of Morocco, Department of Research, Casablanca, Morocco

²Hassan II University of Casablanca, Department of Biology, Casablanca, Morocco

³Institut Pasteur, Biology, Paris, France

⁴Hassan II University of Casablanca, Biology, Casablanca, Morocco

⁵Pasteur Institute of Morocco, Casablanca, Morocco

Background: *Androctonus mauretanicus* (*A.mauretanicus*) is one of the most hazardous scorpions in Morocco and has a highly toxic venom responsible for severe cases of envenomation. However, few studies have focused on deciphering its proteic composition.

Objectives: Herein, we aim to map out the complete proteome of the *A.mauretanicus* venom in order to highlight its complexity and the polymorphism of its toxic content. This, in turn, will lead to a deeper understanding of the toxins' mechanism of action and will help uncover those with therapeutic potential.

Methods: Top-down and bottom-up proteomic approaches were used complementarily to decipher the proteome of the *A.mauretanicus* venom. These approaches were carried out on nano-high liquid chromatography coupled to nano-electrospray tandem mass spectrometry (Nano-LC-ESI-MS/MS).

Results: *A.mauretanicus* venom encloses a complex mixture of 269 different compounds with molecular weights ranging from 1618.74 to 14 214.84 Da. The most abundant ones showed masses from 6185.92 to 7899.53 Da (53.89%) followed by those ranging from 2079.25 to 5969.63 Da (37.81%). Interestingly, the combination of the results of both approaches allowed the screening of a total of 112 peptides (of which 14 were identified by both approaches). The highest percentage was represented by neuropeptides (87%), including NaScTx, KScTx, ClScTx, venom proteins, venom neuropeptides, and myotropic neuropeptides. Moreover, other peptides were identified, such as antimicrobial peptides, amphipathic peptides, cysteine-rich venom peptides, enzymes, kunitz-type inhibitor and orphan peptides.

Conclusion: This study revealed the molecular diversity of the *A.mauretanicus* scorpion venom and identified its components that could be interesting biomolecules with various pharmacological activities.

Pharmacology – Drug transport/delivery and metabolism

P83

Aerosol from a heated tobacco product causes lower induction of hepatic drug metabolism and reduced drug interaction compared with cigarette smoke

D. Bovard¹, K. Renggli¹, D. Marescotti¹, S. Majeed¹, C. Pak¹, A. Iskandar¹, K. Luettich¹, S. Frentzel¹, J. Hoeng¹, M. Peitsch¹

¹Philip Morris International, Neuchâtel, Switzerland

The main mechanism behind drug interactions with cigarette smoke (CS) involves activation of hepatic cytochrome P450 (CYP) isoenzymes by the polycyclic aromatic hydrocarbons present in CS. Activation of these enzymes can alter the metabolism of other drugs, potentially affecting their pharmacologic response.

This study aimed to evaluate the impact of exposure to aerosol generated from Tobacco Heating System 2.2 (THS 2.2; Philip Morris International) on human liver xenobiotic metabolism and subsequent drug metabolism, compared with the impact of exposure to CS. We exposed liver spheroids composed of HepaRG cells to various concentrations of culture medium bubbled through with THS 2.2 or CS aqueous fractions (AF). After exposure for 48 or 96 h, the viability and xenobiotic metabolism of the tissues were analyzed. At 0.8 puffs/mL and just after 48 h of exposure, hepatotoxicity was observed with the CS AF but not with THS 2.2. The activity of 8 CYP enzymes was then measured by liquid chromatography–mass spectrometry (LC–MS) in liver spheroids exposed for 96 h to subtoxic doses of THS 2.2 and CS AF. Notably, exposure to the CS fraction caused a dose-dependent increase in the activity of CYP1A1/1B1, CYP1A2, CYP2A6, and CYP2B6 enzymes; but, it inhibited CYP3A4 activity. At a comparable concentration, exposure to the THS 2.2 aerosol fraction resulted in smaller changes in CYP activity relative to those observed with CS. Liver spheroids exposed to THS 2.2 or CS AF were then coincubated for 48 h with a subtoxic dose of clozapine, an antipsychotic drug. The levels of 7 clozapine metabolites were then measured by LC–MS. CS AF exposure was characterized by a reduction in the levels of 6 clozapine metabolites relative to the untreated condition or to THS 2.2 AF exposure (at a similar concentration as the CS aqueous fraction). Similar effects of the THS 2.2 AF on clozapine metabolism were observable at doses 32 times lower than CS.

In conclusion, CS AF exposure of human liver spheroids resulted in increased hepatotoxicity, increased CYP activity, and altered clozapine metabolism relative to the untreated condition. This latest observation is line with the clozapine pharmacodynamics changes observed in smokers. In contrast, THS 2.2 AF exposure resulted in reduced hepatotoxicity and smaller changes in liver xenobiotic metabolism and clozapine metabolism relative to exposure to similar concentrations of the CS AF.

P84

Examination of the cytotoxic effects of magnetic nanoporous silica nanoparticles on different primary murine cells

R. Storzjohann¹, V. Filor¹, B. Gericke¹, H. Oltmanns¹, T. Herrmann², P. Behrens², M. Kietzmann¹, J. Meißner¹

¹University of Veterinary Medicine Hannover, Department of Pharmacology, Toxicology and Pharmacy, Hannover, Germany

²Leibniz University Hannover, Institute of Inorganic Chemistry, Hannover, Germany

Question: Magnetic nanoporous silica nanoparticles (NP) based on the model described by JAN&EN et al. (Journal of Nanobiotechnology 16, 96, 2018) were functionalized for targeted therapy of implant-associated infections. To study cytotoxic effects proliferation and viability of primary murine macrophages were examined in relation to the NP concentration as well as their phagocytic activity.

Methods: Male BALB/c mice between 8 – 12 weeks were used for the experiments. Macrophages and dendritic cells were differentiated from bone marrow cells over 10 days. Progenitor cells were treated on day 3 with different amounts of NP (15 µg/ml, 50 µg/ml and 150 µg/ml). For comparison an untreated, a stimulated and an attenuated control were included. Adherent macrophages were stained with crystal violet assay at different time points (day 6, 8 and 10) and the cell viability were measured with CellTiter 96® MTS on day 10. Full differentiated macrophages were similarly treated on day 10 and proliferation assay was performed after 24 h. It is intended to examine the amounts of TNF-α. For fluorescence microscopy investigation of phagocytic activity macrophages were incubated with a fluorescent NP (500 µg/ml) for different intervals (10, 20, 60 and 90 min). Furthermore, primary murine osteoblasts were generated and used to study their viability and synthesis of hydroxyapatite.

Results: NP induced a slight increase of proliferation especially after treating with 150 µg/ml. Cell viability was not influenced by the NP, although phagocytosis could be observed within 10 min after contact of macrophages with NP. Osteoblasts showed similar results.

Conclusion: The magnetic NP show good biocompatibility behavior concerning viability and proliferation, although macrophages tend to phagocyte the NP. Thus, further experiments are required to get more information about the impact of NP on different cell activities.

P85

Polyethylenimine (PEI)-based polyplexes and lipopolyplexes for inhalative application of siRNA therapeutics, analyzed in 2D- and air-liquid interface culture

S. Noske¹, A. Ewe¹, A. Aigner¹

¹Rudolf Boehm Institute of Pharmacology and Toxicology, Leipzig, Germany

Question: RNA interference (RNAi) is a highly conserved tool for gene regulation in eukaryotic organisms. It is based on the action of small interfering RNAs (siRNAs) on a target mRNA, which is cleaved and thus degraded. The downregulation of specific gene products offers new perspectives in the treatment of diseases like cancer, viral infections or genetic disorders. Due to its large surface and high vascularization, the lung is an attractive target organ for local and/or systemic application of siRNAs. A major bottleneck, however, is the delivery of active siRNA molecules to their target site. Hence, considerable research efforts have focused on the development and refinement of carriers, for overcoming extracellular and intracellular barriers. Polymeric nanoparticles based on polyethylenimine (PEI), and their corresponding liposomal derivatives (lipopolyplexes), providing a promising systems for gene targeting in the lung.

Methods: PEI/siRNA complexes ("polyplexes") were prepared according to optimized protocols, and also combined with liposomes for the generation of lipopolyplexes. Particle characteristics (size and ζ-potential) of the different PEI-based nanocarriers were determined. By measuring gene knockdown, transfection efficacies were evaluated in lung cancer cell lines in 2D-cell culture and in an air-liquid interface culture system.

Results: A partial loss of siRNA was found during nebulization of polyplexes, which could be largely avoided by using low adhesion tubes. Biological activities of nebulized (lipo)polyplexes were comparable to their non-nebulized counterparts. The ionic strength of the buffer used for complexation was decisive for particle size, and the positive ζ-potential of polyplexes was shielded upon lipopolyplex formation. Transfection efficacy was also observed in the air-liquid interface culture, as determined by fluorescent siRNA uptake and by reporter gene knockdown.

Conclusion: In 2D culture, we have identified polyplexes and lipopolyplexes with high transfection efficacies and sufficient biocompatibility, even after nebulization. First results also indicate their biological activity in 3D models like the complex air-liquid interface system, but this may be affected by their stability towards mucus and their penetration properties. Taken together, this provides the basis for their prospective exploration as pharmacological carriers, aiming at the pulmonary application of siRNA for therapeutic use.

P86

Sex-dependent alterations in neurobehavioral development of offspring of depressive dams treated with antidepressant mirtazapine during pregnancy and lactation

M. Viñas-Noguera¹, K. Belovičová¹, K. Csatossová¹, M. Dubovický¹

¹Institute of Experimental Pharmacology and Toxicology, Experimental Medicine, Bratislava, Slovakia

Depression is a life-threatening form of mental illness which affects up to 20% of women during pregnancy and breastfeeding. The administration of antidepressants in this critical period represents a serious health concern for both the mother and the child. In addition, even treatment is required, the consequences of maternal antidepressant treatment on the developing organism are not well known. New generation antidepressants, such mirtazapine, that targets both the serotonergic and noradrenergic systems in the CNS, represent a new focus of research. However, little is known about the safety of these drugs for the developing organism, neither the long-term consequences.

The aim of the present study was to assess the effects of maternal depression and/or treatment with antidepressant mirtazapine during pregnancy and lactation on the behavioral development of affected offspring.

Female Wistar rats were submitted to a 3-week chronic unpredictable stress (CUS) procedure and then were mated. Dams were treated with either mirtazapine, administered orally from day 10 of gestation until day 21 post-partum at a dose of 10mg/kg/day or vehicle. After weaning, offspring were submitted to behavioral tests: Elevated plus maze (EPM) and Y-maze. The Shapiro-Wilks method was used to check the distribution of data. Behavioral data with normal distribution were analyzed by means of factorial ANOVA and Kruskal Wallis test was used for variables without a normal distribution.

There was present main effect of sex in all parameters of EPM and Y-maze with females being more active than males. In males, we observed main effect of stress ($F(1, 30) = 4.53$; $p < 0.05$) in the percentage of time spent in the closed arm and trend of stress × mirtazapine interaction ($F(1, 30) = 3.37$; $p = 0.07$). In females, we observed marginally significant effect of mirtazapine ($F(1, 32) = 3.70$; $p = 0.06$) and trend in effect of stress ($F(1, 32) = 3.06$; $p = 0.08$) on the percentage of time spent in the open arm. In Y-maze, there was a main effect of treatment ($p < 0.01$) in total distance travelled with treated animals being less active in males. In females, there was a main effect of stress ($p < 0.05$) in total distance travelled with increase of motor activity in stress × mirtazapine group ($p = 0.07$).

The results of our study show that pre-gestational CUS and/or antidepressant treatment with mirtazapine has long-term effects in the neurobehavioral development of the offspring which may be sex dependent.

P87

An efficient nanoscale delivery system for therapeutic nucleic acids, based on the combination of disulfide crosslinking and tyrosine-modification of polyethylenimine (PEI)

M. Karimov¹, D. Appelhans², A. Ewe¹, A. Aigner¹

¹Universität Leipzig, Medizinische Fakultät, Rudolf Boehm Institute of Pharmacology and Toxicology, Leipzig, Germany

²Leibniz Institute for Polymer Research, Macromolecular Chemistry, Dresden, Germany

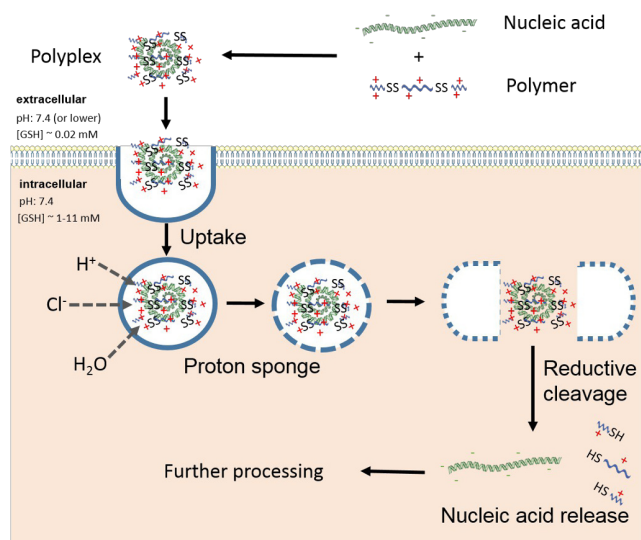
Background: Nucleic acid therapies is a field of major relevance and growing interest, since it offers potent tools in the therapy of cancer, genetic disorders or infections (including e.g. new mRNA COVID-19 vaccines). However, the efficient and non-toxic delivery of nucleic acids is still a major limiting factor. Among the large diversity of non-viral vectors, the cationic polymer polyethylenimine (PEI) plays a prominent role, often considered as a "gold standard". However, the transfection efficacy and biocompatibility of PEIs is strongly dependent on the molecular weight. Higher molecular weight of PEI is beneficial for transfection efficacy, but also leads to higher cytotoxicity.

Methods: In this study, we explored for the first time the combination of two very promising strategies for improving DNA delivery: the bioreversible cross-linking of polymers (a low molecular weight PEI, "P2") through biodegradable disulfide groups ("SS"), in combination with its L-tyrosine-modification ("Y").

Results: *In vitro* transfection experiments demonstrated a strongly synergistic effect of disulfide-crosslinking and tyrosine grafting, as indicated by a marked increase in transfection efficacy. Compared to the 2 kDa PEI as well as its tyrosine-modified or disulfide-crosslinked counterparts, which show very poor transfection properties, the combination of both modifications led to a substantial enhancement of transfection efficacy. This was true for different plasmids and different cell lines, including hard-to-transfect cells. Beyond various cell lines, high biological activity of the SSP2Y-based nanoparticles was also seen in an *ex vivo* tissue slice culture model, more closely mimicking *in vivo* conditions. For this purpose, tumor xenograft tissue slices were transfected with SSP2Y/pEGFP complexes. Subsequent analyses revealed efficient transfection and high EGFP expression in a fraction of the cells, particularly those at the surface of the native tissue slices. However, cryo-sections revealed EGFP expression, with decreasing extent, also in the cell layers below, thus indicating SSP2Y/pEGFP complex penetration.

Conclusions: Taken together, in this study we demonstrate a surprisingly substantial, synergistic enhancement of transfection efficacies of SSP2Y/DNA nanoparticles over their non- or mono-modified polymer counterparts, accompanied by high biocompatibility as well as favorable physicochemical and biological properties.

Fig. 1



Pharmacology – Disease models, drug development

P88

Do highly soluble ibuprofen (400 mg) formulations provide faster headache relief than standard ibuprofen (acid) tablets? Data from head-to-head randomized clinical trials

A. Lampert¹, M. Plomer², T. Weiser¹

¹Sanofi Aventis Deutschland GmbH, Medical Affairs, Frankfurt am Main, Germany

²Sanofi Aventis Deutschland GmbH, Medical Affairs, Frankfurt am Main, Germany

Introduction: Highly soluble (hs) ibuprofen (formulated as e. g. lysine or sodium salts, or soft gel capsule), has been developed with the intention to provide faster pain relief than

standard ibuprofen acid tablets. We analyzed published randomized, double-blind head-to-head comparisons of hs-ibuprofen and ibuprofen acid in headache pain.

Methods: Pubmed and clinicaltrials.gov were searched, and information on the onset of pain relief was extracted from identified studies.

Results: Two studies were identified, which investigated 400 mg hs-ibuprofen (sodium salt) with 400 mg ibuprofen acid for the treatment of acute tension type headache attacks (1, 2). No other head-to-head studies were found (e. g. no studies on ibuprofen lysine vs. ibuprofen acid). In both studies "time to meaningful pain relief" (TTMPR) was a primary/co-primary endpoint. Both studies could not show statistically significant differences in TTMPR for hs- versus standard ibuprofen (Figure 1). In contrast, a study combining 400 mg ibuprofen acid with 200 mg caffeine showed statistically significant and clinically relevant earlier onset of pain relief (3).

Conclusion: Clinical data could not demonstrate shorter TTMPR for hs- vs ibuprofen acid. In contrast, a fixed dose combination of 400 mg ibuprofen acid with caffeine showed statistically shorter TTMPR.

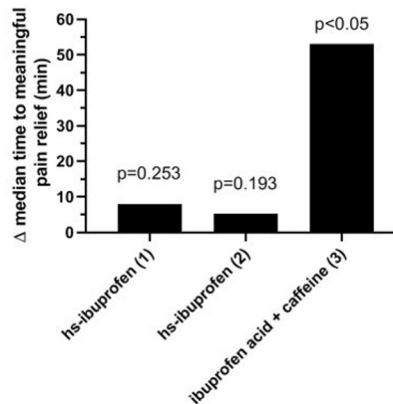
References:

- 1: Packman et al. (2015) Journal of Pharmaceutical Health Care and Sciences 1:13
- 2: NCT01077973 (2012) <https://www.clinicaltrials.gov/ct2/show/NCT01077973>
- 3: Diamond et al. (2000) Clin Pharmacol and Therapeutics 68:3, 312-319

Funding: This study was funded by Sanofi-Aventis Deutschland GmbH.

Fig. 1

Figure 1



Difference in median time to meaningful pain relief (TTMPR) for highly soluble (hs) ibuprofen 400 mg (1, 2), and ibuprofen acid + caffeine (400 + 200 mg; 3), compared to ibuprofen acid 400 mg. Hs-ibuprofen did not relieve pain significantly faster than standard ibuprofen. Caffeine as co-analgesic significantly shortened time to meaningful pain relief.

Study 1: Hs-ibuprofen 91 patients, TTMPR 40.6 min; ibuprofen acid 89 patients, TTMPR 48.5 min, p=0.253

Study 2: Hs-ibuprofen 79 patients, TTMPR 50.3 min; ibuprofen acid 80 patients, TTMPR 55.5 min, p=0.193

Study 3: Ibuprofen + caffeine, 97 patients, TTMPR 108 min; ibuprofen acid 99 patients, TTMPR 161 min, p<0.05

P89

Do highly soluble ibuprofen (400 mg) formulations provide faster pain relief after third molar extraction than standard ibuprofen (acid)? Data from head-to-head randomized clinical trials

T. Weiser¹, M. Plomer², A. Lampert¹

¹Sanofi Aventis Deutschland GmbH, Medical Affairs, Frankfurt am Main, Germany

²Sanofi Aventis Deutschland GmbH, Medical Affairs, Frankfurt am Main, Germany

Introduction: Highly soluble (hs) ibuprofen (formulated as e. g. lysine or sodium salts, or soft gel capsules), has been developed with the intention to provide faster pain relief than standard ibuprofen acid tablets. We analyzed published randomized, double-blind head-to-head comparisons of hs-ibuprofen and ibuprofen acid in the third molar extraction pain model.

Methods: Pubmed and clinicaltrials.gov were searched, and information on the onset of pain relief were extracted from identified studies.

Results: Seven studies (in 6 publications) were identified (1,2,3,4,5,6). Three (4, 5, 6) were excluded, since they investigated ibuprofen arginate, and arginine affects the NO-system and is therefore analgesic on its own (7, 8). Quantitative measures of onset of pain relief were only given in (3); in the other studies pain-score over time figures were used to compare onset of action. Hs-ibuprofen showed 0-7.8 min earlier pain relief (1, 2), compared to ibuprofen acid, no statistical significance was reported. Study (3) failed to show faster onset of action of ibuprofen lysinate compared to ibuprofen acid (Figure 1).

Conclusion: Clinical data could not demonstrate statistically significant faster pain relief for hs- vs standard ibuprofen acid formulations. In contrast, a fixed dose combination of 400 mg ibuprofen acid with caffeine showed statistically significant shorter time to meaningful pain relief (9).

References

(1) Seymour et al. (1991) Br J Clin Pharmacol. 31, 83ff; (2) Seymour et al. (1996) Br J Oral and Maxillofacial Surgery 34, 110ff; (3) Kyselovic et al. (2020) Pain Ther 9(1), 249ff; (4) Black et al. (2002) Clin Therapeutics 24, 1072ff; (5) Desjardin et al. (2002) Eur J Clin Pharmacol 58, 387ff; (6) Mehlisch et al. (2002) J Clinical Pharmacol 42, 904ff; (7) Sprout et al. (2006) J Rheumatol 33, 2515ff; (8) Gomes et al. (2020) Biochem Pharmacol 176, 113862; (9) Weiser et al. (2018) Eur J Pain 22, 28ff

Funding: This study was funded by Sanofi-Aventis Deutschland GmbH.

Fig. 1

Figure 1

Summary of clinical data for onset of analgesic effects of hs-ibuprofen (400 mg) compared to standard formulations of ibuprofen acid.

Study	Hs-ibu-formulation	Hs-ibu patients (n)	Standard ibuprofen acid patients (n)	Delta pain reduction (min)	P value	Comment
1a	Soft gelatine capsule	32	31	~0 min	?	No statistical analysis possible
1b	Soluble	32	30	~4 min	?	No statistical analysis possible
2	Soluble	16	15	~8 min	?	No statistical analysis possible
3	Lysinate	141	139	~5 min	0.863	Median time to meaningful pain relief
9						
	Ibu acid + 100 mg caffeine	213	209	39 min	0.0001	Median time to meaningful pain relief

P90

The influence of gestation on adiponectin levels in a polygenic mouse model with impaired glucose tolerance and dyslipidemia

M. Liebmann¹, K. Grupe¹, S. Scherneck¹

¹Technische Universität Braunschweig, Institute of Pharmacology, Toxicology and Clinical Pharmacy, Braunschweig, Germany

Question: Gestational diabetes mellitus (GDM) is the most common disorder in pregnancy and has severe consequences. There is evidence that the adipokine adiponectin (AdipoQ) could be a marker for GDM and low plasma levels reflect glucose intolerance (GIT) and hyperlipidemia. However, available data are limited and suitable models are needed for better prediction of disease progression. New Zealand obese (NZO)-mice are a polygenic model for impaired glucose tolerance and insulin resistance (IR) before conception, with the latter improving during pregnancy. Moreover, pregnant NZO mice show dyslipidemia with hypertriglyceridemia but reduced hepatic triglycerides. The aim of this project was to investigate whether alterations in AdipoQ levels during pregnancy correlate with metabolic changes in this mouse model.

Methods: Female NZO mice and NMRI controls were examined both preconceptionally (pc.) and on day 14 of gestation (d14). Animals were sacrificed at 9-10 weeks of age and plasma and tissue samples were collected. Plasma AdipoQ was measured by ELISA. Further, gonadal white adipose tissue mass was determined and hepatocyte proliferation was examined in both strains histologically (Ki67-positive nuclei). Hepatic glycogen content was determined by PAS staining and by a colorimetric assay.

Results: NZO mice showed significantly lower AdipoQ levels compared to NMRI controls both at pc. and at d14. Further, NZO showed significantly higher fat pad weight compared to control mice, consistent with lower AdipoQ levels. However, in contrast to NMRI, AdipoQ levels in NZO mice decreased significantly at d14 compared to pc. Both strains showed a significant increase in fat mass and liver weight with a corresponding increase

in hepatocyte proliferation at d14. Further, NZO mice exhibited a significantly decreased hepatic glycogen content at d14 compared to the controls, whereas this did not differ between both strains pc.

Conclusion: As expected, AdipoQ values correlated inversely with increasing fat mass and plasma triglycerides. In general, values were decreased at GIT. However, improvement of IR and the unchanged degree of GIT of the NZO model could not be reflected in AdipoQ levels. A correlation was found with low glycogen levels in the liver during gestation. Thus, determination of AdipoQ is more suitable for monitoring dyslipidemia than impaired glucose tolerance in GDM.

P91

Aldosterone-induced phosphorylation of Nrf2 and its subsequent translocation into the nucleus does not lead to upregulation of Nrf2 target genes in tubuli of mouse kidneys

R. Balhorn¹, N. Schupp¹

¹Institute of Toxicology, Medical Faculty, Heinrich Heine University of Düsseldorf, Düsseldorf, Germany

Question: Hypertensive patients have an increased risk to develop chronic kidney disease. Many of these patients have increased levels of the blood pressure regulating mineralocorticoid aldosterone (Ald), which is known to cause oxidative stress. As a protection against induced oxidative damage, kidney cells are capable to upregulate key regulators of the antioxidant defence, such as nuclear factor erythroid 2-related factor 2 (Nrf2). The aim of the present study is to investigate the aldosterone-induced oxidative damage and Nrf2 activation in kidney cells of mice.

Methods: Male C57BL/6-mice received three different concentrations of Ald combined with 1% NaCl in the drinking water. After 4 weeks the kidneys were isolated for further analysis.

Results: The kidney function of the Ald-infused mice was impaired, as detected by elevated levels of albumin and neutrophil gelatinase-associated lipocalin (NGAL) in urine. Increased systemic oxidative damage in the form of urinary 8-OHdG and 15-isoprostane F2t excretion was measured in the low and middle dose group. Additionally, a higher number of 8-oxodG-positive cells was observed in the low and high dose group on kidney sections. Phosphorylated Nrf2 was significantly increased in the kidney cortex after Ald-infusion. Furthermore, a higher amount of phosphorylated Nrf2 was observed in nuclear kidney protein fractions analyzed via western blot. These facts are usually an indication of Nrf2 activation. However, the observed phosphorylation and translocation did not result in an increased expression of Nrf2 target genes and proteins. On the contrary, a down-regulation of Nrf2-regulated genes was detected on mRNA and protein level in extracts of the whole kidney.

Conclusion: Ald-infusion increased oxidative stress which resulted in Nrf2 phosphorylation and its translocation into the nucleus. The observed down-regulation of Nrf2 targets suggests that the eventually activated Nrf2 somehow did not stimulate the expression of antioxidative proteins as a defense against the oxidative damage.

P92

Effects of serotonin on insulin secretion in a pregnant prediabetic mouse model

M. Asuaje Pfeifer¹, T. Beuerle², K. Grupe¹, S. Scherneck¹

¹Technische Universität Braunschweig, Institute of Pharmacology, Toxicology and Clinical Pharmacy, Braunschweig, Germany

²Technische Universität Braunschweig, Institute of Pharmaceutical Biology, Braunschweig, Germany

Question: Recent studies have revealed a link between serotonin (5-hydroxytryptamine, 5-HT) and the pathophysiology of gestational diabetes mellitus (GDM). In pancreatic islets, 5-HT was found to enhance insulin secretion in most of the studies. However, its specific role in islet function, in particular of pregnant prediabetic mice, needs to be further investigated. For this purpose, female New Zealand obese (NZO) mice, which show an impaired glucose tolerance but no signs of manifest diabetes, are an appropriate model. Interestingly, in vivo but not ex vivo stimulation by glucose shows an improvement of insulin secretion during pregnancy in NZO mice. The aim of this study was to investigate the role of 5-HT as a modulator of insulin secretion during gestation in the NZO model.

Methods: Female NZO mice were examined preconceptionally (pc.) and on day 14 (d14) of gestation. NMRI mice were used as a healthy control. Islet 5-HT was determined immunohistochemically using pancreatic slices and pancreatic 5-HT content was measured after extraction by ELISA and HPLC-ESI-MS/MS. Furthermore, primary islets of pc. mice were isolated by collagenase digestion technique and insulin secretion was measured by ELISA after ex vivo static incubation with glucose (20 mM) and 5-HT (10, 100, 1000 nM).

Results: On d14 histological determination of islet 5-HT showed a trend towards a stronger staining intensity in NZO mice compared to control mice. This was confirmed by ELISA and HPLC-ESI-MS/MS measurement of pancreatic 5-HT content. As expected, both methods indicated an increase in pancreatic 5-HT content in both strains during gestation. This was significantly more pronounced in the NZO mouse. Incubation of isolated islets with 5-HT led to no effect on secretion at low concentrations, but a significant inhibiting effect at 1000 nM 5-HT was observed in the NZO model, which could not be shown in the NMRI control.

Conclusion: Although glucose-stimulated insulin secretion improves during pregnancy in NZO mice *in vivo*, 5-HT with its inhibitory effect does not appear to represent the underlying mediator. The increased 5-HT content in pancreatic islets of pregnant prediabetic NZO mice could lead to an autocrine/paracrine signal on beta cells by decreasing glucose-stimulated insulin secretion in the islets of this mouse model at higher hormone concentrations.

P93

Development of a dexamethasone-induced osteoporosis 2D *in vitro* model

R. Breinbauer¹, W. Weng¹, F. Zanetti², D. Bovard², S. Ehnert¹, J. Hoeng², A. K. Nüssler¹, R. H. Aspera-Werz¹

¹Siegfried Weller Institute, Tübingen, Germany

²PMI R&D, Philip Morris Products S.A, Neuchâtel, Switzerland

Question: Exposure to high doses or over long periods of time to glucocorticoids are associated with osteoporosis due to detrimental effects on bone forming cells. A cell culture model to study treatment strategies and to understand the molecular mechanisms involved in osteoporosis is necessary. Thus, we established an *in vitro* dexamethasone-induced human osteoporosis model to represent the clinical condition.

Methods: Monocyte human cell line (THP-1, for osteoclasts) and immortalized human mesenchymal stem cell line (SCP-1, for osteoblasts) were used. THP-1:SCP-1 cells - ratio 8:1 - were cultured for 14 days in presence of a dose-range of dexamethasone [0.1 – 100 µM]. After 3, 7, and 14 days of cultivation, the mitochondrial activity (Resazurin conversion), tartrate-resistant acid phosphatase (TRAP) activity (osteoclast function), total DNA and total protein content (sulforhodamine B [SRB] staining) were evaluated. Dot Blot for matrix remodeling with NTX (collagen degradation marker) was performed. In addition, matrix formation (Alizarin red staining) was analyzed on day 14.

Results: At day 14, the mitochondrial activity was significantly increased by treatments with dexamethasone ranging from 1 to 50 µM. Total protein and DNA quantification confirmed these results and demonstrated cell proliferation with dexamethasone treatment. Analysis of bone cell function indicated an increase in matrix formation and no effect on osteoclast function at 0.1 µM dexamethasone (a concentration usually used to induce osteogenic differentiation).

Interestingly, significantly decreased matrix formation was demonstrated with 5 µM dexamethasone on day 14. Simultaneously, TRAP activity was significantly increased by treatments with 1 to 5 µM dexamethasone compared to untreated cultures. This result was confirmed with increased NTX levels in cultures exposed to 1 to 50 µM dexamethasone at all-time points.

Conclusion: Our results suggest a bimodal role of dexamethasone, where lower concentrations (≤ 0.5 µM) induced bone formation and higher concentrations (> 0.5 µM) promoted bone resorption in the THP-1:SCP-1 co-culture model. This model could serve as an experimental model to study the mechanisms related to osteoporosis and to design new treatment strategies.

P94

Gelatin-hydroxyapatite-based cryogels as a platform technology for a direct 3D bone coculture system

W. Weng¹, B. Braun¹, S. Ehnert¹, F. Zanetti², D. Bovard², A. K. Nüssler¹, J. Hoeng², R. H. Aspera-Werz¹

¹Siegfried Weller Institute, Tübingen, Germany

²PMI R&D, Philip Morris Products S.A, Neuchâtel, Switzerland

3D cultures improve bone cell attachment, proliferation, and differentiation, as the cells are in physiological and morphological conditions similar to *in vivo* conditions. Scaffolds are a promising carrier for 3D *in vitro* cell culture; they resemble bone tissue and enhance cell function. The "ideal" scaffold should support cell attachment and migration and flow of nutrients/waste to ensure cell proliferation and differentiation. Our aim was to establish a biocompatible gelatin-hydroxyapatite (GE-HA)-based cryogel that mimics the 3D bone microenvironment.

The scaffold was produced by polymerization of 4.8% gelatin, 10% hydroxyapatite, and 1% glutaraldehyde. Physical characterization was performed by measuring porosity, swelling ratio, permeability, computer tomography (CT) and stiffness. Immortalized human SCP-1 and THP-1 cells were selected to differentiate into osteoblasts and osteoclasts, and seeded in a ratio 1:8. Then, 3D bone coculture and monoculture viability was evaluated by resazurin conversion, total DNA quantification, and calcein AM staining. Differentiation was assessed by analyzing enzymatic activity and gene (RT-PCR) and protein (dot plot) expression of bone markers.

The GE-HA scaffolds had a pore size area of 12000 ± 624.9 µm² and stiffness of 25.02 ± 1.34 kPa. Their mean porosity was 85%, and the scaffolds could take up water 6.134 times their dry mass weight. Their mean permeability was 357.6 µm². CT analysis revealed that the basal mineral content in the scaffolds was 124.4 ± 2.6 mg/cm³. SCP-1/THP-1 cells in suspension had a circular mean area of 253.1 ± 8.9 µm² and 182 ± 6.4 µm² respectively, suggesting that the cells are able to migrate inside the scaffold. The bone cell mono- and cocultures showed increased metabolic activity and total DNA content over 14 days, thus demonstrating cell proliferation on the scaffold. After 14 days of monoculture, SCP-1 cells showed a significantly increased mineral content of 132.4 ± 8.2 mg/cm³. However, scaffolds cultured with only THP-1 cells showed a mineral content

of 127.2 ± 7.2 mg/cm³. We found that bone marker genes and proteins were expressed for 14 days.

We have successfully developed a GE-HA scaffold with a highly interconnected structure and reasonable stiffness, which is a suitable 3D platform for bone coculture *in vitro*. Viability and functionality tests demonstrated that bone cells could attach and proliferate on the GE-HA scaffold and revealed the presence of bone markers.

P95

Assessment of the effects of acute and continuous exposure to tobacco heating system 2.4 and cigarette smoke total particulate matter on a direct 2D osteoblast/osteoclast coculture model

R. H. Aspera-Werz¹, W. Weng¹, B. Braun¹, T. Uynuk-Ool¹, F. Zanetti², D. Bovard², J. Hoeng², A. K. Nüssler¹

¹Siegfried Weller Institute, Tübingen, Germany

²PMI R&D, Philip Morris Products S.A, Neuchâtel, Switzerland

Heated tobacco products are potential reduced-risk alternatives to cigarette smoke (CS). The effects of these products on bone cells are, however, not well known. We aim to develop a 2D bone coculture *in vitro* system suitable for investigating the osteoporotic mechanisms of CS and evaluating the impact of reduced-risk products and responsiveness of the system to anti-osteoporotic drugs.

Coculture was generated by using SCP-1 cells (a human immortalized stem cell line) as an osteoblast model and THP-1 cells as osteoclast precursors in a ratio 1:8. A

decellularized (*via* heat treatment at 47°C) Saos-2 cell matrix was used as platform for the

coculture. The effects of total particulate matter extracts from reference cigarette smoke (1R6F) or Tobacco Heating System (THS) 2.4 (Philip Morris Products S.A.) aerosol on bone cell viability and function were tested. After an acute 24-h exposure to various concentrations of 1R6F or THS (corresponding to 10, 2 or 0.4 µg/mL nicotine for both test items). To confirm the appropriate response of the coculture to anti-osteoporotic drugs, the system was treated continuously with 1R6F (2, 0.4 or 0.08 µg/mL nicotine) in combination with zoledronate/alendronate (50 µM) for 14 days. At 3, 7, and 14 days of culture, viability (mitochondrial activity [resazurin conversion], adenosine triphosphate, and lactate dehydrogenase [LDH] content), functionality and morphology were assessed.

Cocultures exposed to 10 µg/mL 1R6F showed a dose-dependent significant decrease in ATP content and mitochondrial activity at days 3, 7, and 14 following exposure, relative to cocultures exposed to vehicle controls. LDH release and morphology analysis confirmed these results. 1R6F exposure at 10 µg/mL significantly reduced osteoclast function and the number of osteoclast- and osteoblast-like cells, relative to vehicle control and THS exposure at comparable concentrations. However, CS exposure did not affect osteoblast activity. The anti-osteoporotic drugs reduced the detrimental effects of daily exposure to 0.4 µg/mL 1R6F for 14 days on coculture cell viability and function.

We demonstrated that acute exposure to 10 µg/mL THS had less impact on the viability and functionality of the 2D bone coculture than 1R6F at a comparable nicotine concentration. Furthermore, anti-osteoporotic drug treatment reduced the pro-osteoclastic effects of continuous exposure to 0.4 µg/mL 1R6F, confirming the relevance of our coculture system in relation to *in vivo* exposure.

P96

Manipulation of miRNA-365 to normalize aberrant action potential duration in human cardiac myocytes

D. Esfandyari¹, B. M. G. Idrissou¹, P. Avramopoulos¹, A. Dueck¹, I. El-Batrawy², L. Gräter¹, M. Meier¹, A. Näger¹, D. P. Ramanujam¹, T. Dorn³, T. Meitinger⁴, C. Hagl⁵, M. Borggrefe⁶, A. Dendorfer⁶, Y. Sassi¹, A. Moretti³, S. Engelhardt¹

¹TUM, Institute of Pharmacology and Toxicology, München, Germany

²University Medical Centre Mannheim, Mannheim, Germany

³TUM, Klinikum rechts der Isar, München, Germany

⁴Helmholtz Zentrum München, München, Germany

⁵University Hospital LMU Munich, München, Germany

⁶LMU, Walter-Brendl Zentrum, München, Germany

Abnormalities of ventricular action potential (AP) repolarization cause malignant cardiac arrhythmias and sudden cardiac death. The regulatory role of microRNAs (miRNAs) in modulating the human ventricular AP is largely unknown. Here we sought to identify miRNAs that control cardiac ion channels and asked whether miRNA manipulation would allow for therapeutic modulation of AP duration (APD) abnormalities. Among miRNAs that are abundantly expressed in human myocardium, we identified miR-365 targeting the largest number of repolarizing ion channels. Carrying out double-fluorescent reporter assays, we confirmed a direct interaction between miR-365 and its binding sites within KCNQ1, KCNH2, KCNJ2, CACNA1C, KCNC3, KCNA1, and KCNJ3 mRNAs. An independent gene enrichment analysis on 2917 predicted targets of miR-365, primarily associated this miRNA to long QT syndrome (LQTS).

To resolve the regulatory function of miR-365, we performed optical AP recordings in patient-specific induced pluripotent stem cell-derived cardiac myocytes (hiPSC-CMs) as a human disease model. In hiPSC-CMs derived from a long QT syndrome type 1 (LQT1) patient, the pathologically prolonged APD was restored to normal levels upon inhibition of miR-365 using specific anti-miRs (median 673 and 418 ms in control and anti-miR-365

groups, respectively, $P < 0.01$). In short QT hiPSC-CMs (SQT1), shortened APD was ameliorated by elevation of miR-365 using synthetic mimics (median 290 ms compared to 431 ms upon mimic-365 treatment, $P < 0.001$).

Transcriptome analyses in hiPSC-CMs at bulk and single-cell level corroborated the key cardiac repolarizing channels as direct targets of miR-365 and revealed that this miRNA exerts its regulatory role by significant repression of the potassium ion transport machinery and the repolarization phase of the cardiac AP.

To determine the relevance of miR-365 in a model that incorporates the complexity and function of the adult human heart, we employed human myocardial tissue slices. Refractory period (RP) measurements upon manipulation of miR-365 revealed 31 ± 6 ms prolongation of the RP upon elevation of miR-365 ($P < 0.05$), whereas treatment with anti-miR-365 reduced the RP about 60 ms compared to respective controls.

Overall, our results delineate miR-365 to regulate cardiac APD through post-transcriptional repression of key determinants of cardiac repolarization. Therefore, manipulation of miR-365 may be employed to modulate AP abnormalities in various human QT syndromes.

P97

Development of a new blood-brain barrier model to characterize inflammatory and toxic-related diseases

J. Hoffrichter¹, S. Doss¹, M. Boomgarden², M. Sauer^{1,3}

¹Fraunhofer-Institut für Zelltherapie und Immunologie IZI, Extracorporeal Immunomodulation EXIM, Rostock, Germany

²Friedrich-Schiller-Universität Jena, Jena, Germany

³Hospital Magdeburg, Clinic for Intensive Care and Rescue Medicine, Magdeburg, Germany

Question: Acute Brain Injury is a common complication of liver- and kidney failure, sepsis and other inflammatory diseases. Especially, sepsis-associated encephalopathy (SAE) is a diffuse brain dysfunction that occurs secondary to infection in the body, and is in up to 70% of sepsis patients. Development of SAE probably involves different mechanisms such as neuroinflammation with excessive expression of cytokines, disruption of the blood-brain barrier (BBB), and neuronal degeneration. Cognitive impairments and substantial neurological morbidities often occur in survivors. The aim of this work was to develop an inflammatory BBB-model including a disrupted BBB integrity and functionality due to cytokines.

Methods: Concentrations of some of the most relevant cytokines (IL-6, IL-1 β , TNF α), ranging from physiologic to pathophysiologic, were chosen to induce inflammation in a BBB model, consisting of co-cultured hCMEC/D3 (endothelial) and SH-SY5Y (neuronal). Cytotoxicity analyses (viability, lactate dehydrogenase level, FACS analysis) were performed. Para- and transcellular BBB integrity was evaluated by FITC-dextran and albumin passage and FITC-insulin transport measurements, respectively. Furthermore, bio-adrenomedullin levels (bio-ADM) as a marker for endothelial stress were analysed. Noradrenaline levels indirectly provide information about dopamine β -hydroxylase activity. To test the sensitivity of this model, a cytokine adsorber was used for dose-dependent and kinetic investigations.

Results: Cytokine cocktails were able to induce significant damage in a concentration dependent manner. Pathophysiological cytokine concentrations showed a reduced viability and permeability and increased bio-ADM for hCMEC/D3 after an incubation period of 24 hours, which was even higher after 3 days of incubation. Cytotoxic effects on SH-SY5Y were only marginal. As a result of the adsorber treatment, especially functionality in both cell lines was maintained.

Conclusions: This study presents an efficient BBB-model and parameter setup for testing in inflammatory diseases such as SAE. The reduction of cytokines and concomitantly, the reduction of cytokine-induced pathological consequences in this model reflects the effect of therapeutic agents. Results of this study are a useful basis for further developments of pathophysiological in vitro models of BBB to assess preclinical therapeutics such as drugs and detoxification devices in future.

P98

A in-vitro model of human proximal tubule cells derived from human pluripotent stem cells for drug test

T. Ngo¹, A. Kurtz¹, B. Rossbach¹, I. Sebastian², J. Neubauer², K. Hariharan^{1,2}

¹BCRT, Berlin, Germany

²IBMT, Fraunhofer, Wurlub, Germany

Proximal tubular epithelial cells (PTECs) are responsible for selective reabsorption of above 60% of fluid and essential compounds from the glomerular filtrate, as well as secretion of waste products into urine. Due to their performance, PTECs are prone to damage resulting in renal disorders. Human PTECs are in high demand for regenerative therapies, tissue modeling using 3D printing, large scale drug-induced nephrotoxicity screening experiments; however, there is a lack of both quantity and quality of these cells. Established cell lines lost many of the critical functional features. We have developed a in-vitro model of PTECs derived from human pluripotent stem cells (hPSCs) for drug testing. PTECs were generated in a 14 days protocol in Cero bioreactor. Using Cero, the PTECs were directly expanded and differentiated on matrix coated alginate beads. PTEC-like cells were differentiate and expanded with a purity of above 90%, providing a suitable window for drug testing studies. Cisplatin, a nephrotoxicant, was used to induce a kidney

injury model in this study. PTECs model showed expression of Kidney Injury Molecule 1 (KIM1) as well as reduction of cellular viability after Cisplatin treatment.

Pharmacology – Pharmacokinetics and PK/PD modeling

P99

Mass spectrometry-based targeted proteomics method for the quantification of clinically relevant drug metabolizing enzymes in human specimens

C. Wenzel¹, M. Drozdziak², S. Oswald³

¹Institute of Pharmacology, University Medicine Greifswald, Center of Drug Absorption and Transport (C_DAT), Greifswald, Germany

²Department of Experimental and Clinical Pharmacology, Pomeranian Medical University, Szczecin, Poland

³Institute of Pharmacology and Toxicology, Rostock University Medical Center, Rostock, Germany

Biotransformation by phase I and II metabolizing enzymes represents the major determinant for the oral bioavailability of many drugs. To estimate the pharmacokinetics, data on protein abundance of hepatic and extrahepatic tissues, such as the small intestine, are required. Targeted proteomics assays are nowadays state-of-the-art for absolute protein quantification and several methods for quantification of drug metabolizing enzymes have been published. However, some enzymes remain still uncovered by the analytical spectra of those methods. Therefore, we developed and validated a quantification assay for two carboxylesterases (CES-1, CES-2), 17 cytochrome P450 enzymes (CYP) (CYP1A1, CYP1A2, CYP2A6, CYP2B6, CYP2C8, CYP2C9, CYP2C18, CYP2C19, CYP2D6, CYP2E1, CYP2J2, CYP3A4, CYP3A5, CYP3A7, CYP4F2, CYP4F12, CYP4A11) and five UDP-glucuronosyltransferases (UGTs) (UGT1A1, UGT1A3, UGT2B7, UGT2B15, UGT2B17). Protein quantification was performed by analyzing proteospecific surrogate peptides after tryptic digestion with stable isotope-labelled standards. Chromatographic separation was performed on a Kinetex® 2.6 μ m C18 100 Å core-shell column (100 \times 2.1 mm) with a gradient elution using 0.1% formic acid and acetonitrile containing 0.1% formic acid with a flow rate of 200 μ l/min. Three mass transitions were simultaneously monitored with a scheduled multiple reaction monitoring (MRM) method for each analyte and standard. The method was validated according to current bioanalytical guidelines and met the criteria regarding linearity (0.1-25 nmol/L), within-day and between-day accuracy and precision as well as multiple stability criteria. Finally, the developed method was successfully applied to determine the abundance of the aforementioned enzymes in human intestinal and liver microsomes. It can further be applied to the absolute quantification of CES, CYPs and UGTs in various human tissues.

Toxicology – Biogenic toxins

P100

Single dose exposure to sulfur mustard induces chronic senescence in primary human dermal fibroblasts

G. Horn¹, C. Schäfers¹, H. Thiermann¹, A. Schmidt², S. Rothmiller¹

¹Institut für Pharmakologie und Toxikologie der Bundeswehr, München, Germany

²Universität der Bundeswehr, München, Germany

Question: Dermal exposure to sulfur mustard (SM) results in skin blisters, ulcerations and characteristic chronic wounds. Cutaneous wound healing is dependent on many cell types including notably fibroblasts which contribute to granulation tissue formation. It is known that different cell types react to SM exposure with transition to a senescent state which might have a negative effect on wound healing. In this study, we investigated the SM sensitivity and the induction of chronic senescence in primary human dermal fibroblasts (HDF).

Methods: HDF were treated with SM at final concentrations from 0.03 μ M to 1000 μ M or solvent control for 24 h and the XTT assay was used to determine the 50 % lethal concentration (LC₅₀). Sub-lethal concentrations were used to investigate the induction of senescence in HDF by SM. Cells were exposed to 3 – 65 μ M SM or 300 – 500 μ M H₂O₂ and senescence-associated β -galactosidase (SA- β -gal) was stained histochemically over 31 days.

Results: The treatment of HDF with SM revealed a LC₅₀ of 161.73 μ M \pm 7.31 μ M. Using the former defined sub-lethal conditions, a time and concentration dependent senescence induction by SM and H₂O₂ was verified. Single doses of 24 μ M, 40 μ M or 65 μ M SM resulted in stable senescence after 10 – 14 days. Senescent cells showed an increased cell size.

Conclusion and outlook: HDF exposure to single, sub-lethal SM concentrations results in chronic senescence. HDF dysfunction may contribute to the chronic cutaneous wound healing disorder after SM exposure. More research concerning the secretome might give an insight into altered cytokine release of senescent HDF. This novel pathomechanism after SM exposure provides a possible new therapeutic target to improve wound healing.

P101

Specific growth factors and vitamins reduce senescence induction after sulfur mustard exposure in mesenchymal stem cells

A. Neu¹, N. Jäger¹, A. Bürkle², H. Thiermann¹, A. Schmidt³, **S. Rothmiller**¹
¹Bundeswehr Institute of Pharmacology and Toxicology, München, Germany
²University of Konstanz, Department of Biology, Konstanz, Germany
³Universität der Bundeswehr München, München, Germany

Introduction: Recently, chronic senescence in mesenchymal stem cells (MSCs) was identified as novel pathomechanism after exposure to the alkylating chemical warfare agent sulfur mustard (SM). Especially the delayed wound healing is a major obstacle, which may result in chronic wounds, and there is still no causal therapy available. These wounds may be caused by senescent MSCs due to their longevity and proinflammatory microenvironment.

Objectives: Preventing senescence induction after SM exposure might be a possible treatment option. In this study, the growth factor FGF-2, the vitamin niacin, and the poly(ADP-ribose)polymerase inhibitor olaparib were tested as pre- or post-exposure treatment.

Materials & methods: Human MSCs were isolated from bone marrow of femoral heads and cell identity was verified by their differentiation potential determined by IncuCyte microscopy. Senescence was induced by exposure to 40 µM SM and senescence-associated β-galactosidase (SA-β-gal) was stained up to 21 days later. 5 ng/ml FGF-2, 15 µM niacin, or 10 µM olaparib were added 23 h before as pre- or starting from 1 h after SM as post-exposure treatment, respectively. Non-senescent solvent controls as well as sham-treated controls were performed simultaneously.

Results: Osteogenic and adipogenic differentiation of MSCs could be tracked on-line and videos showed the process in more detail than histochemical staining at the endpoint. Pretreatment with FGF-2 and niacin significantly reduced the senescence induction 21 days after SM exposure and did not affect non-senescent controls at the same time. Post-exposure treatment with both substances did not show the same effect. In contrast, olaparib pre- and post-exposure treatment itself significantly increased senescence in non-senescent controls but showed no effect after SM exposure.

Conclusion: Single dose prophylactic treatment with the growth factor FGF-2 and the vitamin niacin is sufficient to reduce the induction of chronic senescence in human MSCs. Since senescent MSCs may be unable to fulfil their regenerative role in wound healing, a reduced senescent cell burden already during induction might possibly result in innovative treatment strategies for SM exposure.

Toxicology – Computational Toxicology

P102

In silico screening for novel harm reduction approaches: Identifying physico-chemical neighbours for controlled substances to facilitate technological harm reduction research

F. Steinmetz^{1,2}, H. Stöver^{2,3}

¹Delphic HSE, Schiphol, Netherlands

²Schildower Kreis, Frankfurt am Main, Germany

³Frankfurt University of Applied Sciences, Frankfurt am Main, Germany

Objectives: Controlled substances, such as cocaine or heroin, are used worldwide albeit their legal status may lead to harsh penalties and health issues. Many health risks can be mitigated by harm reduction measures, such as safer-use-education, regulated supply etc. Heroin-assisted treatment and drug-checking services are two examples for such measures, both being conducted in many European metropolises. With regard to heroin and cocaine certain harms are closely related to route of administration, *i.e.* injecting and smoking. Hence, harm-reducing drug formulations and/or devices may be options for public health policies. Due to very strict narcotic regulations and high costs/efforts associated with the purchase, harm reduction research is inhibited massively, particularly for small NGOs. Hence, alternatives to controlled substances are useful for technological development.

Materials & methods: *In silico* screening was used to identify compounds with similar physico-chemical properties as the controlled substance of interest (here: cocaine). These substances were then considered with regard to their accessibility and other potentially relevant features.

Results: In the elaborated example, a harm reduction device for crack cocaine users helping to avoid typical lung injuries, uncontrolled substances were identified as physico-chemical substitutes. These substances were suggested for low budget and/or early stage technological research.

Conclusion: Substances identified in such a procedure may be relevant for feasibility studies and/or technological development in harm reduction research, which is usually driven by health and social sciences. Further uncontrolled substances could be identified for other relevant harm reduction devices/formulations.

P103

Understanding the mechanism of genotoxicity of drugs by analyzing drug-DNA interactions using in-vitro/in-silico method

S. Akermi¹, **S. Sahoo**², S. Jayant¹, A. Nicole³, A. Nigam²
¹Annotation Analytics pvt. Ltd., Biotechnology, Gurgaon, India
²Amity University, Biotechnology, Mumbai, India
³Insight Biosolutions, Biotechnology, Rennes, France

Background: Drug-induced liver injury (DILI) acts by different mechanisms to induce multiple toxicity effects such as inhibition of hepatic transporters in inducing Hepatic cholestasis (accumulation of bile acid within hepatocytes) and Genotoxicity (the property of chemical agents that damages the genetic information within a cell causing mutations) through DILI [1, 2]. Therefore, it becomes particularly important to understand the multiparametric toxicities of drugs.

Objectives: In our work, we want to understand the mechanism of Genotoxicity of cholestatic/non-cholestatic Drugs by analyzing Drug-DNA interactions using the in-vitro/in-silico method.

Method: Three drugs have been selected from the FDA database: [a]. Caffeine (Stimulant, Non-cholestatic, hepatic transporters Non-inhibitors, > IC50 155 µM), [b]. Chlorpromazine (Antipsychotic, Cholestatic, hepatic transporters Non-inhibitors, IC50 147.6 µM), [c]. Troglitazone (Antidiabetic, Cholestatic, hepatic transporter Inhibitors, IC50 5.9 µM) and screened against the modeled DNA structure of {ATGCCGCATA}₂ using molecular docking approach.

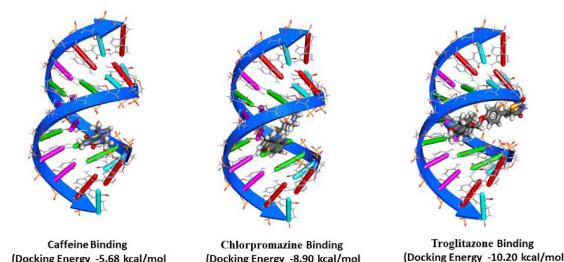
Results: All drugs cause chromosome aberration (CA) and Chlorpromazine causes mutagenicity which is proven experimentally [2,3]. Docking analysis reveals that all drugs make non-covalent interactions with the DNA. Caffeine binds in the DNA groove by making single hydrogen bonds with Cytosine (C5) base with the binding energy of - 5.68 kcal/mol. Chlorpromazine binds in the DNA groove by making two hydrogen bonds with Cytosine (C8) base with the binding energy of - 8.90 kcal/mol. In addition, Troglitazone drug binds in the DNA groove by making two hydrogen bonds with Adenosine (A2) and Guanosine (G6) bases with the binding energy of - 10.20 kcal/mol.

Conclusion: Our study concludes that it is particularly important to evaluate the multiparametric toxicities of drugs at the enzymatic and genomic levels. Our docking results will provide additional insight into molecular interaction to understand the mechanism of Genotoxicity caused by cholestatic/non-cholestatic during the Drug-induced liver injury (DILI) process and emphasizes that non-covalent interactions are also important for Drug Genotoxicity assessment.

Reference:

- [1]: Ren et al, Clinical Focus 2016;31:713–6.
- [2]: Snyder et al, Environmental and Molecular Mutagenesis 2013; 54:668-681.
- [3]: Snyder et al, Environmental and Molecular Mutagenesis 2010; 51:800-814.

Fig. 1



P104

Reactive metabolites from thiazole-containing drugs: Quantum chemical insights into biotransformation and toxicity

S. Khatun¹, C. Jaladanki¹, P. V. Bharatam¹
¹National Institute of Pharmaceutical Education and Research (NIPER), Mohali, Department of Medicinal Chemistry, Chandigarh, India

Drugs containing thiazole (TZ) and aminothiazoles (ATZ) groups are known to generate reactive metabolites (RMs) catalyzed by cytochromes P450 (CYP). These RMs can covalently modify essential cellular macromolecules and lead to toxicity and induce idiosyncratic adverse drug reactions. A quantum chemical DFT study was carried out to explore the molecular mechanisms involved in the biotransformation of TZ and ATZ groups leading to RMs – epoxide, S-oxide, N-oxide, and oxaziridine. The pathways associated with the biotransformation of thiazole ring-containing drugs mediated by CYPs

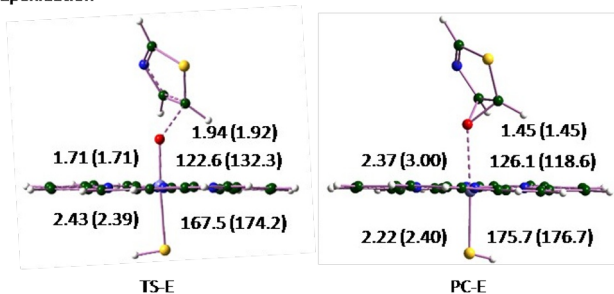
have been explored using quantum chemical methods. The DFT (B3LYP/6-311++G(d,p)/B3LYP/6-31+G(d)) studies were employed to investigate the mechanistic details associated with four important biotransformation pathways (epoxidation, S-oxidation, N-oxidation, and oxaziridine formation) of the model compounds TZ and ATZ. The epoxidation process requires an energy barrier of 13.63 kcal/mol and is exergonic by 24.01 kcal/mol. The alternative reactions require either higher barriers or lead to less stable products. The epoxidation reaction becomes more favorable when the C₂ position of thiazole is substituted by amine group, but the same reaction becomes less favorable when the C₅ position is blocked (e.g., a methyl group at the C₅ position). The four RMs of thiazoles can rearrange to ten more isomers via simple chemical rearrangements. Some of these isomers were found to be highly electrophilic and thus toxic and can directly form covalent adducts due to nucleophilic addition reaction with threonine / serine. The barrier for the reaction between the epoxide RM and MeO⁻ (a model of anionic serine/threonine) was found to be small (~10 kcal/mol), such reactions are probably the cause of mechanism based inhibition (MBI) complex formation. It was also observed that the epoxide metabolite can undergo di-oxidation and form dioxidation metabolite isomers. Few of the metabolites can produce covalent adducts with nucleophilic amino acids, leading to the inactivation of CYPs via MBI. Overall, this study provided the atomic-level details of the metabolic processes associated with thiazole containing drugs and helped in identifying the toxic versus non-toxic reactive metabolites.

References:

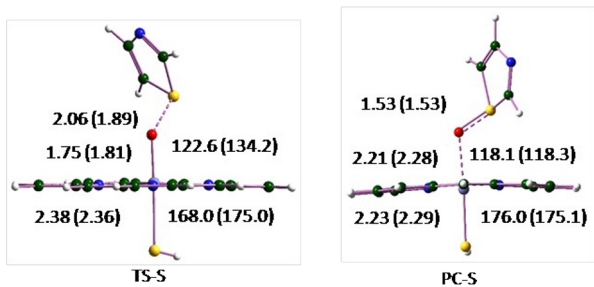
Mizutani, T.; Yoshida, K.; Kawazoe, S. Formation of Toxic From and Other Thiazole n Mice Identification of Thioamides as Ring Cleavage of Products. *Drug Metab. Dispos.* 1994, 22 (5), 750–755.

Fig. 1

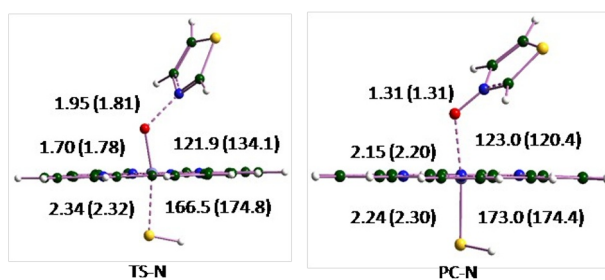
Epoxidation



S-Oxidation



N-Oxidation



Oxaziridine Formation

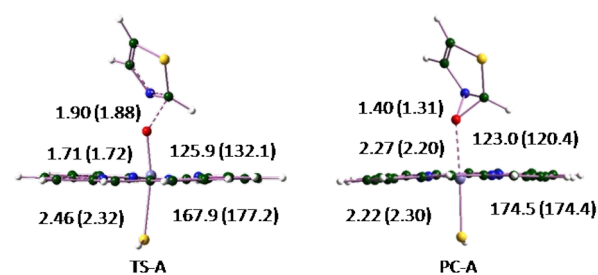
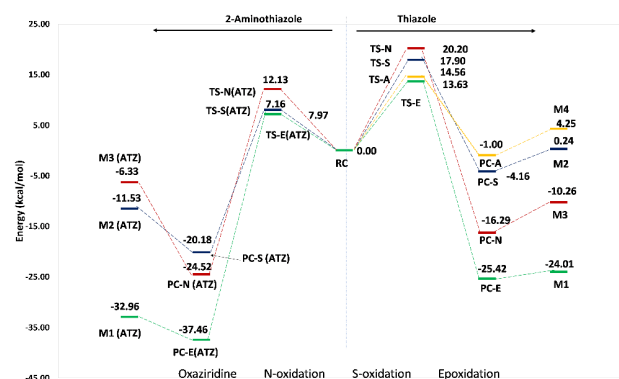


Fig. 2



Toxicology – Emerging topics

P105

Evidence of 2,4,6-trinitrotoluene (TNT) to cause upregulation of the molecular oxidative stress response in *Mytilus* spp

T. M. Schultheiß¹, J. S. Strehse¹, M. Brenner², E. Maser¹

¹University Medical School Schleswig-Holstein, Institute of Toxicology and Pharmacology for Natural Scientists, Kiel, Germany

²Alfred Wegener Institute Helmholtz Centre for Polar and Marine Research, Biosciences - Ecological Chemistry, Bremerhaven, Germany

Marine ecosystems are facing vastly increasing amounts of anthropogenic pollution, although not all pollutants posing a current threat have been recognized. Since World War I excess munitions were dumped in coastal waters and for a long period of time, the dumped munitions were not seen as a concern. But the metal shells are slowly corroding away and toxic compounds such as 2,4,6-trinitrotoluene (TNT) leak into the environment. For endemic organisms these chemicals present a challenge, especially to their cellular defence mechanisms. One crucial cytoprotective mechanism is the oxidative stress response. TNT was shown to lead to accumulated reactive oxygen species, hinting at its capability to unbalance a cell's redox-balance. This leads to the question if the exposure to TNT effects the gene expression of key oxidative stress response genes (biomarkers) in the marine keystone species *Mytilus* spp.

Mussels were exposed to TNT in acute and chronic lab experiments as well as in field studies at a munition dumpsite in the Baltic Sea. mRNA was extracted from the mussel's gills and hepatopancreas. The gene expression of oxidative stress biomarkers was measured with Real-Time PCR and quantified using the relative quantification method 2^{-ΔΔCT}. The respective coding gene sequences of the selected biomarkers *nrf2*, *nf-κb*, *hsp90* and *bcl-2* were bioinformatically predicted and identified in *Mytilus* spp.

In mussels in the controlled as well as natural settings the exposure to sublethal TNT concentrations had significant effects on the regulation of the target genes. TNT induced initially a significant upregulation of both transcription factors (TFs) Nrf2 and NF-κB in the gills and the hepatopancreas. After long-term exposure, in the gills a slight reduction was found, whereas in the hepatopancreas both TFs remained highly upregulated. The anti-apoptotic protein Bcl-2 was also upregulated at short-term exposure but interestingly after long-term exposure significantly decreased. Overall, the regulation was found to be tissue specific and dependent on the length of exposure.

The findings highlight the complexity of the interactions within the oxidative stress response system induced by TNT. On one hand, TNT can lead to a long-lasting imbalanced cellular redox state that can severely impact the organism's health. On the other hand, oxidative stress biomarkers show the potential to be further developed as early warning system for TNT contaminated munition dumping sites.

P106

Induction of the carbonyl reductase 1 (CR1) gene in *Daphnia magna* by TNT, but not by its key metabolites 2-ADNT and 4-ADNT

J. Jacobsen¹, E. Maser¹

¹Institute of Toxicology and Pharmacology for Natural Scientists, Kiel, Germany

After the end of World Wars I and II, surplus ammunition (mines, bombs, torpedos, etc.) was dumped into seas and lakes, with the result that decades later the chemical components such as 2,4,6-trinitrotoluene (TNT) leak out of the already corroding ammunition housings. In addition to its carcinogenic and genotoxic effects, TNT is also known to trigger apoptosis in cells via processes controlled by reactive oxygen species (ROS). Beside the typical enzymatic defense systems against oxidative stress (catalase, superoxide dismutase, glutathione-S-transferase), many species also possess carbonyl

reductases (CR), which play a role in oxidative stress management against reactive carbonyls. *Daphnia magna*, a small planktonic crustacean, has even four copies of the CR (CR1-CR4) and, being a long-established model organism for freshwater biotopes, is well suited as a test organism for this hypothesis.

The aim of this study is to determine whether and which of the CRs in *Daphnia magna* respond to exposure of TNT and its metabolites 2-amino-4,6-dinitrotoluene (2-ADNT) and 4-amino-2,6-dinitrotoluene (4-ADNT).

Gene expression tests were performed with different concentrations (0.5 mg/l to 2.5 mg/L) of TNT, 2-ADNT and 4-ADNT, and incubation times were varied (2 h to 24 h) in experiments with TNT. In addition, experiments with the antioxidant N-acetylcysteine (NAC) were executed. The samples were analyzed using RT-PCR and gel electrophoresis.

It was shown that a concentration and time dependent upregulation of the mRNA expression can only be observed for the CR1 gene under TNT exposition. In experiments with 2-ADNT and 4-ADNT, no upregulation could be observed. Similarly, exposure to TNT has no effect on the mRNA expression of genes coding for CR2, CR3 and CR4. Experiments with TNT and NAC did not show a statistically significant difference between samples with only TNT exposure and those with TNT and Nac combined (although the gels indicate some difference by visual inspection).

In summary, TNT affects the mRNA expression of CR1, in contrast to 2-ADNT and 4-ADNT. This difference could possibly be explained by the lower redox potential of the metabolites, according to the idea that ROS play a role in this hypothesis. However, this would have to be proven by further experiments.

P107

Influence of zinc oxide nanoparticles on Caco-2 monoculture versus Caco-2/HT29-MTX co-culture cells

A. Mittag¹, P. Owesny¹, C. Höra², A. Kämpfe², M. Gle¹

¹Friedrich-Schiller-Universität Jena, Institute of Nutritional Sciences, Department of Nutritional Toxicology, Jena, Germany

²German Environment Agency, Swimming Pool Water, Chemical Analytics, Bad Elster, Germany

Question: Zinc oxide nanoparticles (ZnO NP) are increasingly used in a variety of areas including the food sector because of their special physicochemical properties. This is associated with an increased oral uptake by humans, which makes a toxicological risk assessment essential. For this and in approximation to the physiological situation, the use of *in vitro* intestinal models is reasonable. The aim of our investigations was to examine the cellular ZnO NP uptake, their influence on the cell morphology, the metabolic activity and the intestinal barrier integrity using human cells.

Methods: Differentiated Caco-2 cells were used as monoculture and additionally as co-culture with HT29-MTX cells (ratio 3:1) in a transwell system. They were incubated with 123–614 µmol/l ZnO NP (<50 nm; <100 nm) or ZnCl₂ as salt control for up to 24 h. The cellular zinc content and the zinc permeation through the monolayer were determined using inductively coupled plasma mass spectrometry. By measuring the transepithelial electrical resistance (TEER) and permeability using the fluorescent dye FITC-dextran, conclusions could be drawn about the intestinal integrity. Using cell staining with DAPI and phalloidin, changes in the cytoskeletons and cell nuclei could be investigated. The metabolic activity was examined using the MTT assay.

Results: After treatment with ZnO NP, there was a dose-dependent increase in the cellular zinc content. This was higher in the Caco-2 monoculture than in co-culture. Only very small zinc proportions reached the basolateral transwell area. Compared to the monoculture, the co-culture showed a significantly higher TEER value after incubation with 614 µmol/l ZnO NP. In the co-culture, a significantly increased TEER value was observed at 307 and 614 µmol/l ZnO NP compared to the medium control. ZnO NP did not affect either the permeability or the morphology of the cytoskeletons or cell nuclei. They hardly influenced the metabolic activity of both cultures.

Conclusions: Treatment with ZnO NP leads to an increased cellular zinc uptake. In the co-culture of Caco-2 and HT29-MTX cells, ZnO NP increase the membrane integrity in a concentration-dependent manner. Neither the barrier integrity of the monoculture nor that of the co-culture is negatively influenced by ZnO NP. Concentrations up to 614 µmol/l ZnO NP do not result in morphological changes and cytotoxic effects in differentiated Caco-2 cells in mono- and co-culture.

P108

Cases of exposure to disinfectants from children under 6 years of age in Germany during the COVID-19 pandemic - An analysis of reported cases in the Charité Poisons Information Centre

A. Herrera-Melendez¹, D. Acquarone¹, R. Kreutz¹

¹Charité – Universitätsmedizin Berlin, Institute for Clinical Pharmacology and Toxicology, Berlin, Germany

Prevention has become the most important measure to contain the spread of coronavirus disease 2019 (COVID-19) and resulted in a widespread dissemination of disinfectants following recommendations of health authorities. Young children are particularly susceptible to intoxications with these products such as household and hand sanitizers.

We therefore conducted a retrospective study of exposure characteristics to disinfectants in children younger than 6 years that were reported to the Charité Universitätsmedizin Berlin – Poisons Information Centre during the first half of 2020 and in comparison to the same period of the previous five years.

Our results show that in the first half of 2020 the total number of reported exposures increased by 37.2% ($p < 0.05$) compared to the average of the same period over the last five years. Especially in March 2020 a significantly higher number of reports was observed (+49.3%, $p < 0.001$) compared to the corresponding month in the past five years. Most exposures occurred in male toddlers (aged 1 to 5 years). Despite the increased incidence, most exposures in our cohort were of mild nature. In 2020, 85% of the affected subjects were advised to stay at home, while 13% required medical evaluation, and 2% hospitalization. We observed an (19.5% and 40.9% increase in exposures to both hand sanitizers and disinfectants for the household. Caregivers and healthcare professionals should be aware of the risks associated with disinfectants. Public health strategies should be developed that aim protect children from intoxications with disinfectants.

Fig. 1

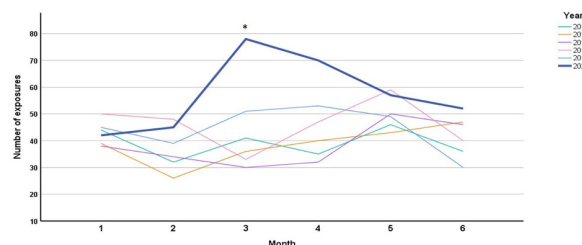


Fig. 2

	Year, n (%)					
	2015 n = 234	2016 n = 229	2017 n = 229	2018 n = 275	2019 n = 266	2020 n = 339
Female	100 (46.9)	94 (43.3)	98 (46.0)	117 (44.5)	129 (48.7)	144 (42.5)
Age category						
Newborn	0 (0)	1 (0.4)	1 (0.4)	1 (0.4)	0 (0)	0 (0)
Infant	31 (13.2)	29 (12.7)	33 (14.4)	42 (15.3)	54 (20.3)	44 (13.0)
Toddler	203 (86.8)	199 (86.9)	195 (85.2)	232 (84.3)	212 (79.7)	294 (87.0)
Route of exposure						
Ingestion	205 (87.6)	197 (86.0)	200 (86.9)	239 (86.9)	230 (86.5)	290 (85.5)
Inhalation	2 (0.9)	0 (0)	2 (0.9)	1 (0.4)	1 (0.4)	4 (1.2)
Dermal	3 (1.3)	5 (2.2)	4 (1.7)	7 (2.5)	5 (1.9)	5 (1.5)
Ocular	8 (3.4)	14 (6.1)	11 (4.8)	9 (3.3)	12 (4.5)	11 (3.2)
Symptoms by the time of calling						
Asymptomatic	188 (80.3)	174 (77.6)	179 (78.2)	208 (75.6)	211 (79.3)	264 (77.9)
Mild symptoms	45 (19.2)	55 (22.4)	48 (20.1)	65 (23.6)	53 (19.9)	75 (22.1)
Moderate symptoms	1 (0.4)	0 (0)	4 (1.7)	1 (0.8)	2 (0.8)	0 (0)
Advice given						
Stay at home	205 (87.6)	203 (88.7)	186 (81.2)	220 (80.0)	221 (83.1)	288 (85.0)
Medical evaluation required	24 (10.3)	25 (10.9)	41 (17.9)	48 (17.5)	36 (13.5)	44 (13.0)
Hospitalized	5 (2.1)	1 (0.4)	2 (0.9)	7 (2.5)	9 (3.4)	7 (2.0)
Product category						
Disinfectants for the household	65 (27.8)	77 (33.6)	63 (27.5)	84 (30.5)	71 (26.7)	122 (36.0)
Hand sanitizers	169 (72.2)	152 (66.4)	166 (72.5)	191 (69.5)	195 (73.3)	217 (64.0)

Newborn, until twenty eight days of age. Infant, from one month until eleven months. Toddler, from one year until five years and eleven months.

P109

Process for the cost-effective separation of problematic substances using the example of drug residues and investigation of the biological effects of anti-inflammatory drugs on *C. elegans*

O. Krings¹, K. Junghanns¹, S. Raabe², B. Schumann^{1,2}, S. Kamalakkannan^{1,2}, F. Glahn¹, K. Krüger², H. Foth¹

¹Institute of Environmental Toxicology, Medical Faculty, Halle, Germany

²GMBU e.V., Department of Environmental Microbiology, Halle, Germany

Drugs and their metabolites unintentionally enter municipal wastewater, as they are difficult to remove in wastewater treatment plants due to their persistence and high water-solubility. For active pharmaceutical ingredients, however, the goal is to have remaining levels without biological effects. For this purpose, criteria are sought that represent a satisfactory cleaning result. The aim of the project is therefore to develop an innovative process for removing pharmaceutical residues in municipal and industrial wastewater and to test its efficiency in model organisms of Environmental Toxicology.

To investigate possible biological effects, the model organism *C. elegans* was cultivated in the culture medium NGM (Nematode Growth Medium) with different concentrations of anti-inflammatory drugs (Diclofenac, Ibuprofen, Naproxen and Acetaminophen). Studies of acute and chronic toxicity (life span assay) and studies of reproductive toxicity (progeny assay) have been established and applied. The trace substances are removed by adsorbing the drug on a catalytically active membrane and then cleaning the surface using UV-C radiation.

Diclofenac and Acetaminophen (0.5; 1; 2 mM) as well as Ibuprofen and Naproxen (2.5; 10; 25 µM) did not lead to any acute toxic effects in *C. elegans*. In studies on the chronic toxicity of diclofenac, the life span of *C. elegans* is shortened by 14 days at the highest concentration (NMG with 2 mM Diclofenac) compared to the untreated control. As the

concentration of Diclofenac in NGM increases, the time in which *C. elegans* lays eggs is significantly longer than in the control (up to five days longer). However, this does not lead to an increase in the progeny. Overall, the absolute number of eggs laid is lowest in the highest concentration group. Previous tests using the planned procedure show that UV-C irradiation can reduce the amount of Diclofenac in water by 84% within 5 minutes and by 96% in 10 minutes.

In an initial assessment, diclofenac shows low toxicity, despite the selection of approximately 600-fold higher concentrations than in previously analyzed wastewater. Further investigations will be carried out on the biological effects of the drugs mentioned and their metabolites that arise during the cleaning process. Also the process will continue to be optimized.

P110

Developing a toolbox for fast and reliable screening of large quantities of marine samples for nitroaromatic explosives by GC-MS/MS on femtogram levels

T. H. Büning¹, A. C. Hollmann¹, J. S. Strehse¹, E. Maser¹

¹University Medical School Schleswig-Holstein, Institute of Toxicology and Pharmacology for Natural Scientists, Kiel, Germany

Objectives: Release of nitroaromatic explosives, e.g. trinitrotoluene, 1,3-dinitrobenzene and 2,4-dinitrotoluene from marine dumped munitions is a worldwide emerging problem. The accumulation of these compounds and their metabolites in marine organisms has been proven in the past. During pilot expeditions along the German Baltic shore, low levels of these compounds could be proven in almost all water samples taken. To draw a picture on how serious the situation in North and Baltic Sea is, and to estimate ecotoxicological consequences, large quantities of various biotic and abiotic samples (e.g. sediment and water, blue mussels, fish bile or filet) must be screened – often at very low compound levels.

Methods: Different workup methods (e.g. lyophilization, ultrasonic-, microwave, liquid-liquid and solid phase extraction, as well as enzymatic treatment for biota samples) were tested and combined. Gas chromatography - tandem quadrupole mass spectrometry parameters were optimized for qualitative and quantitative detection of explosives and their metabolites on levels below 1 ng/mL sample. This was achieved by testing different types and length of columns with different methods of injection. The methods were optimized for fast analysis, as shorter measurement times allow lower detection limits of the temperature-sensitive explosives, and for constant results for at least 100–200 samples.

Results: A toolbox was developed, which allows tailor made processes as demanded by the specific sample type and its expected concentration. Limits of detection between 77 and 333 fg/µL have been achieved. Sample specific LODs are displayed in tab. 1. Even lower LODs for 4- and 2-ADNT were achieved with large volume injection, whereby, however, the sensitivity for TNT decreased. Methods were successfully tested on various sample types.

Conclusion: GC-MS/MS is the ideal technique for screening large quantities of marine samples. With splitless injection, analysis take less than 6.5 minutes for a full scan of all explosives. Even after continuous measurement of several hundred mussel or water samples, the results remained reliable. For biota where almost no unmetabolized TNT is found, large volume injection can offer improved detection limits below 10 pg/g w.w. for the metabolites.

Tab. 1: Limits of detection (LOD) and retention times (RT) of munition compounds in dissimilar samples by the optimized splitless-method, determined by the EU standardized method EUR 28099.

Fig. 1

Compound	RT [min]	LOD _{Water} [pg/L]	LOD _{Sediment} [pg/g]	LOD _{Blue mussel} [pg/g w.w.]
1,3-Dinitrobenzene	2.48	200	99	218
2,4-Dinitrotoluene	2.92	46	25	221
Trinitrotoluene	3.45	91	50	349
4-Aminonitrotoluene	4.27	57	29	154
2-Aminonitrotoluene	4.46	62	31	123

P111

A materiovigilance study: The use of face masks in Romania considering the COVID-19 pandemic

A. Arseniu^{1,2}, A. A. Chis¹, A. Frum¹, C. M. Dobre¹, A. M. Juncan¹, L. L. Rus¹, G. Cormos¹, M. Muresan¹, M. Totan¹, A. C. Muntean¹, F. Gligor¹, S. Ghibu³, C. Morgovan¹
¹"Lucian Blaga" University of Sibiu, Preclinical Department, Sibiu, Romania
²"Iuliu Hatieganu" University of Medicine and Pharmacy, Cluj-Napoca, Romania
³UMF "Iuliu Hatieganu" Cluj-Napoca, Pharmacology, Physiology and Pathophysiology, Cluj-Napoca, Romania

Questions: Medical devices are widely used in the context of the COVID-19 pandemic declared by WHO on 11 March 2020 [1]. In order to assure the patients' quality of life (QoL), the health products need to be of high quality and used correctly [2]. During the pandemic, the pharmacies from Romania have faced numerous problems regarding face masks (FM), such as the absence of certificate of origin or quality documents, the lack of

CE marking, label or instructions for use, the occurrence of counterfeit products; all being considered risks factors for people's QoL.

Methods: The current research of the regulations of FM from EU and Romania was analyzed employing the comparative and interpretation method [3-7].

Results: In Romania, the marketing of FM in pharmacy is regulated by Pharmacy Law no 266/2008. According to the EU regulations, the products must have the CE marking and the Declaration of Conformity. On the EU market, 3 FM categories were identified: 1) **medical or surgical masks** regulated by ASTM F2100, NF EN 14683 or other equivalent standard (the bacteria filtration capacity being over 95%); 2) **respiratory masks** (filtration capacity >95%); FFP2 or FFP3 (EU: EN 149 standard); N95 (US: NIOSH 42 CFR Part 84 standard); KN95 (China: GB2626-2006 standard) etc. and 3) **fabric mask for non-medical use** (filtration capacity: <70%). In addition to the lack of effective protection, improper use of masks has led to facial skin lesions, dermatitis, worsening acne [8]. In order to combat the Covid-19 pandemic, along with other sanitary measures, authorized products must be used correctly, respiratory and medical FM being the most effective.

Conclusions: The pharmacists from Romania have faced a lot of legislative problems regarding FM, which could affect the people's security and QoL. These problems were generated by the explosive demand and limited supply (initially, the authorized products being out of stock) and even limited knowledge considering these products.

References:

- Cucinotta D, Acta Biomed. 2020, 91(1):157-160. doi: 10.23750/abm.v91i1.9397
- Morgovan C et al., Farmacia, 2019, 67(3): 537-544, doi.org/10.31925/farmacia.2019.3.24
- Regulation (EU) 2016/425
- Regulation (EC) No 765/2008
- Decision No 768/2008/Ec
- Cuc Hepcal I et al., Farmacia, 2015, 63(4): 607-612
- Morgovan C et al., Int. J. Environ. Res. Public Health 2020, 17, 4456, https://doi.org/10.3390/ijerph17124456
- Radonovich L.J. et al., JAMA. 2019;322(9):824-33, 10.1001/jama.2019.11645.

Author index

A			
Abdel-Aziz, H.	29		
Abdel-Kahaar, E.	89		
Abdeltawab, N. F.	29		
Abrahamian, C.	P26		
Acali, S.	P48		
Acquarone, D.	P108		
Adam, J.	37		
Adamson, M.	83		
Adler, J.	60, P67		
Aigner, A.	20, 23, 47, P28, P85, P87		
Akermi, S.	P103		
Akinloye, O.	P47		
Al Disi, S.	27		
Albert, B. V.	24, P12		
Albin, J.	55		
Althaus, L.	28		
Altmeppen, H.	25		
Ammar, R. M.	29		
Anangi, B.	P19		
Andreev-Andrievskiy, A.	65		
Andryka, K.	83, P10, P71		
Annibale, P.	34		
Anton, S.	76		
Appelhans, D.	P87		
Arbogast, M.	P58		
Arseni, A.	P111, P31		
Aspera-Werz, R. H.	P93, P94, P95		
Asuaje Pfeifer, M.	P92		
Attila, B.	P07		
Avondet, M.-A.	12		
Avramopoulos, P.	P96		
B			
Bachmann, H. S.	85, P60		
Baier, J.	8		
Balan, M. A.	P06		
Balhorn, R.	P91		
Ban, E.-G.	P06		
Bankoglu, E. E.	36, 40		
Barchet, W.	P11, P71		
Barenys, M.	P37		
Bars, R.	57		
Barth, H.	7, 8, 10, 11, 54		
Bartok, E.	45, 83, P10, P11, P71		
Bass, R.	P52		
Batke, M.	58, P45		
Bätz, V.	17		
Bauer, S.	57		
Bäumer, W.	P04		
Baumgärtner, W.	P05		
Baygün, S.	28		
Bayrak, K.	83		
Becher, F.	12		
Beck, A.	64		
Beck, C.	14, 16		
Beck, K.	P63		
Becker, A.	P81		
Becker, H.	3		
Becker, K.	P05		
Beckmann, L.	52		
Beer-Hammer, S.	P59		
Behrens, P.	P84		
Belkacemi, A.	64, P80		
Belovičová, K.	P86		
Beltzig, L.	P15		
Bender, A.	59		
Benkel, T.	74		
Berit-Seiffert, S.	P42		
Berkut, A.	65		
Bernhard, D.	7		
Bernhardt, G.	P57		
Berning, H.	P61		
Bertold, R.	P68		
Beuck, S.	3		
Beuerle, T.	P92		
Beuerlein, K.	P70		
Beyerle, P.	63		
Bharatam, P. V.	P104		
Birk, B.	4, 5, P36, P39		
Bischof, H.	60, P75		
Bischoff-Kont, I.	78, 79		
Bisha, M.	P01		
Bitsch, A.	30		
Blaszkwicz, M.	P53		
Bleich, M.	33		
Bloch, D.	P43		
Bock, A.	34, 76		
Bockstiegel, J.	81		
Bode, G.	P52		
Bode, H. B.	79		
Boengler, K.	19		
Böhm, R.	86, P27		
Böhmert, L.	68		
Boldt, K.	P67		
Boomgarden, M.	P97		
Boran, B.	12		
Borchardt, H.	23		
Borggreffe, M.	P96		
Bovard, D.	P83, P93, P94, P95		
Bracher, F.	78, P26		
Braeuning, A.	68, 69, P54		
Brandes, R. P.	49		
Braun, B.	P94, P95		
Braun, P.	2		
Braune, M.	11		
Bredeck, G.	P32		
Breinbauer, R.	P93		
Brenner, M.	56, P105		
Bresnick, A.	49		
Breunig, L.	17		
Brinschwitz, B.	75		
Brockmüller, J.	32		
Bruckmüller, H.	P19		
Bruckmüller, J.	P19		
Büch, T.	20		
Buchmüller, J.	69		
Bühler, M.	72		
Bulin, C.	86		
Bünning, T. H.	P110		
Burgers, L.	82		
Burk, O.	P65		
Bürkle, A.	22, P101		
Burns, L.	12		
Busch, H.	52		
Busch, M.	P32		
Busche, M.	3		
Busschots, K.	12		
Butuca, A.	P31		
C			
Cachorro, E.	P61		
Cadi, R.	P82		
Campbell, K.	12		
Canbolat, P. M.	P04		
Carlsson, M. J.	66		
Carstensen, J.	P40		
Cartus, A.	66		
Cascorbi, I.	21, 86, P14, P19		
Chamot Rooke, J.	P82		
Chaudhari, K.	P03		
Chesne, C.	2		
Chevigne, A.	74		
Chis, A. A.	P111, P31		
Chong, R.	46		
Chowdhury, S. A. K.	18		
Christmann, M.	19, 37, 38, 66, P13, P15		
Coch, C.	P11		
Colon, D.	46		
Comes, C.	P42		
Connemann, B. J.	89		
Coricovac, D.	P22, P25		
Corina, U.	P07		
Cosmos, G.	P111		
Creutzenberg, O.	69		
Crispi, F.	P37		
Csatlovová, K.	P86		
D			
Damm, G.	3, 58, P45		
Damm, H.	66		
DAOUDI, K.	P82		
De Coninck, D.	P62		
De-Eknamkul, W.	P26		
DeGrave, A.	27		
Dehelean, C.	P22, P25		
Demuth, P.	19		
Dendorfer, A.	P96		
Denkinger, M.	89		
Dietl, P.	8		
Dietrich, A.	62		
Dimitrijevic, D.	P36		
Dittrich-Breiholz, O.	P02		
Dobrea, C. M.	P111, P31		
Dobrev, D.	13		
Dolghi, A.	P22, P25		
Dolšak, A.	44		
Dooley, S.	55		
Dorn, T.	P96		
Dorner, B.	9, 12, 31		
Dorner, M.	9, 31		
Doss, S.	P97		
Dressler, D.	2		
Dropmann, A.	55		
Drozdzik, M.	P99		
Dubovický, M.	P86		
Dubrall, D.	33		
Dueck, A.	14, 28, P96		
Dunst, S.	1		
Dworschak, M.	21		
Dygai, A.	48		
E			
Ebert, F.	41		
Ebert, M.	55		
Ebmeyer, J.	69		
Ehinger, R.	60, P75		
Ehnert, S.	P93, P94		
Eichenlaub, M.	P72		
El-Armouche, A.	P61		
El-Batrawy, I.	P96		
Elsayed, M.	89		
Elßner, T.	9		
Empl, M.	37		
Engelhardt, S.	14, 16, 28, P50, P96		
Engelhart-Jentsch K, K.	2		
Erdösi, P.	55		
Erhardt, N.	P74		
Erika, B.	P07		
Erkoc, P.	79		
Ermakova, N.	48		
Ernst, K.	10, 11		
Ersche, K. D.	P28		
Eschenhagen, T.	26		
Esfandyari, D.	14, 28, P96		
Esselen, M.	71		
Ewe, A.	P85, P87		
F			
Fabian, E.	P36		
Fabritius, M.	82		
Fahrer, J.	19, 37, 66, 70		
Falk, S.	P78		
Fecher-Trost, C.	64, P74, P76		
Fechter, L.	54		
Felician, G.	14		
Fellermann, M.	54		
Fender, A.	13		
Fender, J.	17		
Feraudet-Tarisse, C.	9		
Filor, V.	P05, P84		
Fischer, B.	P43		
Fischer, S.	8, 54		
Flick, B.	4		
Flockerzi, V.	64, P76, P80		
Flormann, D.	64		
Fois, G.	8		
Folkert, F.	P53		
Forster, L.	P57		
Foth, H.	58, P109, P45, P49		
Freiberger, A.	58, P45		
Freitag, M.	52		
Frentzel, S.	P48, P83		
Frericks, M.	P72		
Frey, O.	P41		
Frick, M.	8		
Fritsche, E.	P37		
Fritz, G.	P16, P17, P18, P20		
Frum, A.	P111, P31		
Fuentes-Amell, M.	P37		
Fuhlbrueck, J. A.	66		

Funk, F.	P63	Herrmann, T.	P84	Karwelat, D.	57
Fürst, R.	78, 79, 82	Herzer, K.	85	Kassler, L.	13
		Hessel-Pras, S.	69, P54	Kazakov, A.	46
G					
Gaedcke, J.	32	Hettwer, K.	15	Kelber, O.	40
Gahr, M.	89	Heylmann, D.	66, P70	Keller, J.	P46
Gall, K.	3	Hiebl, B.	26	Keller, J. G.	P51
Garbe, S.	45	Hilgenfeld, R.	25	Kerner, J.	73
Gastmeier, A.	P27	Hill, K.	35, 61	Khajavi, N.	63
Gastmeier, K.	P27	Himmerkus, N.	33	Khatun, S.	P104
Gebel, T.	58, P45	Hinz, S.	P60	Khayyal, M. T.	29
Gebhardt, R.	3	Ho, M. T.	P66	Khazraei, H.	P08, P09, P79
Geertz, B.	26	Hock, F. J.	18	Khosravani, F.	P01
Gehring, F. K.	2	Hoeng, J.	P48, P83, P93, P94, P95	Khusainov, G.	65
Geiger, F.	62	Hoffmann, C.	74	Kietzmann, M.	P05, P84
Geisen, S.	37	Hoffmann, P.	37	Kildalsen, H.	P19
Gericke, B.	P84	Hofmann, T.	P72	Kim, Y. O.	43
Gerullis, H.	P53	Hofmann, U.	P59	Kipp, A.	41
Gessler, F.	9	Hofrichter, J.	P97	Kirsch, V.	67, 88, P56
Geyer, J.	P78	Höhne, S.	P53	Kisiela, M.	56
Ghibu, S.	P111, P31	Holdenrieder, S.	45	Klaassen, T.	3
Gholamreza-Fahimi, E.	P01	Hollmann, A. C.	P110	Klehr, J.	P61
Giammarino, E. D.	P71	Holze, J.	42, 44	Klein, H.-J.	86
Giralt, A.	P48	Honarvar, N.	P34, P42	Klein, K.	P76
Giri, V.	P39, P46	Höra, C.	P107	Klugbauer, N.	P73, P77
Glahn, F.	P109, P49	Hom, G.	P100	Klutzny, S.	1
Glatzel, M.	25	Hövelmeyer, N.	43	Knapp, F.	P02
Glei, M.	P107	Hövener, J.-B.	53	Knapp, S.	78
Gligor, F.	P111, P31	Huber, G.	53	Knauff, J.	P21, P69
Gnad, T.	73	Huber, L.	53	Kneuer, C.	P40
Göbel, S.	51	Huber, M.	19	Knobloch, J.	52
Goedtke, L.	P54	Huchler, C.	54	Kojda, G.	P01
Golka, K.	P53	Hucho, T.	65	Kolb, P.	74
Gomes, C.	P34	Hughes, S.	P29	Kolle, S.	P44
Gómez-Catalán, J.	P37	Husen, P.	85	Kondylis, A.	P48
Gomeza, J.	74			Konrad, C.	34, 76
Göpfert, A.	P34	I		Kopp, J.	41
Götz, C.	P81	Ibrahim, S.	52	Kopp, L.	79
Grabowski, M.	44	Idrissou, B. M. G.	P96	Kornhuber, M.	1
Gralinski, M. R.	18	Illa, M.	P37	Kosinska, J.	33
Gratacós, E.	P37	Ingelfinger, R.	79	Kostenis, E.	42, 74
Grätz, L.	P57	Inoue, A.	74	Kostka, T.	37
Greim, H.	P55	Isbatan, A.	18	Kracht, M.	24, P02, P12, P21, P64
Grimm, C.	P26	Isbilir, A.	77		P69, P70
Grimm, W.-D.	48	Isensee, J.	65	Krämer, F.	38
Großmann, S.	P73, P77	Iskandar, A.	P48, P83	Krassnig, S.	22
Grundmann, O.	P29	Ivanov, N.	P48	Krause, M.	7
Grupe, K.	P90, P92	J		Kreutz, R.	P108
Grushevskiy, E. O.	77	Jacobsen, J.	P106	Krings, O.	P109
Grüter, L.	P96	Jäger, N.	P101	Krishnathas, G. M.	78
Guan, K.	15	Jaladanki, C.	P104	Krohn, M.	25
Gudermann, T.	47, 62, 63	Janker, T.	75	Kronenbitter, A.	P63
Guedj, E.	P48	Jansson, D.	12	Krüger, K.	P109
Gundert-Remy, U.	58, P45	Jayagopi, S.	46	Krüger, M.	9
Günscht, M.	P61	Jayant, S.	P103	Krüger, M.	P63
Guthale, G.	P03	Jedlitschky, G.	75	Krupin, V.	48
Gutsch, D.	20	Jenke, R.	20	Krybus, M.	P01
H		Johansen, B.	P19	Kubatiev, A.	48
Haag, M.	P59	John, A.	P54	Kühne, B. A.	P37
Haake, V.	P39, P46	Josuran, R.	12	Kühnlenz, J.	57
Haas, M.	70	Juli, J.	P64	Künstner, A.	52
Häberlein, F.	74	Juncan, A. M.	P111, P31	Küpper, J.-H.	70
Hagedorn, P.	P05	Jung, D.	P60	Kuret, A.	60
Hagemann, A.	85	Junghans, K.	P109	Kurtz, A.	P98
Hagen, C.	45	Jurida, L.	P02	Kuth, M. S.	49
Hagl, C.	P96	Jurk, D.	53	Kuzmenkov, A.	65
Hagmeyer, B.	3	Just, K.	84	L	
Hain, T.	P12	K		Lackner, M.	P59
Hammad, S.	55	Kadhun, T.	P53	Laming, S.	45
Hanna, D. M. F.	P58	Kähler, M.	21, P14	Lampe, J.	25
Hariharan, K.	P98	Kaina, B.	P13, P15	Lampen, A.	P54
Hartmann, E.	83	Kalina, D.	P75	Lampert, A.	P30, P88, P89
Hartmann, G.	45, 83, P10, P11, P71	Kallenborn-Gerhardt, W.	49	Landenberger, M.	10
Hasse, M.	15	Kamalakkannan, S.	P109	Landsiedel, R.	4, 5, P34, P36, P42
Hasselwander, S.	43	Kamler, M.	13		P44, P51
Hauert, D.	P60	Kammerer, S.	P61	Langan, E.	52
Heber, S.	54	Kamp, H.	P39, P46	Längst, N.	P67
Hein, L.	P73	Kampa, B.	12	Lauffer, S.	P65
Heiner, M.	P69, P70	Kämpfe, A.	P107	Lechsner, P.	P06
Heise, K.	28	Kämpfer, A.	P32	Lehmann, J.	P33
Hemmler, R.	3	Karaca, M.	P43	Leib, L.	P64
Hengstler, J.	58, 69, P45, P53	Karagiannis, F.	46	Leiss, V.	73
Hennekinne, J.-A.	12	Karimov, M.	P87	Lemichez, E.	12
Herberhold, S.	83	Karin, W.	P74	Leovskiy, C.	51
Herdegen, T.	86, P27	Karl, M.	43	Lezoualch, F.	P23
Herold, M.	P39	Karl, N.	24	Li, H.	43
Herrera-Melendez, A.	P108			Li, W.	15

Li, Y.	82	Mönnich, D.	P57	Peiser, M.	P40
Lichtenberg, J.	P41	Monteleone, S.	74	Peitsch, M.	P48, P83
Liebl, B.	47	Moormann, O.	P53	Pershina, O.	48
Liebmann, M.	P90	Morawski, M.	23	Peschke, E.	53
Lim, V.	74	Moretti, A.	P96	Peter, A.	P67
Linne, U.	24, P64	Morgovan, C.	P111, P31	Pfeifer, A.	73, P62
Linnebacher, M.	19	Moritz, E.	75	Pfitzner, I.	2
Litterst, M.	P14	Morozov, S.	48	Pflock, R.	33
Liu, A.	59	Motoc, A.	P24	Pfuhler, S.	2
Löhr, H.	P74	Muehlich, S.	47	Pham, T.	P75
Lohse, M.	34, 76, 77	Müller, Ch.	5	Philipp, S. E.	P81
Loreiro, C.	P37	Müller, Chr.	24	Philippu, A.	P55
Lorenz, K.	17, P61	Müller, K.	25	Pinzaru, I.	P22, P25
Lossow, K.	41	Müller, L.	71	Plomer, M.	P30, P88, P89
Lübow, C.	80	Müller, P.	45, P71	Pockes, S.	P57
Luch, A.	P66	Müller, R.	82	Poertner, J.	13
Luczak, A.	60	Müller, Sa.	P58	Poetsch, M.	15
Luetlich, K.	P83	Müller, Su.	78	Pöhlmann, C.	9
Luginbühl, W.	12	Müller, Th.	P73, P77	Popoff, M.	12
Lukowski, R.	60, P67, P75	Müller, Ti.	63	Prevot, V.	25
Luo, X.	15	Müller-Fielitz, H.	25	Pueschel, K.	P52
Luong, B.	82	Munoz-Muriedas, J.	59	Püschel, G. P.	6
Lutz, S.	27	Muntean, A. C.	P111	Puustinen, A.	12
Lux, F.	P76	Muresan, M.	P111	Puzicha, T.	13
		Mustea, A.	P23		
		Mustonen, E.-K.	P65		
M				Q	
Ma-Hock, L.	P51			Querdel, E.	26
Maegdefessel, L.	28	N		Quian, Y.	55
Maestro Lavin, D.	27	Nagel, I.	21, P14, P19		
Magauer, T.	61	Näger, A.	P96	R	
Mahrhold, S.	9, 31	Naji Said Aboud, H.	40	Raabe, S.	P109
Maiellaro, I.	76, 77	Nebolsin, V.	48	Raasch, W.	52, 53
Maier, M.	61	Neitzel, C.	19	Ramanujam, D. P.	14, 16, 28, P50, P96
Maier, P.	46	Nemec, K.	77	Ramirez Hincapie, S.	P39, P46
Majeed, S.	P48, P83	Netcharoensirisuk, P.	P26	Raschke, M.	57
Malan, D.	74	Neu, A.	P101	Rasenberger, B.	19, 66
Malihpour, M.	64	Neubauer, J.	P98	Rasetti-Escargueil, C.	12
Malli, R.	60	Neumann, T.	9	Rashidian, A.	P65
Mallmann, R. T.	P73, P77	Neve, V.	25	Rasinger, J. D.	69
Mangerich, A.	22, 58, P45	Neves, L. A. A.	18	Rauch, B. H.	75
Mann, J.	P16	Newel, D.	P69	Raudszus, R.	35
Marescotti, D.	P48, P83	Ngo, T.	P98	Rayk, B.	P68
Martin, D. E.	47	Nguyen, A.	38	Reamon-Büttner, S. M.	30
Martin, F.	P48	Nia, Y.	12	Regenthal, R.	P28
Martinez, T.	18	Nichani, K.	15	Reichel, C.	78, 82
Martus, D.	P80	Nicol, B.	P36	Reifenberg, G.	43
Marx, S.	83	Nicole, A.	P103	Reinders, J.	P53
Marx-Stoeltling, P.	P43	Nieland, J.	10	Reinders, Y.	17
Marzo Solano, M.-D.-L.	P43	Nigam, A.	P103	Reinhard, O.	P68
Maser, E.	56, P105, P106, P110	Nikolaev, V.	74	Remmele, M.	P44
Masquelier, J.	12	Noetger, S.	7	Renggli, K.	P83
Matschl, U.	52, 53	Noske, S.	P85	Renn, M.	45, 83
Matt, L.	P75	Nowakowski, F.	P61	Richling, E.	67, P46
Matthees, E.	74	Nürnberg, B.	73, P59	Rimek, D.	9
Matthes, J.	88, P56	Nüssler, A. K.	P93, P94, P95	Roeder, M.	10
Matz-Soja, M.	3	Nørgaard, K.	10	Röhl, C.	58, P45
Mayer, D.	54			Rohrbach, S.	P02
Mayr, T.	3	O		Roman, A.	P24
Mayr-Buro, C.	24, P12	Odainic, A.	46	Römer, S.	32, P78
Meier, M.	P96	Oelgeschläger, M.	1, P38	Rommel, C.	P73
Meier-Soelch, J.	P12, P69	Oertel, R.	15	Rosbach, B.	P98
Meißner, J.	P05, P84	Offermanns, S.	33	Rösser, S.	78
Meister, G.	14	Ogrodnik, M.	53	Roth, E.	P53
Meitinger, T.	14, P96	Olthoff, S.	61	Roth, N.	4
Mejivang, J.	P19	Oltmanns, H.	P05, P84	Rothmiller, S.	P100, P101
Menne, S.	P11	Onifade, I.	P47	Rottmann, F.	P27
Menzel, R.	P38	Ortega-Torres, L.	P48	Rowe, J. B.	P28
Merches, K.	17	Oswald, S.	32, P99	Rowland, D.	P62
Merg, C.	P48	Othman, O.	P70	Ruggiero, E.	P51
Mertens, C.	P71	Otto, T.	P53	Rühl, P.	P26
Messelhäußer, U.	9, 31	Oukkache, N.	P82	Rülker, C.	P34
Metzner, K.	49	Ovsianikov, D.	P53	Rummel, A.	9, 12, 31
Meyer, F. B.	51	Owesny, P.	P107	Rus, L. L.	P111, P31
Meyer, M. R.	64			Ruth, P.	60, P75
Meyer, M. J.	32, P78	P			
Michaelis, J.	7, 54	Pak, C.	P83	S	
Michalakakis, S.	82	Pakhomova, A.	48	Sacher, J.	P28
Michla, M.	46	Pan, E.	48	Sachs, B.	33
Mierzala, A.-S.	12	Pantsar, T.	P65	Sahoo, S.	P103
Miess, E.	74	Papatheodorou, P.	7, 10	Sailer, J.	11
Mishra, D.	P39	Park, K.-S.	43	Salah, H.	P80
Mittag, A.	P107	Partosa, N.	P42	Salako, K.	P47
Mittendorf, C.	13	Partosch, F.	58, P45	Salako, O.	P47
Mittermeier, C.	47	Pasparakis, M.	25	Sander, L. E.	
Mittmann, L.	78	Patzelt, S.	P06	Santos, G. L.	27
Moer, J.	3	Paul, M.	68	Sasse, P.	74
Mohamed, S. S.	29	Pavlaki, N.	74	Sassi, Y.	P96
Mohan, M.	P03	Pawlak, M.	3	Saudagar, P.	P03
Möller, J.	76	Peigneur, S.	65	Sauer, M.	P97

Sauve, F.	25	Singh, G.	50	Viñas-Noguera, M.	P86
Sawatsky, B.	P11	Sivakumar, N.	P20	Virmani, I.	P35
Schaefer, M.	35, 61	Skandali, N.	P28	Vogel, D.	19
Schäfers, C.	P100	Skiba, M.	12	Vogl, S.	P38
Schaudien, D.	69	Skurikhin, E.	48	Volland, H.	12
Scheffler, A.	44	Soler, S. B.	P10	Vollmer, A. S.	66
Schenke, M.	6	Sova, M.	44	von Berg, L.	31
Scherneck, S.	P90, P92	Sovadinová, I.	P35	von Bibra, C.	26
Scheuer, R.	P81	Sperber, S.	P39	von Kügelgen, I.	P58
Schiffmann, S.	79	Sprenger, H.	69	von Messling, V.	P11
Schihada, H.	77	Šribar, D.	44	Vonica, L.	P31
Schiller, H.	P50	Srivastava, S.	50		
Schins, R.	P32	Staab-Weijnitz, C.	62, P50	W	
Schirmer, B.	87	Steger-Hartmann, T.	57	Wack, G.	49
Schjeide, B.-M.	6	Stegmüller, S.	66	Wagner, A.	P38
Schmid, M.	33	Steinberg, G.	P38	Wagner, C.	64
Schmid, T.	78	Steinberg, M.	31	Waldhoer, M.	74
Schmidt, A.	P100, P101	Steinberg, P.	37	Wandt, V. K.	41
Schmidt, H.	7	Steiner, R.-P.	15	Wang, E.	49
Schmidt, M.	P23	Steinmetz, F.	P102	Wang, X.	43
Schmidt-Supprian, M.	28	Stelzle, M.	3	Wardas, B.	P80
Schmidtko, A.	49	Stenger, S.	54	Wätzig, V.	86, P27
Schmitt, J. P.	P63	Stern, D.	9, 31	Weber, A. G.	5
Schmitt, M.	79	Stingl, J.	84	Weber, A.	24, P64
Schmitt, N.	P44	Stock, V.	68	Wedemeyer, H.	85
Schmitt, V.	46	Stölting, I.	52, 53	Wehr, M.	30
Schmitz, L.	P12	Stolz-Ertych, A.	72	Wein, L.	61
Schmitz, M. L.	24	Stope, M.	P23	Weinberger, F.	26
Schmitz, S.	83, P10, P71	Stopper, H.	36, 40	Weinbrenner, S.	27
Schnabel, J.	3	Storjohann, R.	P84	Weindl, G.	42, 44, 80, 81
Schneider, D.	P49	Stöver, H.	P102	Weisemann, J.	9, 12
Schneider, M. R.	72	Strano, A.	15	Weiser, H.	24, P12, P69
Schneider, M.	15	Stratenwerth, B.	P15	Weiser, T.	P30, P88, P89
Schneider, S.	5, P72	Straub, K.	85	Weiss, R.	P39
Schön, A. P.	14, 16	Strehse, J. S.	56, P105, P110	Weissgerber, P.	P76
Schönfelder, G.	1, 72, P38	Strödke, B.	78	Weng, W.	P93, P94, P95
Schönfeldt-Lecuona, C.	89	Sturla, S.	37	Wenzel, C.	32, P99
Schrenk, D.	70	Summers, N.	P39	Wenzel, J.	25, 53
Schreyer, L.	47	Sündermann, J.	30	Werner, Seb.	P02, P12, P69
Schröder, K.	49	Suresh, M.	P11	Werner, Sim.	3
Schubert, M.	15	Sychrová, E.	P35	Wesely, C.	P74
Schuchhardt, M.	81	Szpakowska, M.	74	Weyrich, A.	P72
Schultheiß, T. M.	P105			Wieland, A.	P11
Schulz, C.	14	T		Wilde, S.	30
Schulz, K.	9	Tang, R.	P26	Wilhelm, C.	46
Schulz, S.	74	Tänzer, L.	P23	Wilk, L.-V.	31
Schulz, T.		Tatsch, L.	P13	Will, O.	53
Schumann, B.	P109, P49	Teichert, J.	P28	Willenbockel, C.-T.	P43
Schupp, N.	P91	Tenekeci, U.	P70	Willuweit, K.	85
Schupp, T.	58, P45	Tenhaken, V.	P19	Wilzopolski, J.	P04
Schuppan, D.	43	Teufel, A.	55	Winkelbeiner, N.	41
Schürmann, L.	P17	Thierbach, R.	51	Winter, M.	P76
Schuster, D. M.	P34	Thiermann, H.	P100, P101	Wirachowski, K.	70
Schuster, R.	25	Thoma, E.	P41	Wissenbach, U.	P74
Schütte, L.	71	Tinschert, R.	64	Wittig, I.	49
Schwab, M.	P59, P65	Tinwell, H.	57	Woelk, S.	4
Schwaninger, M.	25, 33, 53	Tolksdorf, C.	75	Wohlleben, W.	P51
Schwarzenbach, C.	P13	Tölle, M.	81	Wolber, G.	44
Schwerdtle, T.	41	Tom, D.	2	Wolf, A.	P41
Scotto Rosato, A.	P26	Tomicic, M.	38, P13	Wolf, R.	75
Sebastien, I.	P98	Totan, M.	P111	Wollin, K.-M.	58, P45
Seeger, B.	6, 37, P33	Tran, T. M.	P38	Wondany, F.	7, 54
Seidel, A.	P54	Trivedi, K.	P48	Worbs, S.	12
Seidel, E.	43	Tuerkova, A.	32		
Seifert, R.	87	Tytgat, J.	65	X	
Seitz, T.	32	Tzankov, A.	P52	Xia, N.	43
Seiwert, N.	19, 37	Tzvetkov, M. V.	32, P78		
Sekeres, M.	P18			Y	
Selinski, S.	P53	U		Yadav, S.	50
Senese, P.	18	Uhlig, S.	15	Yesildag, B.	P41
Sessler, K.	7	Ullrich, A.	3		
Seternes, O. M.	P19	Ullrich, F.	P10	Z	
Sewer, A.	P48	Ulrich, C.	P42	Zaborosch, C.	12
Shaban, M. S.	24, P12	Uphaus, H.	30	Zanetti, F.	P48, P93, P94, P95
Shay, J.	37	Ureche, C.	P06	Zdrazil, B.	32
Shibamiya, A.	26	Urynuk-Ool, T.	P95	Zech, T.	78
Sickmann, A.	17			Zeiner, J.	74
Sieg, H.	68	V		Zeleny, R.	12
Sievers, H.	40	Vaccarello, P.	14, P50	Zellmer, S.	P66
Simm, S.	P78	van Cann, M.	65	Zhang, L.	25
Simon, K.	74	van den Boom, J. G.	45	Zhou, X.	60
Simon, K.	15	van Ravenswaay, B.	4, 5, P34, P36	Zhukova, M.	48
Simon, L.	41		P39, P46, P72	Ziebuhr, J.	24
Simon, S.	9, 12	Vanninen, P.	12	Ziemann, C.	30
Simon Andreas, P.	P07	Vassilevski, A.	65	Zille, M.	25
Simonsig, S.	P75	Vázquez, P.	P37	Zillinger, T.	P10, P11, P71
Singer, S.	47	Veltri, C.	P29	Zimmermann, M.	74

